LARGE-DEFLECTION ELASTO-PLASTIC ANALYSIS OF DISCRETELY STIFFENED PLATES

A thesis submitted for the degree of Doctor of Philosophy in the Faculty of Engineering of the University of London

by

Parwiz Djahani, Dipl. Ing., M.Sc., D.I.C.

Imperial College of Science and Technology

London, January 1977

To Puran,
Parvin
and Puyan

ABSTRACT

A treatment is presented for the elasto-plastic large-deflection analysis of stiffened (including isotropic) plates subject to lateral and/or in-plane loading, using finite difference approximations to the three governing simultaneous non-linear partial differential equilibrium equations. The discretely stiffened plate has been analysed by considering it as an isotropic plate subjected to interactive line loads at the location of the stiffeners, representing the effect of the stiffeners. Out-of-plane buckling of the structure and in-plane buckling of stiffeners, have been considered. For iterative solution of the set of non-linear equations a method equivalent to the linearly convergent Newton-Raphson method with δ^2-extrapolation has been used which has resulted in a very fast convergence. Ideal elastic-perfectly plastic behaviour (with no strain hardening) is assumed for the material.

For the plasticity of plate, the Ilyushin yield criterion with the associated Prandtl-Reuss flow rule has been adopted, which assumes a sudden plastification through the plate depth. For the plasticity of stiffeners the effect of axial stress has been considered only. Initial deformation of plate and stiffeners and residual stresses in plate and stiffeners have been considered.

Numerical examples are presented for unstiffened and stiffened plates (with eccentric and concentric stiffeners) having different flexural and membrane boundary conditions and various types of loadings (lateral load, direct compression, shear load and combined shear and in-plane bending). Close agreement with the few existing solutions is obtained. The method is also used to check the basis of a proposed

design method for plate- and box-girder webs which will be used in the new British bridge code.

ACKNOWLEDGEMENTS

The investigation reported in this thesis was undertaken in the Department of Civil Engineering of Imperial College, London. It was supervised by Dr. P.J. Dowling, Reader in Steel Structures, to whom the author is deeply indebted for his valuable suggestions and guidance. The author is also grateful to Professor B.G. Neal, Professor of Engineering Structures, for his support during the course of the research and to Professor A.K. Basu for his useful discussions and suggestions during the early stages of the research.

Thanks are due to Dr. P.A. Frieze, Dr. J.E. Harding, Dr. K.R. Moffatt and Mr. L.P.R. Lyons whose computer programs were used to provide results for comparison, and to Mrs. H. Guile for her help with the drawings and Mrs. M. Frieze who helped with the typing.

The author would particularly like to thank his wife Puran and his children Parvin and Puyan for their great understanding.

Financial support was provided by Arya-Mehr University of Technology Tehran and the Iranian Ministry of Higher Education.

CONTENTS

CHAPTER 1

INTRODUCTION AND LITERATURE REVIEW

1.1 INTRODUCTION

1.1.1 General Remarks on Behaviour of Stiffened Plates

In practice thin plates are seldom used in isolation, they are usually connected to beams resulting in stiffened plates or plated grillages which as structures or sub-structures are structurally more efficient and functional. Such systems are used frequently in space, marine and civil engineering metal structures. The function of the plate element in stiffened plates is often to withstand transverse pressure and transfer it to the stiffeners, and/or to act integrally with the stiffeners to sustain in-plane forces. The presence of longitudinal and transverse stiffeners affects the structural behaviour of stiffened plates compared with unstiffened plates in many ways. For example, the mode and character of buckling and failure which may occur can be altered and influenced by stiffener geometry and connection methods.

A great deal of interest has been generated in the ultimate strength of stiffened steel plates in recent years, particularly in the wake of the failure of a number of steel box girder bridges. This has highlighted the need for more powerful theoretical methods for the analysis of plated structures, that can predict their behaviour up to and possibly beyond their maximum load carrying capacities. Ideally, the methods should be able to include all main factors affecting the behaviour of stiffened plates, such as fabrication tolerances and material properties. Such methods need reliable numerical processes to be used in solving the complex equations which govern the non-linear behaviour of the structure. The importance of developing rigorous

methods which take account of both geometric and material non-linearities and fabrication tolerances and therefore can predict more realistically the behaviour of stiffened plates is twofold. In the first place there are insufficient experimental data available to check the validity of simplified approximate methods. The results of a rigorous analysis could thus serve to calibrate approximate methods. Secondly, the relevant design parameters in stiffened plates are too numerous (plate aspect and slenderness ratio, stiffener geometry, spacing and arrangement, boundary conditions, etc.,) to be investigated thoroughly using an experimental approach. Numerical parametric studies could be used, however, to generate results covering the range of practical parameters in a more economic and efficient manner.

The purpose of the present work is to develop an analytical technique to predict the elasto-plastic large-deflection behaviour of stiffened plates subject to different types of loading and having different in-plane and flexural boundary conditions. For developing such a technique all factors governing the behaviour of stiffened plates should be known and their effect should be incorporated into the solution method considered. In view of the lack of relevant experiments there is little known about the behaviour of stiffened plates and, therefore, it is possible only to discuss briefly under what circumstances the influence of different factors will be significant. The main factors governing the behaviour of stiffened plates are:

(a) Boundary Conditions

Stiffened plates are usually considered as sub-structures of the total structure and may be treated in isolation. Often members providing large out-of-plane rigidity support stiffened plates. In most cases the out-of-plane boundary conditions are

easily determined. The nature of the membrane boundary conditions, however, is often very difficult to judge and a close examination and clear definition for any particular problem is required. Frequently edges remain straight, but are free to pull in in-plane. In-plane boundary conditions have a significant influence on the magnitude of membrane stresses and hence on the deflections and surface stresses, which is not possible to predict from small deflection and plane stress solutions alone.

(b) Geometry

The geometry of orthogonally stiffened rectangular plates is defined by the following parameters:

(i) Aspect ratio of stiffened plate (width/length),

(ii) Aspect ratio of plate between stiffeners,

(iii) Slenderness ratio of plate between stiffeners,

(iv) Stiffener geometry (size, shape, etc.) and arrangement.

The different geometric parameters have a significant effect on the behaviour and ultimate strength of stiffened plates and this should be considered both in design and analysis. Stiffened plates with closely spaced stiffeners, generally show a column-like failure mode under axial compression[1]. For a wide integrally uniaxially stiffened plate subject to uniaxial compression the critical modes of bifurcation are either the local buckling of the plate between stiffeners or buckling of the panel as a wide Euler column. By a suitable choice of plate and stiffener rigidities and arrangement, plates may be designed so that theoretically at least, buckling occurs simultaneously in these two modes. Such designs usually maximise the theoretical bifurcation load for a given amount of material[1]. The

simultaneous buckling designs are, however, more imperfection sensitive than other designs due to the strong mode interaction[2,3] and also show a reduction in load carrying capacity compared to alternative designs using a similar amount of material. In practice stiffened plates are often designed so that they bifurcate in the plastic range. The relative importance of some factors such as residual stresses and geometric imperfections depends on geometric parameters. In plates with low slenderness ratio, residual stresses have a more pronounced influence on their ultimate strength than geometric imperfections[4], because such plates have a high buckling stress and therefore a loss of the effective flexural rigidity of the stiffeners becomes considerable due to early partial yielding of the plate. Initial distortion has a significant effect on the behaviour of stiffened plates, specially in cases of in-plane loading. Large initial distortions result in extensive changes in the distribution of the membrane stresses. Two main types of geometric imperfection are important in plated structures. Firstly, the out-of-plane displacement of plate and stiffeners which also induces out-of-straightness in stiffeners. Secondly, additional out-of-straightness of stiffeners. In the present work only the first type of geometric imperfection has been considered, however there is no difficulty in considering the second type of imperfection in the presented method of analysis. Out-of-flatness is often towards the stiffeners.

(c) Material Properties

One of the basic advantages of structural materials such as

steel and aluminium is their ductility - the ability to undergo large plastic deformations without fracture. One type of failure in steel structures is brittle failure by brittle fracture or fatigue cracking. The other type of failure is the ultimate collapse in which the structure fails to carry further load due to partial or full yielding of a critical section. In the present work the first type of failure is disregarded and the ultimate collapse is considered only. Partial yielding in the stiffeners due to applied stress plus residual stresses reduces considerably the buckling strength of the stiffened plates. In order to avoid a great reduction of the strength, "hybrid stiffened plates" have been recommended[4], in which a higher strength steel is used for the stiffener than the plate.

Some materials show a strain-hardening behaviour, but in the case of steel an ideal elastic-perfectly plastic behaviour can be assumed with sufficient accuracy.

(d) Loading

In general a stiffened plate is subjected to several different load conditions composed of combinations of in-plane and lateral loading. The lateral loading is generally distributed pressure, but there are frequently cases of concentrated lateral load such as wheel loading on bridge decks, or truck loading on a ships deck. The actual in-plane loading is dependent on the stiffness of adjacent structural elements, and may be reproduced either as distributed stresses or prescribed displacements along the edges. In marine structures and bridges in-plane loading is often induced by composite action of the stiffened flange with deep girder webs in bending action. Frequently, stiffened plates are

subject to combined lateral pressure and in-plane loading. In rectangular plates under combined axial compression and lateral load an increase in buckling load can be achieved[5]. This is because of the conversion of the flat plate to a segment of cylinder loaded in longitudinal compression. Lateral pressure may however, cause a reduction in the strength of stiffened plates where transverse membrane compression is present. This is because the displacement due to lateral pressure acts as an initial geometric imperfection.

Another important aspect in stiffened plates is the presence of residual stresses. Recent theoretical[6,7] and experimental[8,9] studies have led to a much improved understanding of the influence of residual stresses on the strength of plated structures. The high temperatures involved in the yielding process of plate panels and stiffeners produce large thermal strains, which due to the uneven rate of cooling in the areas near and away from the weld result in considerable residual stresses which are self-balancing. The weld and areas near to it have tension stresses of the order of the metal yield stress and because of statical equilibrium the other parts have compressive residual stresses. Based on experimental results some residual stress patterns have been suggested[7]. The residual stresses will speed up or delay the process of yielding in different parts of the stiffened plate depending upon the applied stresses and residual stresses in that part being of the same or different sign.

1.1.2 Analysis and Design

The rational design of stiffened plates is based on factors such as material properties, geometry, fabrication, loading, method of analysis and some design criteria. To develop rational design criteria the behaviour of the structure under all possible loading conditions should be well understood. Such design procedures should produce structures which are safe and at the same time are not unnecessarily conservative. The analyses on which design methods are based should therefore be able to consider all the main factors which have a significant effect on the behaviour of the structure. The applicability of existing methods is often restricted to special cases of geometry, material properties, type and magnitude of loading and boundary conditions.

The choice of method of analysis depends not only on the type of loading but also on its magnitude. In the case of lateral loading when displacements are small, we can assume with sufficient accuracy that the loading is transferred to supports (or stiffeners) by the bending action of plate and stiffeners, and classical small-deflection analysis will give sufficiently accurate results. With increasing displacements, membrane forces will be developed and the relationship between the applied loading and deflections and stresses will become non-linear. The loading will be partly resisted by the membrane forces of plate and stiffeners, which are significant in magnitude. In some cases such as ship and aircraft structures, under the working condition loadings the components undergo deflections of the order of their thickness. Here a small-deflection solution will overestimate deflections and stresses and so will lead to an unduly conservative design. In such cases a large-deflection non-linear theory should be

employed. This theory allows for the stiffening effect due to membrane stresses which develop under finite deflections. The effect of initial geometric imperfection can be also included in this theory. In some cases under the working conditions, the loadings result in stresses which exceed the proportionality limit of the material. Parts of the plate and/or stiffeners yield and so the elastic large-deflection theory will underestimate the displacements. This is because the theory considers only the geometric non-linearity but not the material non-linearity. A design criterion used for some structures subject to lateral pressure is to limit the level of permanent deflections (e.g. helicopter landing pads, ship decks, etc.). Normally limitations on permanent deflections are dictated by serviceability criteria, e.g. satisfactory functioning of bridge deck surfacing. Apart from satisfactory functioning of the structure under normal service loading there are no other reasons for such a limitation unless compressive membrane forces co-exist with the lateral loading. In practice plates are subject to combined in-plane and lateral loading so that the permanent set limitation is often necessary from considerations of the effect of in-plane loading. Evaluation of permanent set is possible only by using elasto-plastic analysis. Even for structures which have a linear behaviour under working condition loads, an elasto-plastic analysis may be required to predict its behaviour in case of over-loading and its safety with respect to collapse.

If in-plane loads dominate the full advantage can often be taken of the ultimate load as unserviceability is not the controlling limit state. An important principle in the design of such structures is to identify the load-carrying action at collapse so that elements may be sized to meet load and in-plane deformation requirements, and

details arranged so as to prevent premature localised failure. Interaction of elements is known to significantly affect stiffeners and thus load redistribution between components, and consequently their ultimate strength. Local collapse of some elements may influence the overall deformation pattern through sympathetic rotational and membrane interaction with adjacent panels and stiffeners. Redistribution throughout one element may significantly alter total loading on an adjacent one of smaller dimensions. The ultimate collapse of plated structures may occur in the following modes or their interactions[10]:

(a) *Local buckling of plate panel between stiffeners:* In this case the ultimate strength of the plate panel between the stiffeners is exceeded before extensive yield occurs in the stiffeners. By increasing the applied load beyond this point the reduction of load in the plate panel will proceed more rapidly than the increase of load in stiffeners, so that the ultimate load for the stiffened plate is reached before the stiffener failure occurs.

(b) *Flexural buckling of the longitudinally stiffened panel:* In this case the compressively loaded stiffener and the plating as its flange show a column-like flexural buckling between the transverse stiffeners.

(c) *Lateral-torsional buckling of longitudinal stiffeners:* In this case failure occurs by a lateral-torsional buckling of compressively loaded stiffeners. This mode of failure occurs when the stiffeners have small torsional rigidity e.g. flat bars.

(d) *Overall grillage buckling:* In this form of failure the grillage buckles in one or more half waves over its length

with bending in transverse as well as longitudinal stiffeners.

In the past the design of stiffened plates has been based on the results of the linear buckling theory, in which any fabrication tolerances such as geometric imperfection of plate and stiffeners and residual stresses due to welding are ignored. A more correct approach would be the use of ultimate strength of stiffened plate evaluated by an elasto-plastic large-deflection analysis as design basis. The conventionally employed methods for dealing with stiffened plates are based on the "orthotropic plate theory". Such techniques are based on replacement of the stiffened plate by an equivalent continuum obtained by smearing out the stiffener properties. The result is a continuum model which is anisotropic, and in the case of plates with orthogonal stiffeners is orthotropic. If the discontinous system (stiffened plate) is replaced by a continuum (orthotropic plate), the interpretation of the solution for local behaviour e.g. near a stiffener, lacks a rational base. The method gives therefore results that at best predict only the overall behaviour of plates with fairly closely spaced stiffeners. Moreover, this method is not appropriate in the inelastic range since the phenomenon of local yielding in the plating and stiffeners and the spread of the plasticity in the structure can not be examined in terms of overall plate properties used in this theory. Also the method can not deal exactly with initial geometric imperfections in the plating and torsional type initial distortions in the stiffeners and the local buckling of these elements. Finally the requirement that there should be a sufficient number (at least five) of closely spaced stiffeners for the theory to be valid, limits its usefulness even for the study of overall elastic behaviour. There is a tendency in marine structures to increase frame

spacing to reduce costs, and so deck grillages frequently have only a few stiffeners and perhaps only one stiffener between deep frames on bulkhead boundaries.

The other frequently used method for analysis of stiffened plate is the "discrete beam element" technique in which the plated structure is treated as a grillage of discrete beam elements, the plating being represented by equivalent effective flanges acting with the stiffeners according to the beam theory. Elements are normally taken as the segments of beams between grillage intersections, but additional subdivisions may be necessary if discontinuities in the sectional properties, loading or initial imperfections occur between intersections. In this technique plasticity can be considered, but in general its use is restricted only to cases where a beam-column behaviour is expected.

The purpose of the present work is to develop an analytical technique to predict the non-linear elasto-plastic behaviour and to predict the ultimate capacity of discretely stiffened plates including cases with eccentric stiffeners. For the numerical part of this work the finite difference method has been used which has in this case some advantages compared with other available techniques. At each node there are three variables (u, v, and w), which is less than the five degrees of freedom often used in the finite element method. A further advantage of this method is that the treatment of stiffeners involves only some changes in the rigidities at the respective nodes, rather than the addition of new elements as in the finite element method.

1.2 LITERATURE REVIEW

The review is concentrated mainly on works concerned with the analysis of unstiffened and stiffened plates which are related to the present work. Basic information on the subject can be found in standard text books[11-15]. A detailed review of theoretical and experimental research on unstiffened and stiffened plates is presented in Ref. (16). A review and references of works on this subject using the finite element method can be found in Refs. (17-20).

1.2.1 Elastic Linear Solutions

Unstiffened Plates: Linear small-deflection solutions and the problem of critical buckling of plates has been tackled by many investigators. Elastic critical buckling solutions for rectangular plates having various boundary conditions are extensively reported in Refs. (11,21,22,24), and by many others.

Stiffened Plates: Pflueger[25,26] has derived three simultaneous fourth order linear partial differential equations which govern the three displacement components u, v and w for two way reinforced plates in the linear elastic range, considering interaction between plate and stiffeners. Gienke[27-31] reduced these to two fourth order linear differential equations in terms of lateral displacement w and stress function F. By elimination of u and v, Trenks[28] reduced Pflueger's equations to a single eighth order differential equation for w. The complexity of solution was not lessened by this modification. Dean and Omidvaran[29] presented a discrete continuous field approach to the analysis of rectangular plates reinforced in one direction by straight ribs. The reinforced continuum has been analysed by dealing with each rib as a line of discontinuity in

loading. A closed form field approach is indicated, in which one attempts to find a field or functional solution that will yield the stresses or deflections at the desired point through substitution of the co-ordinates into the solution formula, which is valid for all points. A similar approach was also presented by Wah and Calcote[30]. The first solutions for critical buckling of plates having longitudinal or transverse stiffenerswere reported by Timoshenko[32], and were based on energy principles. He presented solutions for plates subjected to uniform uniaxial compression and pure shear load. Exact solutions were later reported by Loshkin[33] and Barbré[34,35] who investigated the buckling of plates with one and several longitudinal stiffeners. Froehlich[36] presented buckling loads for plates with one longitudinal and one transverse stiffener at the centre. Solutions for buckling of eccentrically stiffened plates in the elastic range are reported by Tvergaard[2,3]. Elastic critical buckling solutions of rectangular plates having various boundary conditions are extensively reported[21, 22,24].

The most common approach for the analysis of stiffened plates is the orthotropic plate theory, in which the stiffened plate is replaced by an equivalent anisotropic continuum obtained by 'smearing out'[4] the stiffener properties. Huber[37], working with concrete as an orthotropic material, first formulated the linear differential equations which govern the small deflection behaviour of orthotropic plates. Using these equations Pelikan and Esslinger[38] developed a practical design procedure for stiffened plates considering them as equivalent orthotropic plates. Based on Huber's equations many finite difference solutions have been reported[144].

1.2.2 Geometric Non-linearity

Unstiffened Plates: The equations governing the elastic non-linear behaviour of isotropic plates were first derived by von Karman[45] in the form of two fourth order simultaneous partial differential equations in terms of lateral deflection of the plate and a stress function for the membrane action of the plate. They can be written also in the form of three simultaneous partial differential equations in terms of lateral and in-plane displacements of the plate (u,v,w). The direct solution of von Karman's differential equations is lengthy, but several approximate and indirect methods of solution (Ritz energy, Fourier Series and finite difference methods) have been presented. Solutions using the Ritz energy method were presented by Marguerre[46] and Way[55] for plates under lateral loading. Levy[49,50] and Levy and Greenman[51] using a double Fourier Series presented general solutions for simply supported and clamped plates under the combined action of lateral and in-plane loading. Finite difference solutions were obtained by Kaiser[48] which agreed closely with his experimental results. Wang[52] presented finite difference solutions by forming and solving two sets of simultaneous non-linear partial differential equations. Von Karman's equations were extended by Marguerre[47] to include the effect of out-of-flatness of the plate. Most of the later work on the initially deformed plates are based on his formulation. Solutions for laterally loaded plates using dynamic relaxation technique are reported by Rushton[54] and Williams[53]. Chien and Yeh[56] and Thompson and Walker[57] used a perturbation procedure for the analysis of plates. Based on Levy's method Coan[58] investigated the post-buckling behaviour of an initially deformed plate under uniaxial compression. Yamaki[59] extended Levy and Coan's work to obtain solutions for rectangular plates with simply

supported and clamped edges and different membrane boundary conditions. Other series solutions for post-buckling of plates are presented by Walker[60] and Dawson and Walker[61]. Elastic large-deflection analyses of plates using the finite element method are reported by many investigators[17-20,62-68].

Stiffened Plates: The equations governing the elastic non-linear behaviour of orthotropic or discretely stiffened plates were first presented by Lekhnitzkii[24] in the form of two fourth order simultaneous partial differential equations in terms of lateral displacement and Airy stress function. Based on Lekhnitzkii's work Vogel[69,76] derived a new compatibility equation which more closely represents the behaviour of stiffened plates. He used a technique based on the Ritz energy method for the solution of the large deflection problem. Soper[77] extended Levy's method (Fourier Series) to the solution of rectangular stiffened plates, replacing them as equivalent orthotropic plates. Solutions were obtained which agreed well with his test results. Basu[70, 71] and Aalami[72] extended Wang's (finite difference) computational method and obtained solutions for a wide range of orthotropic and isotropic plates with various flexural and membrane boundary conditions. In all solutions based on orthotropic plate theory, the local buckling of plate panels between stiffeners and the lateral torsional buckling of stiffeners cannot be considered. Massonnet and Maquoi[40], however, used the orthotropic plate approach for the analysis of stiffened plates in compression. To allow for the effects of stiffener eccentricity the extensional, flexural and torsional rigidities for the equivalent orthotropic plate were modified according to Pflueger[25]. Some allowance for the local buckling of plate panels between longitudinal stiffeners was achieved by using an approximate effective width approach based on

Faulkner's[73] formula and an approximate collapse criterion.

Rubin[74,75] presented solutions for longitudinally eccentric stiffened plates with initial geometric imperfection by considering the stiffeners as discrete members acting with an adjoining effective width of flange plating. The effective width is again based on Faulkner's[73] formula. For the deflection in the longitudinal direction he assumes a sinusoidal mode but lateral deflections in the transverse direction are free and are established by minimising the total potential energy. Only normal stress and shear stress resulting from pure torsion (Saint-Venant) are considered for bending of stiffeners and for its membrane action only normal stress. Skaloud and Novotny[78] investigated the post-buckling behaviour of rectangular plates with one stiffener. As in all earlier works they assume a lateral displacement $w(x,y)$ function in the longitudinal as well as transverse direction. They presented solutions for a rectangular plate with one symmetric longitudinal stiffener at the centre. Bilstein[79,80] recently presented solutions for elastic non-linear buckling of plates stiffened eccentrically in the longitudinal direction. He considers the stiffened plate as discrete plate panels and beams and satisfies compatibility at their junction. For lateral displacement in the longitudinal direction he assumes a sinusoidal function and derives ordinary differential equations for the transverse direction from the two partial differential equations of non-linear buckling theory. A modified reduction method in connection with the numerical integration of the ordinary differential equations is used for the solution. He presents solutions for isotropic plates with discrete eccentric stiffeners both having initial imperfection. The differential equations are derived from a variational principle for finite elastic deformations. Variation of the Airy stress function and of the deformations yields the

compatibility equations and equilibrium equations in the out-of-plane direction.

Weiss and Zaenkert[81] presented solutions for rectangular plates with one eccentric longitudinal or transverse stiffener under uniaxial compression. They transformed the two non-linear partial differential equations in terms of lateral displacement (w) and stress function (F) by means of the Hermitian method into a system of non-linear finite difference equations and solved them by means of a step-by-step iteration method. The effect of stiffeners is taken into account for introducing the continuity conditions for stiffener and plate. The edges of plates are assumed to be simply supported and free of shear stresses and to remain straight after buckling. The calculations are carried out for flat plates as well as for plates with sinusoidal initial deflections between the plates' edges and the stiffeners.

1.2.3 Material Non-linearity

Elasto-plastic analysis of plates has been investigated by two different approaches, the "Area Approach" and the "Volume Approach". The first approach is based on an area integration using the Ilyushin[89] yield criterion which assumes a sudden plastification through the plate depth. The second approach, in which the plate is assumed to be multi-layered, involves a volume integral and is based on the Von Mises[83] yield criterion. In both methods the relation between stress and strain increments in the plastic stage is determined by the Prandtl[91]-Reuss flow rule.

Unstiffened Plates: Bhaumik and Hanley[82] using finite differences presented a lower bound elasto-plastic solution to the ultimate load carrying behaviour of a square sandwich plate under uniformly

distributed lateral load. Results are presented for three different yield criteria, von Mises'[83], Tresca[84] and Johansen[85], each one being applied as a plane stress yield criterion to the thin outer layers of the sandwich plate.

An entirely different method is used by Lin and Ho[86] to determine stress and deflections of rectangular plates beyond the elastic range. An analogy method is used which links the plastic strain to an equivalent lateral load. By using influence coefficients the inelastic response of an aluminum plate is calculated which includes in the solution the Von Mises yield criterion and its associated flow rule.

Elasto-plastic solutions assuming sudden plastification of the whole section have been presented by Yam and Das[87] using finite differences, Bleytschko and Velebit[90] using a complementary energy formulation, and Ang and Lopez[88] using a discrete model approach in which the plate consists symbolically of a system of flexible nodes, rigid bars and torsional elements. Finite element solutions allowing for the progressive growth of plasticity through the depth of the plate and simplified solutions based on sudden plastification of the whole section are presented in Refs. (92-95).

Stiffened Plates: One of the main disadvantages of the "orthotropic plate approach" is that its use is restricted to elastic cases only, because the location and shape of stiffeners are ignored in the analysis. Finite element solutions for buckling of eccentrically stiffened plates are presented by Terazawa et al.[96]. Tvergaard and Needleman[1] investigated the plastic buckling due to axial compression for an elastic-plastic wide panel with eccentric stiffeners. Mode interaction and imperfection sensitivity were investigated numerically by application of an incremental method. The bifurcation behaviour for a perfect panel compressed into

the plastic range is determined analytically. Wegmuller and Kostem[97] presented finite element solutions for elasto-plastic material behaviour with linear hardening. They investigated plates reinforced in one direction and subject to lateral load. To the author's knowledge solutions based on finite differences or dynamic relaxation techniques are not reported.

1.2.4 Combined Geometric and Material Non-Linearities

Unstiffened Plates: Solutions including both geometric and material non-linearities have been obtained recently by different methods. Moxham[101] used a Ritz energy method for the analysis of isotropic plates under compression. He used eight Fourier coefficients to present the plate displacements u, v and w. For calculating the potential energy, the quarter plate was divided into 405 volume units (9x9x5). The energy was minimized using an iterative minimization procedure due to Powell[102]. The plasticity was included by means of a combination of flow and deformation theories. Lin[135] extended his earlier work[86] to include the large-deflection effect. Crisfield[17,103-106] developed tangential elasto-plastic matrices for "area" and "volume" approaches based on Ilyushin and Von Mises yield criteria respectively. Using these approaches in his finite element program, he presented solutions for unstiffened plates subject to different types of loadings and having different membrane boundary conditions. He showed that the Ilyushin criterion is in general satisfactory. However it tends to overstimate the strength of plates in direct compression, and he proposed a modification to the Ilyushin surface to allow for the intermediate loss of stiffness, which improves the accuracy in the computation of collapse loads of plates in compression. Yam[108-110], using finite differences, presented solutions based on an "area" approach. For each node he used two non-linear partial

differential equations in terms of out-of-plane displacement w and in-plane strains ε_x, ε_y and γ_{xy}. Frieze[111] and Frieze, Dowling and Hobbs [112] using dynamic relaxation and adopting the "area approach" presented solutions for isotropic plates under in-plane loads. Harding[113] and Harding et al[114,143] also used dynamic relaxation but adopted the "volume approach" and presented solutions for plates subject to different in-plane load conditions (compression, compression and shear, shear and bending). In his program the tangential elasto-plastic matrix is computed at each load increment and remains constant for the following iterations. The effect of initial out-of-plane displacements and residual stresses has been considered by many investigators[17,101,111-114,143]. A detailed parametric study on the effect of residual stresses on the ultimate load of plates is presented in Refs. (111-114,143). Further research on the combined geometric and material non-linear behaviour of plates using the finite element method are reported in Refs. (18-20, 115-120).

Stiffened Plates: Considering the combined geometric and material non-linearity in the analysis of stiffened plates results in a set of complex non-linear equations which have to be solved by approximate numerical techniques. Due to lack of reliable numerical methods to solve the set of complex non-linear equations, a complete study of load carrying behaviour of stiffened plates up to collapse and beyond it has been limited. Some investigators have considered stiffened plates as grillages of discrete beam elements, the plates being represented by equivalent effective flanges acting with the stiffeners according to beam theory. The elements are normally taken as the segments of beams between grillage intersections. Additional subdivisions may be necessary if discontinuities in the internal properties, loading or initial deformation occur between intersections. This method has been used widely

for elastic analysis of stiffened plates[121-123]. Recently it has been used also for elasto-plastic analysis of stiffened plates[124]. A special "beam-column grillage approach" for stiffened plates has been presented by Moolani[125]. In this method the average stress-strain curve for the plate panel between the stiffeners is first generated using a large-deflection elasto-plastic program for isotropic plates and considering approximate loading and edge conditions. Knowing the moment-curvature-thrust relationships of the cross-section, the equilibrium shape of the beam-column for the required load and boundary conditions can be obtained using an iterative numerical procedure. The effect of initial geometric imperfection and residual stresses has been considered. Kagan and Kubo[99] reported a solution technique based on orthotropic plate theory, which is of little practical use. They used the Vogel's[69,76] coupled partial differential equations of orthotropic plates and extended these to include the effect of yielding. By distributing a portion of membrane forces to the stiffeners and assuming that no unloading occurs, and that first yield occurs in the ribs and the plate remains elastic, they presented a solution for a laterally loaded ideal elastic-perfectly plastic stiffened plate. The distribution of residual stresses in welded plates and their effect on the ultimate strength has been discussed by Dwight, Chin and Ractliffe[6,9], Ractliffe[126] and by Nishino, Ueda and Tall[8]. Further theoretical and experimental work has been reported in Refs. 7, 10,39-41,128-133, and 145-146.

Systematic finite difference solutions for combined geometric and material non-linearity considering the whole stiffened plate and its different collapse modes is not known. To the author's knowledge this present work seems to be the first in this area. Elasto-plastic large-deflection analysis of stiffened plates using the finite element method has been only

recently reported by Soreide, Bergan and Moan[18-20]. The plasticity is considered by dividing plate as well as stiffeners in layers. Crisfield[17] presented solutions for stiffened plates under shear load in which he assumed an elastic behaviour for stiffeners. Later an approximate solution for stiffened plates was reported[117]. In his recent works[107,147] he investigated the behaviour of stiffened load-bearing diaf-ragms in which a modified Ilyushin criterion for the plasticity of stiff-eners is adopted. Moeller[134] presented a finite element solution for longitudinally stiffened plates under lateral load. Special assumptions are made so that its application is restricted.

1.3 SCOPE AND AIM OF THESIS

Considerable attention has been given recently to the collapse behaviour of plated steel components, following the extensive research on its elastic behaviour. It is clear from the foregoing review that there is a lack of systematic solution techniques to study theoretically the real behaviour of stiffened plates considering geometric or material non-linearity and especially their combination. Concurrently with the development of the present method some alternative solutions have been reported. The present method with the special technique employed for the solution of the system of simultaneous non-linear equations can be used, (and indeed shows an improvement compared with the available meth-ods) for the analysis of isotropic plates, especially in the plastic range. However the main aim of the thesis is to develop a systematic solution technique to predict the behaviour of discretely stiffened plates subject to lateral and/or in-plane loading up to and beyond their ultimate load carrying capacity. The method developed for the analysis of stiffened plates should be able to consider different possible modes

of buckling which may occur and their interaction and to take accurate account of fabrication tolerances. A further aim of this thesis is to present results for a range of different problems so as to prove the validity and to demonstrate the scope of the present method. A general computer program has been developed and a systematic study of different aspects of plated structures can follow.

1.4 GENERAL OUTLINE OF PRESENTED METHOD

The analysis of stiffened plates is in fact a three dimensional problem, but practically useful solutions can be obtained by idealising the plate as a two dimensional continuum acting integrally with a one dimensional beam. The discretely stiffened plate can be analysed by considering it as an isotropic plate subjected to interactive line loads at the location of stiffeners. The nature and the magnitude of the line loadings can be determined by considering the equilibrium and compatibility conditions of plate-stiffener intersection. Considering the equilibrium of beam elements, the interactive loads can be expressed in terms of geometric and material properties of the stiffeners and the three mid-plane displacements (u, v and w) of the plate. Considering the equilibrium of plate elements with the interactive line loads as body forces the three governing non-linear partial differential equations may be obtained in terms of forces. These are different for each of the basic node types. For nodes lying on the plate itself these are the same as the usual equilibrium equations for isotropic plates. Considering the linear terms of the equilibrium equations only and using strain-displacement relationships and considering equilibrium and continuity of deformations at the plate and stiffener junctions, three simultaneous linear partial differential

equations in terms of displacements are obtained for different types of nodes. These,with the equilibrium equations in terms of forces, and expressions to evaluate internal forces, are replaced by their finite difference equivalents. The non-linear equations are solved by an iterative method which uses the linearised equations in terms of displacements from which the matrix of coefficients is generated and its inverse is computed only once. The iteration procedure starts with an arbitrary assumed set of displacements. (In practice for the first load increment, the small-deflection solution will be used as an initial guess.). For every set of displacements the internal forces and moments are evaluated and equilibrium checked by substituing these forces and moments in the non-linear equilibrium equations. When no equilibrium exists the residual forces are used to obtain correction displacements using the linearised equilibrium equations. These are added to the assumed displacements to obtain new displacements. Then the same procedure is repeated till either residual forces or correction displacements are sufficiently small. This linearly convergent method is a modified Newton-Raphson method. To accelerate the convergence, Aitken's δ^2-method has been applied in which two subsequent displacement corrections are used to obtain a better correction. For the elasto-plastic analysis, ideal elastic-perfectly plastic behaviour is assumed (with no strain hardening). The Ilyushin yield criterion with the Prantl-Reuss flow rule is employed which assumes a sudden plastification of the plate throughout the depth. Stiffeners have been divided into volume units by horizontal and vertical sections, and for the plasticity the effect of normal stress (axial force, vertical and horizontal bending moments) has been considered only. Due to the incremental relation between stresses and strains in the plastic range, the equilibrium equations and expressions to calculate forces in the plate and stiffeners are written in their incremental form.

CHAPTER 2

MATHEMATICAL FORMULATION

2.0 ASSUMPTIONS

The formulation is based on the usual assumptions of thin plate and beam theory:

1 Stresses normal to the midplane of the plate and the stiffener axis are ignored and the transverse shear deformation is neglected in both the plate and the stiffener, so that the hypothesis of preservation of straight normals during deformation is retained.

2 The stiffeners are of solid rectangular cross-section and undergo negligible warping deformations under torsion.

3 The Lagrangian fixed co-ordinate system is used, thus implying small gradients.

4 Stress-strain curves are reversible.

5 Material has ideal elastic-perfectly plastic behaviour (with no strain hardening).

6 The Ilyushin yield criterion and the Prantl-Reuss flow rule are employed.

7 The effect of shear stress on the stiffener plasticity is neglected.

2.1 LARGE-DEFLECTION THEORY OF ECCENTRICALLY STIFFENED ISOTROPIC PLATE.

2.1.1 Derivation of Governing Equations

2.1.1.1 *Displacement Compatability at the Stiffener-Plate Interface*

Let x, y and z be a set of rectangular cartesian co-ordinates with the z-axis pointing downwards and x- and y-axes in the midplane of the plate, and let the net components of displacements in the midplane of the plate along x, y and z directions be denoted by u, v and w respectively. The net components of displacements at the centre of stiffeners will be shown as u_c, v_c and w_c. Forces, moments and displacements in longitudinal stiffeners (x-direction stiffeners) are represented by index 1 and those in transverse stiffeners (y-direction stiffeners) have the index 2. Indices A, H, V and T have been used for axial, horizontal, vertical and torsional forces and moments respectively for both longitudinal and transverse stiffeners.

Interaction between plate and stiffeners can be achieved by enforcing equilibrium of forces and moments and continuity of deformations at the plate and stiffener junctions. Because of the flat deflection curve we can assume that the distance from the stiffener centresto the mid-plane of the plate is very small with respect to the radii of curvature so that the curvature of the stiffeners can be set equal to that of the plate. Now we can write the following relationships between midplane displacements of the plate and displacements at the centre of the stiffeners (Fig. 1).

For longitudinal stiffeners:

$$\left.\begin{aligned} u_{c1} &= u - e_1 \frac{\partial w}{\partial x} \\ v_{c1} &= v - e_1 \frac{\partial w}{\partial y} \\ w_{c1} &= w \end{aligned}\right\} \qquad (1)$$

Similarly for transverse stiffeners:

$$\left.\begin{aligned} u_{c2} &= u - e_2 \frac{\partial w}{\partial x} \\ v_{c2} &= v - e_2 \frac{\partial w}{\partial y} \\ w_{c2} &= w \end{aligned}\right\} \qquad (2)$$

Defining initial imperfection by index 0 and total displacements by $\bar{}$, and considering that the plate will have only lateral imperfections ($u_0 = 0$, $v_0 = 0$ and $w_0 = 0$), we can write the following relationships. For longitudinal stiffeners:

$$\left.\begin{aligned} u_{c10} &= - e_1 \frac{\partial w_0}{\partial x} \\ v_{c10} &= - e_1 \frac{\partial w_0}{\partial y} \\ w_{c10} &= w_0 \end{aligned}\right\} \qquad (3)$$

and:

$$\left.\begin{aligned} \bar{u}_{c1} &= u - e_1 \frac{\partial \bar{w}}{\partial x} \\ \bar{v}_{c1} &= v - e_1 \frac{\partial \bar{w}}{\partial y} \\ \bar{w}_{c1} &= \bar{w} \end{aligned}\right\} \qquad (4)$$

The corresponding relations for the transverse stiffeners are obtained by writing 2 in place of the subscript 1 in the above equations.

2.1.1.2 *Derivation of Equilibrium Equations in Terms of Forces*

The governing partial differential equations in terms of forces can be obtained by considering the equilibrium of an element of stiffened plate (Fig. 2). First we consider a plate element having only one rectangular bar stiffener in the x-direction. The sectional actions on an element cut by two pairs of planes parallel to x-z and y-z planes are shown in Figs. 3 and 5. For clarity moments and forces for both beam element and plate element are shown separately. Figures 3a and 3b show moments and forces respectively for beam element and Figs. 5a and 5b show the same for plate element. Figures 4a, 4b and 4c show sectional actions in a deformed element of beam. F_{xl}, F_{yl} and F_{zl} are the interaction forces and T_l is the interaction moment per unit length of stiffener assumed acting at the level of the midplane of the plate, F_{xl} and F_{yl} acting in the plane of the bent plate in x-z and y-z plane respectively. The intensities of these forces and moment per unit area, required while considering the equilibrium of the plate element, are $F_{xl}/\Delta y$, $F_{yl}/\Delta y$, $F_{zl}/\Delta y$ and $T_l/\Delta y$, where Δy is a finite distance perpendicular to the stiffener over which the forces and moment are assumed to be distributed. As will be seen later Δy is the length of finite difference mesh in the y-direction. Flexural and membrane actions in the beam are forces and moments, while those of the plate are forces and moments per unit width of plate. To derive the governing equilibrium equations we consider first the equilibrium of a beam element (Figs. 3a and 3b).

(a) Beam element:

Taking moment about x, y and z-axes with origin in the midplane of plate, and considering equilibrium of forces in x, y and z-directions, we obtain the following 6 equations.

Taking moments about x-axis:

$$\frac{\partial M_{T1}}{\partial x} dx + \frac{\partial N_{H1}}{\partial x} dx\, e_1 - T_1\, dx = 0$$

which gives:

$$T_1 = \frac{\partial M_{T1}}{\partial x} + \frac{\partial N_{H1}}{\partial x} e_1 \tag{5}$$

Taking moments about y-axis similarly gives:

$$\frac{\partial M_{V1}}{\partial x} - N_{V1} + \frac{\partial N_{A1}}{\partial x} e_1 = 0 \tag{6}$$

and about z-axis:

$$\frac{\partial M_{H1}}{\partial x} - N_{H1} = 0 \tag{7}$$

Equilibrium of forces in x-direction:

$$\frac{\partial N_{A1}}{\partial x} dx - F_{x1}\, dx = 0$$

which gives:

$$F_{x1} = \frac{\partial N_{A1}}{\partial x} \tag{8}$$

For equilibrium of forces in y-direction considering the component of N_{A1} in y-direction we can write:

$$\frac{\partial N_{H1}}{\partial x} dx - F_{y1}\, dx + N_{A1} \frac{\partial^2 \bar{v}_{c1}}{\partial x^2} dx + \frac{\partial N_{A1}}{\partial x} \frac{\partial \bar{v}_{c1}}{\partial x} dx = 0$$

Substituing $\frac{\partial N_{H1}}{\partial x}$ from (7) in the above equation we have:

$$F_{y1} = \frac{\partial^2 M_{H1}}{\partial x^2} + N_{A1} \frac{\partial^2 \bar{v}_{c1}}{\partial x^2} + \frac{\partial N_{A1}}{\partial x} \frac{\partial \bar{v}_{c1}}{\partial x} \tag{9}$$

Similarly considering the normal components of N_{A1}, F_{x1}, and F_{y1}, the equilibrium equation for z-direction will be:

$$\frac{\partial N_{V1}}{\partial x} dx + N_{A1} \frac{\partial^2 \bar{w}}{\partial x^2} dx + \left(\frac{\partial N_{A1}}{\partial x} \frac{\partial \bar{w}}{\partial x} - F_{x1} \frac{\partial \bar{w}}{\partial x}\right) dx - F_{y1} \frac{\partial \bar{w}}{\partial y} dx - F_{z1}\, dx = 0$$

From (8) the term in the bracket is zero and substituing $\frac{\partial N_{V1}}{\partial x}$ from (6) in the above equation, we then have:

$$F_{z1} = \frac{\partial^2 M_{V1}}{\partial x^2} + \frac{\partial^2 N_{A1}}{\partial x^2} e_1 + N_{A1} \frac{\partial^2 \bar{w}}{\partial x^2} - F_{y1} \frac{\partial \bar{w}}{\partial y} \tag{10}$$

Substituting $\frac{\partial N_{H1}}{\partial x}$ from (7) in (5) and substituting F_{y1} from (9) in (10) ignoring third order terms and writing equation (8) and (9) again, we will have all interaction forces in terms of internal forces of the stiffeners:

$$F_{x1} = \frac{\partial N_{A1}}{\partial x} \tag{11}$$

$$F_{y1} = \frac{\partial^2 M_{H1}}{\partial x^2} + N_{A1} \frac{\partial^2 \bar{v}_{c1}}{\partial x^2} + \frac{\partial N_{A1}}{\partial x} \frac{\partial \bar{v}_{c1}}{\partial x} \tag{12}$$

$$F_{z1} = \frac{\partial^2 M_{V1}}{\partial x^2} + e_1 \frac{\partial^2 N_{A1}}{\partial x^2} + N_{A1} \frac{\partial^2 \bar{w}}{\partial x^2} - \frac{\partial^2 M_{H1}}{\partial x^2} \frac{\partial \bar{w}}{\partial y} \tag{13}$$

$$T_1 = \frac{\partial M_{T1}}{\partial x} + e_1 \frac{\partial^2 M_{H1}}{\partial x^2} \tag{14}$$

(b) Plate element:

Now consider the equilibrium of the plate element (Figs. 5a and 5b). The body forces acting on the element are $F_{x1}/\Delta y$, $F_{y1}/\Delta y$, $F_{z1}/\Delta y$ and q the applied transverse loading. The line couple T_1 is replaced by two equal and opposite vertical line loads $T_1/(2\Delta y)$ per unit length acting at a distance Δy on either side of the stiffener. These forces are to be (algebraically) added to the given transverse loading when considering equilibrium at these lines.

The equilibrium equations in terms of moments and in-plane forces work out to be identical to those in customary thin plate theory except for the body force terms[100] and are given below:

$$\frac{\partial N_x}{\partial x} + \frac{\partial N_{xy}}{\partial y} + \frac{F_{x1}}{\Delta y} = 0 \tag{15}$$

$$\frac{\partial N_y}{\partial y} + \frac{\partial N_{xy}}{\partial x} + \frac{F_{y1}}{\Delta y} = 0 \tag{16}$$

$$\frac{\partial^2 M_x}{\partial x^2} + 2\frac{\partial^2 M_{xy}}{\partial x \partial y} + \frac{\partial^2 M_y}{\partial y^2} + \left(N_x \frac{\partial^2 \bar{w}}{\partial x^2} + 2 N_{xy} \frac{\partial^2 \bar{w}}{\partial x \partial y} + N_y \frac{\partial^2 \bar{w}}{\partial y^2} \right) + q + \frac{F_{z1}}{\Delta y} = 0 \tag{17}$$

Finally, substituting for F_{x1}, F_{y1} and F_{z1} from equations (11)-(13) in equation (15)-(17), the three equilibrium equations for the plate-stiffener combination at the line of interaction can be obtained in terms of internal forces in the plate and the stiffener.

$$\frac{\partial N_x}{\partial x} + \frac{\partial N_{xy}}{\partial y} + \frac{1}{\Delta y}\frac{\partial N_{A1}}{\partial x} = 0 \tag{18}$$

$$\frac{\partial N_y}{\partial y} + \frac{\partial N_{xy}}{\partial x} + \frac{1}{\Delta y}\left(\frac{\partial^2 M_{H1}}{\partial x^2} + N_{A1}\frac{\partial^2 \bar{v}_{c1}}{\partial x^2} + \frac{\partial N_{A1}}{\partial x}\frac{\partial \bar{v}_{c1}}{\partial x} \right) = 0 \tag{19}$$

$$\frac{\partial^2 M_x}{\partial x^2} + 2\frac{\partial^2 M_{xy}}{\partial x \partial y} + \frac{\partial^2 M_y}{\partial y^2} + \left(N_x \frac{\partial^2 \bar{w}}{\partial x^2} + 2 N_{xy} \frac{\partial^2 \bar{w}}{\partial x \partial y} + N_y \frac{\partial^2 \bar{w}}{\partial y^2} \right) + q + \frac{1}{\Delta y}\left(\frac{\partial^2 M_{V1}}{\partial x^2} + \frac{\partial^2 N_{A1}}{\partial x^2} e_1 + N_{A1}\frac{\partial^2 \bar{w}}{\partial x^2} - \frac{\partial \bar{w}}{\partial y}\frac{\partial^2 M_{H1}}{\partial x^2} \right) = 0 \tag{20}$$

The equilibrium equations of the plate and a y-direction (transverse) stiffener can be found by writing for body forces $F_{x2} / \Delta x$, $F_{y2} / \Delta x$ and $F_{z2} / \Delta x$ in equations (15), (16) and (17) respectively. These body forces themselves are found from equations (11), (12) and (13) by re-

placing displacement v by u, subscript 1 by 2 and interchanging x and y. The equilibrium equations at intersections of longitudinal and transverse stiffeners are obtained by writing for body forces ($F_{x1}/\Delta y + F_{x2}/\Delta x$, $F_{y1}/\Delta y + F_{y2}/\Delta x$ and $F_{z1}/\Delta y + F_{z2}/\Delta x$) in equations (15)-(17), and then expressing the interaction forces in terms of internal forces in plate and stiffeners as in the previous cases. The equilibrium equations at all other points are obviously those for unstiffened plates and are given by equations (15)-(17) with the body forces omitted. All the above mentioned equations are given in Appendix A.

2.1.1.3 *Force-Displacement Equations*

The internal forces in the plate and stiffeners can be related to the plate mid-plane displacements u, v and w in terms of rigidities of the plate and the stiffeners which are defined as follows:

$$\left.\begin{aligned} E' &= \frac{E\ t}{1-\nu^2} \\ E_1' &= \nu\ E' \\ E_{xy}' &= G\ t = \frac{E\ t}{2(1+\nu)} \end{aligned}\right\} \qquad (21)$$

and

$$D = \frac{E\ t^3}{12(1-\nu^2)} \qquad (22)$$

For stiffeners in x-direction:

$$\left.\begin{aligned} C_{s1} &= E\ A_{s1} = E\ t_{s1}\ h_{s1} \\ B_{V1} &= \frac{E\ t_{s1}\ h_{s1}^3}{12} \\ B_{H1} &= \frac{E\ h_{s1}\ t_{s1}^3}{12} \end{aligned}\right\} \qquad (23)$$

$$B_{T1} = K_1 \, G \, h_{s1} \, t_{s1}^3$$

where K_1 is the torsional rigidity factor and depends on the h_{s1} / t_{s1} ratio. The rigidities of stiffeners in the y-direction are C_{s2}, B_{V2}, B_{H2} and B_{T2} and are obtained by replacing 1 by 2 in equation (23). The force-displacement equations for the plate are now given by:

$$\left.\begin{aligned} N_x &= E' \varepsilon_x + E'_1 \varepsilon_y \\ N_y &= E' \varepsilon_y + E'_1 \varepsilon_x \\ N_{xy} &= E'_{xy} \gamma_{xy} \end{aligned}\right\} \qquad (24)$$

$$\left.\begin{aligned} M_x &= - D \left(\frac{\partial^2 w}{\partial x^2} + \nu \frac{\partial^2 w}{\partial y^2} \right) \\ M_y &= - D \left(\frac{\partial^2 w}{\partial y^2} + \nu \frac{\partial^2 w}{\partial x^2} \right) \\ M_{xy} &= - M_{yx} = - D \, (1-\nu) \frac{\partial^2 w}{\partial x \partial y} \end{aligned}\right\} \qquad (25)$$

with

$$\left.\begin{aligned} \varepsilon_x &= \frac{\partial u}{\partial x} + \frac{1}{2} \left(\frac{\partial w}{\partial x} \right)^2 + \left(\frac{\partial w}{\partial x} \frac{\partial w_0}{\partial x} \right) \\ \varepsilon_y &= \frac{\partial v}{\partial y} + \frac{1}{2} \left(\frac{\partial w}{\partial y} \right)^2 + \left(\frac{\partial w}{\partial y} \frac{\partial w_0}{\partial y} \right) \\ \gamma_{xy} &= \frac{\partial u}{\partial y} + \frac{\partial v}{\partial x} + \frac{\partial w}{\partial x} \frac{\partial w}{\partial y} + \frac{\partial w}{\partial x} \frac{\partial w_0}{\partial y} + \frac{\partial w}{\partial y} \frac{\partial w_0}{\partial x} \end{aligned}\right\} \qquad (26)$$

Similarly the following force-displacement relationships can be written for the stiffeners in the x-direction.

$$N_{A1} = C_{s1} \left[\frac{\partial u_{c1}}{\partial x} + \frac{1}{2} \left(\frac{\partial w}{\partial x} \right)^2 + \frac{\partial w}{\partial x} \frac{\partial w_0}{\partial x} + \frac{1}{2} \left(\frac{\partial v_{c1}}{\partial x} \right)^2 + \frac{\partial v_{c1}}{\partial x} \frac{\partial v_{c10}}{\partial x} \right]$$

$$N_{A1} = C_{s1}\{[\frac{\partial u}{\partial x} + \frac{1}{2}(\frac{\partial w}{\partial x})^2 + \frac{\partial w}{\partial x}\frac{\partial w_0}{\partial x} - e_1\frac{\partial^2 w}{\partial x^2}] + \frac{1}{2}(\frac{\partial v}{\partial x} - e_1\frac{\partial^2 w}{\partial x\partial y})^2$$

$$+ (\frac{\partial v}{\partial x} - e_1\frac{\partial^2 w}{\partial x\partial y})(-e_1\frac{\partial^2 w_0}{\partial x\partial y})\}$$

$$= C_{s1}\{[\frac{\partial u}{\partial x} + \frac{1}{2}(\frac{\partial w}{\partial x})^2 + \frac{\partial w}{\partial x}\frac{\partial w_0}{\partial x} - e_1\frac{\partial^2 w}{\partial x^2}] + (\frac{\partial v}{\partial x} - e_1\frac{\partial^2 w}{\partial x\partial y})$$

$$(\frac{1}{2}\frac{\partial v}{\partial x} - \frac{e_1}{2}\frac{\partial^2 w}{\partial x\partial y} - e_1\frac{\partial^2 w_0}{\partial x\partial y})\} \qquad (27)$$

$$M_{V1} = -B_{V1}\frac{\partial^2 w_{c1}}{\partial x^2} = -B_{V1}\frac{\partial^2 w}{\partial x^2} \qquad (28)$$

$$M_{T1} = -B_{T1}\frac{\partial^2 w_{c1}}{\partial x\partial y} = -B_{T1}\frac{\partial^2 w}{\partial x\partial y} \qquad (29)$$

$$M_{H1} = -B_{H1}\frac{\partial^2 v_{c1}}{\partial x^2} = -B_{H1}(\frac{\partial^2 v}{\partial x^2} - e_1\frac{\partial^3 w}{\partial x^2\partial y}) \qquad (30)$$

$$N_{H1} = \frac{\partial M_{H1}}{\partial x} = -B_{H1}\frac{\partial^3 v_{c1}}{\partial x^3} = -B_{H1}(\frac{\partial^3 v}{\partial x^3} - e_1\frac{\partial^4 w}{\partial x^3\partial y}) \qquad (31)$$

The force-displacement equations for stiffeners in the y-direction are obtained by interchanging (x and y) and (u and v) and replacing subscript 1 by 2 in equation (27)-(31).

2.1.1.4 *Presentation of Equilibrium Equations in Terms of Displacements*

For the solution method employed in this work, as mentioned in 1.4, it is not necessary to obtain explicitly the non-linear equilibrium equations in terms of displacements. However the linear parts of these equations are needed to provide, through finite difference approximations, the matrix of coefficients which will be used for finding corrections to trial displacements in the iteration process.

Now we consider again points on stiffeners in the x-direction. Using equations (24)-(31) and considering the linear terms only, equations (18)-(20) can be written in terms of displacements as follows:

$$E' \frac{\partial^2 u}{\partial x^2} + (E'_1 + E'_{xy}) \frac{\partial^2 v}{\partial x \partial y} + E'_{xy} \frac{\partial^2 u}{\partial y^2} + \frac{C_{s1}}{\Delta y} \frac{\partial^2 u_{c1}}{\partial x^2} = 0 \qquad (32)$$

$$E' \frac{\partial^2 v}{\partial y^2} + (E'_1 + E'_{xy}) \frac{\partial^2 u}{\partial x \partial y} + E'_{xy} \frac{\partial^2 v}{\partial x^2} - \frac{B_{H1}}{\Delta y} \frac{\partial^4 v_{c1}}{\partial x^4} = 0 \qquad (33)$$

$$(D + \frac{B_{V1}}{\Delta y}) \frac{\partial^4 w}{\partial x^4} + D \frac{\partial^4 w}{\partial y^4} + 2 D \frac{\partial^4 w}{\partial x^2 \partial y^2} - \frac{C_{s1}\, e_1}{\Delta y} \frac{\partial^3 u_{c1}}{\partial x^3} = q \qquad (34)$$

In equation (32) the term $\frac{C_{s1}}{\Delta y} \frac{\partial^2 u_{c1}}{\partial x^2}$ represents the contribution of the stiffener to the in-plane displacement in the stiffener direction, and the term $\frac{B_{H1}}{\Delta y} \frac{\partial^4 v_{c1}}{\partial x^4}$ in equation (33) denotes the in-plane bending of the stiffener. The terms $\frac{B_{V1}}{\Delta y} \frac{\partial^4 w}{\partial x^4}$ and $\frac{C_{s1}\, e_1}{\Delta y} \frac{\partial^3 u_{c1}}{\partial x^3}$ in equation (34) show the effect of stiffener flexural and extensional rigidities on plate bending.

Equations (32)-(34) can be written also in terms of displacements of the mid-plane of the plate:

$$(E' + \frac{C_{s1}}{\Delta y}) \frac{\partial^2 u}{\partial x^2} + (E'_1 + E'_{xy}) \frac{\partial^2 v}{\partial x \partial y} + E'_{xy} \frac{\partial^2 u}{\partial y^2} - \frac{C_{s1}\, e_1}{\Delta y} \frac{\partial^3 w}{\partial x^3} = 0 \qquad (35)$$

$$E' \frac{\partial^2 v}{\partial y^2} + (E'_1 + E'_{xy}) \frac{\partial^2 u}{\partial x \partial y} + E'_{xy} \frac{\partial^2 v}{\partial x^2} - \frac{B_{H1}}{\Delta y} (\frac{\partial^4 v}{\partial x^4} - e_1 \frac{\partial^5 w}{\partial x^4 \partial y}) = 0 \qquad (36)$$

$$(D + \frac{B_{V1}}{\Delta y} + \frac{C_{s1}\, e_1^2}{\Delta y}) \frac{\partial^4 w}{\partial x^4} + D \frac{\partial^4 w}{\partial y^4} + 2D \frac{\partial^4 w}{\partial x^2 \partial y^2} - \frac{C_{s1}\, e_1}{\Delta y} \frac{\partial^3 u}{\partial x^3} = q \qquad (37)$$

Note that the last term in each equation represents coupling between bending and membrane action and each has been entirely missed by the orthotropic plate theory.

Similar equations can be written for other node types and are given in Appendix B.

2.1.2 Boundary Conditions

The deflected shape and the distribution of membrane forces in the plate is greatly influenced by the boundary conditions. At the boundaries the deformation in the plate and the stiffener must be the same at the junction. This means that the slope in both components is the same in magnitude and sign. The edges of the plate are assumed not to have any stiffeners and to be rigidly supported. At the boundaries it is assumed that only the plate is supported and stiffeners are free. In general four boundary conditions are required on each boundary for the complete solution of plate behaviour. Two conditions are associated with the bending equations and two with plane stress equations. The boundary conditions in mathematical form are now presented for edges parallel to the y-axis.

(a) Flexural Boundary Conditions:

The two flexural conditions are associated with lateral displacement (sinking) and rotation of the edges.

(i) Simply supported edge:

(1) The edge is rigidly supported so that the first condition is:

$$w = 0 \qquad (38)$$

(2) The edge has complete rotational freedom, so that plate and stiffener can rotate freely in the vertical plane. Under such a condition the curvature normal to the edge at the end of the plate and the stiffener would be zero (curvature along

the edge is zero because of w = 0), so we have:

$$\frac{\partial^2 w}{\partial x^2} = 0 \qquad (39)$$

(This condition implies that both M_x and M_{V1} are zero, that is, the bending moment at the edge of the plate and the end of the x-direction stiffener in the vertical plane are both zero.)

(ii) Built-in edge:

(1) The edge is rigidly supported

$$w = 0 \qquad (40)$$

(2) The end rotation is zero, that is:

$$\frac{\partial w}{\partial x} = 0 \qquad (41)$$

(Note that here both the plate and the stiffener are built-in and the stiffener has moment at the end. Specification of zero moment at the end of the stiffener (M_{V1}=0) will automatically mean zero curvature, hence zero moment in the plate at stiffener locations. This is not permissible.)

(iii) Symmetric edge:

For edges the case of symmetry has been also considered so that for symmetric and double symmetric plates only a half or a quarter of the plate needs to be considered respectively.

(1) For lateral displacement (depending on the type of the node) one of equations (37), (B-3), (B-6),and (B-9) can be used.

(2) The rotation in nodes on the line of symmetry is zero:

$$\frac{\partial w}{\partial x} = 0 \qquad (42)$$

(b) Membrane Boundary Conditions:

At each edge each of the in-plane displacements (u and v) can be free or given:

u = free u = constant

v = free v = constant

Restrained edges are special cases of given displacements, where constant=0.

(I) Free extensional displacement, u=free (K_x=0)

In this case at stiffener locations the resultant normal force in plate-stiffener combination should be zero, since in general N_x and N_{Al} cannot both be zero, thus we have:

$$\left(N_x + \frac{N_{Al}}{\Delta y} \right) = 0 \qquad (43)$$

Elsewhere:

$$N_x = 0 \qquad (44)$$

(II) Free tangential displacement, v=free (S_x=0)

At all points

$$N_{xy} = 0 \qquad (45)$$

(III) A given extensional displacement, u=constant

At all points:

$$u = \text{constant} \qquad (46)$$

(Note that specification of the additional condition of N_{Al}= 0 is not permissible here, since it amounts to the specification of N_x as well. For example for simply supported edges with v = 0, the condition N_{Al} = 0 leads to N_x = 0)

(IV) A given tangential displacement, v=constant.

At all points:

$$v = \text{constant} \qquad (47)$$

(V) An additional boundary condition used in some cases is that the edge is constrained to remain straight such that there is no resultant transverse edge load. In this case for the edge x=0 (i=0 mesh line, Fig. 7) for one edge node we have:

$$\sum_{j=1}^{J-1} \left(N_x + \frac{N_{A1}}{\Delta y} \right)_{0,j} = 0 \qquad (48)$$

and for other nodes:

$$\frac{\partial^2 u}{\partial y^2} = 0 \qquad (49)$$

The cases of given edge displacements are used for edges subject to in-plane loading in the form of displacements.

The boundary conditions obtained so far are based on the recognition of four independent displacements (u, v, w and $\partial w/\partial x$ or $\partial w/\partial y$) at the plate edges, as is appropriate in the customary thin plate theory. There is however another edge displacement corresponding to the rotation of the stiffeners in the horizontal plane and is given by $\partial v_{cl} / \partial x$ for a x-direction stiffener. Due to continuity of displacements at the plate and stiffener junctions this value depends on displacements of fictitious nodes and therefore it is prescribed by the above four displacements, since

$$\frac{\partial v_{cl}}{\partial x} = \frac{\partial v}{\partial x} - e_1 \frac{\partial^2 w}{\partial x \partial y}$$

2.2 ELASTO-PLASTIC LARGE-DEFLECTION ANALYSIS OF ECCENTRICALLY STIFFENED ISOTROPIC PLATES

2.2.1 Introduction

For the ultimate strength analysis of structures the non-linear behaviour of the material should be taken into account. For this purpose,

first the stress-strain relationships which describe adequately the plastic deformation of the metal should be defined, and by making some idealizations the material behaviour should be described by a mathematical model (plasticity theory). Secondly these effects are to be incorporated in the numerical analysis of the structure.

The "deformation" and the "flow" theories are the two major plasticity theories[139]. The deformation theory assumes a unique relation between total stresses and total strains. But the stress-strain relationship for a real elasto-plastic material is not only a function of the present loading, and the load history of the structure should be also considered. In the "flow theory" the load history is considered in the way that the plastic deformations are "memorized" by integrating an equivalent plastic strain increment over the load history and gives an incremental relationship between stresses and strains. The flow theory consists of two parts, yield criterion and flow rule.

The "yield criterion" assumes that there exists a loading function (yield surface) in stress space which governs the transition between the elastic and plastic states. Many different yield criteria have been suggested, but most experimental work on steel structures favours the Von Mises yield criterion[83].

The other part of the "flow theory" is the "flow rule" which gives the incremental stress-strain relationship.

The Von Mises yield criterion and its associated Prantl-Reuss flow rule can be used for the so called "volume approach" where the plate is divided in some layers in its depth. Due to the large computer time and storage needed for this approach, and because the main aim of the present work is to verify the presented method for the analysis of stiffened plates a single layer approach using an approximate yield criterion

formulated by Ilyushin has been employed. Based on the deformation theory (which ignores the load history), Ilyushin developed a yield criterion for thin shells. He assumed a sudden full-depth plastification of the section, which is determined on the basis of stress resultants rather than stresses. This approach has been recently used by Frieze[111] (dynamic relaxation) and Crisfield[17] (finite element method) for the elasto-plastic analysis of isotropic plates. Although the Ilyushin criterion is based on the deformation theory, Mikeladze[137] and Robinson[136] who investigated its suitability, concluded that it should be still applicable even when a flow rule is employed. Crisfield[17] assumed that the expressions for the generalized stresses in the Ilyushin yield function can be treated as a plastic potential such that the generalized plastic strain rates are proportional to the partial derivatives of the potential so the Prantl-Reuss flow rule which was originally intended for stresses was used for stress resultants. This resulted in a single-layer formulation (area Approach) which he used in his recent work and he also made some modifications to the Ilyushin yield criterion for cases which are "in-plane dominant".

In the present work for the plate itself the "area approach" derived by Crisfield is employed which gives the following incremental stress-strain relationships:

$$\{\Delta N\} = [C^*]\ \{\Delta\varepsilon_t\} + [cd]\ \{\Delta\chi_t\}$$
$$\{\Delta M\} = [cd]^T\ \{\Delta\varepsilon_t\} + [D^*]\ \{\Delta\chi_t\} \qquad (50)$$

The tangential elasto-plastic modular matrices $[C^*]$, $[D^*]$ and $[cd]$ are each functions of the six current stress resultants $\{N\}$ and $\{M\}$. The Ilyushin yield criterion and the derivation of the above incremental stress-strain relationships are given in detail in Appendix C.

For the stiffeners, it is assumed that they are slender and the

shear forces as well as the twisting moment do not significantly affect the yielding. They are divided horizontally and vertically in Layers.

2.2.2 . Presentation of Governing Equations in Incremental Form

Due to the incremental nature of the stress-strain relationship in the post-elastic range the equilibrium equations in terms of forces and the force-displacement equations are modified to represent the incremental behaviour and are given in Appendix D. To get a better convergence for elastic instability problems it is also desirable to employ the incremental approach.

2.2.3 Boundary Conditions

The boundary conditions for the generation of the matrix of coefficients for elasto-plastic problems are basically the same as those for the elastic problems discussed under 2.1.2. Necessary changes and modifications are considered in the checking program where equilibrium is checked and out-of-balance forces are calculated.

For a non-deflecting simply supported edge along the y-axis, in the elastic range the condition $M_x=0$ was reduced to zero curvature transverse to the edge:

$$\chi_x = - \frac{\partial^2 w}{\partial x^2} = 0$$

But in the plastic range this condition becomes:

$$\Delta\chi_x = -(cd_{11}\,\Delta\varepsilon_x + cd_{21}\,\Delta\varepsilon_y + cd_{31}\,\Delta\gamma_{xy} + D^*_{21}\,\Delta\chi_y + D^*_{31}\,\Delta\chi_{xy})/\,D^*_{11} \qquad (51)$$

CHAPTER 3

METHOD OF SOLUTION

3.1 INTRODUCTION

An analytical solution of the simultaneous non-linear differential equations of equilibrium is not generally possible. The method of finite differences has therefore been adopted, being particularly powerful for regular geometries like the rectangle considered here. The plate has been divided into (I+1) divisions in the x-direction and (J+1) divisions in the y-direction. The mesh lengths in the two directions are Δx and Δy respectively (Fig. 7). In the governing equations Δx and Δy have been equated to dx and dy respectively. The mesh is chosen such that plate-stiffener intersections coincide with mesh lines. First-order central difference formulae have been used throughout to approximate the derivatives of the governing equations.

3.2 SMALL-DEFLECTION SOLUTION

The linear small-deflection solution will be discussed first. This solution is useful for problems where the deflections are small and the material remains elastic. In the present work, it is used to obtain the starting approximation for the iterative large-deflection solution at the first load level and, what is more important, the evaluation of the displacement corrections vector in each iteration involves a small-deflection solution.

There are $(I_X J)$ internal mesh points in the plate and at each node there are three unknown displacements u, v and w. For each internal node three equilibrium equations (B-4)-(B-6) or their special cases depending on the node type can be written as difference equations with u,

v and w as unknowns. The equilibrium equations in finite difference form, when applied at nodes near an edge, generally involve displacements on or outside the edge, the latter being termed fictitious displacements. Hence the total number of equations for internal points (3xIxJ) is less than the total number of unknown displacements involved in the difference equations. In a properly formulated problem the number of these additional unknowns would be exactly matched by the number of available boundary conditions.

In principle the equilibrium equations and the boundary conditions are solved together to yield values for all displacements including the fictitious ones. It is more economical to eliminate the additional displacements by using the boundary conditions, where such elimination is practicable, and to solve the reduced set of equations. (The number of arithmetic operations involved in equation solution varies approximately as the cube of the number of equations in the set). In some cases however this method can be laborious and it is easier to add the boundary conditions to the internal equilibrium equations. To keep the present computer program general the first approach has been employed and the equilibrium equations and boundary conditions are solved together. The use of boundary conditions to complete the matrix of coefficients will now be illustrated with reference to the edge x=0 (i=0 mesh line) (Fig. 7). It is assumed for clarity of illustration, that there is no y-direction stiffener at i=1 or i=2. The relevent equilibrium equations are therefore those which correspond to points either on the plate or on the intersections of plate and x-stiffeners. The latter, equations (32)-(34) are listed here again:

$$E' \frac{\partial^2 u}{\partial x^2} + (E'_1 + E'_{xy}) \frac{\partial^2 v}{\partial x \partial y} + E'_{xy} \frac{\partial^2 u}{\partial y^2} - \frac{C_{s1}}{\Delta y} \frac{\partial^2 u_{c1}}{\partial x^2} = 0 \qquad (52)$$

$$E' \frac{\partial^2 v}{\partial y^2} + (E'_1 + E'_{xy}) \frac{\partial^2 u}{\partial x \partial y} + E'_{xy} \frac{\partial^2 v}{\partial x^2} - \frac{B_{H1}}{\Delta y} \frac{\partial^4 v_{c1}}{\partial x^4} = 0 \qquad (53)$$

$$(D + \frac{B_{V1}}{\Delta y}) \frac{\partial^4 w}{\partial x^4} + D \frac{\partial^4 w}{\partial y^4} + 2 D \frac{\partial^4 w}{\partial x^2 \partial y^2} - \frac{C_{s1} e_1}{\Delta y} \frac{\partial^3 u_{c1}}{\partial x^3} = q \qquad (54)$$

The equations for points on the plate only can be obtained by omitting the terms associated with the stiffeners.

1. Flexural Boundary Conditions

(a) Lateral Displacement:

The edge is rigidly supported so:

$$w_{0,j} = 0 \qquad (\text{for } j = 0 \text{ to } J+1) \qquad (55)$$

(b) Rotational Conditions:

The edge can be either simply supported or built-in.

(i) Simply supported:

The boundary condition for this case is:

$$\frac{\partial^2 w}{\partial x^2} = 0$$

This expression can be written in form of a difference equation as:

$$w_{-1,j} - 2 w_{0,j} + w_{1,j} = 0$$

and since $w_{0,j} = 0$ then

$$w_{-1,j} = - w_{1,j} \qquad (\text{for } j = -1 \text{ to } J+2) \qquad (56)$$

(ii) Built-in:

The boundary condition is:

$$\frac{\partial w}{\partial x} = 0$$

which written in the form of a difference equation gives:

$$w_{-1,j} - w_{1,j} = 0 \qquad \text{or}$$

$$w_{-1,j} = w_{1,j} \qquad (\text{for } j = -1 \text{ to } J + 2) \tag{57}$$

In equation (54) the highest derivative of w in each direction is of the fourth order. This equation relates to the lateral displacement and is used only for internal points (all edges are rigidly supported), so that lateral displacements on lines i=-1, j=-1 and j=J+2 are involved, which are defined by boundary conditions. For the stiffened plate shown in Fig. 7 with I=8 and J=5, the total number of lateral displacements will be (I+4)x(J+4)=108. The number of flexural equilibrium equations for internal points is IxJ=40. The lateral displacements for 2(J+I+2)=30 boundary nodes are defined as zero. Finally the lateral displacements for the 2(J+I+6)=38 fictitious points are defined by other flexural boundary conditions of the type given by equations (56) or (57). So the number of available flexural equations equals the number of unknown lateral displacements.

For symmetric edges, for lateral displacements (depending on the type of node) one of equations (37), (B-3), (B-6) or (B-9) is used. The displacements of nodes behind the line of symmetry are given by symmetry.

2. Membrane Boundary Conditions

At each node,in-plane displacements may be either free or known as a given constant, hence four different types of boundary conditions are possible. As an additional boundary condition for plates subject to in-plane loading the case of a straight unloaded edge has been considered.

I Both in-plane displacements are known.

II In-plane displacement normal to edge is free and the tangential displacement is known.

III In-plane displacement normal to edge is known and the tangential displacement is free.

IV Both in-plane displacements are free.

V The edge is constrained to remain straight such that there is no resultant transverse load.

Now each of the above cases will be discussed in detail with reference to the edge x = 0 (i=0 mesh line).

Membrane Boundary Condition I

Consider the edge to have given (zero or constant) normal and tangential displacements and to be simply supported or built-in flexurally. The in-plane boundary conditions are:

$$u = \text{constant} \tag{58}$$

$$v = \text{constant} \tag{59}$$

Generally for all cases where boundary displacements are given, equilibrium equations (52)-(54) are applied at the interior nodes only. The highest derivatives of in-plane displacements for nodes without stiffeners are of the second order and therefore in-plane displacements of fictitious points are not involved. For nodes lying on stiffeners, the in-plane displacements of fictitious nodes along the stiffeners $(u_{c1})_{-1,j}$ and $(v_{c1})_{-1,j}$ are required and should be defined by using other relationships. To determine $(v_{c1})_{-1,j}$ we consider that

$$N_{H1} = -B_{H1} \frac{\partial^3 v_{c1}}{\partial x^3} \tag{60}$$

we also note that

$$(N_{H1})_{1,j} = \left(\frac{\partial M_{H1}}{\partial x}\right)_{1,j} = \frac{(M_{H1})_{2,j} - (M_{H1})_{0,j}}{2\,\Delta x} = -B_{H1}\left(\frac{\partial^3 v_{c1}}{\partial x^3}\right)_{1,j}$$

or $$(M_{H1})_{0,j} = 2\,\Delta x\, B_{H1} \left(\frac{\partial^3 v_{c1}}{\partial x^3}\right)_{1,j} + (M_{H1})_{2,j}$$

in terms of displacements the above equation becomes:

$$\left(\frac{\partial^2 v_{c1}}{\partial x^2}\right)_{0,j} = -2\,\Delta x \left(\frac{\partial^3 v_{c1}}{\partial x^3}\right)_{1,j} + \left(\frac{\partial^2 v_{c1}}{\partial x^2}\right)_{2,j} \qquad (61)$$

From the above equation written in finite difference form $(v_{c1})_{-1,j}$ can be eliminated and substituted in equation (52) when written in finite difference form. Similarly, to determine $(u_{c1})_{-1,j}$ we can use the following relationships:

$$\left(\frac{\partial N_{A1}}{\partial x}\right)_{1,j} = \frac{(N_{A1})_{2,j} - (N_{A1})_{0,j}}{2\,\Delta x} = C_{s1}\left(\frac{\partial^2 u_{c1}}{\partial x^2}\right)_{1,j}$$

$$\text{or } (N_{A1})_{0,j} = -2\,\Delta x\, C_{s1}\left(\frac{\partial^2 u_{c1}}{\partial x^2}\right)_{1,j} + (N_{A1})_{2,j}$$

which can be written in terms of displacements as:

$$\left(\frac{\partial u_{c1}}{\partial x}\right)_{0,j} = -2\,\Delta x \left(\frac{\partial^2 u_{c1}}{\partial x^2}\right)_{1,j} + \left(\frac{\partial u_c}{\partial x}\right)_{2,j} \qquad (62)$$

For the plate shown in figure 7, in addition to equilibrium equations for the interior nodes, equations (61) and (62) are applied on nodes (0,2) and (0,4) to take account of four unknown fictitious displacements $(u_{c1})_{-1,2}$, $(v_{c1})_{-1,2}$, $(u_{c1})_{-1,4}$ and $(v_{c1})_{-1,4}$. The total number of boundary displacements is 3 (J+2) for which 3 (J+2) equations

$u_{0,j}$ = constant , $v_{0,j}$ = constant , $w_{0,j} = 0$ (for j=0 to J+1)

are available. For (J+2) unknown fictitious lateral displacements there are (J+2) equations of the type of equations (56) or (57).

Membrane Boundary Condition II

For a flexurally simply supported or built-in edge with free in-plane displacement normal to the edge and given displacement along the edge, the in-plane boundary conditions for a stiffener point are:

$$\left(N_x + \frac{N_{A1}}{\Delta y}\right) = \text{constant} \qquad (63)$$

$$v = 0 \qquad (64)$$

For all other nodes the above conditions reduce to

$$N_x = 0 \tag{65}$$

$$v = 0$$

Using the force-displacement relations for N_x and N_{A1} (equations 24, 26 and 27) and ignoring the non-linear terms, the first condition becomes:

$$(E' + \frac{C_{s1}}{\Delta y}) \frac{\partial u}{\partial x} + E'_1 \frac{\partial v}{\partial y} - \frac{e_1 C_{s1}}{\Delta y} \frac{\partial^2 w}{\partial x^2} = 0 \tag{66}$$

In the membrane equilibrium equations applied on nodes (1,j), displacements on the boundary are involved, but in this case displacements normal to the edge are unknown and cannot be obtained by the boundary condition (66), and an extra equation is needed. For this reason the governing equation (52) expressing the equilibrium of forces in the x-direction is now applied at the edge nodes (0,j). But in this equation the terms $\partial^2 v/\partial x \partial y$, $\partial^2 u/\partial x^2$ (and for nodes on stiffeners also the term $\partial^2 u_{c1}/\partial x^2$) are involved. This means that the fictitious in-plane displacements $(u)_{-1,j}$, $(v)_{-1,j}$ and $(v_{c1})_{-1,j}$ are needed. (The fictitious lateral displacements for nodes (-1,j) were discussed earlier under flexural boundary conditions.). The unknown $(u)_{-1,j}$ will be taken into account by applying equation (66) on nodes (0,j). To determine $(v)_{-1,j}$ for nodes without a stiffener the equilibrium equation (53), and for nodes with a stiffener equation (61), are used. The fictitious displacement $(u_{c1})_{-1,j}$ can be found from the boundary condition (63) written as:

$$E' \frac{\partial u}{\partial x} + E'_1 \frac{\partial v}{\partial y} + \frac{C_{s1}}{\Delta y} \frac{\partial u_{c1}}{\partial x} = 0 \tag{67}$$

and substituted in equation (52) when written in finite difference form. For the plate shown in figure 7 the total number of unknown in-plane displacements involved at edge x = 0 are 4(J+2) for which the same number of

equations are available as follows:

J+2 equations v = constant for $(v)_{0,j}$ (j=0 to J+1)

J equations (52) without stiffener terms for $(u)_{0,j}$ (j=0 to J+1 but j≠2 and j≠4)

2 equations (52) for $(u)_{0,j}$ (j=2 and j=4)

J equations $N_x = 0$ for $(u)_{-1,j}$ (j=0 to J+1 but j≠2 and j≠4)

2 equations $N_x + N_{A1}/\Delta y = 0$ for $(u)_{-1,j}$ (j=2 and j=4)

J equations (53) without stiffener terms for $(v)_{-1,j}$ (j=0 to J+1 but j≠2 and j≠4)

2 equations (61) for $(v)_{-1,j}$ (j=2 and j=4)

The two fictitious displacements $(u_{c1})_{-1,2}$ and $(u_{c1})_{-1,4}$ are eliminated from equation (67), applied at nodes (0,2) and (0,4), and substituted in the corresponding equations, so that no other equation is added to the system of equations.

Membrane Boundary Condition III

For an edge with free in-plane displacement along the edge and given displacement normal to the edge, the in-plane boundary conditions for all points are:

$$u = \text{constant} \tag{68}$$

$$N_{xy} = 0 \tag{69}$$

Using the force-displacement relations for N_{xy}, equations (24) and (26), and ignoring the non-linear terms, the second condition becomes:

$$E_{xy} \left(\frac{\partial u}{\partial y} + \frac{\partial v}{\partial x} \right) = 0 \tag{70}$$

The boundary displacements $(v)_{0,j}$ cannot be found from the above equation, and an additional equation is needed. Therefore the equilibrium equation

(53) expressing equilibrium of in-plane forces in the y-direction is applied at the edge nodes (0,j). For nodes without a stiffener the fictitious in-plane displacements $(u)_{-1,j}$ and $(v)_{-1,j}$ are needed, and for nodes on a stiffener, in addition to these $(v_{c1})_{-2,j}$ is also required. For determining $(u)_{-1,j}$ the governing equation (52), and for determining $(v)_{-1,j}$ the boundary condition (70), are applied at nodes (0,j). To eliminate $(u_{c1})_{-1,j}$, which involves $(w)_{-1,j}$, equation (62) is used. To eliminate $(v_{c1})_{-2,j}$ from equation (53) we note that

$$\left(\frac{\partial N_{H1}}{\partial x}\right)_{1,j} = \frac{(N_{H1})_{2,j} - (N_{H1})_{0,j}}{2\,\Delta x} = -B_{H1}\left(\frac{\partial^4 v_{c1}}{\partial x^4}\right)_{1,j}$$

or $$(N_{H1})_{0,j} = 2\,\Delta x\, B_{H1}\left(\frac{\partial^4 v_{c1}}{\partial x^4}\right)_{1,j} + (N_{H1})_{2,j}$$

which can be written in terms of displacements as:

$$\left(\frac{\partial^3 v_{c1}}{\partial x^3}\right)_{0,j} = -2\,\Delta x\left(\frac{\partial^4 v_{c1}}{\partial x^4}\right)_{1,j} + \left(\frac{\partial^3 v_{c1}}{\partial x^3}\right)_{2,j} \qquad (71)$$

From the above equation written in finite difference form $(v_{c1})_{-2,j}$ can be eliminated and substituted in equation (53) when written in finite difference form.

For the plate shown in figure (7) the total number of unknown in-plane displacements involved in edge x = 0 are 4(J+2) for which the same number of equations are available as follows:

J+2 equations u = constant for $(u)_{0,j}$ (j=0 to J+1)

J equations (53) without stiffener terms for $(v)_{0,j}$ (j=0 to J+1 but $j\neq2$ and $j\neq4$)

2 equations (53) for $(v)_{0,j}$ (j=2 and j=4)

J+2 equations $N_{xy} = 0$ for $(v)_{-1,j}$ (j=0 to J+1)

J equations (52) without stiffener terms for

$(u)_{-1,j}$ (j=0 to J+1 but j≠2 and j≠4)

2 equations (52) for $(u)_{-1,j}$ (j=2 and j=4)

The four other unknown displacements $(u_{c1})_{-1,2}$, $(v_{c1})_{-2,2}$, $(u_{c1})_{-1,4}$ and $(v_{c1})_{-2,4}$ are eliminated from equations (62) and (71), applied on nodes (0,2) and (0,4), and are substituted in the corresponding equations.

Membrane Boundary Condition IV

This case is similar to case III, but here both normal and tangential in-plane displacements are free. The boundary conditions for a stiffener point are:

$$N_x + \frac{N_{A1}}{\Delta y} = 0 \tag{72}$$

$$N_{xy} = 0 \tag{73}$$

Fot other nodes they reduce to

$$N_x = 0 \tag{74}$$

$$N_{xy} = 0$$

The equations used in this case are the same as those for case III, and only equation (68) has been replaced by equation (72) which in terms of displacements is given as equation (66).

In cases where on two adjacent edges, e.g. edge x = 0 and edge y = 0, both normal and tangential displacements are free, additional equations are needed. Considering the our nodes (0,0), (0,-1), (-1,0) and (-1,-1), the total number of unknown in-plane displacements is 8, but only the following five equations are available. These are the two equilibrium equations (52) and (53) without stiffener terms and the three boundary conditions $N_x = 0$, $N_{xy} = 0$ and $N_y = 0$. Therefore three additional equations are needed to determine $(u)_{-1,-1}$, $(v)_{-1,-1}$ and $(u)_{0,-1}$ (or

$(v)_{-1,0}$). The term $(u)_{-1,-1}$ is found by extrapolation from other u-values on the line i = -1, and similarly $(v)_{-1,-1}$ is determined by extrapolation from v-values on the line j = -1. The unknown $(u)_{0,-1}$ is also extrapolated from u-values on the line j = -1.

Membrane Boundary Condition V

For the case of a shear free straight edge with no resultant transverse edge force, the boundary conditions can be written as:

$$N_{xy} = 0 \tag{75}$$

$$\frac{\partial^2 u}{\partial y^2} = 0 \tag{76}$$

$$\sum_{j=1}^{J-1} \left(N_x + \frac{N_{A1}}{\Delta y} \right)_{0,j} = 0 \tag{77}$$

This case is similar to case III but instead of using equation (68) for each edge node, here equation (77) is applied at one edge node and equation (76) is used for all other edge nodes. The application of equation (77) involves the displacements of all edge nodes and thus results in a large band width for the matrix of coefficients.

The total number of unknown displacements in most cases is 3(I+2)(J+2), and these are to be found from the same number of simultaneous linear algebraic equations, obtained by using finite difference approximations to the differential equations of equilibrium and from boundary conditions.

3.3 LARGE-DEFLECTION SOLUTION

3.3.1 Elastic Large-Deflection Solution

The equilibrium equations in the large-deflection range are non-linear and require an iterative method of solution (Fig. 8). The

solution method used here utilises the linear small-deflection equations as noted earlier. Let the small-deflection problem in terms of unknown nodal displacements u, v and w be stated as:

$$[A]\ \{R\} = \{P\} \tag{78}$$

where $\{R\}$ is the vector of nodal displacements, $\{P\}$ is the given load vector and $[A]$ is the square matrix of coefficients obtained from the linearised equilibrium equations in their finite difference form, called "the initial stiffness matrix" in the present text. The solution of these equations gives the nodal displacements:

$$\{R\} = [A]^{-1}\ \{P\} \tag{79}$$

One cycle of the iterative method for the solution of the non-linear equations for a given load vector consists of the following steps:

1. Assume a trial displacement vector $\{R\}_1$.
2. Calculate the strains (including the effect of the quadratic terms) and, hence, the internal forces and moments at various nodes in the plate, using the force-displacement equations (24), (25) and (27)-(30). The boundary conditions are utilised in this step, either to avoid the computation of nodal forces at the boundaries or to obtain their values at or outside the boundaries, if these values are needed in the following step.
3. These forces and moments are substituted in the non-linear equilibrium equations in terms of forces at the interior nodes, and also in those equations at the boundaries that correspond to the displacements not specified at that boundary. In general the equilibrium equations (and some boundary conditions) will not be exactly satisfied by these substitutions for the given loading $\{P\}$, but will indicate that the plate is in equilibrium with a fictitious loading $\{P\} - \{dP\}_1$, where $\{dP\}_1$ is called the

vector of "out-of-balance forces".

4. The additional displacements needed to bring the load level up by $\{dP\}_1$ are found approximately by assuming that the plate behaves linearly under this load as in the small-deflection case. Thus the additional (correction)displacements are given by:

$$\{dR\}_1 = [A]^{-1} \{dP\}_1 \qquad (80)$$

If the individual components of $\{dR\}_1$ are sufficiently small compared with those of $\{R\}_1$, then $\{R\}_1$ is the required solution, otherwise the new approximation for the displacements is

$$\{R\}_2 = \{R\}_1 + \{dR\}_1 \qquad (81)$$

5. Same as step 2

6. Same as step 3 to find $\{dP\}_2$

7. Same as step 4 to find $\{dR\}_2$. If $\{dR\}_2$ components are sufficiently small, $\{R\}_2$ is the solution. Otherwise proceed to step 8.

8. Rather than using $\{dR\}_2$ as correction displacements to obtain the new approximation, an improved approximation to the displacements is now found by using Aitken's δ^2-extrapolation

$$\{R\}_* = \{R\}_1 + \{dR\}_* \qquad (82)$$

where each element of $\{dR\}_*$ is found from the corresponding elements of the two subsequent correction displacements $\{dR\}_1$ and $\{dR\}_2$ using the formula

$$dR_* = \left(\frac{dR_1}{dR_1 - dR_2} \right) dR_1 = \alpha \, dR_1 \qquad (83)$$

When dR_1 and dR_2 are very close for a particular displacement component, the factor α becomes very large. In such cases an upper limit has been imposed on the value of α.($|\alpha| = 4$ if

$|\alpha| > 6$). If the individual components of $\{dR\}_*$ are sufficiently small compared with those of $\{R\}_1$, then $\{R\} = \{R\}_*$ is the required solution, otherwise $\{R\}_*$ is the new approximation and setting $\{R\}_1 = \{R\}_*$ completes a cycle (Fig. 8).

The whole iterative procedure is given in flow chart form in Appendix E. The initial approximation for $\{R\}$ at the first load level is found from the small-deflection solution-equation (79). For subsequent load levels the initial approximation is found by linear extrapolation of the individual converged displacements obtained at the previous two load levels. Assuming the load increment is constant, and the large-deflection displacements of the previous two load levels (i-th and i-1st) can be represented as $\{R\}_i$ and $\{R\}_{i-1}$, and displacement at each node and direction can be shown by $R_{i,k}$ and $R_{i-1,k}$ then:

$$R_{i+1,k} = \left(2 - \frac{R_{i-1,k}}{R_{i,k}} \right) R_{i,k} \qquad (84)$$

For instability problems an improved procedure for obtaining the initial approximation for the third and the subsequent load levels has been adopted. For this case a parabolic extrapolation of the displacements obtained at the previous three load levels has been used.

To obtain a better convergence for instability problems, and due to the incremental nature of the stress-strain relationships in the elasto-plastic problems, for both cases an incremental iterative approach has been adopted (Fig. 8).

3.3.2 Elasto-Plastic Large-Deflection Solution

For elasto-plastic problems the solution procedure is basically the same as for elastic cases. Here because of the incremental nature of force-displacement relationships in the plastic range a combined incremental iterative solution technique has been adopted. For this purpose all govern-

ing equations have been used in their incremental form (Appendix D) to compute the displacement and force increments for a particular load increment. These displacement and force increments have been added to the previous total displacements and forces up to the application of the present load increment to obtain the total displacements and forces for the present load level. For instability problems this approach has been employed even in the elastic range and a faster convergence has been achieved. One cycle of the incremental iterative method for a given load increment vector $\{\Delta P\}$ consists of the following steps:

1. Assume a trial displacement increment vector $\{\Delta^p\}_1$ for the load increment vector $\{\Delta P\}$.
2. Calculate the increments of the strains, forces and moments for various nodes of plate, using the incremental force-displacement equations (D-3), (D-5)-(D-6), or equations (D-7), (D-12)-(D-14), depending on the plate and stiffener at the particular node being in the elastic or plastic range respectively. The boundary conditions are utilized in this step, either to avoid the computation of nodal forces at the boundaries or to obtain their values at or outside the boundary, if these values are needed in the following step.
3. These incremental values and the total values of displacements, forces and moments are substituted in the incremental equilibrium equations in terms of forces (D-2) at the interior nodes and also in those equations at the boundaries that correspond to the displacements not specified at that boundary. In general the equilibrium equations will not be exactly satisfied for the load vector $\{\Delta P\}$, but for a fictitious loading $\{\Delta P\} - \{d\Delta P\}_1$ with $\{d\Delta P\}_1$ as vector of out-of-balance forces.

4. The correction displacements needed to satisfy the equilibrium are approximately found by assuming that the plate behaves linearly under this small load as in the small-deflection case. Thus the correction displacements vector is given by:

$$\{d\Delta R\}_1 = [A]^{-1} \{d\Delta P\}_1 \qquad (85)$$

When the individual elements of $\{d\Delta R\}_1$ are small compared to $\{\Delta R\}_1$ then $\{\Delta R\}_1$ is the required solution, set $\{\Delta R\} = \{\Delta R\}_1$ and proceed to step 9. Otherwise the new approximation for the displacements is:

$$\{\Delta R\}_2 = \{\Delta R\}_1 + \{d\Delta R\}_1 \qquad (86)$$

5. Same as step 2.

6. Same as step 3 to calculate $\{d\Delta P\}_2$.

7. Same as step 4 to calculate $\{d\Delta R\}_2$.

8. Rather than using $\{d\Delta R\}_2$ to obtain a new approximation for displacement increments, an improved correction displacement vector $\{d\Delta R\}_*$ is found by using the Aitken's δ^2-extrapolation, from corresponding elements of $\{d\Delta R\}_1$ and $\{d\Delta R\}_2$ by the formula:

$$d\Delta R_* = \frac{d\Delta R_1}{d\Delta R_1 - d\Delta R_2} d\Delta R_1 = \alpha \, d\Delta R_1 \qquad (87)$$

When $d\Delta R_1$ and $d\Delta R_2$ are very close for a particular displacement component on a node, the factor α becomes very large, in such cases an upper limit has been imposed on the value of α. ($|\alpha| = 4$ if $|\alpha| > 6$). If each individual element of $\{d\Delta P\}_*$ is sufficiently small compared with $\{\Delta R\}_1$, then

$\{\Delta R\}_* = \{\Delta R\}_1 + \{d\Delta R\}_*$

is the required solution, set $\{\Delta R\} = \{\Delta R\}_*$ and proceed to step 9. Otherwise $\{\Delta R\}_*$ is the new approximation for the displacement

increments and by setting $\{\Delta R\}_1 = \{\Delta^p\}_*$ and proceeding to step 2 an iteration cycle is closed.

9. Using $\{\Delta R\}_i$ (displacement increment vector for the current i-th load increment) and the total displacements up to application of the current load increment $\{R\}_{i-1}$, force and moment increments are computed and by adding these to total forces and moments up to application of the current load increment, the total forces and moments for the present load level are obtained.

$$\{N\}_i = \{N\}_{i-1} + \{\Delta N\}_i$$
$$\{M\}_i = \{M\}_{i-1} + \{\Delta M\}_i \qquad (88)$$

Now at each node the plate and the stiffener are checked for plasticity. At a particular node one of the following four cases may occur:

(a) The plate has been elastic and it remains so at the end of present load increment. In this case elastic rigidities will be used in the next load increment to compute plate forces and moments.

(b) The plate has changed from plastic to elastic during the last load increment (unloading). Also here as in case (a) elastic rigidities will be used for the next load increment.

(c) The plate has been plastic at the beginning and it remains so at the end of present load increment. In this case the new tangential elasto-plastic rigidities (Appendix C) are computed from the present total forces and moments, and they are stored to be used in the next load increment. (Tangential elasto-plastic rigidities are computed for each node at each load increment and not at each iteration).

(d) The plate has changed from elastic to plastic during the

last load increment. The present force and moment increments which were computed using elastic rigidities are not exact, and the following approach is employed[17] to obtain a more exact approximation for force and moment increments. Let f_{i-1} be the elastic value of the yield function at the end of i-1st load increment ($f_{i-1} < 1$) and f_i be the plastic value of the yield function at the end of present load increment ($f_i > 1$). The strain increments to cause the stress resultants that just reach the yield surface may then be approximated as "β" times the total incremental strains. Where

$$\beta = \frac{1 - f_{i-1}}{f_i - f_{i-1}} \tag{89}$$

The present estimate of resultant forces and moments, computed using elastic rigidities for the last load increment is

$$\begin{aligned} \{N\}_{i,e} &= \{N\}_{i-1} + \{\Delta N\}_i = \{N\}_{i-1} + [E]\ \{\Delta\varepsilon_t\} \\ \{M\}_{i,e} &= \{M\}_{i-1} + \{\Delta M\}_i = \{M\}_{i-1} + [D]\ \{\Delta\chi_t\} \end{aligned} \tag{90}$$

Now the resultant forces and moments to reach the yield surface can be estimated as:

$$\begin{aligned} \{N\}_{i,yield} &= \{N\}_{i-1} + \beta\ [E]\ \{\Delta\varepsilon_t\} \\ \{M\}_{i,yield} &= \{M\}_{i-1} + \beta\ [D]\ \{\Delta\chi_t\} \end{aligned} \tag{91}$$

The better estimate for forces and moments at the end of the last load increment is:

$$\begin{aligned} \{N\}_i &= \{N\}_{i,yield} + (1-\beta)\ ([E]^*\ \{\Delta\varepsilon_t\} + [cd]\ \{\Delta\chi_t\}) \\ \{M\}_i &= \{M\}_{i,yield} + (1-\beta)\ ([cd]^T\ \{\Delta\varepsilon_t\} + [D]^*\ \{\Delta\chi_t\}) \end{aligned} \tag{92}$$

Using the total forces and moments up to the present load level,

the tangential elasto-plastic rigidities for the particular node are computed and stored to be used for the next load increment. The plasticity of the stiffener at a particular node is checked at each iteration of a load increment for computing the stiffener forces and moments. The total stress at each area element of stiffener is checked and if it exceeds yield stress, the stress increment is made zero. Force and moment increments are calculated using equations (D-9)-(D-14). Having displacements, forces and moments for the present load level, a new load increment can be applied. The first approximation for displacement increments of the new load increment can be found by linear extrapolation from previous displacement increments. Having the first estimate for displacements, proceed to step 2 to begin the first iteration.

3.4 DISCUSSION ON SOLUTION METHOD

3.4.1 General

The iterative method described here is a modified Newton-Raphson method, since it uses the "initial stiffness matrix" [A] throughout the iterations (Fig. 8), rather than a different "tangent stiffness matrix" at each iteration as required by the original method. It thus avoids the necessity of generating a new tangent stiffness matrix and of solving the corresponding linear equations each time when a new vector of correction displacements is to be computed. In the present method $[A]^{-1}$ is evaluated only once and is stored in the computer; the computation of a new vector of correction displacements merely requires $[A]^{-1}$ to be multiplied by a vector {dP} as indicated in equations (80) or (85). (In fact in the present program [A] is a band matrix, and to save computer time and storage

it has been decomposed into an upper and a lower triangular matrix which have been stored in the computer). Thus the computation per cycle is greatly reduced from that required by the original Newton-Raphson method. The present method is linearly convergent, whereas the original method converges quadratically. The application of the Aitken's δ^2-extrapolation on the individual displacements in the same way as in the case of single equations, partly restores the loss in the speed of convergence, and in many instances ensures convergence where the modified Newton-Raphson method would have failed.

3.4.2 Acceleration of Convergence

It has been possible to achieve further improvement in the rate of convergence by noting the change in the actual stiffness characteristics of the problem with the loading, and taking this into consideration in an empirical way by modifying the displacement increments. Thus, in place of equation (81) we have:

$$\{R\}_2 = \{R\}_1 + \beta \{dR\}_1 \tag{93}$$

and similarly for the next iteration we have:

$$\{R\}_3 = \{R\}_2 + \beta \{dR\}_2 \tag{94}$$

The use of the same β in both iterations allows the application of the extrapolation procedure in spite of this modification. Clearly β should be different for each displacement component at each node. The β-values to be used for the next load level for a particular displacement component at a particular node is calculated so that using β we could get the converged result for the last load level R from the first trial R_1 and the correction displacement of the first iteration dR_1:

$$R = R_1 + \beta \, dR_1 \tag{95}$$

or

$$\beta = (R - R_1) / dR_1 \tag{96}$$

Whereas for bending problems the use of β has resulted in a faster convergence, in some buckling problems it has not helped and therefore it has been ignored in such cases.

3.4.3 Convergence Criteria

For defining the convergence criteria many factors such as the expected behaviour of the structure under the applied type and range of loading and also the possible errors and sources of inaccuracy in the solution method should be taken into account. Therefore in the present work different convergence criteria have been considered for different types of problems.

For elastic bending problems where an iterative solution method has been used, two restrictions are considered for convergence. Firstly, the out-of-plane correction displacement at each node should be less than $e_1 = 0.01$ times the total out-of-plane displacement at the same node:

$$\frac{|dw_k|}{|w_k|} < e_1 = 0.01 \tag{97}$$

Secondly, the Euclidean norm of correction displacements should be less than 0.01 times the Euclidean norm of total displacements:

$$\frac{(\{dR\}^T \{dR\})^{1/2}}{(\{R\}^T \{R\})^{1/2}} < e_2 = 0.01 \tag{98}$$

For elastic instability problems the satisfaction of each of the above restrictions has been considered as convergence.

For problems where the combined incremental iterative solution method has been used, the total out-of-plane correction displacement at each node should be less than $e_3 = 0.01$ times the displacement increment plus 0.1% of the total displacement:

$$|d\Delta w_k| < |(0.01\ \Delta w_k + 0.001\ w_k)| \tag{99}$$

In addition, the Euclidean norm of correction displacements should be less than e_4 = 0.015 times the Euclidean norm of displacement increments

$$\frac{(\{d\Delta R\}^T \cdot \{d\Delta R\})^{1/2}}{(\{\Delta R\}^T \cdot \{\Delta R\})^{1/2}} < 0.015 \tag{100}$$

However, if after five iterations both criteria are not satisfied, then for the next iteration the satisfaction of each of the two criteria has been considered as convergence.

For elasto-plastic problems after the onset of plasticity the same technique as for elastic instability problems with the combined incremental iterative solution method has been used, but the limiting factors e_3 and e_4 have been increased as the load increment is reduced, to a maximum of 0.04 and 0.06 respectively.

In elastic bending problems the convergence is fast and generally after 2 to 3 iterations the convergence is achieved. Also in elastic instability problems the convergence is fast at the beginning, but as the loading approaches the buckling load and beyond the convergence is slower and generally 3 - 7 iterations are needed. If after 10 iterations no convergence is achieved the load increment is halved and this is repeated. If there is still no convergence the solution will be terminated. For elasto-plastic problems in the plastic range generally 1 - 3 additional iterations are needed compared to the elastic range.

3.5 COMPUTER PROGRAM

A computer program for the non-linear analysis of stiffened plates was developed according to the previous theory. The program can

be used to analyse both geometric and material non-linearity separately or simultaneously. Also ordinary linear (small-deflection) solutions can be obtained.

Initial imperfections such as initial out-of-plane deformations of plate and the out-of-straightness of stiffeners caused by these deformations, as well as residual stresses in plate and stiffeners due to welding are considered in the program.

Although the previous theory was derived for rectangular bar sections, but ignoring the effect of warping,other types of sections (L and T) have been included in the program. As special cases grillages ages and unstiffened isotropic plates can be analysed. The program may also be used to analyse plates with eccentric stiffeners. Plate and stiffener material properties are defined separately and may be different, hence hybrid structures may be analysed.

The input data are plate and stiffener geometry, material properties, stiffener locations, boundary conditions, type and size of loading, and mesh size. As output, plate and stiffeners forces and moments, displacements at mid-plane of plate and at centroid of stiffeners are printed.

In the present examples in-plane loading has been specified as applied displacement along the edges, however loading can be defined also as known stresses on edge nodes.

For large deflection solutions, lateral and in-plane loads have been applied incrementally (both in iterative and in combined incremental iterative methods). The load increment does not need to be small because it will automatically reduce if no convergence is achieved after 10 iterations. For plasticity cases the load increment is automatically reduced

when the structure approaches the plastic range. A flow-chart of the computer program is shown in Appendix E.

CHAPTER 4

NUMERICAL EXAMPLES

4.1 GENERAL

The following examples are presented to prove the validity of the present theory and to demonstrate its scope of application. The results have been compared with related existing solutions where possible. Plates subject to three different types of loading have been studied.

I - Plates subject to lateral load.

II - Plates subject to uniaxial in-plane load.

III - Plates subject to combined in-plane shear and compression.

In all three cases both unstiffened isotropic plates and stiffened plates in the elastic as well as in the plastic range have been studied. To the author's knowledge the present theory and solution technique (in particular the modified Newton-Raphson method with Aitken's δ^2-extrapolation) has not been used for isotropic plates before. It has distinct advantages compared to some existing methods, especially for elasto-plastic analyses. However isotropic plates have been included mainly to prove the theory since comparable results for stiffened plates are scarce.

4.2 PLATES SUBJECT TO LATERAL LOADING

For plates subject to lateral loading two types of flexural boundary conditions are considered.

(a) all edges simply supported

(b) all edges built-in

For membrane boundary conditions five different cases are studied. In all cases the opposite edges have the same conditions. If K_x and S_x are the extensional and shear stiffness respectively of the supports parallel to the y-axis, and similarly K_y and S_y are those of the supports parallel to the x-axis, then the boundary conditions for different cases can be shown as:

I. $K_x = S_x = K_y = S_y = \infty$

II. $K_x = 0,\ S_x = K_y = S_y = \infty$

III. $K_x = K_y = 0,\ S_x = S_y = \infty$

IV. $K_x = S_x = K_y = S_y = 0$

V. $K_x = K_y = \infty,\ S_x = S_y = 0$

4.2.1 Isotropic Plates

4.2.1.1 *Elastic Isotropic Plate*

For a square isotropic plate subject to a uniformly distributed lateral load, linear and non-linear elastic solutions are obtained. Four different in-plane boundary conditions (type I to IV) and two flexural boundary conditions (simply supported and built-in) are considered.

The load-deflection curves for simply supported plates are given in figure 9. The solutions are checked against comparable results presented by Levy[49] (Fourier Series), Kaiser[48] (theoretical and experimental), Basu[71] (finite differences) and Crisfield[17] (finite element method), and a very close agreement is observed. For the plate with in-plane boundary conditions of type I, membrane stresses (figure 10) and extreme fibre bending stresses (figure 11) have been compared with Levy's and Crisfield's results. Here a larger discrepancy is found with that of central deflections, however closer agreement is obtained with Levy's results.

The load-deflection curves for built-in plates are given in figure 12 and are compared with results produced by Levy[50] (Fourier Series) and Basu[71] (finite differences). The agreement is good but a finer mesh than in the case of the simply supported plate is required. This is to be expected because of the difference in the deflection shape. In general, in cases where the edges are restrained, the results are more accurate and have a closer agreement with available solutions. In such cases also convergence is faster.

4.2.1.2 *Mesh Convergence*

The mesh convergence has been investigated for the simply supported restrained plate for both elastic linear and non-linear solutions. The results are shown in figures 13a and 13b. For the small-deflection (linear) solution a finer mesh results in larger displacements. Figure 13a shows the percentage increase in displacement due to mesh fineness compared to displacements found by a 2x2 mesh. (Mesh size is quoted for a quarter of plate). The same figure shows that even using a 4x4 mesh an accuracy of 0.18%, and using a 6x6 mesh one of 0.07% can be achieved.

The mesh convergence for the elastic large deflection (non-linear) solution has been investigated for the same plate subject to the pressure ratio $qa^4/Et^4 = 119.05$ which results in a central deflection of about 1.34 times the plate thickness. The limiting percentage set for convergence was 0.5% (see section 3.4.3).

The large-deflection result is more closely predicted by a finer mesh, i.e. a finer mesh results in smaller out-of-plane displacements at the centre. The percentage decrease in central displacement compared to the results obtained using a 2x2 mesh is shown in figure 13b. This figure shows that a 4x4 mesh will give results with an accuracy of 1% and that an accuracy of 0.4% can be expected using a 6x6 mesh.

The load-central deflection curves for the same plate with

different mesh sizes (2x2, 4x4 and 12x12) are plotted in figure 14 and, as can be seen, the results for the last two mesh sizes are very close.

4.2.1.3 *Elasto-Plastic Isotropic Plate*

For a square isotropic plate with in-plane boundary conditions type V two solutions considering material non-linearity and combined geometric and material non-linearity are presented. For the simply supported case a plate slenderness a/t = 40 has been chosen.

The first solution (considering material non-linearity only) for a simply supported plate has been compared with results reported by Crisfield[103] (finite element 6x6 mesh, Ilyushin yield criterion) and Yam and Das[87] (finite differences) and close agreement is observed (figure 15). The second solution (considering both geometric and material non-linearity) is compared with a solution obtained by a program developed by Frieze[111] using a dynamic relaxation method (figure 15). The agreement is excellent.

For the built-in case a plate with a/t = 60 has been analysed and two elasto-plastic solutions are obtained (figure 16). The elasto-plastic small deflection solution has been compared with results presented by Bhaumik[82] (finite differences, 5x5 mesh) and the agreement is very good. The elasto-plastic large deflection solution has been compared again with results from Frieze's program and good agreement is obtained. The small discrepancy for higher load levels may be due to different mesh sizes used in both solutions.

4.2.2 Stiffened Plates

In this section some stiffened plates are analysed and elastic and elasto-plastic solutions are obtained. For many cases no comparable solutions could be found in the literature and so the number of case studies

is restricted.

4.2.2.1 *Elastic Linear Solution for a Discretely Stiffened Plate*

The elastic linear solution is obtained for a simply supported plate with a longitudinal and a transverse stiffener at the centre for two different in-plane boundary conditions. The plate is subject to a uniformly distributed lateral load on the plate side so that the stiffeners are in tension. The plate dimensions are shown in figure 17.

For the plate with restrained edges ($K_x = S_x = K_y = S_y = \infty$), displacements and forces and moments in plate and stiffener at different sections of the plate are compared with results obtained from a finite element program developed by Moffatt[23] (figures 18 and 19). The results for the plate with free in-plane displacements at the edges ($K_x = K_y = S_x = S_y = 0$) are compared with the solution found by a program developed by Lyons[142] using a finite element method (figures 20 and 21). In both cases the agreement is very good, only some discrepancies are observed in in-plane displacements, particularly for plate with restrained edges.

Figures 18 - 21 show very clearly the expected deflection shape and the distribution of forces and moments in discretely stiffened plates which cannot be predicted by orthotropic plate theory.

4.2.2.2 *Elastic Non-Linear Solution for a Discretely Stiffened Plate*

For a square plate with a longitudinal and a transverse stiffener at the centre, elastic non-linear solutions are obtained for different boundary conditions. The plate is subject to uniformly distributed lateral load on the plating side, so the stiffeners are in tension. The plate and stiffener dimensions are given in figures 22 and 23 in non-dimensionalised form.

Two different flexural boundary conditions (simply supported and built-in) and three different in-plane boundary conditions (type I, III and IV) are studied. The load-central deflection curves for simply supported and built-in plates are given in figures 22 and 23 respectively. No comparable results could be found for these cases.

4.2.2.3 *Mesh Convergence for Elastic Linear and Non-Linear Solutions*

The mesh convergence has been investigated for both elastic linear and non-linear solutions for the plate shown in figure 24 with restrained edges. The two solutions have been obtained for different mesh sizes for the case of uniformly distributed lateral load. Figure 24 shows the percentage improvement in the prediction of out-of-plane displacements for points A and C for finer mesh sizes compared to results obtained using a 4x4 mesh. It is clear here that because of the stiffener a finer mesh is needed compared to unstiffened plates. This is because the quarter plate is similar to a plate partially built-in at two edges. Even so, figure 24 shows that with a 6x6 mesh the small deflection solutions for points C and A can be achieved with an accuracy of 1% and 2% respectively.

The large-deflection solutions used to test the mesh convergence are obtained for a pressure ratio of $qa^4/Et^4 = 285.7$ which results in a central deflection of about 1.21 times the plate thickness. The limiting percentage for convergence in the iterative solution method was set at 1% (see section 3.4.3).

4.2.2.4 *Elastic Stiffened Plate*

To obtain solutions which can be compared with results of available solution methods three equivalent stiffened plates with seven stiffeners in each direction have been analysed. The first plate has eccentric stiffeners underneath so that when the uniformly distributed load

is applied on top the stiffeners are in tension. The second plate has concentric stiffeners but the stiffener dimensions are chosen such that their elastic rigidity as an orthotropic plate is the same as the first plate. The third plate is similar to the first one but the stiffeners are connected to the top side so that they are in compression for the given loading. Load-central displacement curves for all three cases have been obtained and are presented in figure 25. Since the three plates have equivalent rigidities a load-central deflection curve has been produced from a program developed by Frieze[111] using orthotropic plate approach. Whereas the solution found for the concentric stiffened plate shows a very close agreement with the solution based on orthotropic plate theory, the other two solutions show very different displacements especially at higher load levels. The difference is caused by stiffener eccentricity the effects of which can only be crudely approximated by "orthotropic plate theory" in the evaluation of the orthotropic plate rigidities.

4.2.2.5 *Elasto-Plastic Beam*

A simply supported beam subject to uniform lateral loading has been analysed as a special case to check the stiffener part of elasto-plastic solution. The beam is hinged and horizontally restrained at both ends. Its dimensions are given in figure 26. The mesh length is L/10 (5 meshes over half the length, n = 5) and the beam section is divided into six layers for plastic analysis. Three different solutions are obtained and are presented in figure 26. The elastic linear solution is compared with the elementary beam theory solution. The elastic non-linear solution has been compared with results presented by Timoshenko and Winowsky-Krieger[12] and excellent agreement is observed. The solution considering both geometry and material non-linearity is compared with

results presented by Baecklund[141] and Moan and Soreide[20] and very good agreement is found (especially with Moan's results). Unloading occurred after reaching a load of .8 MN/m and a load-central deflection curve was obtained. The unloading curve shows close agreement with Moan's result.

4.2.2.6 *Elasto-Plastic Analysis of Longitudinally Stiffened Plate*

The longitudinally stiffened plate shown in figure 27 has been tested by Pelikan[38] for a point load at the centre. The geometry and boundary conditions are shown in figures 27 and 28. The same plate has been analysed by Moeller[134] using a finite element method. Elasto-plastic large deflection solutions have been obtained for two different boundary conditions for the plate ignoring the two edge stiffeners. In case I it is assumed that all edges are free to displace in-plane. In case II the edges parallel to the x-axis are the same as in case I but the other two edges are free to pull in but tangentially restrained. The present load-central deflection curves and Pelikan's and Moeller's results are shown in figure 27. The result for case II which is nearer to the actual test boundary conditions is fairly close to the test result. The larger displacements obtained may be caused by neglecting the edge stiffener and assuming free normal-to-edge displacements for edges parallel to the y-axis. Figure 28 shows the lateral displacement profiles for centre-line sections at different load levels.

4.2.2.7 *Elasto-Plastic Analysis of Orthogonally Stiffened Plate*

The simply supported square plate reinforced in both directions by open rib sections as shown in figure 29 has been analysed by Kagan and Kubo[99]. They used Vogel's[69,76] coupled partial differential equations for orthotropic plates and extended these to include

the effect of yielding. They distributed a portion of the membrane forces to the stiffeners and assumed that no unloading occurred in the ribs and that the plate remained elastic. They have presented three solutions for the above mentioned stiffened plate. Firstly, an elastic linear solution using Huber's[37] equations and secondly, an elastic non-linear solution based on Vogel's equations, and finally, an elasto-plastic solution using the assumption that the plate remains elastic and only the stiffeners yield in tension. In reference (99) it is not clear whether for the elasto-plastic solution geometric non-linearity is also taken into account or only material non-linearity has been considered. Neither are the in-plane boundary conditions given but it would seem that the edges were free to displace in-plane. The same plate has been analysed for this boundary condition using the present program and four different solutions have been obtained and are given in the form of load-central deflection curves in figure 29. Where the elastic results show very close agreement to Kagan's solutions, the present elasto-plastic solutions differ very much from Kagan's elasto-plastic solution.

4.2.2.8 *Elasto-Plastic Analysis of Discretely Stiffened Plate*

The elasto-plastic behaviour of a simply supported plate with a longitudinal and a transverse stiffener subject to uniformly distributed lateral load has been investigated. The plate's dimensions and the elasto-plastic large-deflection solution in the form of a load-central deflection curve are given in figure 30. In the same figure the elastic non-linear solution for the same plate and both the elastic and elasto-plastic non-linear solutions for the same plate without stiffeners are also given for comparison. The spread of plasticity in the plate and stiffeners and the deflection profiles for different load levels are shown in figures 30

and 31.

4.3 PLATES SUBJECT TO UNIAXIAL IN-PLANE LOADING

In this section some unstiffened and stiffened plates subject to uniaxial in-plane loading have been analysed. The in-plane loading has been achieved by applying two opposite but equal and constant displacements normal to the edges parallel to the x-axis. In most cases it is assumed that the other two unloaded edges are free to displace normally and tangentially to the edge. Other boundary conditions used in some cases will be discussed when dealing with the particular examples.

All plates have initial out-of-plane displacements and in the case of stiffened plates the stiffeners have an initial out-of-flatness. In some cases the effect of residual stresses in plate and stiffeners has been also taken into account.

In all examples because of geometric and loading symmetry only a quarter of the plate needed to be considered in the analysis.

4.3.1 Isotropic Plates

4.3.1.1 *Elastic Isotropic Plate*

The post-buckling behaviour of an initially imperfect square isotropic plate subject to uniform direct compression has been investigated. The loading is achieved by the application of a constant displacement normal to the edge. The tangential displacement at the loaded edge is free. The unloaded edges are free to displace normally and tangentially to the edge. Two solutions, for simply supported and built-in plates are obtained and are given in the form of average stress-central deflection curves in figure 32. The solution found for the simply supported plate is compared with results presented by Yamaki[59] and Crisfield[17]. Yamaki used

double trigonometric series with four coefficients to solve Marguerre's[46] fundamental equations for initially imperfect plates. Crisfield used the finite element method. The present solution for the built-in plate has been compared also with Yamaki's result. Whereas the stress-deflection curve for the simply supported plate is very close to both Yamaki's and Crisfield's results, the solution for the built-in plate shows larger central displacements, especially for higher stresses due to the mesh size. A better agreement will be achieved with a finer mesh also for the built-in plate.

4.3.1.2 *Elasto-Plastic Isotropic Plates*

In this section the elasto-plastic behaviour of three different isotropic plates subject to uniform compressive displacement are investigated. Residual stresses and different initial geometric imperfections have been considered to check the different aspects of the present theory and the program. The examples are chosen so that the effects of different parameters such as plate slenderness, initial out-of-plane displacements and residual stresses can be observed.

Plate with b/t = 40: For three different initial out-of-plane displacements, the load-shortening and load-central deflection curves are given in figures 33 and 34. These curves are compared with results reported by Harding[113], who used dynamic relaxation and the von Mises' yield criterion. The agreement is very good and the differences are typical for the two different yield criteria used in both solutions. However in all three cases the ultimate loads are very close.

Plate with b/t = 55: For this plate two solutions with and without residual stresses are obtained. The residual stresses are assumed to be due to the welding of the edges parallel to the y-axis. For the

distribution of residual stresses the simplified rectangular block distribution proposed by Dwight and Moxham[7] has been adopted (figure 35). The results for both cases are given in the form of load-shortening curves in figure 36 and load-central displacement curves in figure 37. These curves have been compared with results presented by Moxham[101], Crisfield[17] and Harding[113]. Moxham adopted the Ritz approach and used Fourier series to calculate the potential energy. He used a 9x9 mesh and the plate was divided into 5 layers. Crisfield used the finite element method and his results are based on the Ilyushin yield criterion. The present results show excellent agreement with Crisfield's results for both cases with and without residual stresses. But the present ultimate loads are higher by 6% than those presented by Moxham and Harding who used a different yield criterion.

Plate with b/t = 80: Figure 38 shows the plate dimensions and the present average stress-average strain curve which is compared with solutions presented by Moxham[101] and Crisfield[17]. The average stress-central deflection curve is given in figure 39. For both curves a close agreement, especially with Crisfield's results, can be observed.

4.3.2 Stiffened Plates

4.3.2.1 *Elastic Plate with a Single Stiffener*

The elastic post-buckling behaviour of a wide range of simply supported plates with a single stiffener at the centre has been investigated by Weiss and Zaenkert[81] using an improved finite difference method. The effect of different parameters such as initial out-of-plane displacements of the plate, stiffener eccentricity and its extensional and flexural rigidity have been studied. Here two plates have been chosen to be

analysed by the present program to assess its accuracy. In both plates the stiffener is in the direction of loading and at the plate's centre-line. Both plates are equivalent in respect of elastic rigidity ratios δ and γ . The only difference is in the arrangement of the stiffener which is concentric in one case (fig. 40) and eccentric in the other (fig. 41). For each plate two different types of in-plane boundary conditions have been considered. In the first case all edges are shear free and the unloaded edges are restrained to remain straight such that there is no resultant transverse edge load. The same conditions have been adopted by Weiss and Zaenkert. In the second case the unloaded edges are free to displace in-plane. The plate panels between the edges and the stiffener have sinusoidal initial out-of-plane displacements towards the stiffener as:

$$w_0 = \max w_0 \left(\cos \frac{\pi y}{L_y} \right) \left| \sin \frac{2\pi x}{L_x} \right|$$

For the plate with concentric stiffener, the average stress-maximum deflection curves for both cases of constrained and free unloaded edges are given in figure 40. Figure 41 shows the same curve for the plate with the eccentric stiffener. For both plates the solutions for constrained cases are compared with results presented by Weiss and Zaenkert and good agreement is observed. The buckling loads given by Weiss and Zaenkert for both plates are also shown in figures 40, 41. A comparison of the curves of figure 40 with those of figure 41 shows that for the stiffeners with the same δ and γ the plate with eccentric stiffener is more rigid and shows smaller out-of-plane displacements for the same load level.

4.3.2.2 *Elasto-Plastic Analysis of a Plate with a Single Stiffener*

For a simply supported plate with a longitudinal stiffener subject to uniform compressive displacement, the elastic and elasto-plastic behaviour have been investigated. Also the behaviour of a hybrid plate (assuming a higher yield stress than that of the plate for the stiffener $\sigma_{os} = 1.4\ \sigma_o$) has been studied. The plate's dimensions are given in figure 42. The linear buckling load is very high since,because of the flexurally strong stiffener, the buckling occurs in plate panels between the edges and the stiffener. The load-shortening curves for both elastic and elasto-plastic analyses are given in figure 42. The load-deflection curves for points A and C are shown in figure 43. Figure 44 shows the spread of plasticity in the stiffener and plate and the deflection profiles for different sections. The ultimate stress is about 0.8 times the yield stress and only a half of the buckling stress.

4.3.2.3 *Longitudinally Stiffened Plate*

The elastic post-buckling behaviour of the longitudinally stiffened plate shown in figure 45 has been investigated by Bilstein[79,80]. The plate has a low buckling stress of 788 Kp/cm^2 compared with the yield stress of 2400 Kp/cm^2. The plate has sinusoidal initial out-of-plane displacements with $w_o = 1.0$ t. Although the present theory has been derived for stiffeners with solid rectangular cross-section, ignoring the effect of warping, the above mentioned plate with L-stiffeners has been analysed approximately. The elastic load-central deflection curve is shown in figure 45. The results are very close to Bilstein's solution up to 1.1 times of the buckling stress, but later the present method gives larger displacements and at 1.84 times of the buckling stress the stiffeners fail. The larger deflections observed in the present method will be also caused by in-plane buckling of the stiffener which has not been included in Bilstein's solution.

4.3.2.4 *Elasto-Plastic Stiffened Plate with Residual Stresses*

A range of simply supported longitudinally stiffened steel plates has been tested by Fukomoto et al.[4] for uniformly distributed edge compression in one direction. One of these, shown in figure 46 has been analysed using the present program. The actual and the assumed residual stress patterns are shown in figure 46. The assumed residual stress patterns are so determined that the self-equilibrating conditions are satisfied independently within each plate subpanel and within each stiffener. The maximum values of measured initial plate deflection and of initial displacement along the free edges of stiffeners are 1.03 mm and 0.54 mm respectively. The loaded edges were simply supported and the specimen was set in position so that the axial line load was applied through the centroidal axis of the end cross-section of the specimen. The unloaded edges were simply supported and stress free. These edges were supported vertically by steel pipes of 22 mm diameter of 75 mm spacing along the edge.

The load-deflection (figure 47) and load-shortening curves (figure 48) have been obtained for three different values of initial deflections and residual stresses. The ultimate stress obtained for the initial deflection and residual stresses similar to the test conditions is 0.96 times of the yield stress which is about 13% higher than that of 0.835 found by testing. The analysis shows an overall buckling of the stiffened plate towards the stiffener, which was also observed in the test. The difference in ultimate load will be caused mainly by the support conditions at unloaded edges. Fukumoto et al. mention in their report that their results seem to be low in strength compared with the other test results as well as the theoretical predictions. As one

of the main reasons for the discrepancy, they recognize that the deflections of the plate were not rigidly constrained along their unloaded edges. In the present solution the initial out-of-flatness of stiffeners was also less than those of the test specimen. The ultimate stress obtained for a maximum initial deflection of 1.0 times of plate's thickness is only 4,5% larger than the test result. The deflection profiles and the spread of plasticity in stiffeners and plate for different load levels are given in figures 49, 50 and 51.

4.4 PLATES SUBJECT TO COMBINED DIRECT AND SHEAR IN-PLANE LOADING

As a further example to demonstrate the application of the present theory, the response of stiffened and unstiffened plates subject to combined shear and in-plane bending has been studied. This type of loading occurs in the web panels of plate and box girders such as those used in bridges. The behaviour of isotropic plates subject to such loading has been investigated by Crisfield[17], Harding [113] and Frieze[111]. Harding et al.[114,143] have presented a detailed study on this subject, discussing the effect of different parameters such as plate slenderness ratio, initial imperfection and residual stresses. The direct and shear in-plane loading has been applied as in-plane normal and shear displacements along the edges.

4.4.1 Isotropic Plates

4.4.1.1 *Elastic Plate Under Shear Load*

The post-buckling behaviour of the simply supported plate shown in figure 52 has been investigated earlier by Williams[53] and Crisfield[17] using a dynamic relaxation and a finite element method respectively.

All edges are constrained to remain straight and the loading is applied as axial and shear displacements. The average shear stress-central deflection curve is obtained for two different mesh sizes and is compared with results presented by Williams and Crisfield. A very close agreement with Williams' solution is obtained (figure 52). The out-of-plane deflection profiles across the tensile and compressive diagonals for different load levels are also shown in figure 52.

4.4.1.2 *Elasto-Plastic Square Plate*

A simply supported square plate with the slenderness ratio a/t = 120 has been analysed for combined shear and in-plane bending. The loading is applied as in-plane normal and shear displacements along the left and right hand sides of the plate and shear displacements along the top and bottom edges as shown in fig. 53. The top and bottom edges are unrestrained and there are no transverse in-plane stress components along these edges. Average stress-strain curves are plotted in fig. 53 and are compared with results presented by Harding et al.[143]. Although they used a different yield criterion (von Mises' yield criterion, multi-layer approach) than that used in the present solution, a close agreement can be observed between results. For different load levels, out-of-plane deflection profiles along the tensile and compressive diagonals are plotted in figure 54, which show the upward buckles along the compressive diagonal. The out-of-plane deflection contours expressed as multiples of the plate thickness t are shown in figure 56.

4.4.2 Stiffened Plates

Stiffened web panels are used frequently in marine and civil engineering structures and in general they are subjected to combined in-

plane bending and shear loading. In this section some stiffened web panels are analysed and since no similar solutions are available, the results are compared with solutions obtained by Harding et al.[143] for isolated plates with restrained and unrestrained edges. It is of particular interest to note that the examples presented form part of a series used to validate a design procedure currently being incorporated into the new British bridge code. Five different plates each with two stocky flat stiffeners have been analysed. The square centre panels of three plates have a slenderness ratio a/t = 60 and this ratio for the other two plates is 120. The depth/thickness ratio is constant and equal to 8 for all stiffeners. For plates with a/t = 60, three different stiffeners thickness values of 0.5 t, 1.0 t and 2.0 t and for plates with a/t = 120 values of 0.5 t and 2.0 t have been considered. Harding[143] has analysed two plates with the same dimensions with stiffener positions represented by zero deflection nodal lines but without stiffeners. Loading and plates dimensions are shown in figure 55. This figure also shows the average shear stress-strain curvesfor the centre panels of plates with a/t = 60 and a/t = 120 respectively. Harding's results for similar restrained and unrestrained single panels and the three panel deep webs are also plotted for comparison. In both cases of a/t = 60 and a/t = 120, the restrained single panels are the strongest, but for plates with stronger stiffeners ($t_s/t = 2$) the centre panel strength is very close to that the restrained single panel. In the case of a/t = 120 the difference in ultimate strength for the restrained single panel and the stiffened plate with $t_s/t = 2.0$ is about 3% and for a/t = 60 this value is about 4%. For a/t = 60 the ultimate strengths for $t_s/t = 0.5$ and $t_s/t = 1.0$ are about $0.88\tau_0$ and $0.93\tau_0$ respectively. For $t_s/t = 2.$ no convergence

was achieved after $\gamma / \gamma_0 = 0.95$ with $\tau = 0.93 \tau_0$ which may indicate stiffener failure. For a/t = 120 the computed ultimate strengths are $0.78 \tau_0$ and $0.89 \tau_0$ for $t_s/t = 0.5$ and $t_s/t = 2.0$ respectively. In figure 55 the results for plates with a/t = 60 show that even for a large stiffener thickness , stiffener failure is occurring, probably due to the failure of the adjacent compression panels. Figure 55 shows also that for plates with weak stiffeners the strength is even less than that of an unrestrained single panel which is due to the out-of-plane displacements along the stiffe er location. In the case of plates with strong stiffeners although the ultimate strength is close to that of restrained single panels the deflection shapes are completely different. This can be seen from figure 56 comparing the contours of out-of-plane displacements for the stiffened plates with that of the single panel. Figure 57 shows the average shear stress-strain curves for the whole stiffened plates. The variation of shear stress distribution for the plate with a/t = 120 is shown in figure 58. Figure 59 shows the distribution of transverse stress components along the top and bottom edges for two different load levels. The distribution of normal stress in right and left-hand sides and at the centre-line are shown in figure 60. The practical implications of this study are discussed in the conclusions to the thesis.

CHAPTER 5

CONCLUSIONS AND FUTURE WORK

5.1 CONCLUSIONS

(1) The three governing simultaneous non-linear partial differential equilibrium equations presented for the first time in this thesis can account for the real elasto-plastic behaviour of discretely stiffened plates by considering plate and stiffeners separately rather than assuming an orthotropic continuum. The main advantage of the present method is its ability to consider different possible types of buckling which may occur and their interaction. Factors which have a significant effect on the behaviour of stiffened plates such as material properties, initial deflection and residual stresses are included in the present theory.

(2) The use of non-linear equilibrium equations in terms of forces rather than displacements makes the method especially suitable for elasto-plastic analysis.

(3) The finite difference method used for the numerical part of this work has some advantages compared to other available techniques. At each node there are three variables which is less than the five degree of freedoms used by the finite element method. Furthermore, in this method, the treatment of stiffeners involves only some changes in the rigidities of the appropriate nodes rather than the addition of new elements as in the finite element method. These result in savings on computer time and

storage and also help to avoid numerical instability even for reasonably large problems.

(4) The non-linear equilibrium equations are solved by a modified Newton-Raphson iterative method which uses the linearised equations in terms of displacements from which the matrix of coefficients is generated and its inverse is computed only once. It thus avoids the necessity of generating a new "tangent stiffness matrix" and solving the corresponding equations at each iteration. The application of Aitken's δ^2-extrapolation partly restores the loss in the speed of convergence (compared to the quadratically convergent original Newton-Raphson method) and in many instances ensures convergence where the modified Newton-Raphson method would have failed.

(5) In general, for cases of lateral loading the convergence is very quick and only 2-4 iterations are needed for each load increment. For instability problems, particularly for slender plates, a larger number of iterations is required. In such cases the convergence speed and also the result depend very much on the size of the load increments. Different convergence criteria have been used depending on the type of the structure and loading.

(6) The examples presented demonstrate the wide range of applicability of the present method to the analysis of stiffened plates subject to different types of loading and having different flexural and membrane boundary conditions.

(7) The comparisons of solutions from the new analysis with existing theoretical and experimental results have established its accur-

acy. Although the present method was derived for solid rectangular sections, the analysis of a plate with L-stiffeners showed that even in such cases fairly accurate results can be achieved. Although the von Mises' yield criterion (multi-layer approach) can be easily incorporated into the present analysis, the examples quoted herein have shown that sufficiently accurate solutions can be achieved in most cases using the Ilyushin approximate yield criterion.

(8) The method has been used to help formulate a new design method for longitudinally stiffened plate or box girder webs. The basic philosophy used in this method is to design outer plate panels of such webs as unrestrained (against in-plane movement) and inner panels as restrained. It was essential to establish the criteria which should be met to ensure the validity of this approach. Comparisons between existing elasto-plastic plate programs developed for isolated panels and the present program which can accurately represent a multi-stiffened panel, quickly established that the stiffeners bounding inner panels would have to provide sufficient axial stiffness to ensure that inner panels could be safely treated as restrained panels - a factor which had been overlooked in the original formulation of the design procedure.

5.2 FUTURE WORK

(1) The relevant design parameters for stiffened plates are too numerous to be investigated thoroughly using an experimental approach. However, numerical studies using the present method could generate results covering the range of practical parameters

in a more economical and efficient manner. Thus the analysis may be used for future parametric studies on which limit state design rules for multi-stiffened plated structures can be based.

(2) The present analysis should be extended to allow for the effects of stiffener warping so that sections other than flats can be more accurately covered by the method.

(3) The edges of the plate are assumed to be rigidly supported and not to have any stiffeners in the analysis presented, but often the plates have some edges which are free and even more often edge stiffeners are present. Therefore, it would be useful to extend the range of boundary conditions covered by the analysis.

(4) In the present work the initial out-of-plane displacements of plate and also the out-of-straightness induced in stiffeners due to these displacements have been considered. However, it is not difficult to include the additional initial bow of stiffeners.

(5) Future research is needed to consider the effect of shear stress due to torsion on the stiffener yielding.

(6) Future research should be directed towards the optimization of solution techniques for non-linear equations for special problems such as stiffened plates.

(7) Further analysis with finer mesh divisions should be undertaken and more experimental verification is needed.

REFERENCES

1. Tvergaard, V. and A. Needleman. "Mode interaction in an eccentrically stiffened elastic-plastic panel under compression". DCAMM Report No. 69, June 1974, The Technical University of Denmark, Lyngby, Denmark.

2. Tvergaard, V. "Imperfection-sensitivity of a wide integrally stiffened panel under compression". Int. J. Solids Structures, Vol. 9, p.177, 1973.

3. Tvergaard, V. "Influence of post-buckling behaviour on optimum design of stiffened panels". Int. Journal of Int. J. Solids Structures, 9, pp.1519, 1973.

4. Fukumoto, Y., T. Usami and Y. Okamoto. "Ultimate compressive strength of stiffened plates". Preprints ASCE Specialty Conference on Metal Bridges. St. Louis, November 12-13, 1974, pp.201-230.

5. Levy, S., D. Goldenberg and G. Zibritosky. "Simply supported long rectangular plates under combined axial load and normal pressure". NACA TN 949, Oct. 1944.

6. Dwight, J.B., T.K. Chin and A.T. Ratcliffe. "Local buckling of thin-walled columns, effect of locked-in welding stresses". CIRIA Res. Rep. No. 12, (Pt. 2) May, 1968.

7. Dwight, J.B. and K.E. Moxham. "Welded steel plates in compression". The Structural Engineer, Vol. 47, No. 2, Feb. 1969, pp.49-66.

8. Nishino, F., Y. Ueda and L. Tall. "Experimental investigation of buckling of plates with residual stresses. Test methods for compression members". ASTM STP419, Am. Soc. Testing Mats, 1967, p.12.

9. Dwight, J.B., T.K. Chin and A.T. Ratcliffe. "Local buckling of thin-walled columns, effect of locked-in residual stresses". CIRIA Res. Rep. No. 12 (Pt. 1), May, 1968.

10. Smith, C.S. "Compressive strength of welded steel ship grillages". Trans. R.I.N.A., Vol. 117, (Spring Meeting) 1975.

11. Timoshenko, S.P. and J.M. Gere. "Theory of elastic stability". McGraw-Hill Book Co. N.Y., 1961.

12. Timoshenko, S.P. and S. Woinowsky-Krieger. "Theory of plates and shells". McGraw-Hill Book Co., N.Y. 1959.

13. Timoshenko, S.P. and J.N. Goodier. "Theory of elasticity". McGraw-Hill Book Co., N.Y. 1970.

14. Bleich, J.F. "Buckling strength of metal structures". McGraw-Hill Book Co., London, 1952.

15. Girkman, K. "Flaechentragwerke". Springer-Verlag, Wien, 1959.

16. Dean, J.A. "The collapse behaviour of steel plating subject to complex loading". PhD Thesis, University of London (Imperial College), 1975.

17. Crisfield, M.A. "Large-deflection elasto-plastic buckling analysis of plates using finite elements". Department of the Environment, TRRL Report LR 593, Crowthorne, England, 1973.

18. Søreide, T.H., P.G. Bergan and T. Moan. "Ultimate collapse behaviour of stiffened plates using alternative finite element formulations". Proc. International Conference on Steel Plated Structures, Imperial College, London, July 6-9, 1976.

19. Søreide, T.H. and T. Moan. "Non-linear material and geometric behaviour of stiffened plates". Report No. SK/M31, Division of Ship Structures, The Norvegian Institut of Technology, The University of Trondheim, Norway, 1975.

20. Moan, T. and T.H. Søreide. "Analysis of stiffened plates considering non-linear material and geometric behaviour using finite element method". Proc. World Congress on Finite Element Methods in Structural Mechanics, Bournemouth, England, Oct. 12-17, 1975.

21. Bulson, P.S. "The stability of flat plates". Chatto and Windus Co., London, 1970.

22. Column Research Committee of Japan (Edited by). "Handbook of structural stability". Corona Publishing Ltd., Tokyo, 1971.

23. Moffatt, K.R. "Finite element analysis of box girder bridges". PhD Thesis, University of London (Imperial College), 1974.

24. Lekhnitskii, S.G. "Anisotropic plates". Gordon and Breach, Science Publisher Ltd., London, 1968.

25. Pflueger, A. "Zum Beulproblem anisotroper Rechteckplatten". Ingenieur-Archiv, Vol. 16, 1947, p.111.

26. Pflueger, A. "Die Orthotrope Platte mit Hohlsteifen". Oesterreichishes Ingenieur-Archiv, Vol. 9, No. 2-3, 1955, pp.199-207.

27. Gienke, E. "Die Grundgleichungen fuer die Orthotrope Platte mit exzentrischen Steifen". Der Stahlbau, Vol. 24, June 1955, pp.128-129.

28. Trenks, K. "Beitrag Zur Berechnung orthogonal anisotroper Rechteckplatten". Der Bauingenieur 29, 1954, p.372.

29. Dean, D.L. and C. Omid'varan. "Analysis of ribbed plates". J. of Struct. Div., Proc. A.S.C.E., Vol. 95, No. ST3, March 1969, pp.411-440.

30. Wah, T. and L.R. Calcote. "Structural analysis by finite difference calculus". Van Nostrand Reinhold Co., New York, N.Y. 1970.

31. Gienke, E. "Einfluss der Steifen-Exzentrizität auf Biegung und Stabilitaet orthotroper platten". Beitrag aus Statik und Stahlbau, Stahlbau-Verlag G.m.b.H., Koeln, 1961.

32. Timoshenko, S. "Ueber die Stabilitaet versteifter Platten". Eisenbau Vol. 12, 1921, p.147.

33. Loshkin, A.S. "On the calculation of plates with ribs". J. Applied Math. and Mechanics, Vol. 2, Moscow, 1935, p.225.

34. Barbré, R. "Beulspannungen von Rechteckplatten mit Laengssteifen bei gleichmaessiger Druckbeanspruchung". Der Bauingenieur Vol. 17, 1936, No. 25/26, pp.268-273.

35. Barbré, R. "Stabilitaet gleichmaessig gedrueckter Rechteckplatten mit Laengs oder Quersteifen". Ingenieur-Archiv, Vol. 8, 1937, p.117.

36. Froehlich, H. "Stabilitaet der gleichmaessig gedrueckten Rechteckplatte mit Steifenkreuz". Der Bauingenieur Vol. 29, Oct. 1937.

37. Huber, M.T. "Die Theorie der Kreuzweise bewehrten Eisenbetonplatten nebst Anwendungen auf mehrere bautechnisch wichtige Aufgaben ueber rechteckige Platten". Bauingenieur, Vol. 4, 1923, pp.354-392.

38. Pelikan, W. and M. Esslinger. "Die Stahlfahrbahn". Berechnung und Konstruction, M.A.N. Forshungsheft, No. 7, 1957.

39. Murray, N.W. "Analysis and design of stiffened plates for collapse load". The Structural Engineer, Vol. 53, No. 3, March 1975.

40. Massonnet, Ch. and R. Maquoi. "New theory and tests on the ultimate strength of stiffened box girders". Proc. Int. Conference on Steel Box Girder Bridges, I.C.E., London, 13-14 Feb. 1973.

41. Dowling, P.J., S. Chatterjee, P.A. Frieze and F.M. Moolani. "The experimental and predicted behaviour of rectangular stiffened steel box girders". Proc. Int. Conference on Steel Box Girder Bridges, I.C.E., London, 13-14 Feb. 1973.

42. Dorman, A.P. and J.B. Dwight. "Tests on stiffened compression plates and plate panels". Proc. Int. Conference on Steel Box Girder Bridges, I.C.E., London, 13-14 Feb. 1973.

43. Clarkson, J. "Test of flat plated grillages under uniform pressure". Trans. R.I.N.A., Vol. 105, No. 4, 1963.

44. Clarkson, J. "Small-scale grillage tests". Trans. R.I.N.A., Vol. 109, No. 2, 1967.

45. Von Karman, Th. "Festigkeitsprobleme in Maschinenbau". Encyklopaedie der Mathematischen Wissenshaften, IV, 1910.

46. Marguerre, K. "Die mittragende Breite der gedrueckten Platte". Luftfahrt-Forschung, Vol. 14, 1937.

47. Marguerre, K. "Zur Theorie der gekruemmter Platte grosser Formaenderung". Proc. of the Fifth Int. Cong. for Appl. Mech., Cambridge, 1938.

48. Kaiser, R. "Rechnerische und experimentelle Ermittlung der Durchbiegung und Spannungen von quadratischen Platten bei freier Auflagerung an den Raendern, gleichmaessig verteilter Last und grossen Ausbiegungen". Z.f.A.M.M., Band 16, Heft 2, April 1936.

49. Levy, S. "Bending of rectangular plates with large deflection". NACA, TN 846, 1942.

50. Levy, S. "Square plate with clamped edges under normal pressure producing large deflections". NACA, TN 847, 1942.

51. Levy, S. and S. Greenman. "Bending with large deflection of a clamped rectangular plate with length width ratio of 1.5 under normal pressure". NACA, TN 853.

52. Wang, C.T. "Bending of rectangular plates with large deflections". NACA, TN 1462, 1948.

53. Williams, D.G. "Some examples of the elastic behaviour of initially deformed bridge panels". Civil Eng. and Pub. Wks. Rev., Oct. 1971, pp.1107-1112.

54. Rushton, K.R. "Large deflection of plates with unsupported edges". Journal of Strain Analysis, Vol. 7, No. 1, 1972, pp.44-53.

55. Way, S. "Uniformly loaded, clamped, rectangular plates with large deflection". Proc. Fifth Int. Cong. of Appl. Mech., Cambridge, Mass., 1938, p.123.

56. Chien, W.Z. and K.Y. Yeh. "On the large deflection of rectangular plates". Proc. Ninth Int. Cong. Appl. Mech., Brussels, Belgium, Vol. 6, 1957, pp.403-412.

57. Thompson, J.M.T. and A.C. Walker. "A non-linear perturbation analysis of discrete structural systems". Int. Journal of Solids and Structures, 4, 1968, pp.757-767.

58. Coan, J.M. "Large deflection theory for plates with small initial curvature loaded in edge compression". Journal of Appl. Mech., 18, 2, June 1951, pp.143-151.

59. Yamaki, N. "Post-buckling behaviour of rectangular plates with small initial curvature loaded in edge compression". Journal of Appl. Mech., 26, 3 Sept. 1959, pp.407-414.

60. Walker, A.C. "The post-buckling behaviour of simply supported square plates". Aeronautical Quarterly, 20, 3 Aug. 1969, pp.203-226.

61. Dawson, R.C. and A.C. Walker. "Post-buckling of geometrically imperfect plates". Journal of Struct. Div., Proc. ASCE, Jan. 1972, ST1, pp.75-94.

62. Turner, M.J., E.H. Dill, H.C. Martin and R.J. Melosh. Large deflection of structures subject to heating and external loads". Journal of Aerospace Sciences, Vol. 27, Feb. 1960.

63. Mallet, R.H. and P.V. Marcel. "Finite element analysis of non-linear structures". Journal of Struct. Div. Proc. ASCE, Vol. 94, No. ST9, Sept. 1968, pp.2081-2105.

64. Murray, D.W. and E.L. Wilson. "Finite element large deflection analysis of plates". Journal of Eng. Mech. Div., Vol. 95, No. EM1, Feb. 1969, pp.143-165.

65. Murray, D.W. and E.L. Wilson. "Finite element post-buckling analysis of thin elastic plates". American Inst. of Aero. and Astro, Jrnal, Vol. 7, 1969, pp.1915-1930.

66. Oden, J.T. "Numerical formulation of non-linear elasticity problems". Journal of Struct. Div. Proc. ASCE, Vol. 93, No. ST3, June 1967.

67. Brebbia, C. and J. Connor. "Geometrically non-linear finite element analysis". Journal of Eng. Mech. Div. Proc. ASCE, Proc. Paper 6516, April 1969.

68. Zienkiewicz, O.C. "The finite element in engineering science". McGraw-Hill, London, 1971.

69. Vogel, U. "Der Biege und Membranspannungszustand der rechteckigen orthotropen Platten mit grosser Durchbiegung unter gleichmaessig verteilter Vollast bei Navierschen Randbedingungen, naeherungweise behandelt mit Hilte der Energie-Methode". Thesis presented to the Stuttgart Technischen Hochschule for the degree of Doctor-Ingenieurs. Stuttgart, West Germany, 1960.

70. Basu, A.K. "The theory of orthotropic plates under lateral pressure and its application to corrugated plates". PhD thesis, University of London (Imperial College), 1964.

71. Basu, A.K. and J.C. Chapman. "Large deflection behaviour of transversely loaded rectangular orthotropic plates". Proc. Inst. Civ. Engrs., Vol. 35, Sept. 1966.

72. Aalami, B. "Non-linear behaviour of rectangular orthotropic plates under in-plane and transverse loading". PhD thesis, University of London (Imperial College), 1967.

73. Faulkner, D. "A review of effective plating to be used in the analysis of stiffened plating in bending and compression". Journal of Ship Research, Vol. 19, No. 1, March 1975.

74. Rubin, H. "Longitudinally stiffened and compressed plates of box girders". ECCS Commission 8, Working Group 3 Document.

75. Rubin, H. "Das Tragverhalten Laengsversteifter, vorverformter Rechteckplatten unter Axialbelastung nach der nichtlinearen Beultheorie". Schriftenreihe, Heft 1, 1976, Institut fuer Baustatik und Messtechnik, Universitaet Karlsruhe, Karlsruhe, West Germany.

76. Vogel, U. "Herleitung der Differentialgleichungen der orthogonal-anisotropen Platte mit grosser Durchbiegung (nach der Theorie II Ordnung) durch Anwendung der Variationsrechnung". Der Stahlbau 31, 1962, p.119.

77. Soper, W.G. "Large deflection of stiffened plates". Journal of Appl. Mech., Dec. 1958.

78. Skaloud, M. and R. Novotny. "Ueberkritisches Verhalten einer anfaenglich gekruemmten, gleichfoermig gedrueckten in der Mitte mit einer Laengsrippe versteiften Platte". Acta Technica CSAV, No. 2, 1965.

79. Bilstein, W. "Anwendung der nichtlinearen Beultheorie auf Vorverformte, mit discreten Laengssteifen verstaerkte Rechteckplatten unter Laengsbelastung. Heft 25, Veroeffentlichungen des Institutes fuer Statik und Stahlbau der Technischen Hochschule Darmstadt, Darmstadt, West Germany, 1974.

80. Bilstein, W. "Beitrag zur Berechnung Vorverformter, mit discreten Laengssteifen ausgesteifter, ausschliesslich in Laengsrichtung belasteter Rechteckplatten nach der nichtlinearen Beultheorie". Der Stahlbau 43, 1974, p.193.

81. Weiss, S. and O. Zaenkert. "Uber das Nachbeulverhalten einachsig gedrueckter, einfach ausgesteifter Rechteckplatten und ihre Beanspruchung bei Anfangsausbiegungen". Bericht No. 42, 1974, Forschungszentrum des Deutschen Schiffbaus (FDS), Hamburg, West Germany.

82. Bhaumik, A.K. and J.T. Hanley. "Elasto-plastic plate analysis by finite differences". Journal of Struct. Div., Proc. ASCE, No. ST5, Oct. 1967, pp.279-294.

83. Von Mises. "Mechanik der festen Koerper in plastisch deformablen Zustand". Nach Math. Phys. Klasse, Goettingen, West Germany, 1913, pp.582-592.

84. Tresca, H. "Comptes Rendus". Academie des Sciences, Paris, Vol. 59, 1864, p.754.

85. Johansen, K.W. "The ultimate strength of reinforced concrete slabs". Final Report, 3rd. Congress, IABSE, Belgium Sept. 1948, pp.565-570.

86. Lin, T.H. and E. Ho. "Elasto-plastic bending of a thin rectangular plate". Journal of Eng. Mech. Div., Proc. ASCE, Vol. 94, EM1, 1968, pp.199-210.

87. Yam, L.C.P. and P.C. Das. "Elasto-plastic analysis of reinforced concrete slabs - some implications of limit state design". Proc. Int. Conf. on Developments in Bridge Design and Construction, Cardiff, 1971, edited by K.C. Rockey, J.O. Bannister and H.R. Evans, Pub. Crosby Lockwood, London, pp.144-160.

88. Ang, A.H.S. and L.A. Lopez. "Discrete model analysis of elastic-plastic plates". Journal of Eng. Mech. Div., Proc. ASCE, Vol. 94, No. EM1, Feb. 1968, pp.271-293.

89. Ilyushin, A.A. "Plasticité". Editions Eyrolles, Paris, 1956.

90. Bleytschko, T. and M. Velebit. "Finite element method for elastic plastic plates". Journal of Eng. Mech. Div., Proc. ASCE, EM1, Feb. 1972, pp.227-242.

91. Mendelson, A. "Plasticity: Theory and application". The Macmillan Company, New York, 1968.

92. Marcal, P.V. and R.H. Mallet. "Elasto-plastic analysis of plates by the finite element method". Proc. ASME, Winter Annual Meeting, Paper 68-WA3PVB-10, Dec. 1968.

93. Marcal, P.V. and I.P. King. "Elastic-plastic analysis of two dimensional stress systems by the finite element method". Int. Journal of Mech. Sci. Vol. 9, No. 3, 1967, pp.143-155.

94. Yamada, Y., N. Yoshimura and T. Sakurai. "Plastic stress-strain matrix and its application for the solution of elasto-plastic problems by the finite element method". Int. Journal of Mech. Sci., No. 10, 1968, pp.343-354.

95. Whang, B. "Elasto-plastic orthotropic plates and shells". Proc. Symp. on Application of Finite Element Methods in Civil Engineering, School of Eng. Vanderbilt University, ASCE, 1969, pp.481-516.

96. Terazawa, K., et al. "Elasto-plastic buckling of plates using the finite element method". Journal of the Society of Naval Architecture of Japan, Vol. 127, 1970.

97. Wegmuller, A.W. and C.N. Kostem. "Finite element analysis of elastic-plastic plates and eccentrically stiffened plates". Report No. 378A.4, Finite Engineering Laboratory, Lehigh University, 1973.

98. Wegmuller, A.W. "Full-range analysis of eccentrically stiffened plates". Journal of Struct. Div. Proc. ASCE, Vol. 100, No. ST1, Jan. 1974, pp.143-159.

99. Kagan, H.A. and G.G. Kubo. "Elasto-plastic analysis of reinforced plates". Journal of Struct. Div. Proc. ASCE, Vol. 94, No. ST4, April 1968.

100. Djahani, P. "Large-deflection elastic analysis of discretely stiffened plates subject to transverse and/or in-plane loading". MSc thesis, University of London (Imperial College), 1974.

101. Moxham, K.E. "Theoretical prediction of the strength of welded steel plates in compression". Cambridge University Report No. CUED/C-Struct/TR2, 1971.

102. Powell, M.J.D. "An iterative method for finding stationary values of a function of several variables". The Computer Journal, Vol. 5, 1966, p.147.

103. Crisfield, M.A. "On an approximate yield criterion for thin steel shells". Department of the Environment, TRRL Report LR 658, Crowthorne, England, 1974.

104. Crisfield, M.A. "Some approximations in the non-linear analysis of rectangular plates using finite elements". Department of the Environment, TRRL Report No. SR 51 UC, Crowthorne, England, 1974.

105. Crisfield, M.A. "Collapse analysis of box girder components using finite elements". Department of the Environment, Symposium on non-linear techniques and behaviour in structural analysis. Transport and Road Research Laboratory, Crowthorne, Dec. 1974, SR 164 UC.

106. Crisfield, M.A. "Combined material and geometric non-linearity for thin steel plates". World Congress on finite element methods in structural mechanics, Ed. J. Robinson, Bournemouth, England, 1975.

107. Crisfield, M.A. and R. Puthli. "A finite element method applied to the collapse analysis of stiffened box girder diaphragms". Proc. International Conference on Steel Plated Structures, Imperial College, London, July 6-9, 1976.

108. Yam, L.C.P. "Finite difference method for non-linear plate problems and parametric study". Department of the Environment, Symposium on Non-Linear Techniques and Behaviour in Structural Analysis. Transport and Road Research Laboratory, Crowthorne, England, Dec. 1974.

109. Yam, L.C.P. "Problem classification and basic techniques in analysis of inelastic stability of plates". Department of the Environment, TRRL Report No. LR 657, Crowthorne, England, 1974.

110. Yam, L.C.P. "New developments in theory and method of analysis for inelastic plates and shells". Department of the Environment, Symposium on Non-Linear Techniques and Behaviour in Structural Analysis. Transport and Road Research Laboratory, Crowthorne, England, Dec. 1974.

111. Frieze, P.A. "Ultimate load behaviour of steel box girders and their components". PhD thesis, University of London (Imperial College), 1975.

112. Frieze, P.A., P.J. Dowling and R.E. Hobbs. "Steel Box Girders. Parametric study on plates in compression". Engineering Structures Laboratories, Civil EngineeringDepartment, Imperial College, London. CESLIC Report BG39, January 1975.

113. Harding, J.E. "Bolted spliced panels and stress redistribution in box girder components up to collapse". PhD thesis, University of London (Imperial College), 1975.

114. Harding, J.E., R.E. Hobbs and B.G. Neal. "Ultimate load behaviour of plates under combined direct and shear in-plane loading". Proc. International Conference on Steel Plated Structures, Imperial College, London, July 6-9, 1976.

115. Marcal, P.V. "Finite element analysis of combined problems of non-linear material and geometric behaviour". Proc. American Soc. Mech. Eng. Conference on Computational Approaches in Applied Mech. June 1969.

116. Bergan, P.G. "Nonlinear analysis of plates considering geometric and material effects". Report No. 72-1, Division of Structural Mechanics, The Norwegian Institute of Technology. The University of Trondheim, Norway, 1972.

117. Crisfield, M.A. "Full-range analysis of steel plates and stiffened plating under uniaxial compression". Proceedings Institution of Civil Engineers, Vol. 59, 1975.

118- Stricklin, J.A., W.A. Von Rieseman, J.R. Tillerman, W.E. Haisler. "Static geometric and material nonlinear analysis". Proceedings Advances in Computational Methods in Structural Mechanics and Design. J.T. Oden, R.W. Clough and Y. Yamamoto,(eds.) University of Alabama Press, 1972.

119. Stricklin, J.A., W.E. Haisler and W.A. Von Rieseman. "Computation and solution procedures for non-linear analysis by combined finite element - finite difference methods". Computers and Structures, Vol. 2, Dec. 1972, pp. 965-974.

120. Stricklin, J.A., W.E. Haisler and W.A. Von Rieseman. "Formulation, computation and solution procedures for material and/or geometric non-linear analysis by the finite element method". Report SC-CR-72, 3102, Saudia Laboratories, Albuquerque, New Mexico, Livermore, California, July 1972.

121. Wah, T. "The buckling of gridworks". Journal of Mech. Phys. Solids, Vol. 13, 1965, pp. 1.

122. Cox, H.L. and P.H. Denke. "Stress distribution, instability and free vibrations of beam gridworks on elastic foundations". Journal of Aero. Sciences,Vol. 23, 1956.

123. Smith, C.S. "Elastic buckling and beam-column behaviour of ship grillages". Trans. RINA, Vol. 110, Jan. 1968.

124. Smith, C.S. and W. Kirkwold. "Influence of initial deformations and residual stresses on inelastic flexural buckling of stiffened plates and shells". Proc. International Conference on Steel plated Structures, Imperial College, London, July 6-9, 1976.

125. Moolani, F.M. "Ultimate load behaviour of steel box girder stiffened compression flanges". PhD Thesis, University of London (Imperial College), 1976.

126. Ractliffe, A.T. "The strength of plates in compression". PhD Thesis, Cambridge University, 1966.

127. Vojta, J. and A. Ostapenko. "Design curves for longitudinally stiffened plate panels with large b/t". Fritz Engineering Laboratory, Report No. 248.19, Lehigh University, August 1967.

128. Parsanejad, S. "Ultimate strength analysis of plate grillages under combined loads using a grid model". PhD Thesis, Lehigh University, 1972.

129. Horne, M.R. and R. Narayanan. "An approximate method for the design of stiffened steel compression panels". Proc. Inst. of Civil Engineers, Part 2, Vol. 59, Sept. 1975.

130. Horne, M.R. and R. Narayanan. "(i) Ultimate load capacity of longitudinally stiffened panels. (ii) Further tests on the ultimate load capacity of longitudinally stiffened panels". Simon Engineering Laboratories, University of Manchester, 1974.

131. Virdi, K.S. "Inelastic column behaviour: Its application to composite columns in biaxial bending and stiffened plates in compression". PhD Thesis, University of London (I.C.), 1973.

132. Dowling, P.J. "Strength of steel box girder bridges". Journal of Struct. Div. Proc. ASCE. Vol. 101, No. ST9, Sept. 1975.

133. Dowling, P.J. "Some approaches to the non-linear analysis of plated structures". Symposium on Non-Linear Techniques and Behaviour in Structural Analysis. Transport and Road Research Laboratory, Crowthorne, England, Dec. 11-12, 1974.

134. Moeller, B. "Berechnung orthotroper Stahlplatten in Traglast-breich". Int. Assoc. for Bridge and Struct. Engineering (IABSE). Vol. 32-1, 1972, pp. 167-177.

135. Lin, T.H., S.R. Lin and B. Mazelsky. "Elasto-plastic bending of rectangular plates with large deflection". Journal of Applied Mech., Dec. 1972, pp. 978-982.

136. Robinson, M. "A comparison of yield surfaces for thin shells". Int. J. Mech. Sci., Vol. 13, No. 4, 1971, pp. 345-354.

137. Mikeladze, M.Sh. "Theory of perfectly plastic thin shells". Proc. Symp. IASS. Warsaw (1963), Ed. Olszak and Sawzuk, North-Holland, Amsterdam, 1964, pp. 722-731.

138. Massonet, C. "General theory of elasto-plastic membrane plates". Engineering Plasticity, edited by J. Heyman and F.A. Leakie, Cambridge University Press, 1968, pp. 443-473.

139. Hill, R. "The mathematical theory of plasticity". Oxford University Press, 1950.

140. Baecklund, J. and H. Wennerstrom. "Finite element analysis of elasto-plastic shells". Int. J. for Num. Meth. in Engng., Vol. 8, 1974, pp. 415-424.

141. Baecklund, J. "Finite element analysis of non-linear structures". Department of Structural Mechanics, Chalmers University of Technology, 1973.

142. Lyons,L.P.R. "A general finite element system with special references to the analysis of cellular structures". PhD Thesis, University of London (Imperial College), 1977.

143. Harding, J.E., R.E. Hobbs, B.G. Neal and J. Slatford. "Parametric study on plates under combined direct and shear in-plane loading". Engineering Structures Laboratories, Civil Engineering Department, Imperial College, London. CESLIC Report BG44, Oct. 1976.

144. Dowling, P.J. "The behaviour of stiffened plate bridge decks under wheel loading". PhD Thesis, University of London (Imperial College), 1968.

145. Walker, A.C. and P. Davies. "An elementary study of non-linear buckling phenomena in stiffened plates". Symposium on Non-Linear Techniques and behaviour in structural analysis. Transport and Road Research Laboratory, Crowthorne, England, Dec. 1974.

146. Walker, A.C. and N.W. Murray. "A plastic collapse mechanism for a compressed plate". IABSE, Vol. 35/I, 1975.

147. Crisfield, M.A. "Large-deflection elasto-plastic buckling analysis of eccentrically stiffened plates using finites elements". Department of the Environment, TRRL Report No. LR 725, Crowthorne, England, 1976.

APPENDIX A

EQUILIBRIUM EQUATIONS IN TERMS OF FORCES FOR DIFFERENT NODE TYPES

In 2.1.1.2 the interactive forces at the junction of plate and a longitudinal (x-direction) stiffener were obtained. The interactive forces of the plate and a transverse (y-direction) stiffener are found from equations (11)-(14) by replacing displacement v by u, subscript 1 by 2 and interchanging x and y:

$$F_{x2} = \frac{\partial^2 M_{H2}}{\partial y^2} + N_{A2} \frac{\partial^2 \bar{u}_{c2}}{\partial y^2} + \frac{\partial N_{A2}}{\partial y} \frac{\partial \bar{u}_{c2}}{\partial y} \tag{A-1}$$

$$F_{y2} = \frac{\partial N_{A2}}{\partial y} \tag{A-2}$$

$$F_{z2} = \frac{\partial^2 M_{V2}}{\partial y^2} + e_2 \frac{\partial^2 N_{A2}}{\partial y^2} + N_{A2} \frac{\partial^2 \bar{w}}{\partial y^2} - \frac{\partial \bar{w}}{\partial x} \frac{\partial^2 M_{H2}}{\partial y^2} \tag{A-3}$$

$$T_2 = \frac{\partial M_{T2}}{\partial y} + e_2 \frac{\partial^2 M_{H2}}{\partial y^2} \tag{A-4}$$

Similar to equations (18)-(20), the equilibrium equations for nodes on stiffeners in y-direction can be written:

$$\frac{\partial N_x}{\partial x} + \frac{\partial N_{xy}}{\partial y} + \frac{1}{\Delta x} \left(\frac{\partial^2 M_{H2}}{\partial y^2} + N_{A2} \frac{\partial^2 \bar{u}_{c2}}{\partial y^2} + \frac{\partial N_{A2}}{\partial y} \frac{\partial \bar{u}_{c2}}{\partial y} \right) = 0 \tag{A-5}$$

$$\frac{\partial N_y}{\partial y} + \frac{\partial N_{xy}}{\partial x} + \frac{1}{\Delta x} \frac{\partial N_{A2}}{\partial y} = 0 \tag{A-6}$$

$$\frac{\partial^2 M_x}{\partial x^2} + 2 \frac{\partial^2 M_{xy}}{\partial x \partial y} + \frac{\partial^2 M_y}{\partial y^2} + \left(N_x \frac{\partial^2 \bar{w}}{\partial x^2} + 2 N_{xy} \frac{\partial^2 \bar{w}}{\partial x \partial y} + N_y \frac{\partial^2 \bar{w}}{\partial y^2} \right) + q +$$

$$\frac{1}{\Delta x} \left(\frac{\partial^2 M_{V2}}{\partial y^2} + \frac{\partial^2 N_{A2}}{\partial y^2} e_2 + N_{A2} \frac{\partial^2 \bar{w}}{\partial y^2} - \frac{\partial \bar{w}}{\partial x} \frac{\partial^2 M_{H2}}{\partial y^2} \right) = 0 \tag{A-7}$$

The equilibrium equations at the intersections of longitudinal and transverse stiffeners are obtained by writing for interaction forces $(F_{x1} / \Delta y + F_{x2} / \Delta x)$ etc....in equations (15)-(17), and then expressing the interaction forces in terms of internal forces in plate and stiffeners as in the previous cases:

$$\frac{\partial N_x}{\partial x} + \frac{\partial N_{xy}}{\partial y} + \frac{1}{\Delta y}\frac{\partial N_{A1}}{\partial x} + \frac{1}{\Delta x}\left(\frac{\partial^2 M_{H2}}{\partial y^2} + N_{A2}\frac{\partial^2 \bar{u}_{c2}}{\partial y^2} + \frac{\partial N_{A2}}{\partial y}\frac{\partial \bar{u}_{c2}}{\partial y}\right) = 0 \qquad \text{(A-8)}$$

$$\frac{\partial N_y}{\partial y} + \frac{\partial N_{xy}}{\partial x} + \frac{1}{\Delta x}\frac{\partial N_{A2}}{\partial y} \quad \frac{1}{\Delta y}\cdot\frac{\partial^2 M_{H1}}{\partial x^2} + N_{A1}\frac{\partial^2 \bar{v}_{c1}}{\partial x^2} + \frac{\partial N_{A1}}{\partial x}\frac{\partial \bar{v}_{c1}}{\partial x}\Big) = 0 \qquad \text{(A-9)}$$

$$\frac{\partial^2 M_x}{\partial x^2} + 2\frac{\partial^2 M_{xy}}{\partial x \partial y} + \frac{\partial^2 M_y}{\partial y^2} + \left(N_x\frac{\partial^2 \bar{w}}{\partial x^2} + 2N_{xy}\frac{\partial^2 \bar{w}}{\partial x \partial y} + N_y\frac{\partial^2 \bar{w}}{\partial y^2}\right) + q +$$

$$\frac{1}{\Delta y}\left(\frac{\partial^2 M_{V1}}{\partial x^2} + \frac{\partial^2 N_{A1}}{\partial x^2}e_1 + N_{A1}\frac{\partial^2 \bar{w}}{\partial x^2} - \frac{\partial \bar{w}}{\partial y}\frac{\partial^2 M_{H1}}{\partial x^2}\right) +$$

$$\frac{1}{\Delta x}\left(\frac{\partial^2 M_{V2}}{\partial y^2} + \frac{\partial^2 N_{A2}}{\partial y^2}e_2 + N_{A2}\frac{\partial^2 \bar{w}}{\partial y^2} - \frac{\partial \bar{w}}{\partial x}\frac{\partial^2 M_{H2}}{\partial y^2}\right) = 0 \qquad \text{(A-10)}$$

Finally for all other points the usual equilibrium equations of unstiffened isotropic plates can be written as a special case of equations (18-20) with the body forces omitted:

$$\frac{\partial N_x}{\partial x} + \frac{\partial N_{xy}}{\partial y} = 0 \qquad \text{(A-11)}$$

$$\frac{\partial N_y}{\partial y} + \frac{\partial N_{xy}}{\partial x} = 0 \qquad \text{(A-12)}$$

$$\frac{\partial^2 M_x}{\partial x^2} + 2\frac{\partial^2 M_{xy}}{\partial x \partial y} + \frac{\partial^2 M_y}{\partial y^2} + \left(N_x\frac{\partial^2 \bar{w}}{\partial x^2} + 2N_{xy}\frac{\partial^2 \bar{w}}{\partial x \partial y} + N_y\frac{\partial^2 \bar{w}}{\partial y^2}\right) + q = 0 \qquad \text{(A-13)}$$

APPENDIX B

EQUILIBRIUM EQUATIONS IN TERMS OF DISPLACEMENTS FOR DIFFERENT NODE TYPES

Equations (35)-(37) in 2.1.1.4 are the linearised equilibrium equations in terms of mid-plane displacements of the plate for points on the longitudinal (x-direction) stiffeners. Similar to these, the equilibrium equations for nodes on stiffeners in y-direction can be written:

$$E' \frac{\partial^2 u}{\partial x^2} + (E'_1 + E'_{xy}) \frac{\partial^2 v}{\partial x \partial y} + E'_{xy} \frac{\partial^2 u}{\partial y^2} - \frac{B_{H2}}{\Delta x} (\frac{\partial^4 u}{\partial y^4} - e_2 \frac{\partial^5 w}{\partial x \partial y^4}) = 0 \qquad (B\text{-}1)$$

$$(E' + \frac{C_{s2}}{\Delta x}) \frac{\partial^2 v}{\partial y^2} + (E'_1 + E'_{xy}) \frac{\partial^2 u}{\partial x \partial y} + E'_{xy} \frac{\partial^2 v}{\partial x^2} - \frac{C_{s2}\, e_2}{\Delta x} \frac{\partial^3 w}{\partial y^3} = 0 \qquad (B\text{-}2)$$

$$(D + \frac{B_{V2}}{\Delta x} + \frac{C_{s2}\, e_2^2}{\Delta x}) \frac{\partial^4 w}{\partial y^4} + 2 D \frac{\partial^4 w}{\partial x^2 \partial y^2} + D \frac{\partial^4 w}{\partial x^4} - \frac{C_{s2}\, e_2}{\Delta x} \frac{\partial^3 v}{\partial y^3} = q \qquad (B\text{-}3)$$

Combination of equations (B-1)-(B-3) and (35)-(37) gives the equilibrium equations for nodes lying on intersection of stiffeners:

$$(E' + \frac{C_{s1}}{\Delta y}) \frac{\partial^2 u}{\partial x^2} + (E'_1 + E'_{xy}) \frac{\partial^2 v}{\partial x \partial y} + E'_{xy} \frac{\partial^2 u}{\partial y^2} - \frac{C_{s1}\, e_1}{\Delta y} \frac{\partial^3 w}{\partial x^3} -$$

$$\frac{B_{H2}}{\Delta x} (\frac{\partial^4 u}{\partial y^4} - e_2 \frac{\partial^5 w}{\partial x \partial y^4}) = 0 \qquad (B\text{-}4)$$

$$(E' + \frac{C_{s2}}{\Delta x}) \frac{\partial^2 v}{\partial y^2} + (E'_1 + E'_{xy}) \frac{\partial^2 u}{\partial x \partial y} + E'_{xy} \frac{\partial^2 v}{\partial x^2} - \frac{C_{s2}\, e_2}{\Delta x} \frac{\partial^3 w}{\partial y^3} -$$

$$\frac{B_{H1}}{\Delta y} (\frac{\partial^4 v}{\partial x^4} - e_1 \frac{\partial^5 w}{\partial x^4 \partial y}) = 0 \qquad (B\text{-}5)$$

$$(D + \frac{B_{V1}}{\Delta y} + \frac{C_{s1}\, e_1^2}{\Delta y}) \frac{\partial^4 w}{\partial x^4} + (D + \frac{B_{V2}}{\Delta x} + \frac{C_{s2}\, e_2^2}{\Delta x}) \frac{\partial^4 w}{\partial y^4} + 2 D \frac{\partial^4 w}{\partial x^2 \partial y^2} -$$

$$\frac{C_{s1}\, e_1}{\Delta y}\frac{\partial^3 u}{\partial x^3} - \frac{C_{s2}\, e_2}{\Delta x}\frac{\partial^3 v}{\partial y^3} = q \qquad \text{(B-6)}$$

Finally for all other points the usual small-deflection equilibrium equations of isotropic plates can be written as a special case of equations (B-4)-(B-6):

$$E'\frac{\partial^2 u}{\partial x^2} + \left(E_1' + E_{xy}' \right)\frac{\partial^2 v}{\partial x \partial y} + E_{xy}'\frac{\partial^2 u}{\partial y^2} = 0 \qquad \text{(B-7)}$$

$$E'\frac{\partial^2 v}{\partial y^2} + \left(E_1' + E_{xy}' \right)\frac{\partial^2 u}{\partial x \partial y} + E_{xy}'\frac{\partial^2 v}{\partial x^2} = 0 \qquad \text{(B-8)}$$

$$D\left(\frac{\partial^4 w}{\partial x^4} + 2\frac{\partial^4 w}{\partial x^2 \partial y^2} + \frac{\partial^4 w}{\partial y^4} \right) = q \qquad \text{(B-9)}$$

APPENDIX C

ILYUSHIN YIELD CRITERION AND DERIVATION OF ELASTO-PLASTIC TANGENTIAL RIGIDITIES

(a) Ilyushin Yield Criterion

Ilyushin used the von Mises' yield criterion to derive a complex yield surface for thin shells[89]. Using mid-plane strain- and curvature components, he determined equivalent strains e_{i1} on the top surface, e_{i2} on the bottom surface and e_{i0} the minimum value of e_i on a distance z_0 from the plate centre. Depending on whether z_0 lies inside or outside the section, the case was described as "bending dominant" or "in-plane dominant" respectively. The yield surface was derived as :

$$f(Q_t, Q_m, Q_{tm}) = 0 \qquad \text{(C-1)}$$

where Q_t, Q_m and Q_{tm} are non-dimensional quadratic stress intensities:

$$\left.\begin{aligned} Q_t &= \frac{\overline{N}}{N_0} = f_1(\phi, \mu) \\ Q_m &= \frac{\overline{M}}{M_0} = f_2(\phi, \mu) \\ Q_{tm} &= \frac{\overline{MN}}{M_0\, N_0} = f_3(\phi, \mu) \end{aligned}\right\} \qquad \text{(C-2)}$$

with

$$\left.\begin{aligned} \overline{N} &= N_x^2 + N_y^2 - N_x N_y + 3 N_{xy}^2 \\ \overline{M} &= M_x^2 + M_y^2 - M_x M_y + 3 M_{xy}^2 \\ \overline{MN} &= M_x N_x + M_y N_y - \tfrac{1}{2} M_x N_y - \tfrac{1}{2} M_y N_x + 3 M_{xy} N_{xy} \\ N_0 &= t\,\sigma_0 \qquad \text{and} \quad M_0 = t^2 \sigma_0 / 4 \end{aligned}\right\} \qquad \text{(C-3)}$$

and the two parameters ϕ and μ:

$$\phi = e_{i2} / e_{i1} \quad , \quad \mu = e_{i0} / e_{i1} \tag{C-4}$$

Ilyushin gave two sets of functions f_1-f_3 for the "bending dominant" and "in-plane dominant" cases. Subsequently considering the two limiting conditions of pure bending and pure in-plane action and variation of the surface due to Q_{tm}, he proposed a simple approximation to the exact surface for the bending dominant case in which the parameters ϕ and μ are eliminated:

$$Q_t + Q_m + \frac{1}{\sqrt{3}} |Q_{tm}| = 1 \tag{C-5}$$

Using equations (C-2), (C-3) and (C-5), the yield criterion can be written in terms of the six stress resultants as:

$$f = \frac{\overline{N}}{t^2 \sigma_0^2} + \frac{4}{\sqrt{3}} s \frac{\overline{MN}}{t^3 \sigma_0^2} + \frac{16 \overline{M}}{t^4 \sigma_0^2} \leq 1 \tag{C-6}$$

where

$$s = \frac{\overline{MN}}{|\overline{MN}|}$$

This criterion is based on the assumption that the equivalent stress is at yield throughout the full depth of the section, hence the surface yield and the gradual spread of plasticity through the depth of the plate can not be considered. It has been used recently for isotropic plates by Crisfield[17] and Frieze[111] who gives also its derivation in detail. Crisfield found that the present criterion is less satisfactory for problems involving instability since the "full section yield criterion" underestimates the loss of stiffness at loads for which the curvatures are not very large, and he proposed some modifications to the Ilyushin criterion for "in-plane dominant" cases[103].

(b) Derivation of Elastic-Plastic Tangential Rigidities

The Ilyushin criterion was derived for two dimensional problems as:

$$f = \frac{\bar{N}}{t^2\,\sigma_0^2} + \frac{4\,s\,\overline{MN}}{\sqrt{3}\,t^3\,\sigma_0^2} + \frac{16\,\bar{M}}{t^4\,\sigma_0^2} \leq 1 \qquad \text{with} \qquad s = \frac{\overline{MN}}{|\overline{MN}|}$$

For plastic flow to remain on the yield surface, any variation in the generalised stress resultants must be such that no variation occurs in f:

$$\delta f = \{f_n\}^T \{\Delta N\} + \{f_m\}^T \{\Delta M\} = 0 \qquad \text{(C-7)}$$

where

$$\left.\begin{aligned} \{f_n\} &= \frac{1}{t^2}\left\{\frac{\partial \bar{N}}{\partial N}\right\} + \frac{2\,s}{\sqrt{3}\,t^3}\left\{\frac{\partial \bar{M}}{\partial M}\right\} \\ \{f_m\} &= \frac{2\,s}{\sqrt{3}\,t^3}\left\{\frac{\partial \bar{N}}{\partial N}\right\} + \frac{16}{t^4}\left\{\frac{\partial \bar{M}}{\partial M}\right\} \end{aligned}\right\} \qquad \text{(C-8)}$$

To avoid the discontinuity in the partial derivatives of f as $\overline{MN} \to 0$, s is made zero when $\overline{MN}$ is very small ($|4\,\overline{MN}/(\sqrt{3}\,t^3\,\sigma_0^2)| < 10^{-4}$). Although the Ilyushin criterion is based on a deformation theory stress-strain law, it is concluded by some investigators[136, 137] that it should still be applicable when a flow rule is employed. Based on this conclusion, assuming that equation (C-6) may be treated as a plastic potential, Crisfield[17] used the Prantl-Reuss flow rule which was originally intended for materials obeying von Mises' yield criterion. Using the Prantl-Reuss flow rule, the plastic strain component is normal to the yield surface:

$$\left.\begin{aligned} \{\Delta\varepsilon_p\} &= \lambda\,\{f_n\} \\ \{\Delta\chi_p\} &= \lambda\,\{f_m\} \end{aligned}\right\} \qquad \text{(C-9)}$$

where λ is a positive scalar. The elastic incremental stress resultants are determined by assuming a Hookean incremental stress-strain relation-

ship[138].

$$\left.\begin{aligned} \{\Delta N\} &= t\,[E]\,(\{\Delta\varepsilon_t\} - \{\Delta\varepsilon_p\}) \\ \{\Delta M\} &= \frac{t^3}{12}\,[E]\,(\{\Delta\chi_t\} - \{\Delta\chi_p\}) \end{aligned}\right\} \qquad (C\text{-}10)$$

where ε_t and χ_t are the total strains and curvatures and ε_p and χ_p are the plastic portion of them. Substituting equations (C-9) into (C-10) and these into equation (C-7), the plastic strain rate multiplier can be found as:

$$\lambda = \frac{1}{(m+n)}\left(t\,\{f_n\}^T\,[E]\,\{\Delta\varepsilon_t\} + \frac{t^3}{12}\,\{f_m\}^T\,[E]\,\{\Delta\chi_t\}\right) \qquad (C\text{-}11)$$

where

$$\left.\begin{aligned} n &= t\,\{f_n\}^T\,[E]\,\{f_n\} \\ m &= \frac{t^3}{12}\,\{f_m\}^T\,[E]\,\{f_m\} \end{aligned}\right\} \qquad (C\text{-}12)$$

Substituting for λ from (C-11) into (C-9), the plastic strain increments may be related to the total strain increments:

$$\left.\begin{aligned} \{\Delta\varepsilon_p\} &= \frac{1}{(m+n)}\left(t\,[N]\,[E]\,\{\Delta\varepsilon_t\} + \frac{t^3}{12}\,[NM]\,[E]\,\{\Delta\chi_t\}\right) \\ \{\Delta\chi_p\} &= \frac{1}{(m+n)}\left(t\,[NM]^T\,[E]\,\{\Delta\varepsilon_t\} + \frac{t^3}{12}\,[M]\,[E]\,\{\Delta\chi_t\}\right) \end{aligned}\right\} \qquad (C\text{-}13)$$

where

$$\left.\begin{aligned} [N] &= \{f_n\}\,\{f_n\}^T \\ [N] &= \{f_m\}\,\{f_m\}^T \\ [M] &= \{f_n\}\,\{f_m\}^T \end{aligned}\right\} \qquad (C\text{-}14)$$

Substituting equation (C-13) in equation (C-10) gives the relationship between the increments of the generalised stress resultants and the

increments of total generalised strain:

$$\left.\begin{aligned} \{\Delta N\} &= [C^*]\ \{\Delta\varepsilon_t\} + [cd]\ \{\Delta\chi_t\} \\ \{\Delta M\} &= [cd]^T\ \{\Delta\varepsilon_t\} + [D^*]\ \{\Delta\chi_t\} \end{aligned}\right\} \qquad \text{(C-15)}$$

where $[C^*]$, $[D^*]$ and $[cd]$ are the tangential elasto-plastic modular matrices and are given by:

$$\left.\begin{aligned} [C^*] &= t\ [E]\ \left([I] - \frac{t}{(m+n)}\ [N]\ [E] \right) \\ [D^*] &= \frac{t^3}{12}\ [E]\ \left([I] - \frac{t^3}{12\ (m+n)}\ [M]\ [E] \right) \\ [cd] &= \frac{-t^4}{12\ (m+n)}\ [E]\ [NM]\ [E] \end{aligned}\right\} \qquad \text{(C-16)}$$

with $[I]$ as unit matrix.

APPENDIX D

EQUILIBRIUM AND FORCE-DISPLACEMENT EQUATIONS IN INCREMENTAL FORM

Interactive forces and equilibrium equations (11)-(17) for nodes lying on a longitudinal (x-direction) stiffener are given below in incremental form. Corresponding equations for other types of nodes can be written similarly and are omitted here.

Interactive forces:

$$\Delta F_{x1} = \frac{\partial \Delta N_{A1}}{\partial x}$$

$$\Delta F_{y1} = \frac{\partial^2 \Delta M_{H1}}{\partial x^2} + \Delta N_{A1} \frac{\partial^2 \bar{v}_{c1}}{\partial x^2} + N_{A1} \frac{\partial^2 \Delta v_{c1}}{\partial x^2} + \frac{\partial \Delta N_{A1}}{\partial x} \frac{\partial \bar{v}_{c1}}{\partial x} + \frac{\partial N_{A1}}{\partial x} \frac{\partial \Delta v_{c1}}{\partial x}$$

$$\Delta F_{z1} = \frac{\partial^2 \Delta M_{V1}}{\partial x^2} + e_1 \frac{\partial^2 \Delta N_{A1}}{\partial x^2} + \Delta N_{A1} \frac{\partial^2 \bar{w}}{\partial x^2} + N_{A1} \frac{\partial^2 \Delta w}{\partial x^2} - \frac{\partial^2 \Delta M_{H1}}{\partial x^2} \frac{\partial \bar{w}}{\partial y} - \frac{\partial^2 M_{H1}}{\partial x^2} \frac{\partial \Delta w}{\partial y}$$

$$\Delta T_1 = \frac{\partial \Delta M_{T1}}{\partial x} + e_1 \frac{\partial^2 \Delta M_{H1}}{\partial x^2}$$

(D-1)

Equilibrium equations:

$$\frac{\partial \Delta N_x}{\partial x} + \frac{\partial \Delta N_{xy}}{\partial y} + \frac{\Delta F_{x1}}{\Delta y} = 0$$

$$\frac{\partial \Delta N_y}{\partial y} + \frac{\partial \Delta N_{xy}}{\partial x} + \frac{\Delta F_{y1}}{\Delta y} = 0$$

(D-2)

$$\frac{\partial^2 \Delta M_x}{\partial x^2} + 2\frac{\partial^2 \Delta M_{xy}}{\partial x \partial y} + \frac{\partial^2 \Delta M_y}{\partial y^2} + \left(\Delta N_x \frac{\partial^2 \bar{w}}{\partial x^2} + 2\,\Delta N_{xy} \frac{\partial^2 \bar{w}}{\partial x \partial y} + \Delta N_y \frac{\partial^2 \bar{w}}{\partial y^2} \right) +$$

$$\left(N_x \frac{\partial^2 \Delta w}{\partial x^2} + 2\,N_{xy} \frac{\partial^2 \Delta w}{\partial x \partial y} + N_y \frac{\partial^2 \Delta w}{\partial y^2} \right) + \frac{\Delta F_{z1}}{\partial y} + \Delta q = 0$$

N_x, N_y, N_{xy}, N_{A1} and M_{H1} are the total stress resultants up to the application of the current load increment. $\bar{w}$, $\bar{v}_{c1}$ and $\bar{u}_{c1}$ are total displacements including the current displacement increments. For example, for the i-th load increment we have:

$$\bar{w} = w_{i-1} + \Delta w_i + w_0$$

Incremental stress-strain relationships for the elastic-plastic plate were given in Appendix C in matrix form as:

$$\left.\begin{aligned} \{\Delta N\} &= [c^*]\,\{\Delta \varepsilon_t\} + [cd]\,\{\Delta \chi_t\} \\ \{\Delta M\} &= [cd]^T\,\{\Delta \varepsilon_t\} + [D^*]\,\{\Delta \chi_t\} \end{aligned}\right\} \qquad \text{(D-3)}$$

where $$\{\Delta \chi_t\}^T = \left(-\frac{\partial^2 \Delta w}{\partial x^2}\,,\; -\frac{\partial^2 \Delta w}{\partial y^2}\,,\; -2\frac{\partial^2 \Delta w}{\partial x \partial y} \right)$$

$$\{\Delta \varepsilon_t\}^T = (\Delta \varepsilon_x\,,\; \Delta \varepsilon_y\,,\; \Delta \gamma_{xy})$$

with

$$\left.\begin{aligned} \Delta \varepsilon_x &= \frac{\partial \Delta u}{\partial x} + \frac{1}{2}\left(\frac{\partial \Delta w}{\partial x}\right)^2 + \frac{\partial \Delta w}{\partial x}\frac{\partial w}{\partial x} + \frac{\partial \Delta w}{\partial x}\frac{\partial w_0}{\partial x} \\ \Delta \varepsilon_y &= \frac{\partial \Delta v}{\partial y} + \frac{1}{2}\left(\frac{\partial \Delta w}{\partial y}\right)^2 + \frac{\partial \Delta w}{\partial y}\frac{\partial w}{\partial y} + \frac{\partial \Delta w}{\partial y}\frac{\partial w_0}{\partial y} \\ \Delta \gamma_{xy} &= \frac{\partial \Delta u}{\partial y} + \frac{\partial \Delta v}{\partial x} + \frac{\partial \Delta w}{\partial x}\frac{\partial \Delta w}{\partial y} + \frac{\partial \Delta w}{\partial x}\frac{\partial w}{\partial y} + \frac{\partial \Delta w}{\partial y}\frac{\partial w}{\partial x} + \\ &\quad \frac{\partial \Delta w}{\partial x}\frac{\partial w_0}{\partial y} + \frac{\partial \Delta w}{\partial y}\frac{\partial w_0}{\partial x} \end{aligned}\right\} \qquad \text{(D-4)}$$

w is the net displacement up to application of the current load increment. The force-displacement relationships for stiffeners in the elastic range of given by equations (27)-(30). For the incremental iterative solution of instability problems in the elastic range, they are given here in their incremental form. However after the onset of plasticity they are not valid and have to be modified.

Incremental force-displacement equations for stiffeners in elastic range:

$$\Delta N_{A1} = C_{s1} \left[\frac{\partial \Delta u_{c1}}{\partial x} + \frac{1}{2} \left(\frac{\partial \Delta w}{\partial x} \right)^2 + \frac{\partial \Delta w}{\partial x} \frac{\partial w}{\partial x} + \frac{\partial \Delta w}{\partial x} \frac{\partial w_0}{\partial x} + \right.$$

$$\left. \frac{1}{2} \left(\frac{\partial \Delta v_{c1}}{\partial x} \right)^2 + \frac{\partial \Delta v_{c1}}{\partial x} \frac{\partial v_{c1}}{\partial x} + \frac{\partial \Delta v_{c1}}{\partial x} \frac{\partial v_{c10}}{\partial x} \right]$$

$$= C_{s1} \left\{ \Delta \varepsilon_x - e_1 \frac{\partial^2 \Delta w}{\partial x^2} + \left(\frac{\partial \Delta v}{\partial x} - e_1 \frac{\partial^2 \Delta w}{\partial x \partial y} \right) \left[\left(\frac{\partial v}{\partial x} + \right. \right. \right.$$

$$\left. \left. \left. \frac{1}{2} \frac{\partial \Delta v}{\partial x} \right) - e_1 \left(\frac{\partial^2 w}{\partial x \partial y} + \frac{1}{2} \frac{\partial^2 \Delta w}{\partial x \partial y} + \frac{\partial^2 w_0}{\partial x \partial y} \right) \right] \right\} \qquad \text{(D-5)}$$

$$\left.
\begin{aligned}
\Delta M_{V1} &= - B_{V1} \frac{\partial^2 \Delta w}{\partial x^2} \\
\Delta M_{T1} &= - B_{T1} \frac{\partial^2 \Delta w}{\partial x \partial y} \\
\Delta M_{H1} &= - B_{H1} \frac{\partial^2 \Delta v_{c1}}{\partial x^2} = - B_{H1} \left(\frac{\partial^2 \Delta v}{\partial x^2} - e_1 \frac{\partial^3 \Delta w}{\partial x^2 \partial y} \right)
\end{aligned}
\right\} \qquad \text{(D-6)}$$

For the plastic range the stiffener section is subdivided into rectangular elements (Fig. 6). Consistent with the assumption that plane sections before bending remain plane after bending, the strain at the centre of each element can be found from the mid-plane strains and curvatures of the plate.

The axial strain at the centre of element i of a longitudinal (x-direction) stiffener cross-section is given by:

$$\varepsilon_{xi} = \varepsilon_x - e_{vi} \frac{\partial^2 w}{\partial x^2} - e_{hi} \frac{\partial^2 v_i}{\partial x^2}$$

$$= \varepsilon_x - e_{vi} \frac{\partial^2 w}{\partial x^2} - e_{hi} \left(\frac{\partial^2 v}{\partial x^2} - e_{vi} \frac{\partial^3 w}{\partial x^2 \partial y} \right) \qquad \text{(D-7)}$$

and its incremental form is:

$$\Delta\varepsilon_{xi} = \Delta\varepsilon_x - e_{vi} \frac{\partial^2 \Delta w}{\partial x^2} - e_{hi} \left(\frac{\partial^2 \Delta v}{\partial x^2} - e_{vi} \frac{\partial^3 \Delta w}{\partial x^2 \partial y} \right) \qquad \text{(D-8)}$$

e_{vi} and e_{hi} are the distances from the centre of the element i to the reference axes. The increment in axial stress will be:

$$\Delta\sigma_{xi} = E \, \Delta\varepsilon_{xi} \qquad \text{(D-9)}$$

At each iteration the total stress at each element is checked and if it exceeds the yield stress, the stress increment for that element will be set equal zero. With the stress increment known, the force increment for the element with the area δA_i is given by:

$$\Delta\delta N_{Ali} = \Delta\sigma_{xi} \, \delta A_i \qquad \text{(D-10)}$$

Summation of the element force increments for the entire cross-section results in the total axial force increment of the stiffener:

$$\Delta N_{Al} = \Sigma \, \Delta\delta N_{Ali} \qquad \text{(D-11)}$$

The vertical moment ΔM_{Vl} is obtained by summing up the moments of all the element force increments about the stiffener's horizontal axis, that is:

$$\Delta M_{Vl} = \Sigma \, \Delta\delta N_{Ali} \, (e_{vi} - e) \qquad \text{(D-12)}$$

Similarly the horizontal moment increment ΔM_{Hl} can be written as:

$$\Delta M_{Hl} = \Sigma \, \Delta\delta N_{Ali} \, e_{hi} \qquad \text{(D-13)}$$

APPENDIX E

FLOW CHART FOR THE ITERATIVE SOLUTION PROCEDURE

k denotes no. of displacement

K denotes the total no. of displacements

i denotes no. of load increment

Loops: (1) Load increments

(2) Modified Newton-Raphson iteration (combined with Aitken's δ^2-extrapolation)

(3) Displacements

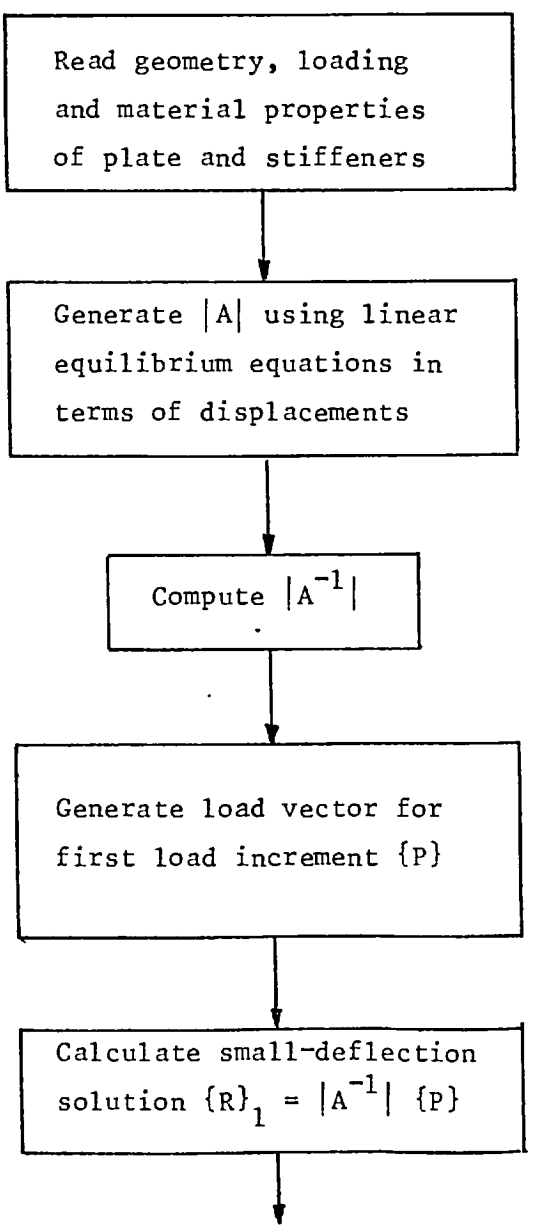

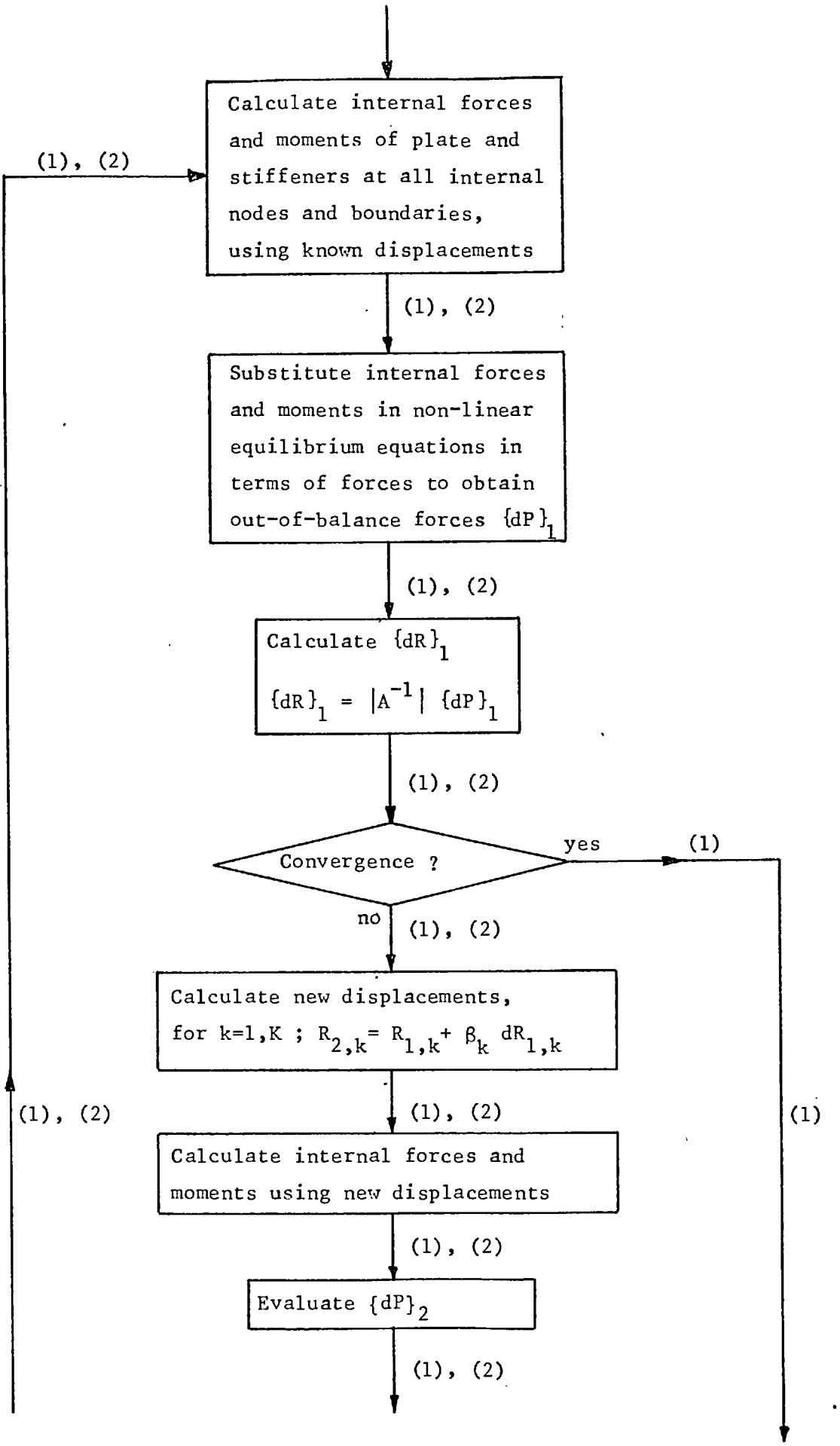
Calculate internal forces and moments of plate and stiffeners at all internal nodes and boundaries, using known displacements
(1), (2)
Substitute internal forces and moments in non-linear equilibrium equations in terms of forces to obtain out-of-balance forces {dP}1
(1), (2)
Calculate {dR}1
{dR}1 = |A-1| {dP}1
(1), (2)
Convergence ?
yes
(1)
no
(1), (2)
Calculate new displacements, for k=1,K ; R2,k= R1,k+ βk dR1,k
(1), (2)
(1), (2)
(1)
Calculate internal forces and moments using new displacements
(1), (2)
Evaluate {dP}2
(1), (2)

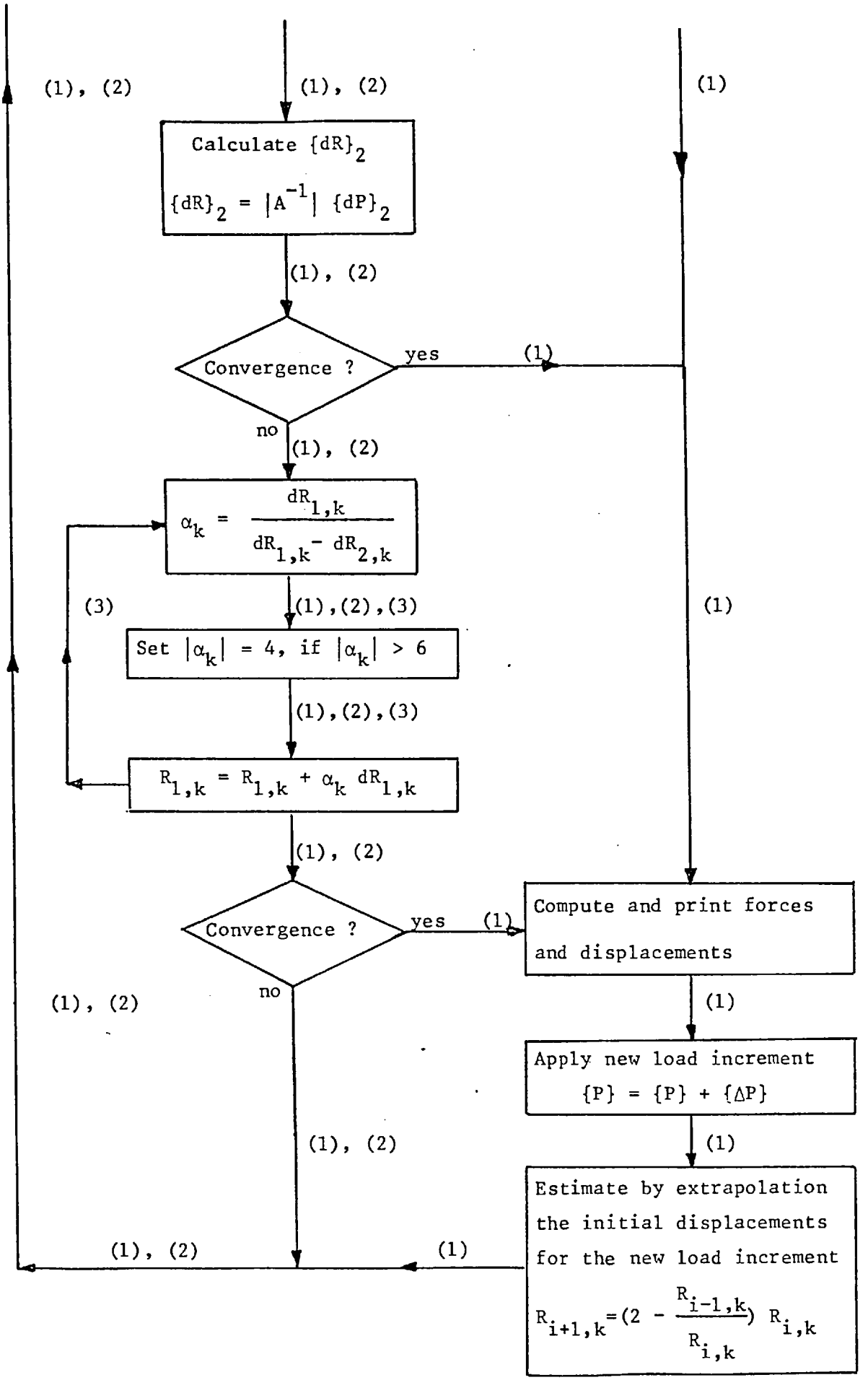
(1), (2)
(1), (2)
(1)
Calculate {dR}2
{dR}2 = |A-1| {dP}2
(1), (2)
Convergence ?
yes
(1)
no
(1), (2)
αk = dR1,k / (dR1,k - dR2,k)
(3)
(1),(2),(3)
(1)
Set |αk| = 4, if |αk| > 6
(1),(2),(3)
R1,k = R1,k + αk dR1,k
(1), (2)
Convergence ?
yes
(1)
Compute and print forces and displacements
no
(1), (2)
(1)
Apply new load increment
{P} = {P} + {ΔP}
(1)
(1), (2)
Estimate by extrapolation the initial displacements for the new load increment
Ri+1,k = (2 - Ri-1,k / Ri,k) Ri,k
(1), (2)
(1)

NOMENCLATURE

A	area
a	length of plate
A_s	area of cross-section of stiffener
B_V	flexural rigidity of stiffener for bending in the vertical plane
B_H	flexural rigidity of stiffener for bending in the horizontal plane
B_T	torsional rigidity of stiffener
b	width of plate
C_s	extensional rigidity of stiffener
D	flexural rigidity of plate
dx, dy	finite difference mesh lengths in x and y-direction
h_s	depth of plate
E	Young's modulus of plate and stiffeners
e	stiffener eccentricity, distance from stiffener's centre to the mid-plane of plate
f	yield function
F_x, F_y, F_z	interaction forces between plate and stiffeners in x, y and z-direction per unit length of stiffener
G	shear modulus of elasticity
I_0	stiffener's moment of inertia about its centre line
I_s	for symmetric stiffeners $I_s = I_0$
	for unsymmetric stiffeners $I_s = I_0 + A_s\ (e - t/2)^2$
K	factor for torsional rigidity of rectangular stiffener
K_{cr}	critical buckling coefficient
L_x, L_y	length of plate in x- and y-direction
M_x, M_y	bending moments per unit length of plate

M_{xy}, M_{yx}	twisting moments per unit length of plate
M_V, M_H	bending moments in stiffener
M_T	twisting moment in stiffener
N_x, N_y, N_{xy}, N_{yx}	in-plane forces per unit length of plate
N_A, N_H, N_V	forces in stiffeners
$\overline{N}$, $\overline{MN}$, $\overline{M}$	quadratic"stress intensities" in Ilyushin yield function
Q_x, Q_y	normal shear forces per unit length of plate
q	intensity of lateral pressure
T	interaction moment between plate and stiffener
t	thickness of plate
t_s	thickness of stiffener
u, v, w	net deflections in x, y and z-direction of mid-plane of plate
$\overline{u}$, $\overline{v}$, $\overline{w}$	total deflections in x, y and z-direction of mid-plane of plate
x, y, z	rectangular cartesian co-ordinate axes
γ_{xy}	shear strain at mid-plane of plate
ε_x, ε_y	strains in x- and y-direction respectively at mid-plane of plate
ε_0	uniaxial yield strain
λ	plastic strain rate multiplier
σ	direct stress
σ'	σ/σ_0
σ_0	uniaxial yield stress
σ_{RC}	residual compression due to welding
τ	shear stress
ν	Poisson's ratio

δ	$A_s/(b\ t)$
γ	$12\ (1 - \nu^2)\ I_s\ /(b\ t^3)$

Subscripts

1	relates to the x-direction stiffener
2	relates to the y-direction stiffener
0	denotes initial values
c	relates to the centre of cross-section of stiffener
x, y, z	denote the directions x, y and z respectively
A, V, H, T	denote axial, vertical, horizontal and torsional quantities respectively
cr	critical
e	elastic
p	plastic
s	stiffener
t	total (elastic + plastic)

Vectors

$\{\chi\}$	curvatures with $\{\chi\}^T = \{-\frac{\partial^2 w}{\partial x^2}\ ,\ -\frac{\partial^2 w}{\partial y^2}\ ,\ -2\frac{\partial^2 w}{\partial x \partial y}\}$, increments $\{\Delta\chi\}$
$\{\varepsilon\}$	strains with $\{\varepsilon\}^T = \{\varepsilon_x, \varepsilon_y, \gamma_{xy}\}$, increments $\{\Delta\varepsilon\}$
$\{N\}$, $\{M\}$	forces and moments per unit length of plate with $\{N\}^T = \{N_x, N_y, N_{xy}\}$ and $\{M\}^T = \{M_x, M_y, M_{xy}\}$, incrs. $\{\Delta N\}$, $\{\Delta M\}$
$\{P\}$	nodal forces, increments $\{\Delta P\}$
$\{dP\}$	nodal out-of-balance forces, increments $\{d\Delta P\}$
$\{R\}$	nodal displacements at mid-plane of plate, increments $\{\Delta R\}$
$\{dR\}$	nodal displacement corrections, increments $\{d\Delta R\}$

Matrices

$[E]$ modular matrix $\frac{E}{1-\nu^2}\begin{bmatrix} 1 & \nu & 0 \\ \nu & 1 & 0 \\ 0 & 0 & \frac{1-\nu}{2} \end{bmatrix}$

$[D]$ $\frac{t^3}{12}[E]$

$[I]$ unit matrix (3x3)

$[C^*]$, $[D^*]$, $[cd]$ tangential elasto-plastic matrices relating to generalised stress resultants

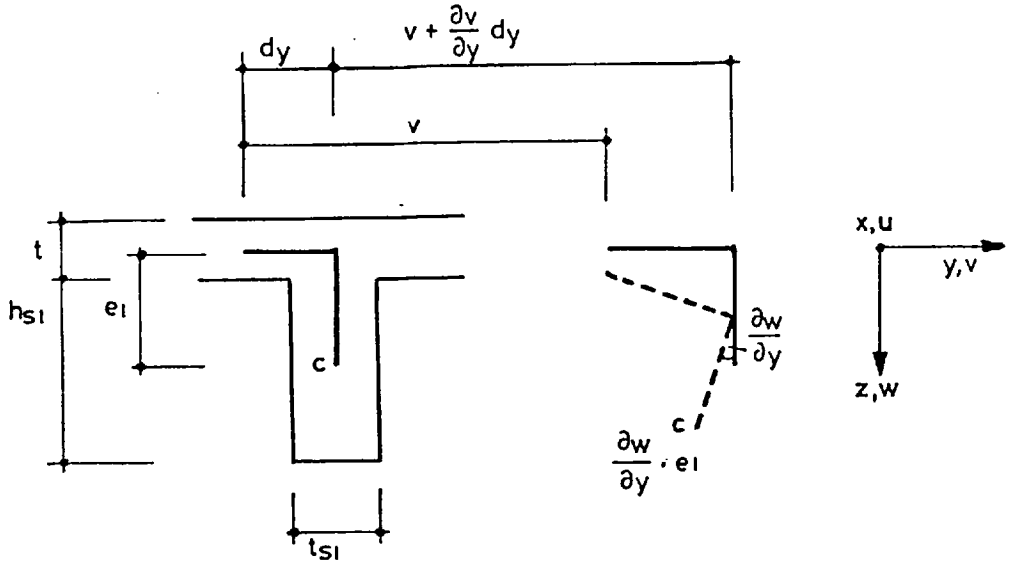

Fig. 1

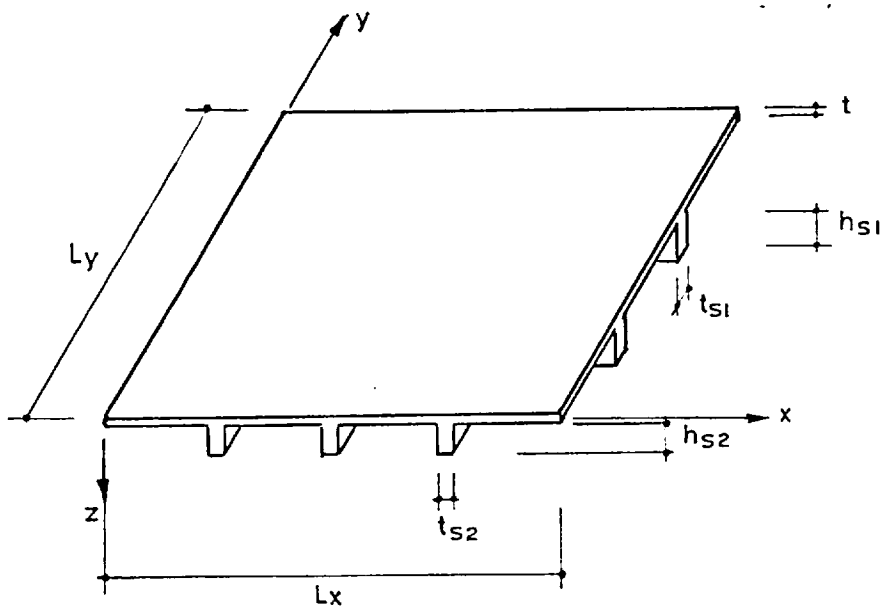

Dimensions of the stiffened plate

Fig. 2

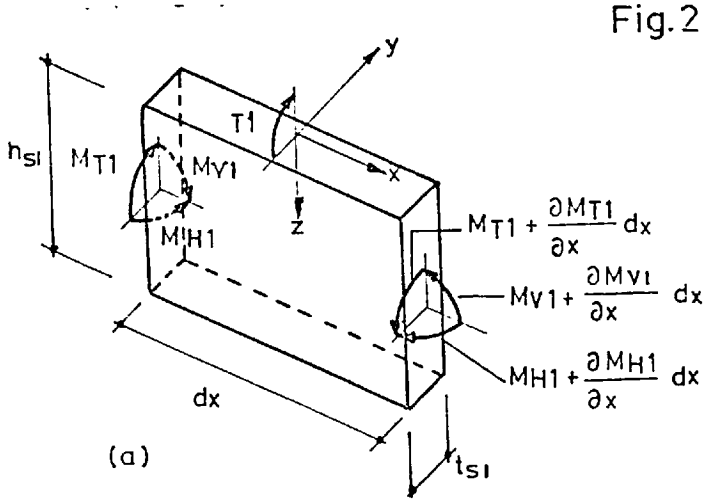

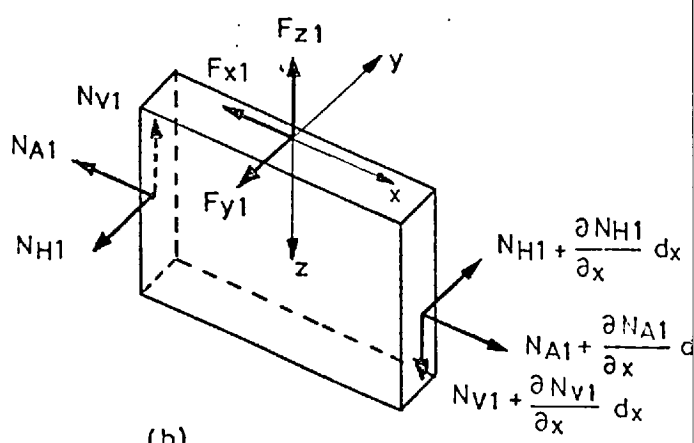

Sectional actions on an element of a longitudinal beam

Fig. 3

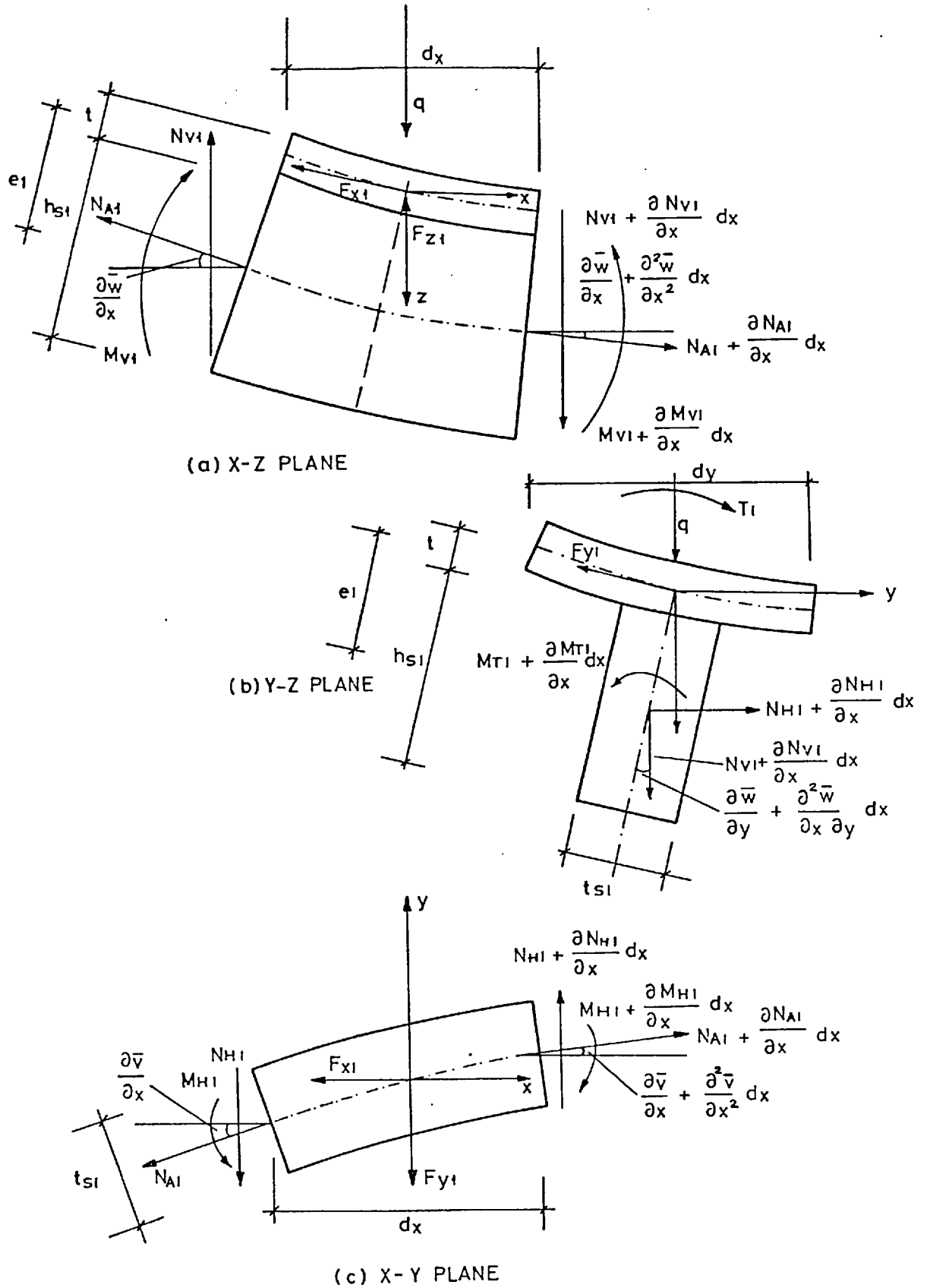

Fig. 4 Sectional actions on a deformed element of beam

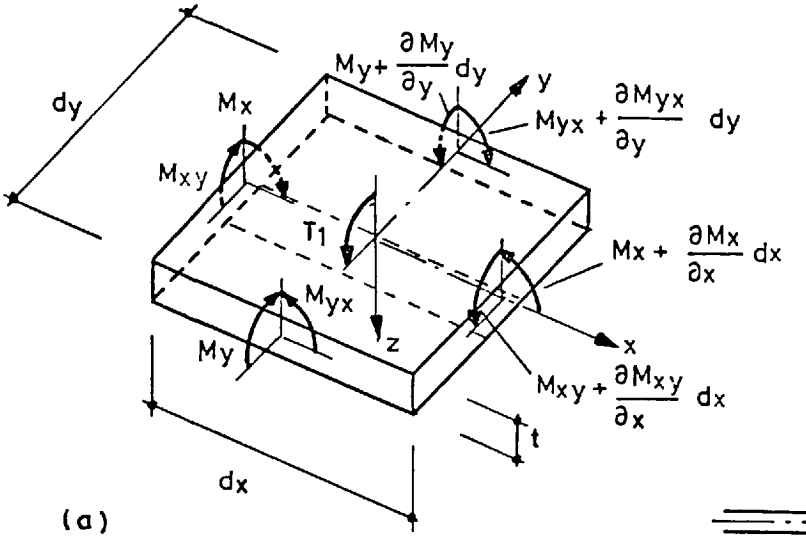

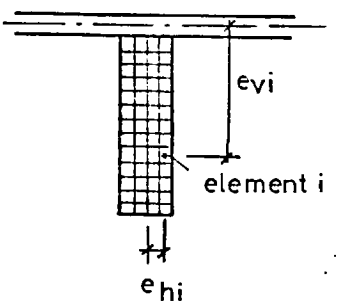

Fig. 6

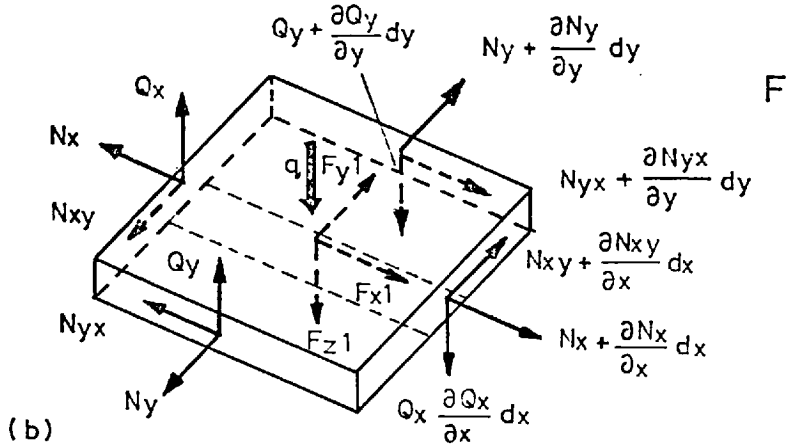

Sectional actions on an element of plate

Fig. 5

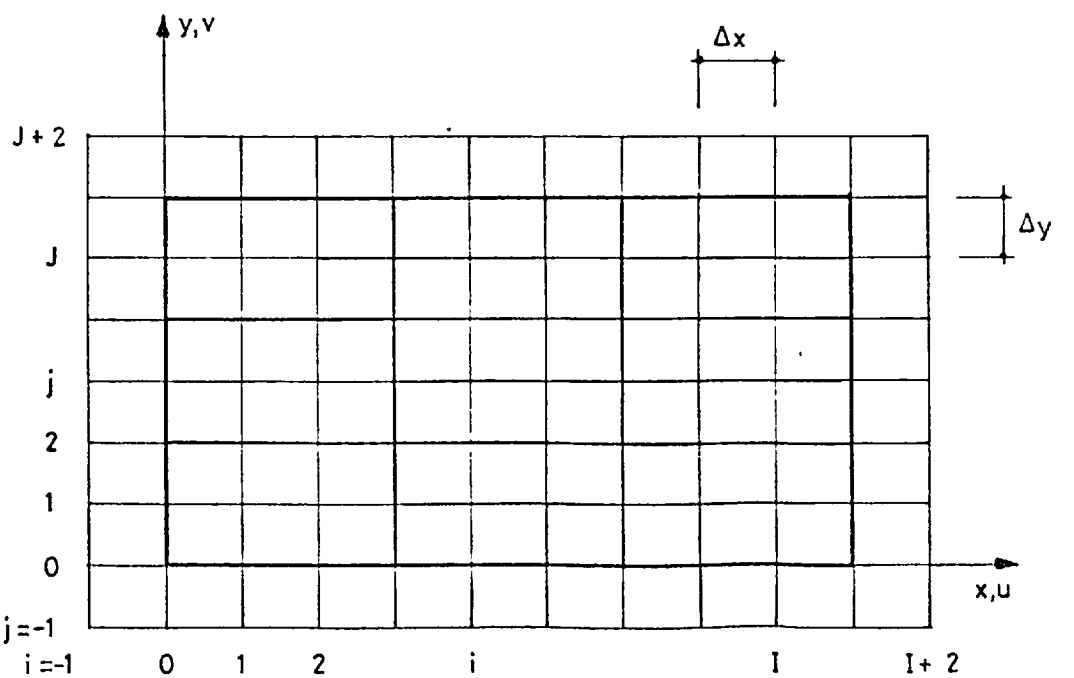

Fig. 7

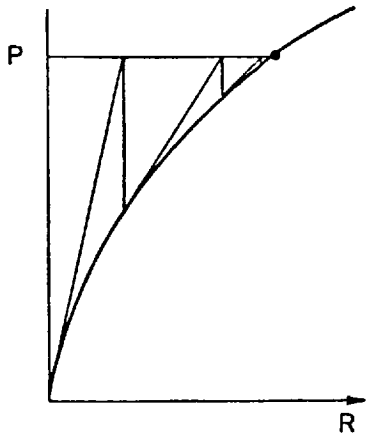

Iterative method

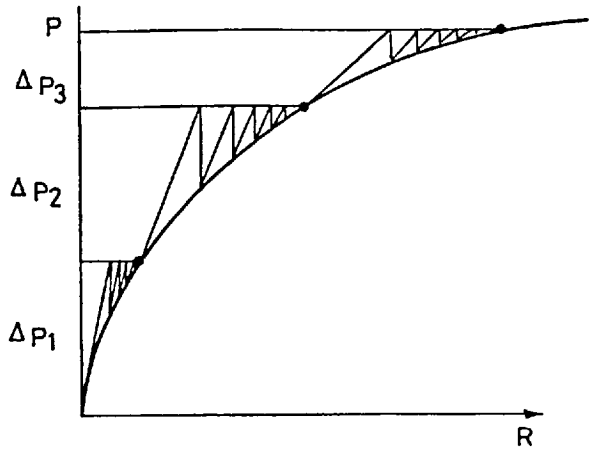

Combined incremental iterative method

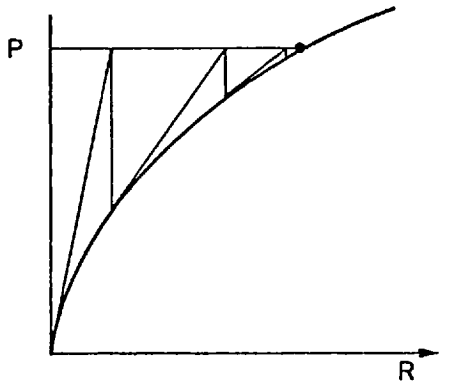

Newton-Raphson method

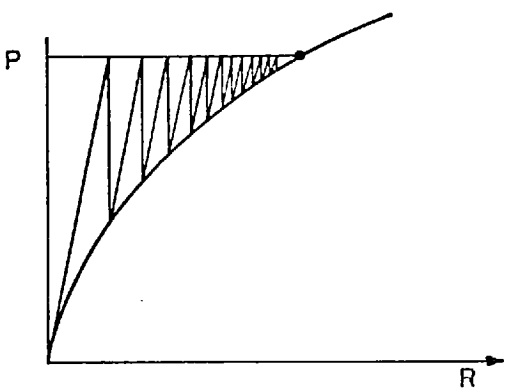

Modified Newton-Raphson method

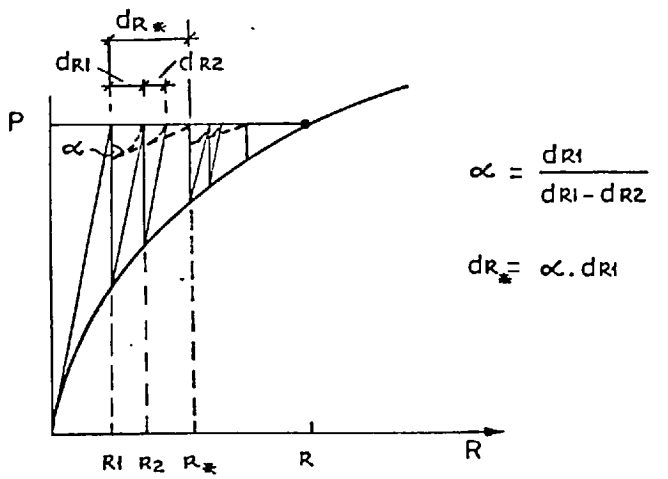

$$\alpha = \frac{dR_1}{dR_1 - dR_2}$$

$$dR_* = \alpha . dR_1$$

Modified Newton-Raphson with Aitken's δ^2-extrapolation

Fig. 8

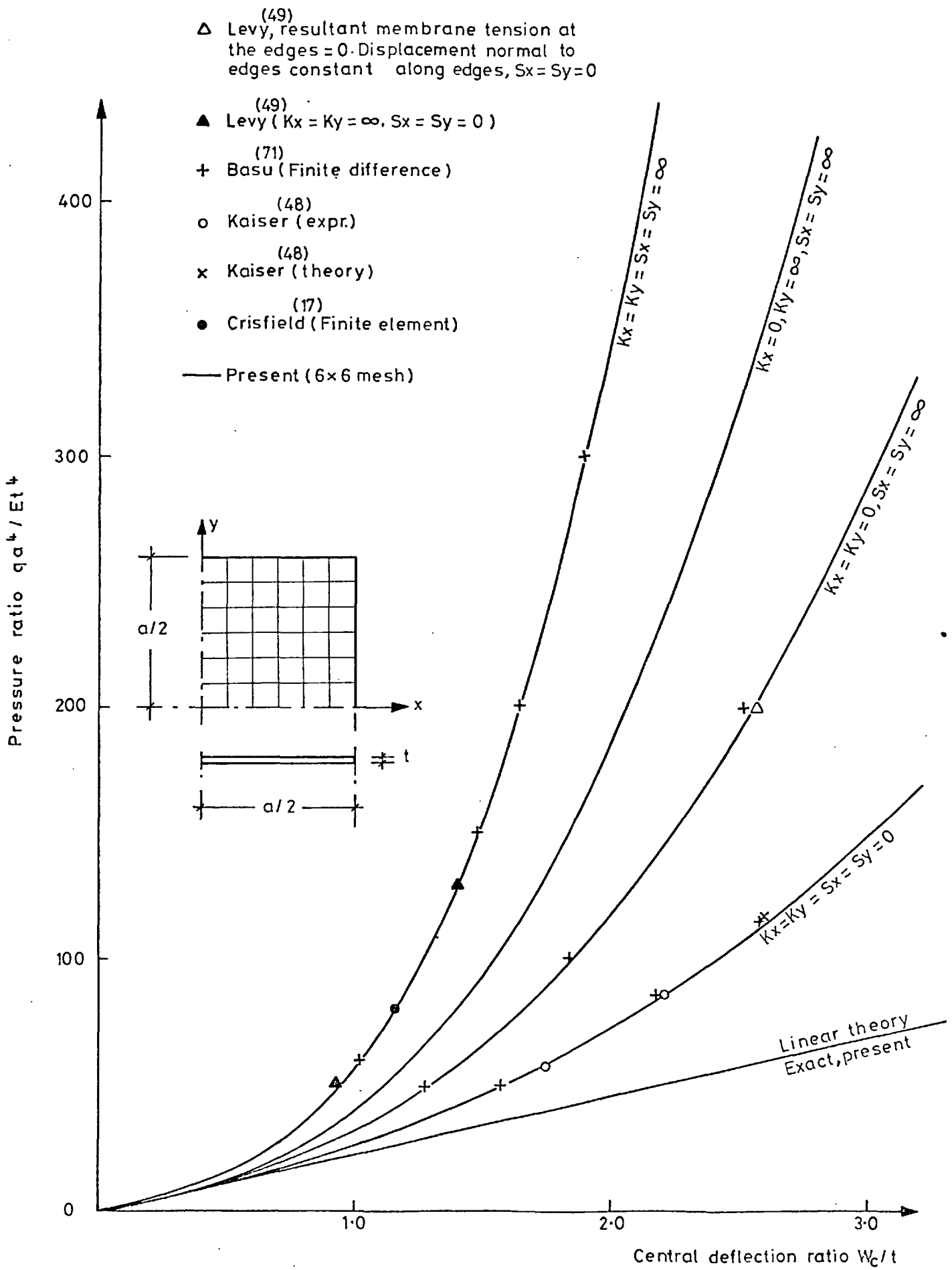

Fig. 9 Simply supported elastic isotropic plate under uniform lateral load. Central deflection (ν = 0·3)

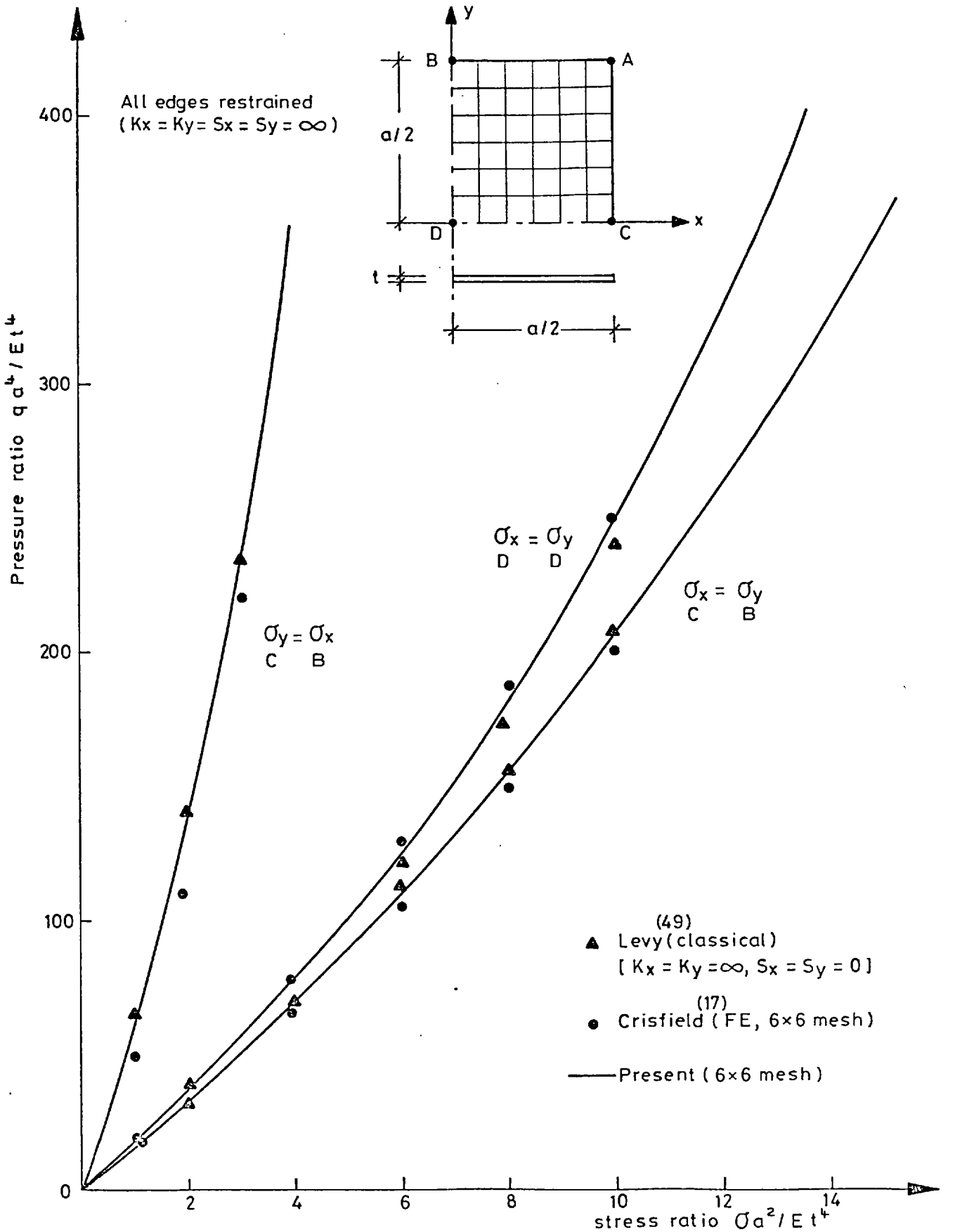

Fig. 10 Simply supported isotropic plate under uniform lateral load, membrane stresses ($\gamma = 0{\cdot}3$)

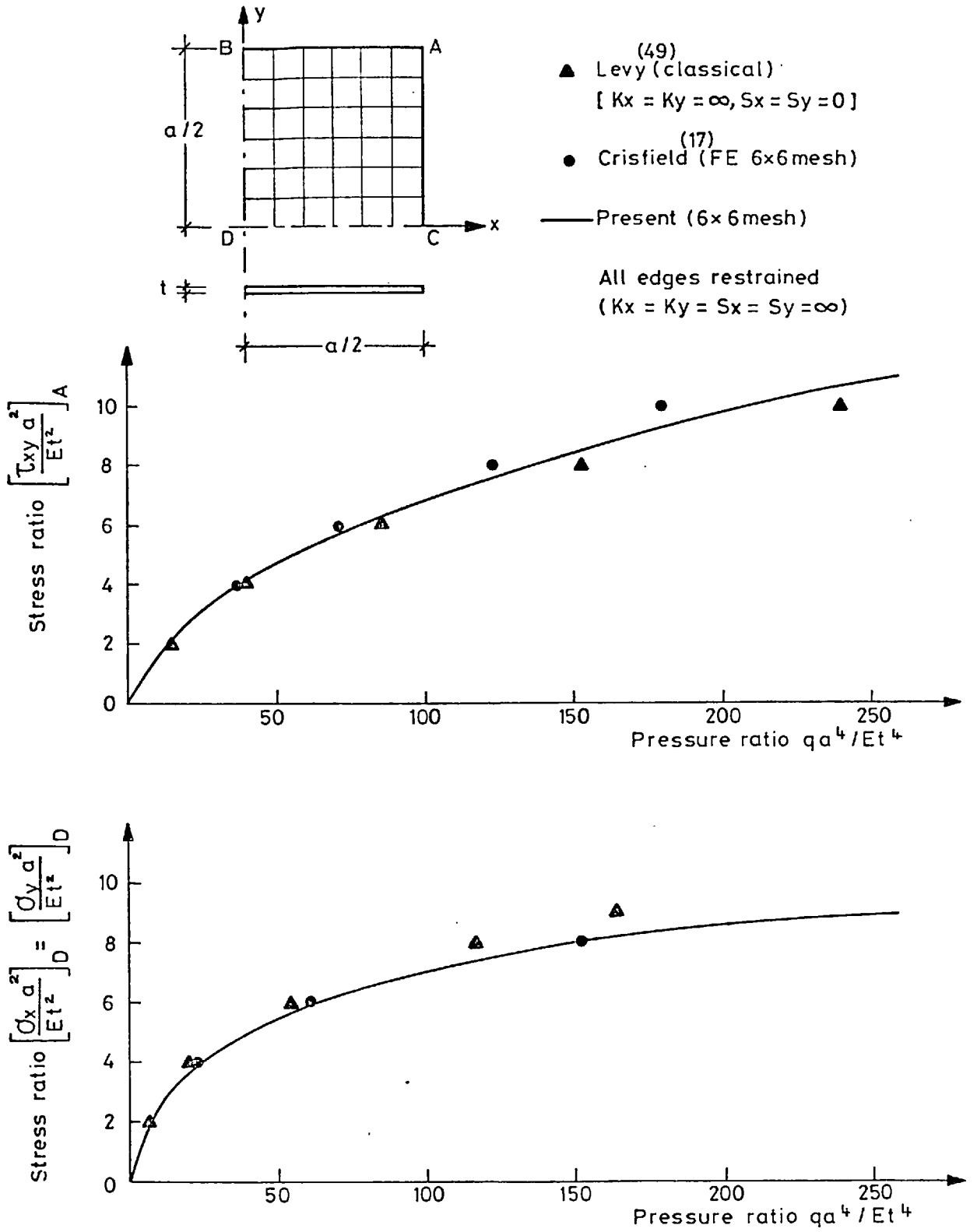

Fig. 11 Elastic simply supported isotropic plate under uniform lateral load. Extreme fibre bending stresses ($\sigma_x^b \sigma_y^b \tau_{xy}^b$)($\nu$=·3)

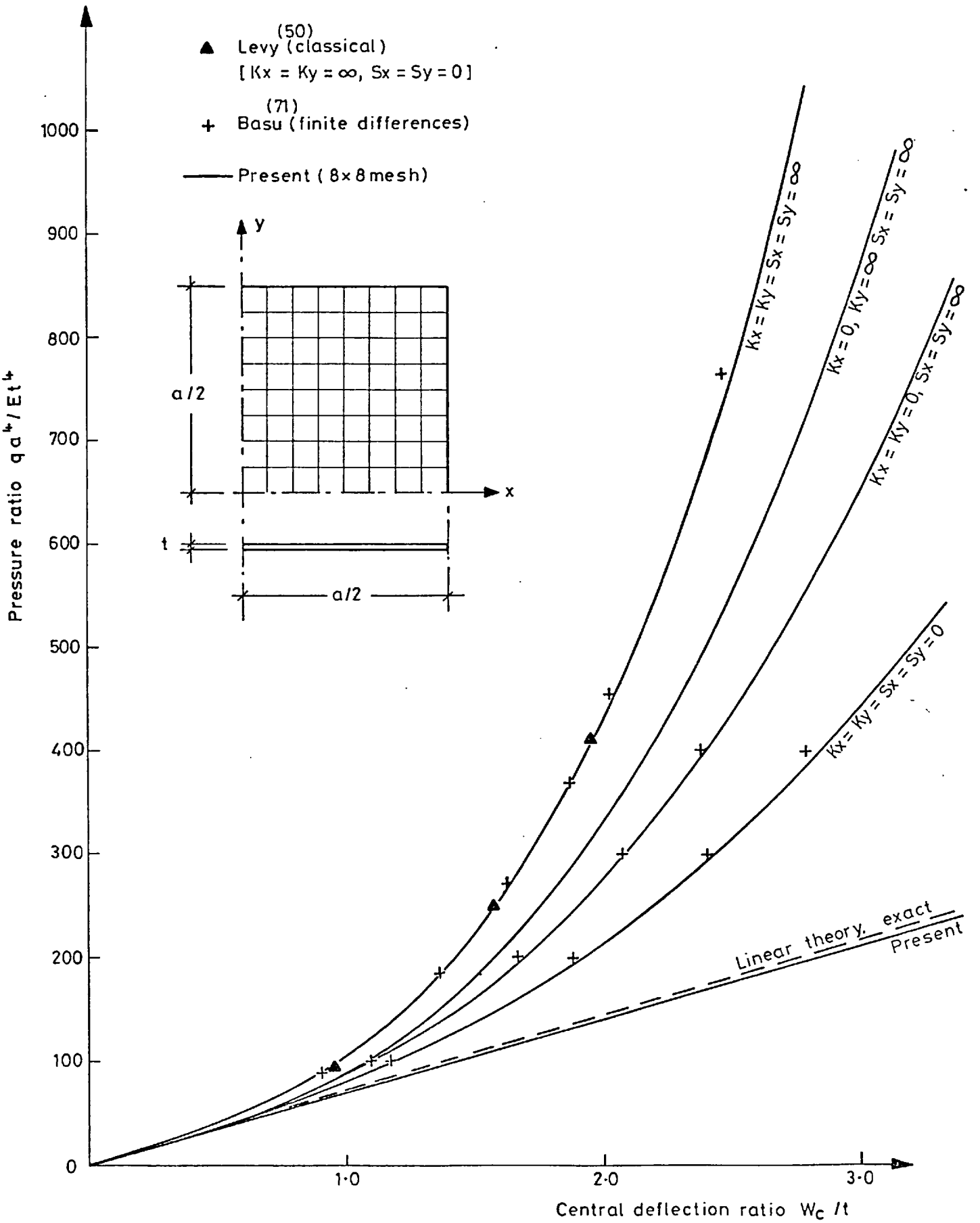

Fig. 12 Built - in isotropic plate under uniform lateral load, central deflection ($\nu = 0{\cdot}3$)

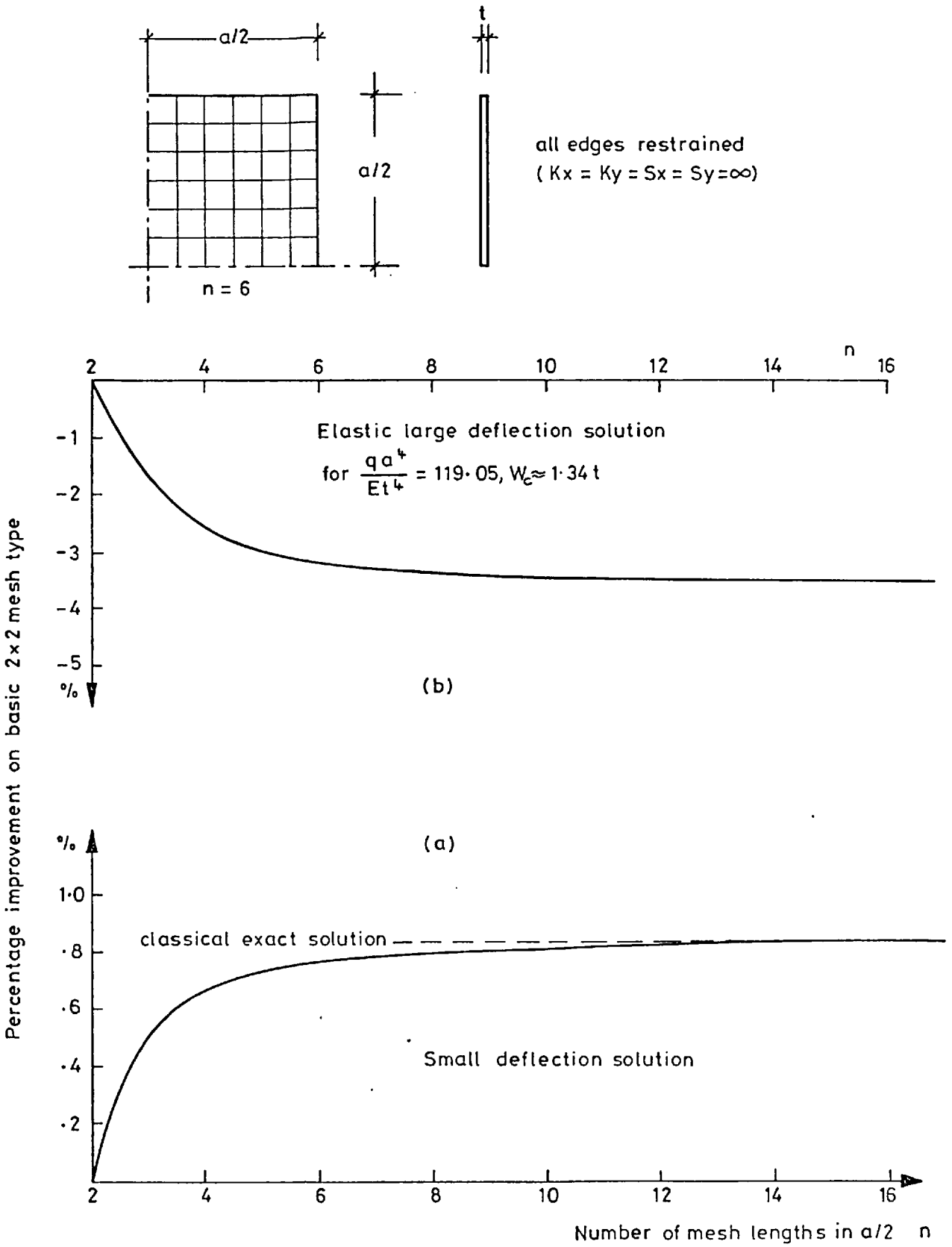

Fig. 13 Simply supported isotropic plate under uniform lateral load. Mesh convergence on basis of central deflection.

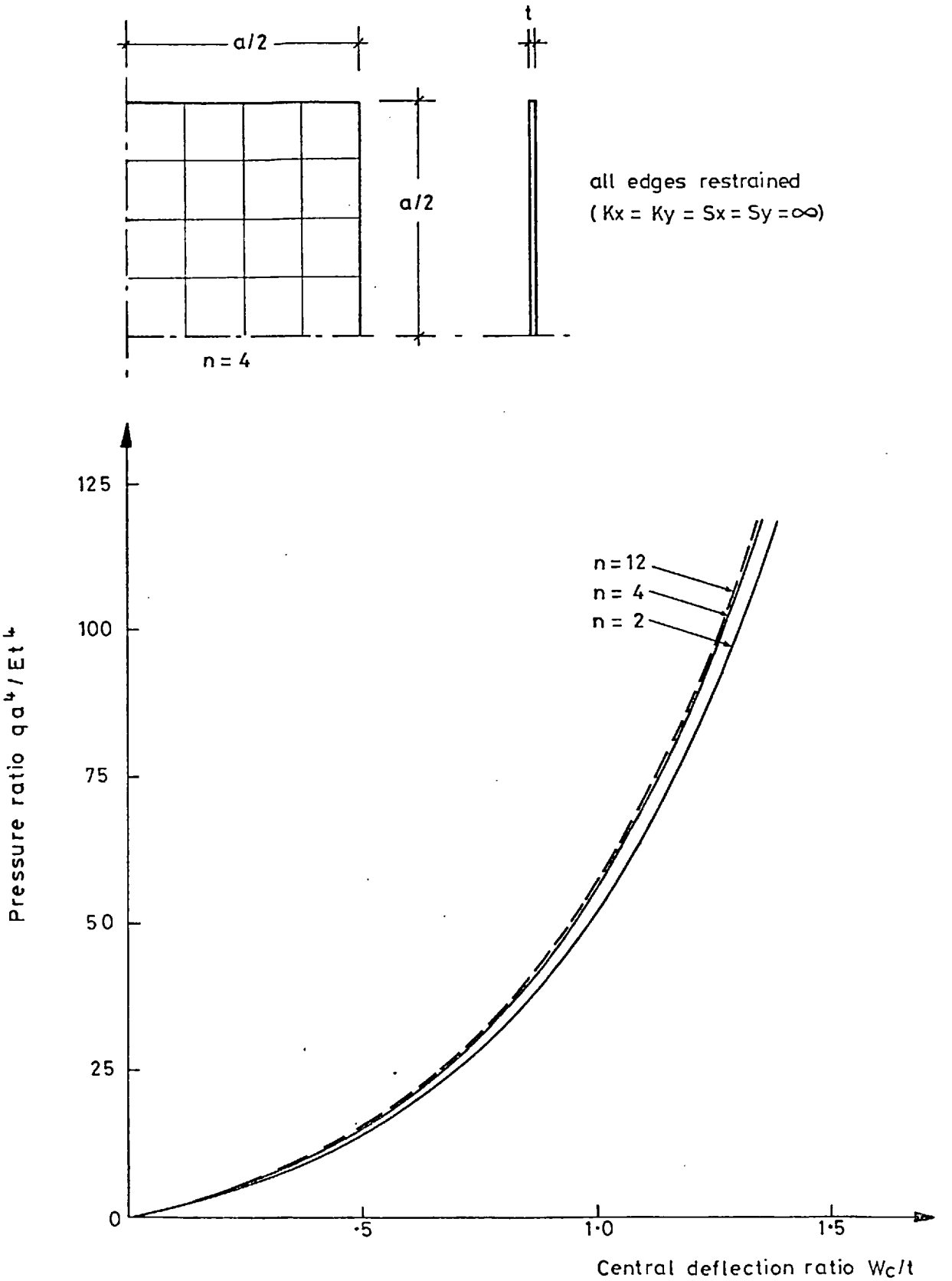

Fig. 14 Simply supported isotropic plate under uniform lateral load. Mesh convergence test for elastic large deflection solution (Central deflection)

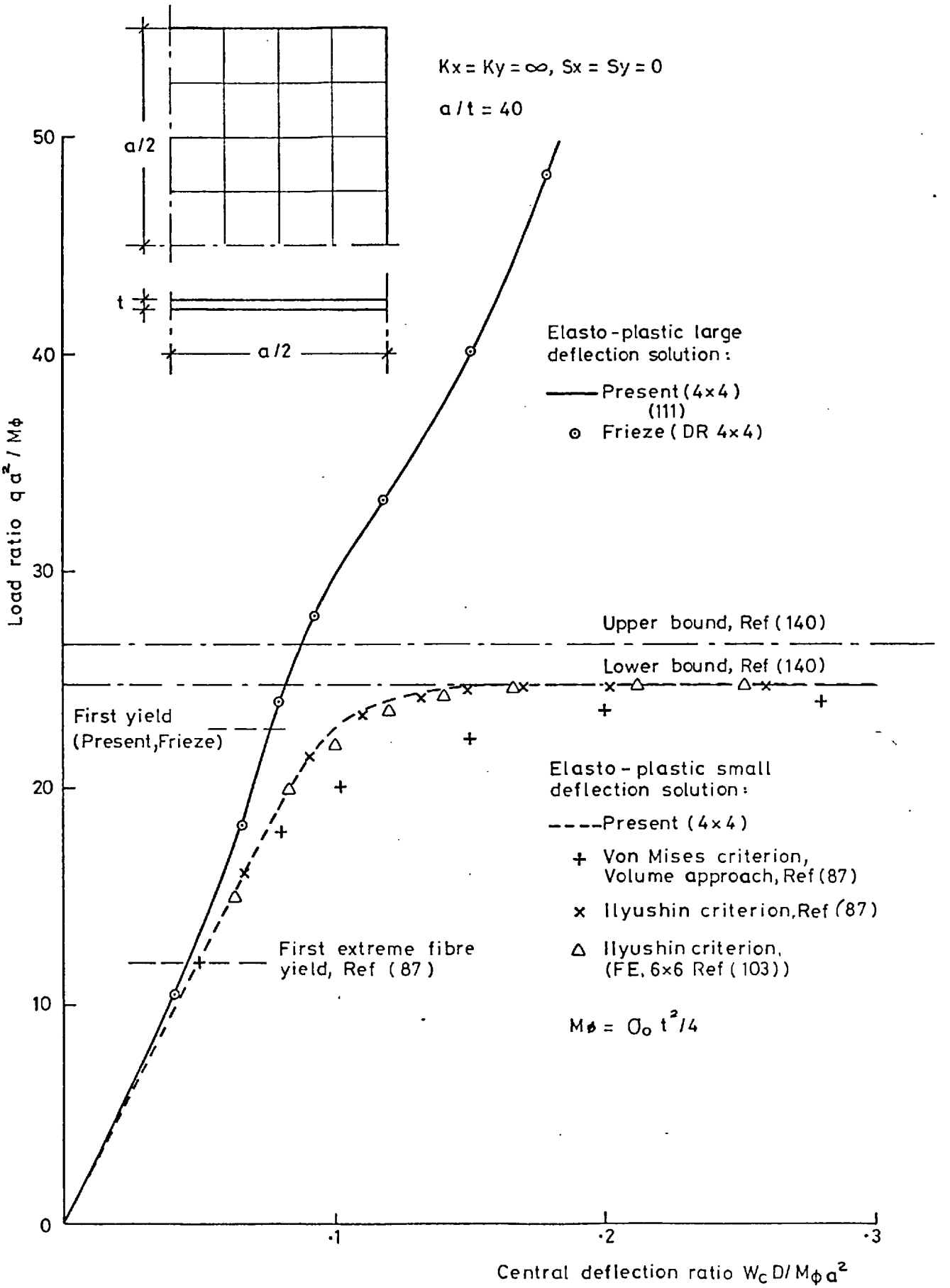

Fig. 15 Simply supported isotropic plate under lateral load. Central deflection (ν = 0·3)

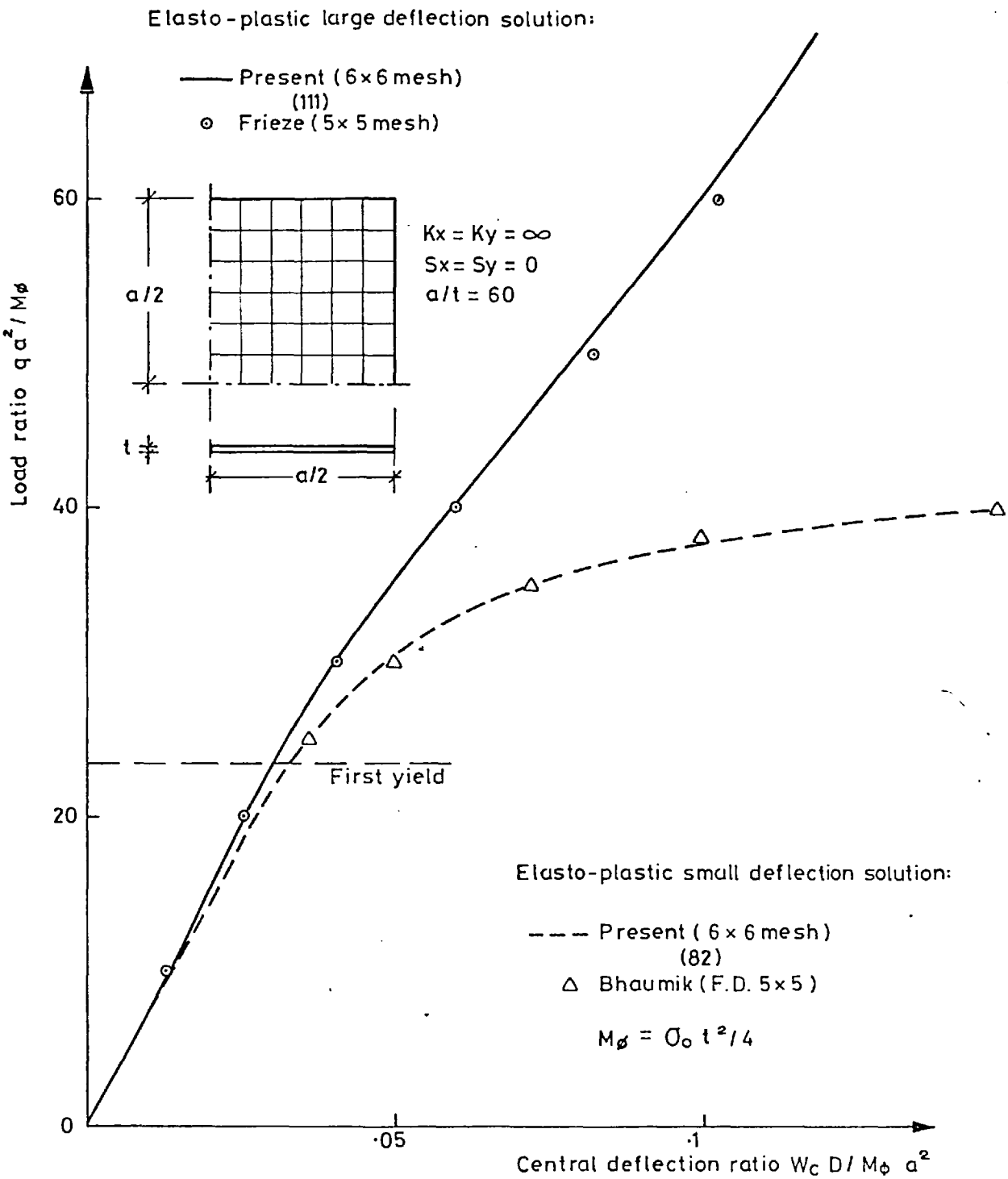

Fig. 16 Built-in isotropic plate under lateral load
Central deflection ($\nu = 0{\cdot}3$)

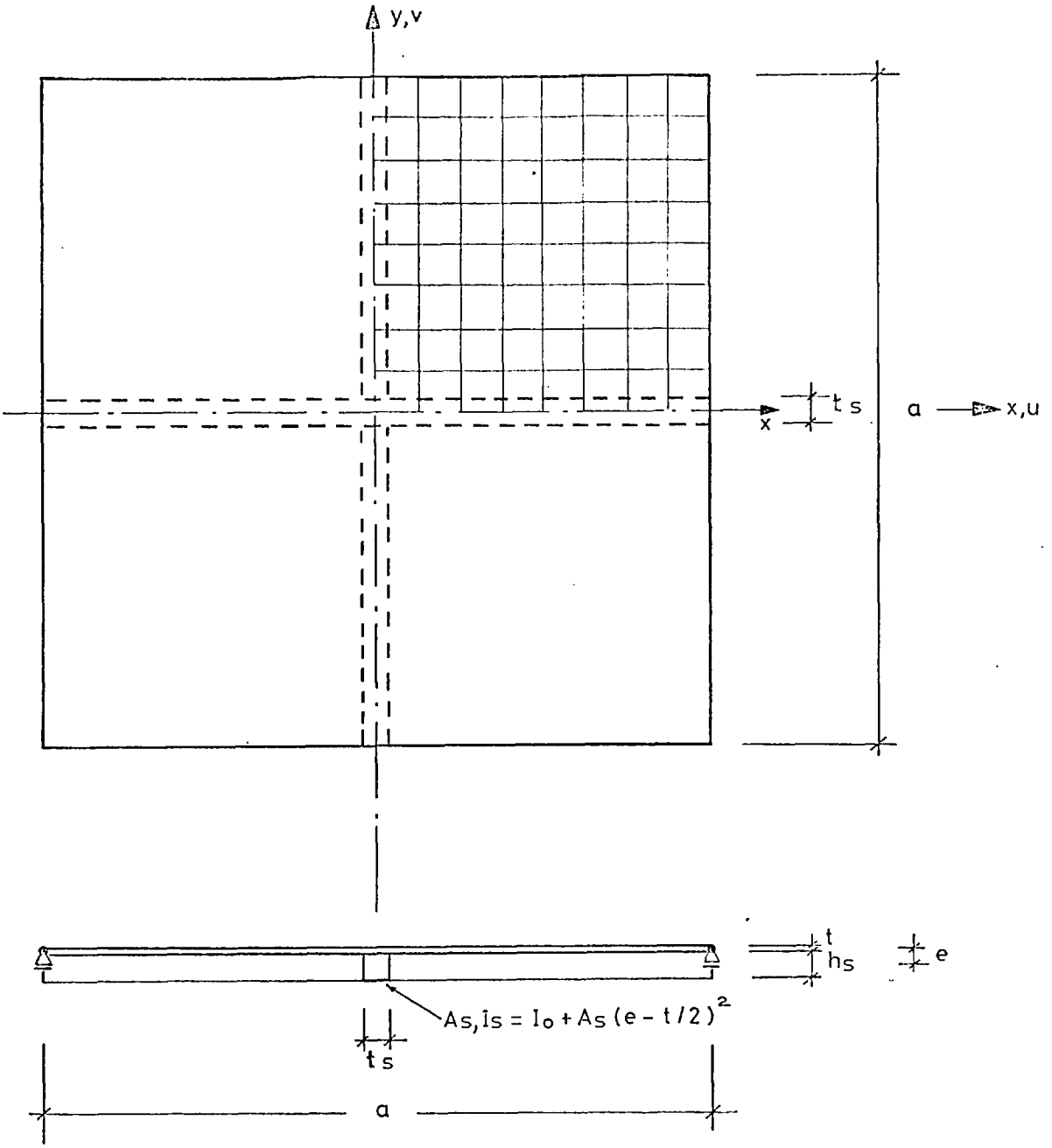

$a = 200\,mm$ $\quad E = 210000\ N/mm^2$

$t = 2\,mm$ $\quad \nu = \cdot 3$

$t_s = h_s = 8mm$ $\quad \bar{e} = e/t = 2 \cdot 5$

$\delta = \frac{A_s}{a \cdot t} = 0 \cdot 16$ $\quad \gamma = \frac{12\,(1-\nu^2)\,I_s}{a \cdot t^3} = 9 \cdot 32$

Fig. 17 Plate with one longitudinal and one transverse stiffener

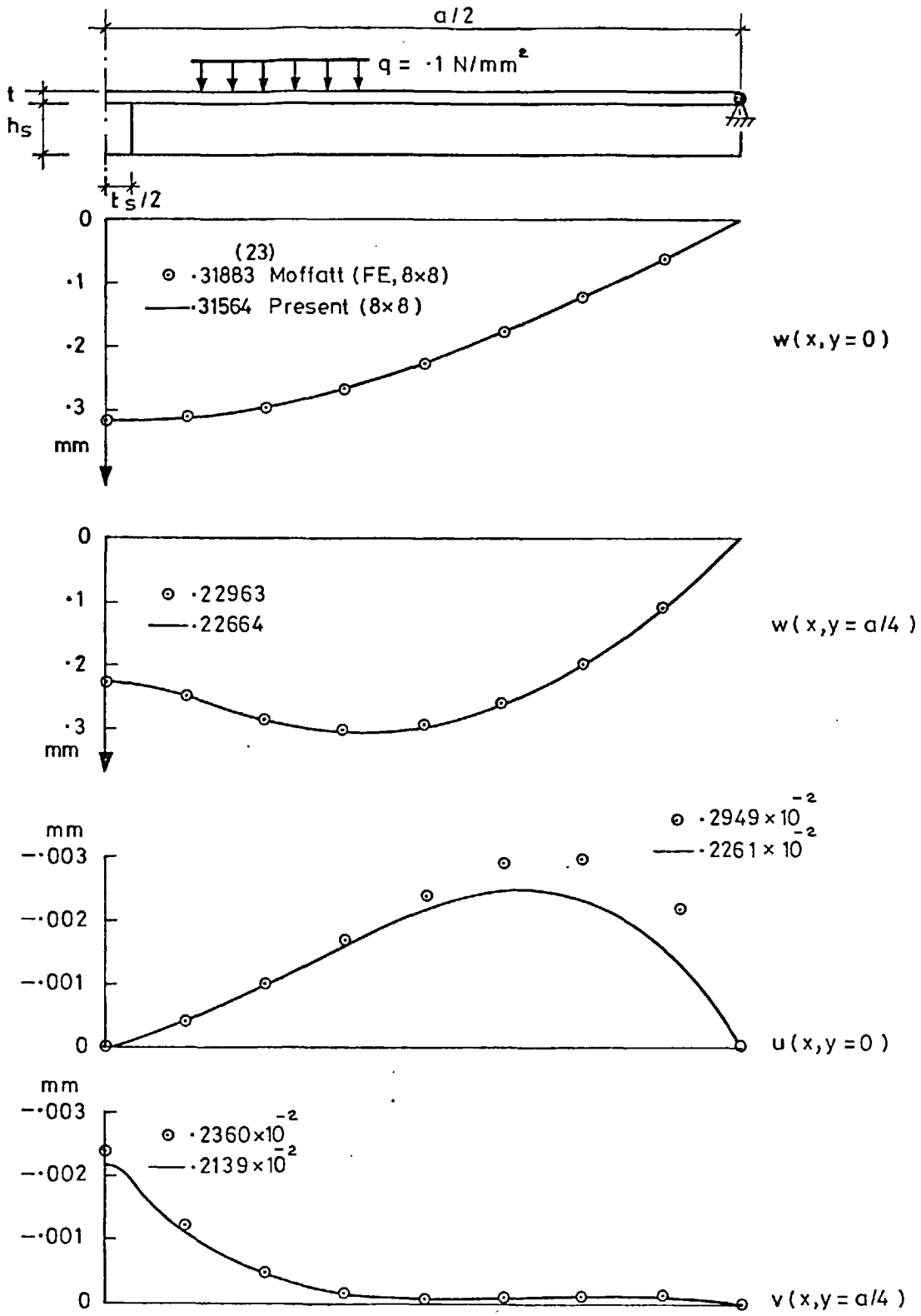

Fig. 18 Simply supported plate with one longitudinal and one transverse stiffener. Small deflection solution. (Kx = Ky = Sx = Sy = ∞)

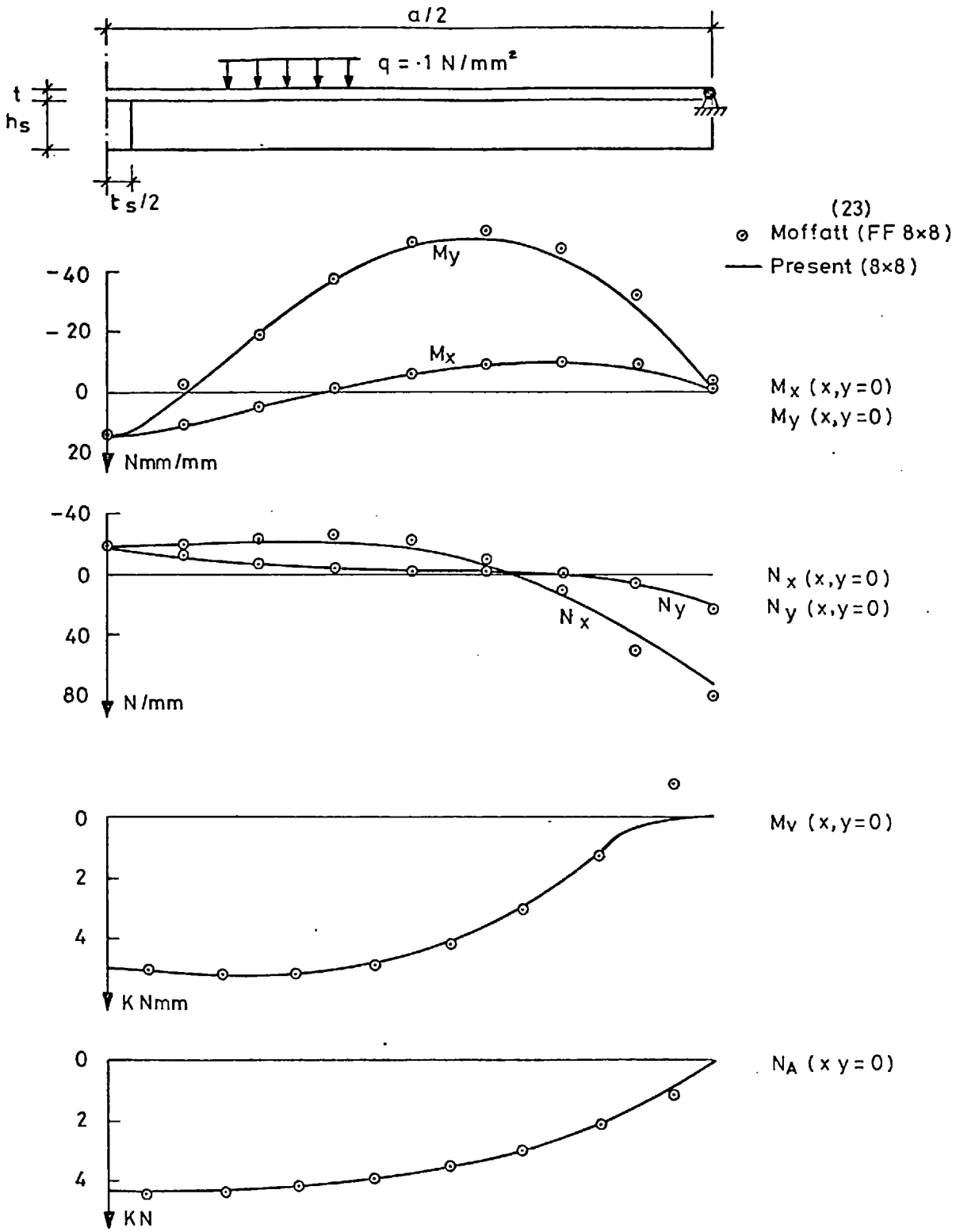

Fig. 19 Simply supported plate with one longitudinal and one transverse stiffener. Small deflection solution ($K_x = K_y = S_x = S_y = \infty$)

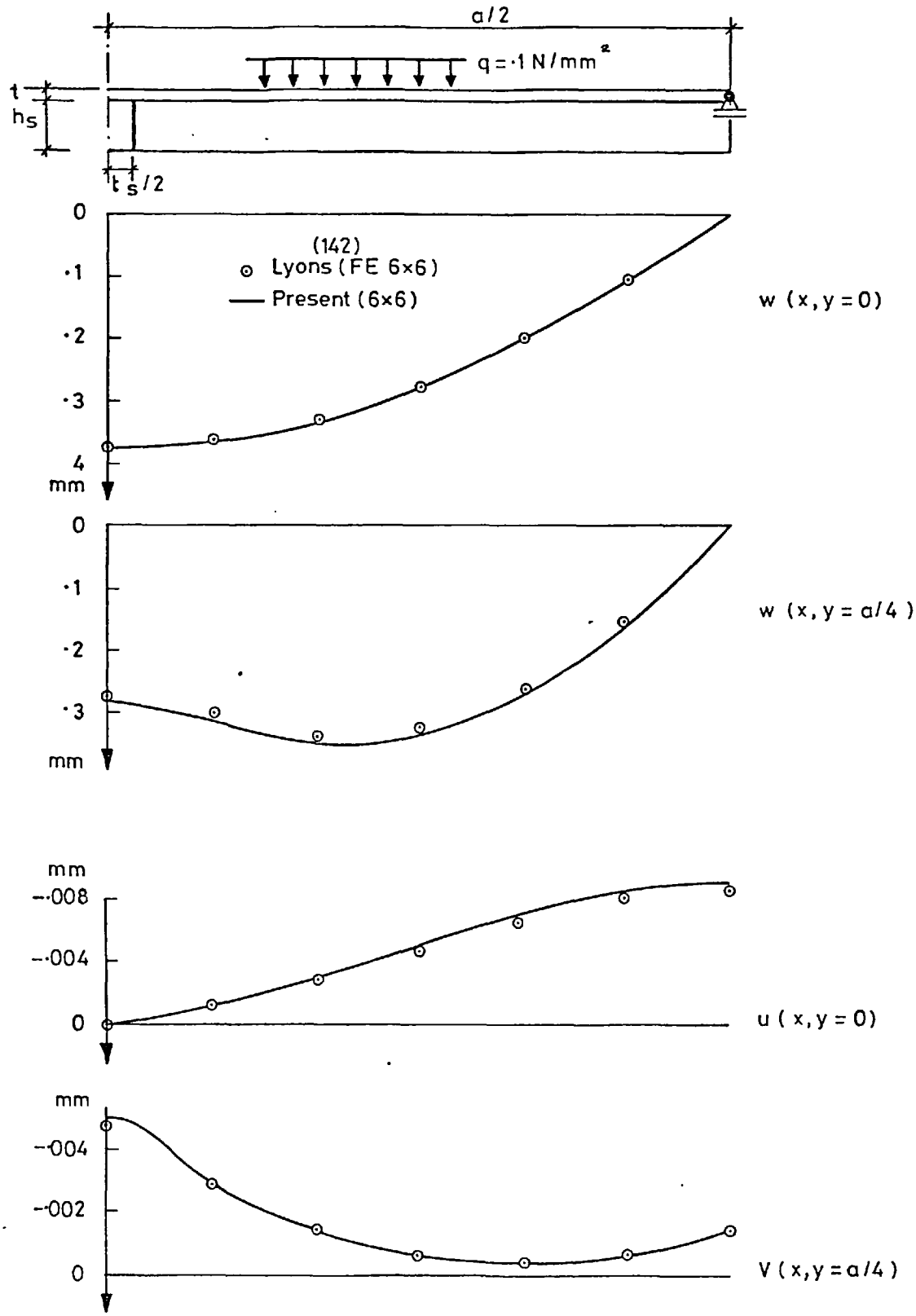

Fig. 20 Simply supported plate with one longitudinal and one transverse stiffener. Small deflection solution (Kx = Ky = Sx = Sy = 0)

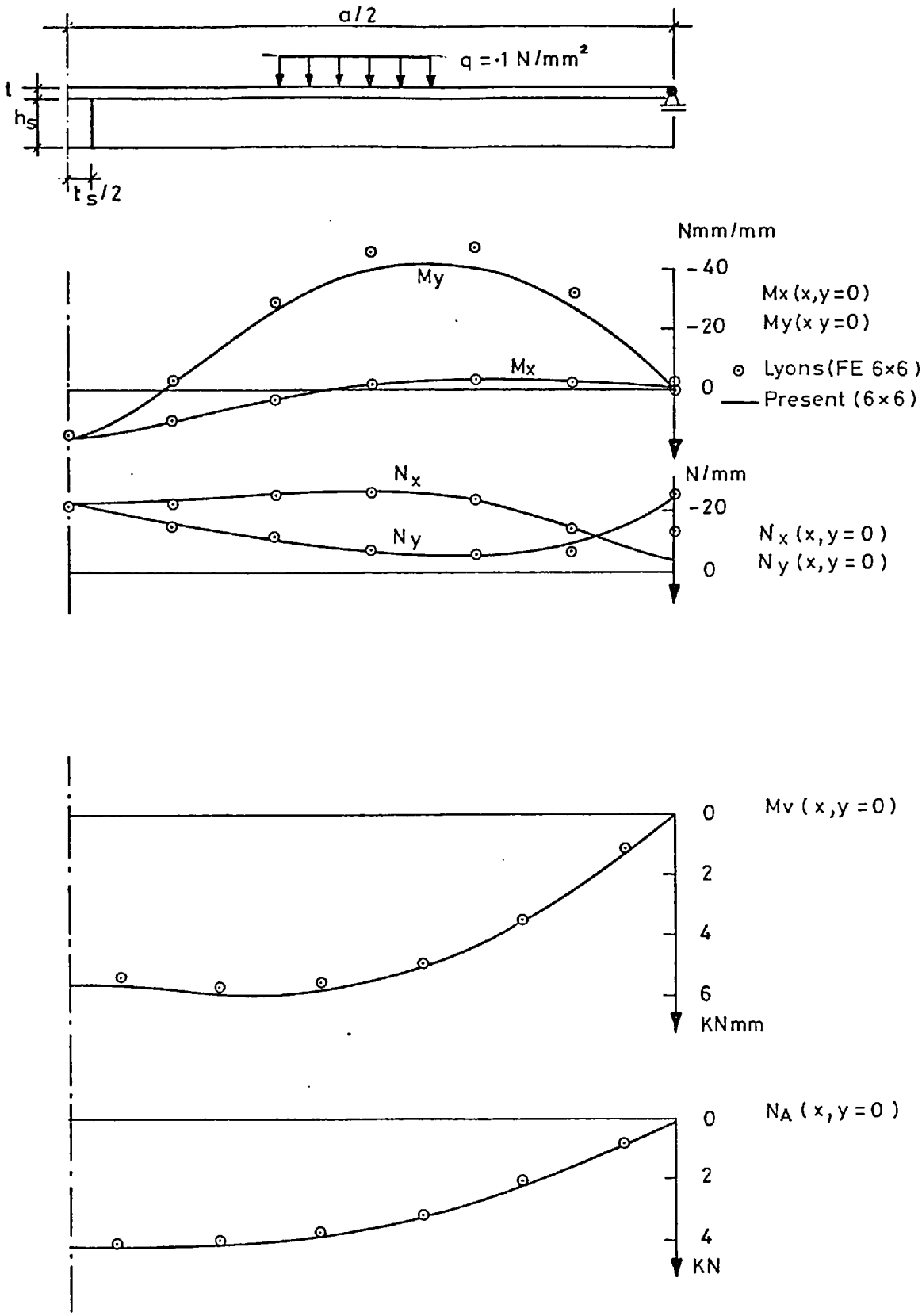

Fig. 21 Simply supported plate with one longitudinal and one transverse stiffener. Small deflection solution (Kx = Ky = Sx = Sy = 0)

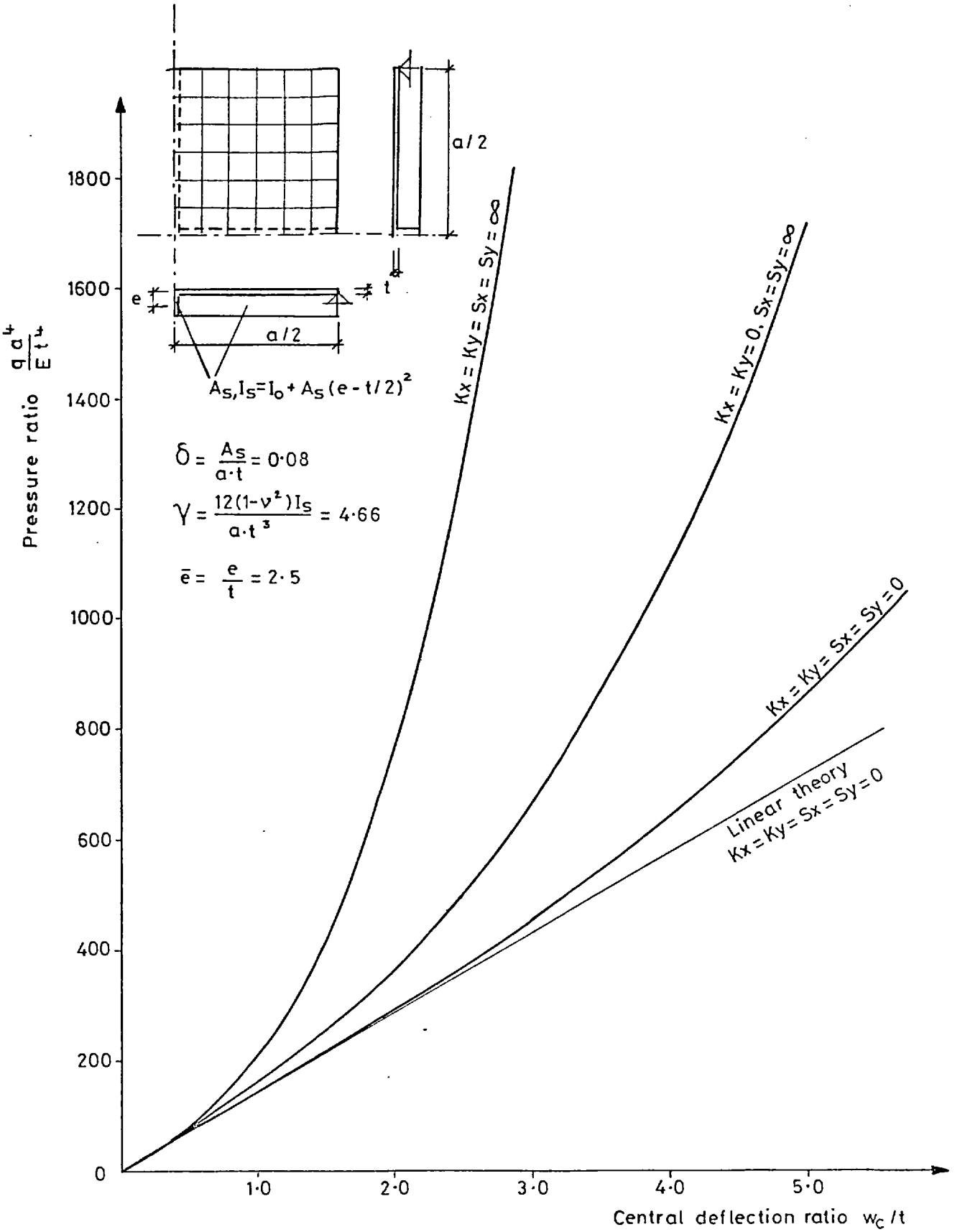

Fig. 22 Simply supported plate with one longitudinal and one transverse stiffener subject to uniform lateral load, central deflection.

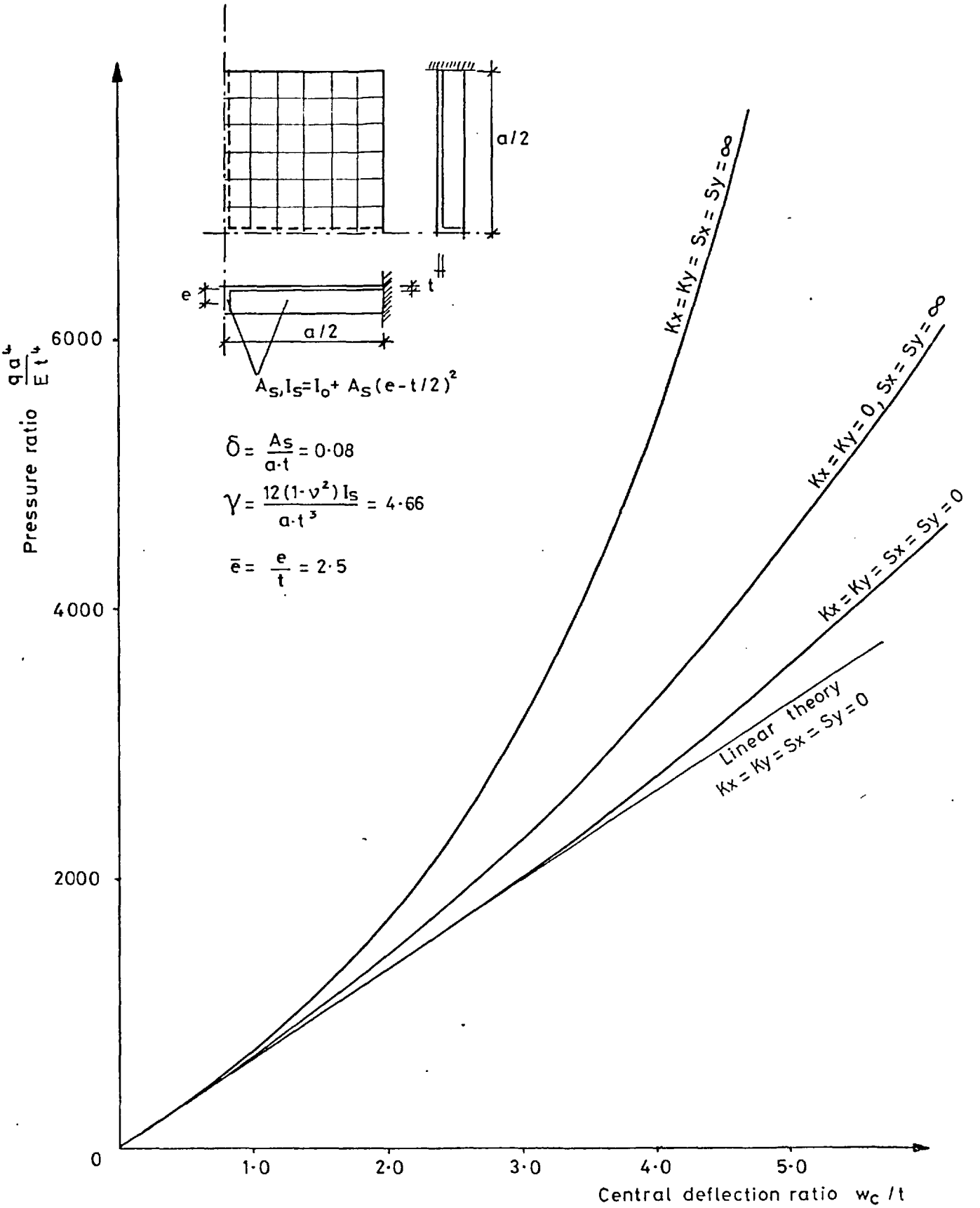

Fig. 23 Built-in plate with one longitudinal and one transverse stiffener under uniform lateral load, central deflection.

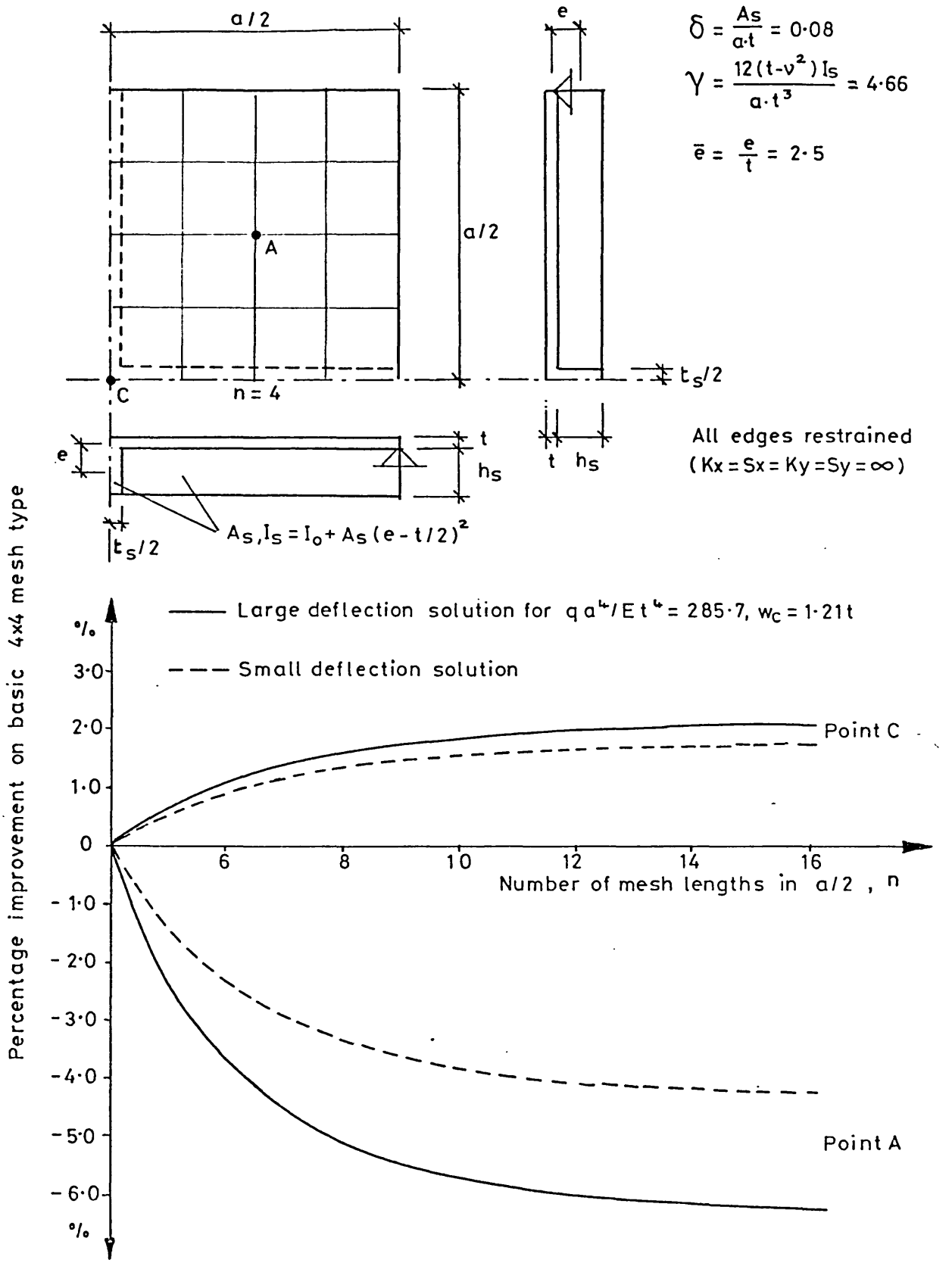

Fig. 24 Simply supported discretely stiffened plate under uniform lateral load, Mesh convergence on basis of central deflection

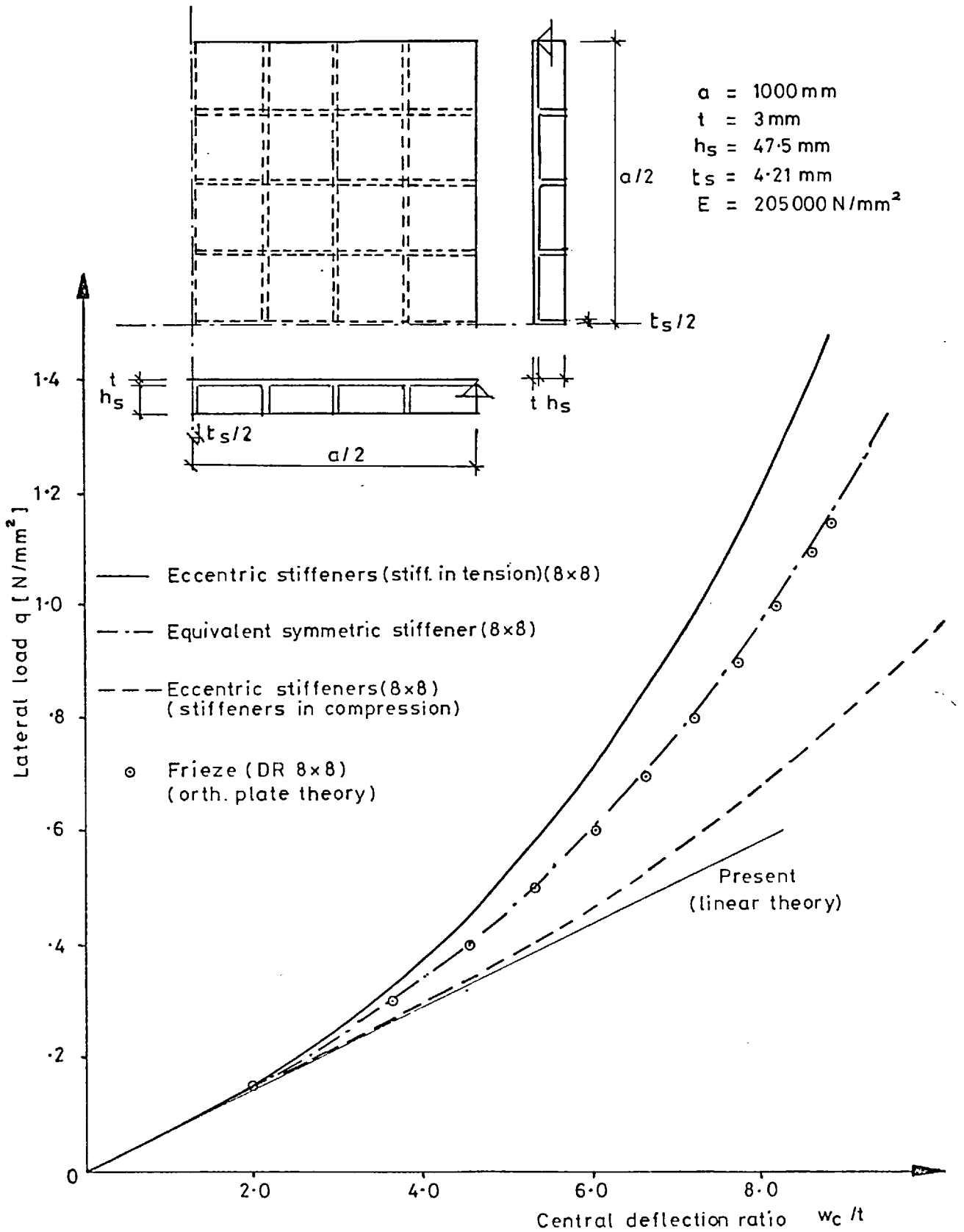

Fig. 25 Simply supported stiffened plate under uniform lateral load central deflection ($K_x = K_y = S_x = S_y = \infty$)

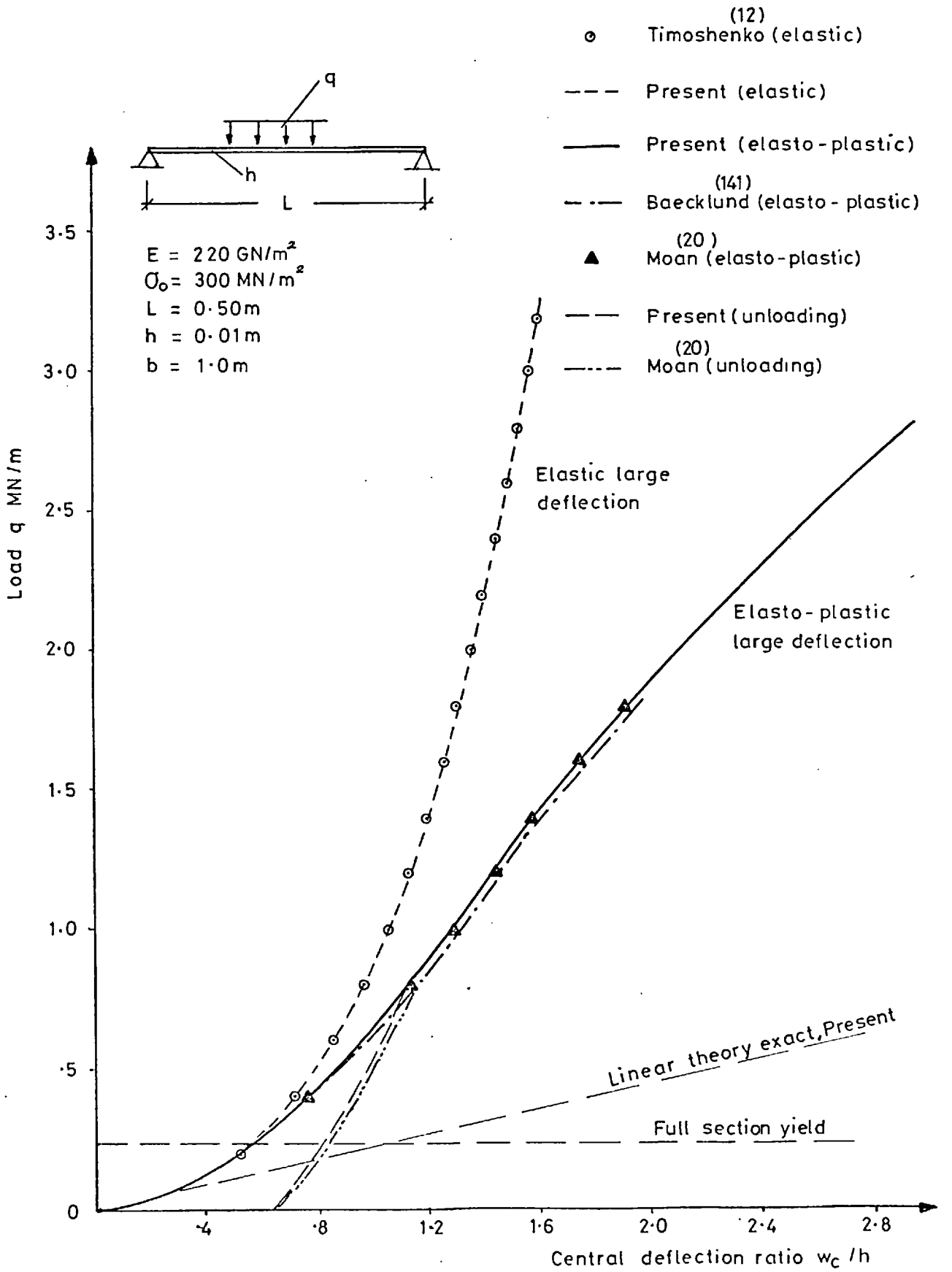

Fig. 26 Load - deflection curve for stiffener analysis

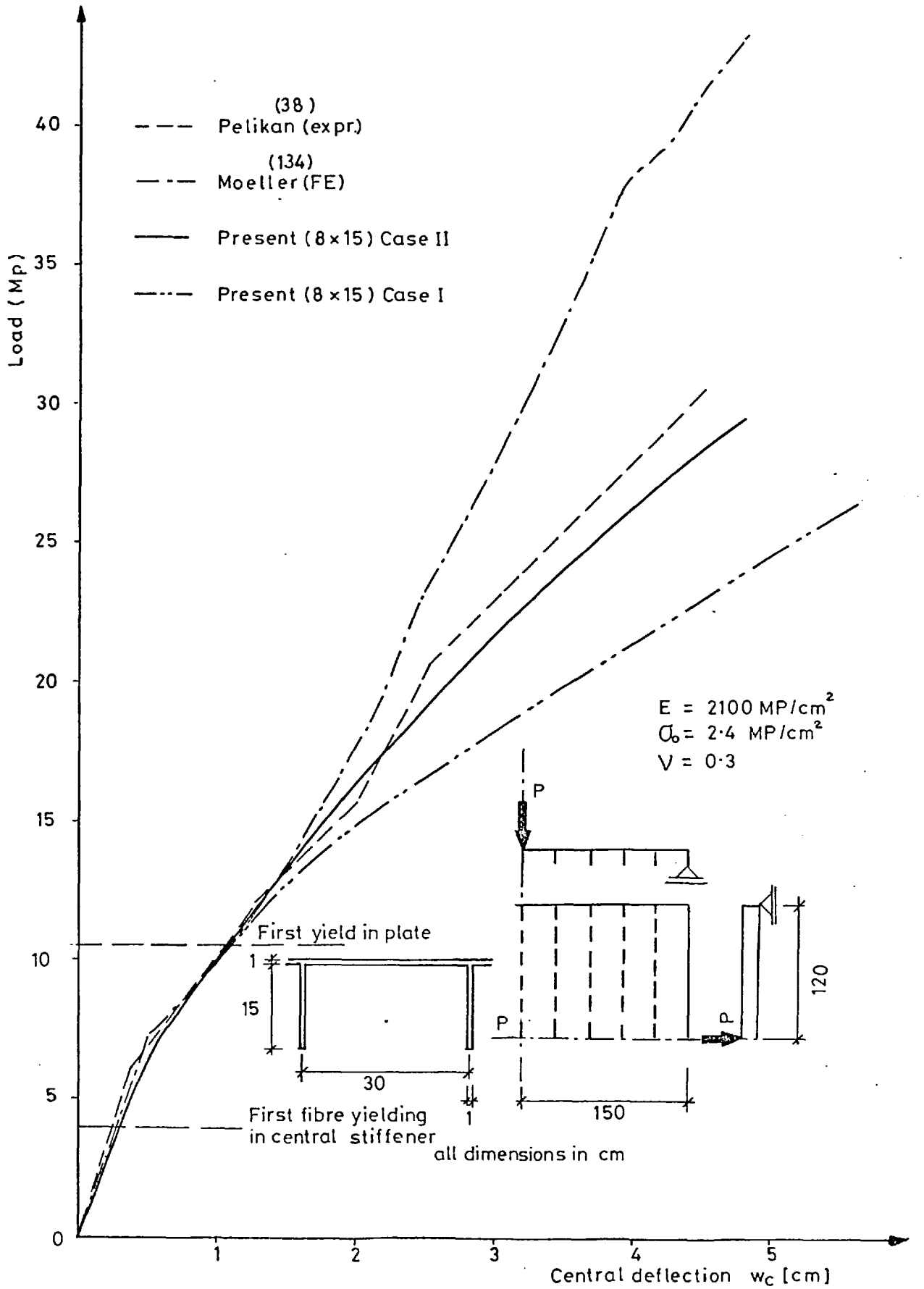

Fig. 27 Load-deflection curve for longitudinally stiffened plate under lateral point load.

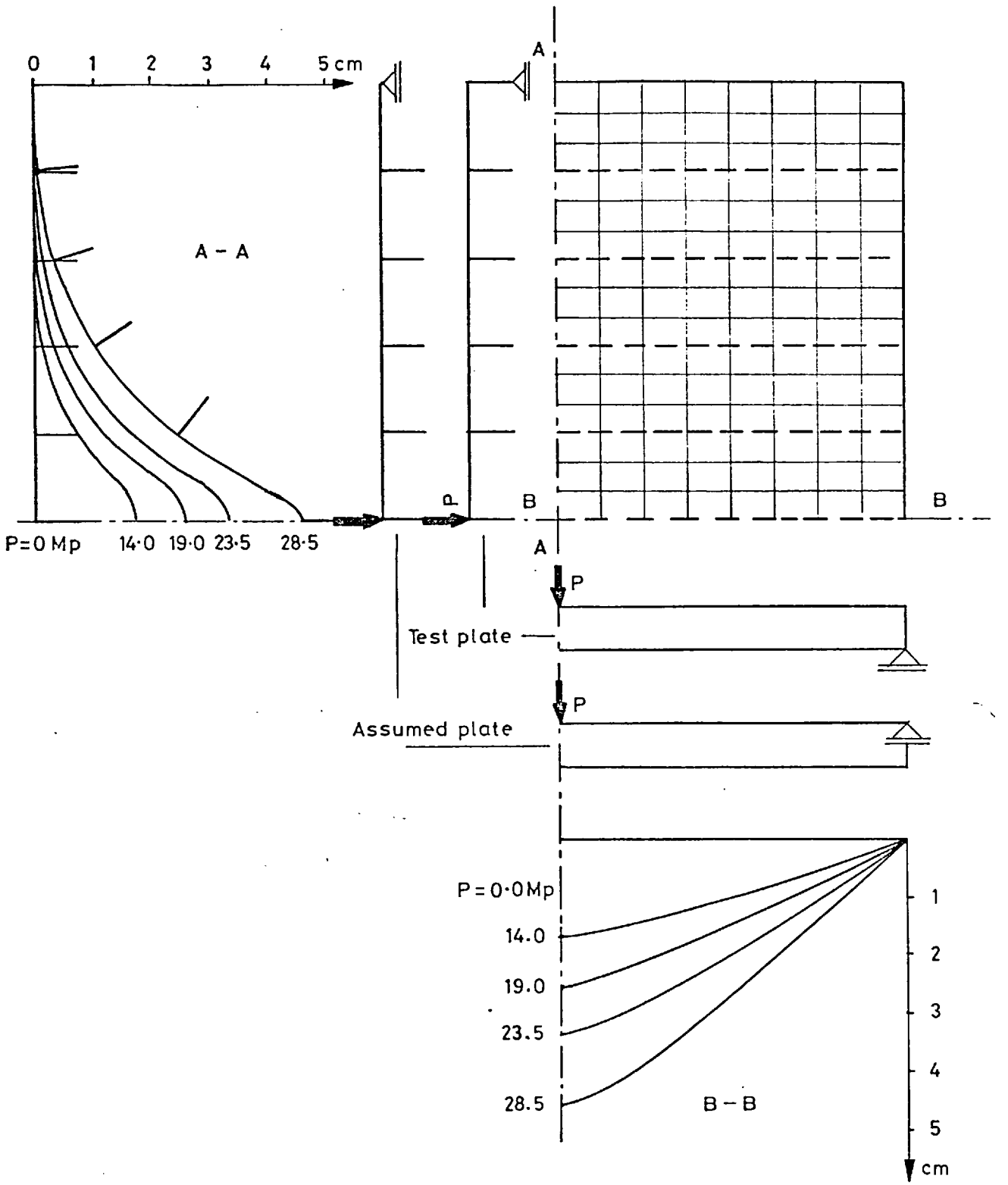

Fig. 28 Longitudinally stiffened plate under lateral point load
Lateral displacement profiles for case II

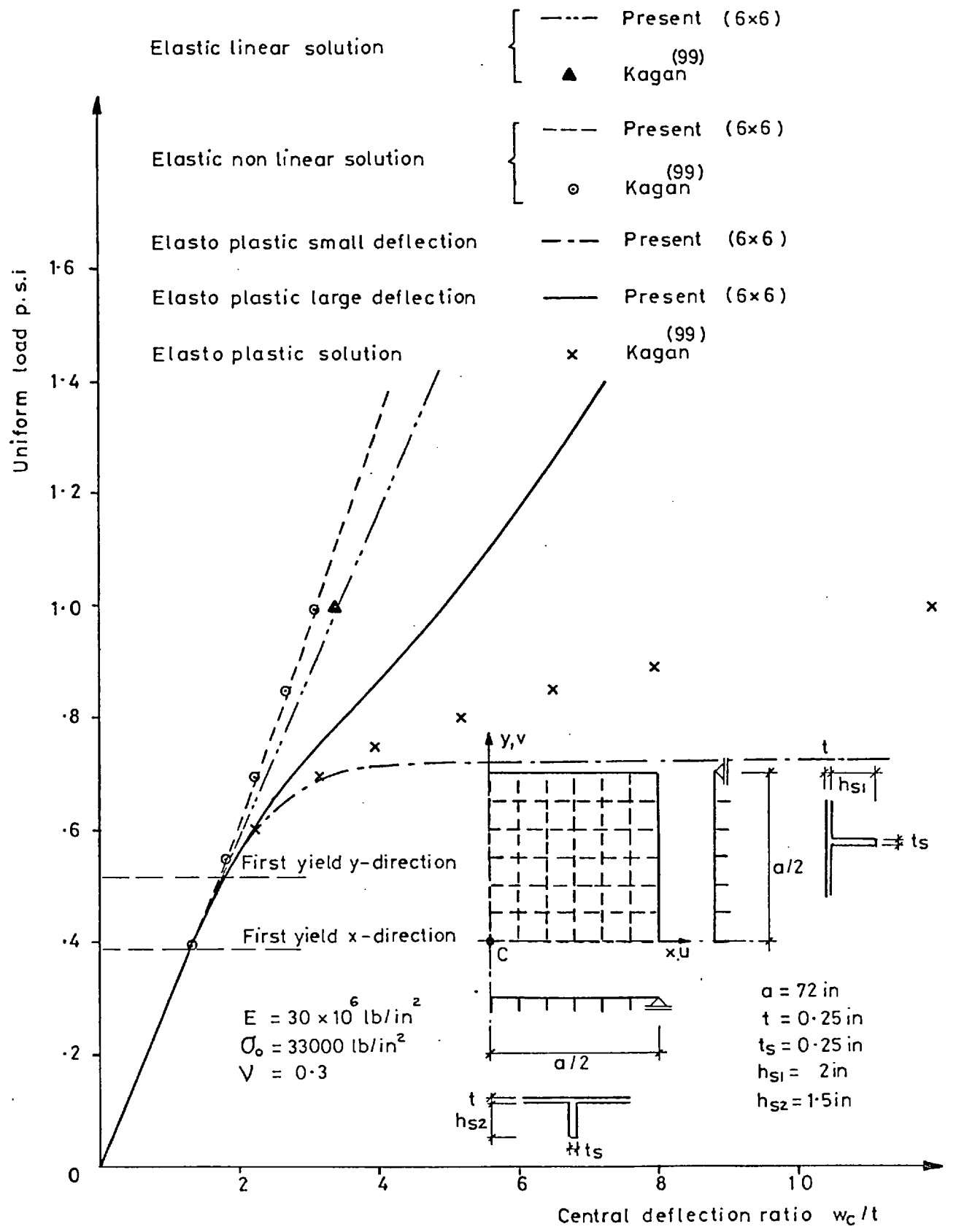

Fig. 29 Load-deflection curve for a two-way reinforced plate under uniform lateral load.

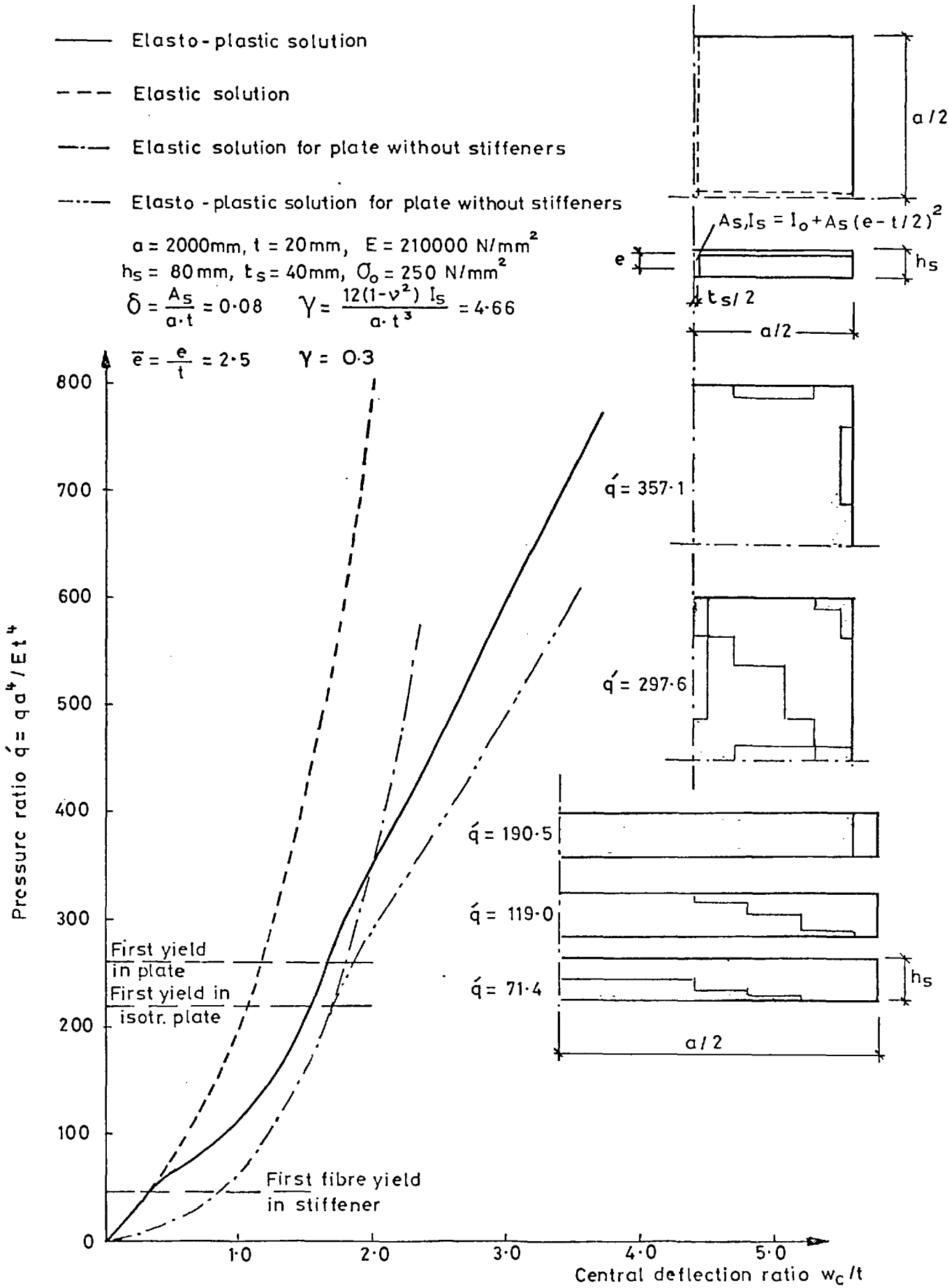

Fig.30 Simply supported discretely stiffened plate subject to lateral loading

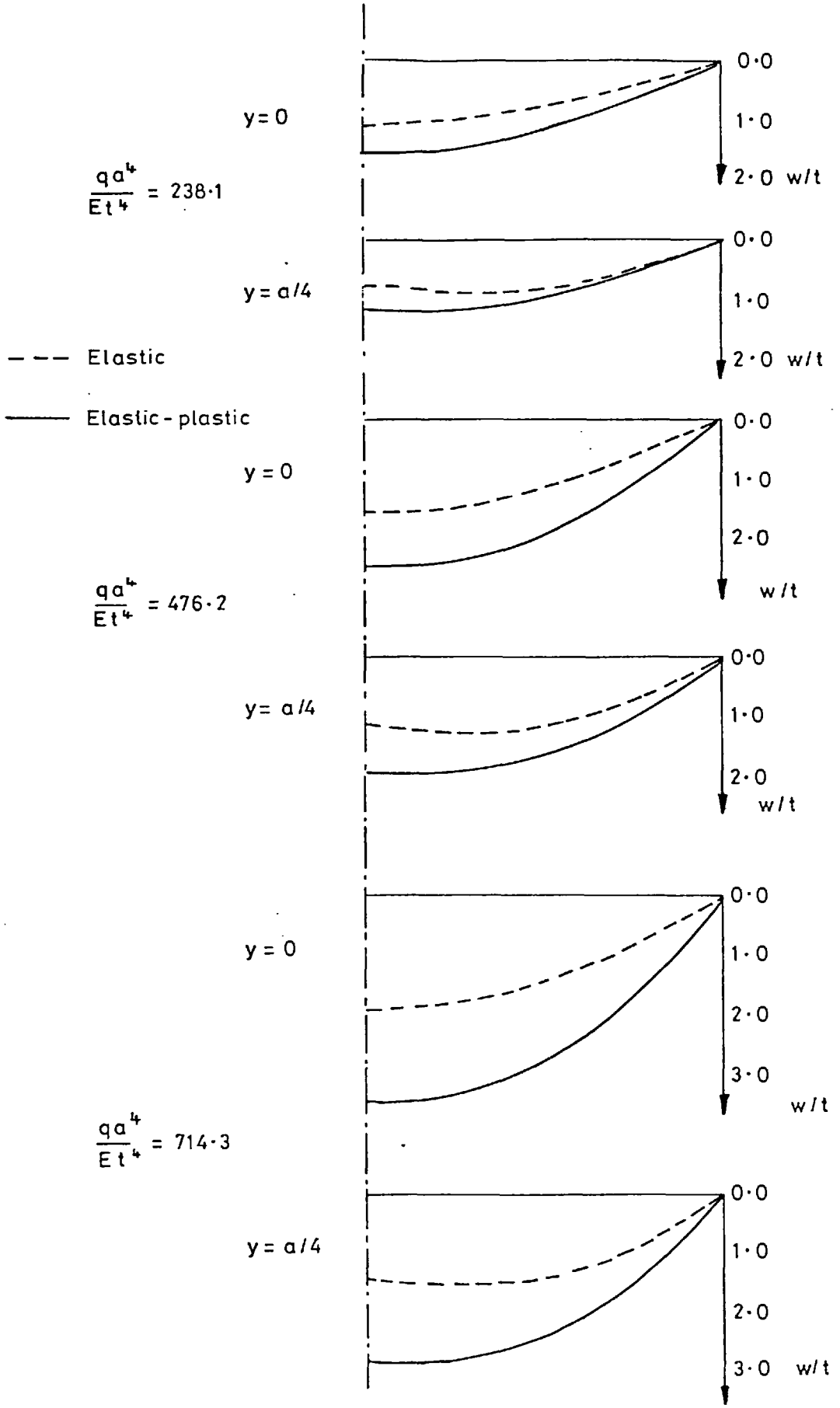

Fig. 31 Simply supported discretley stiffened plate subject to uniform lateral load. Elastic and elastic-plastic deflection profiles.

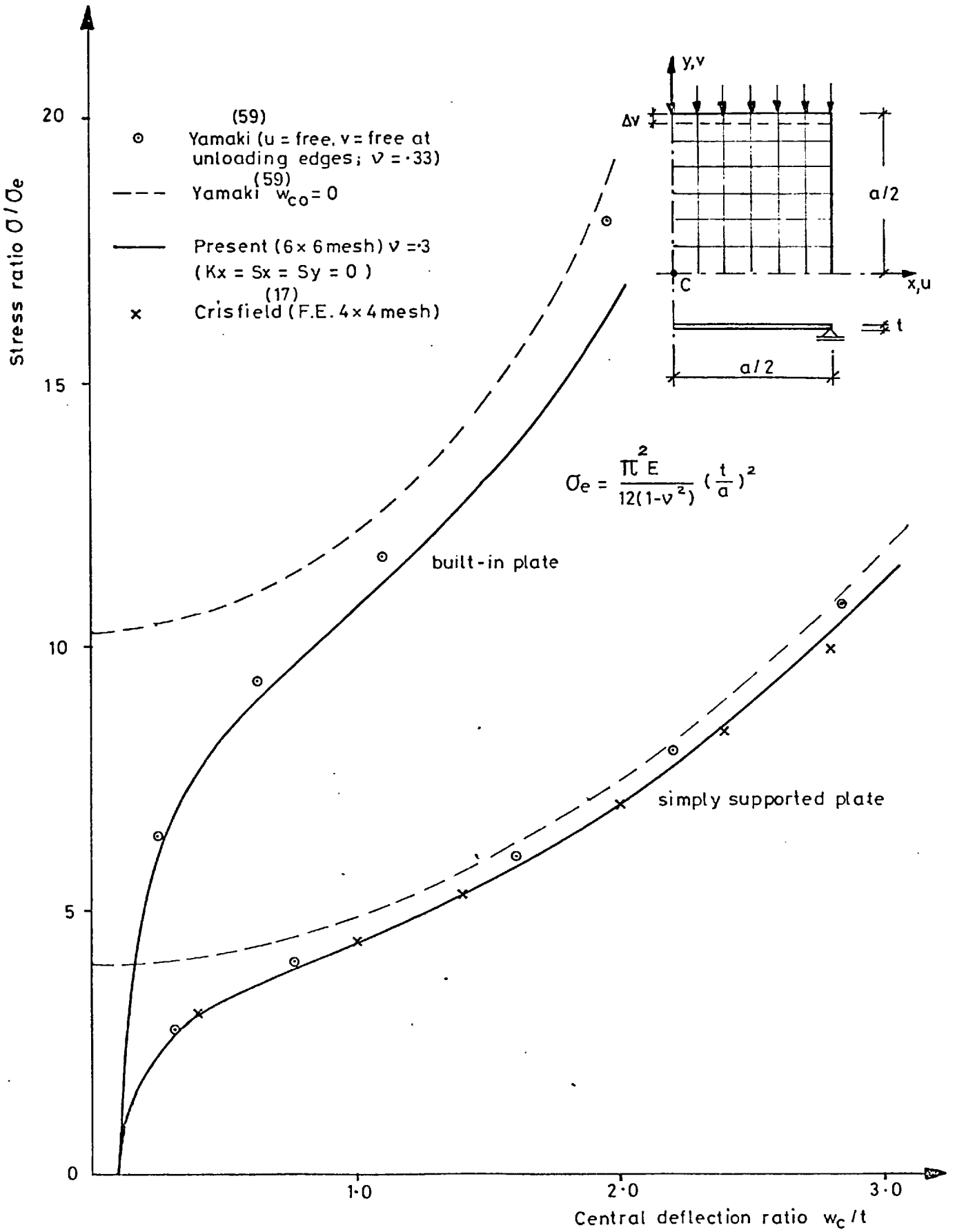

Fig. 32 Imperfect isotropic plate under in-plane load

Central deflection (ν = 0·3)

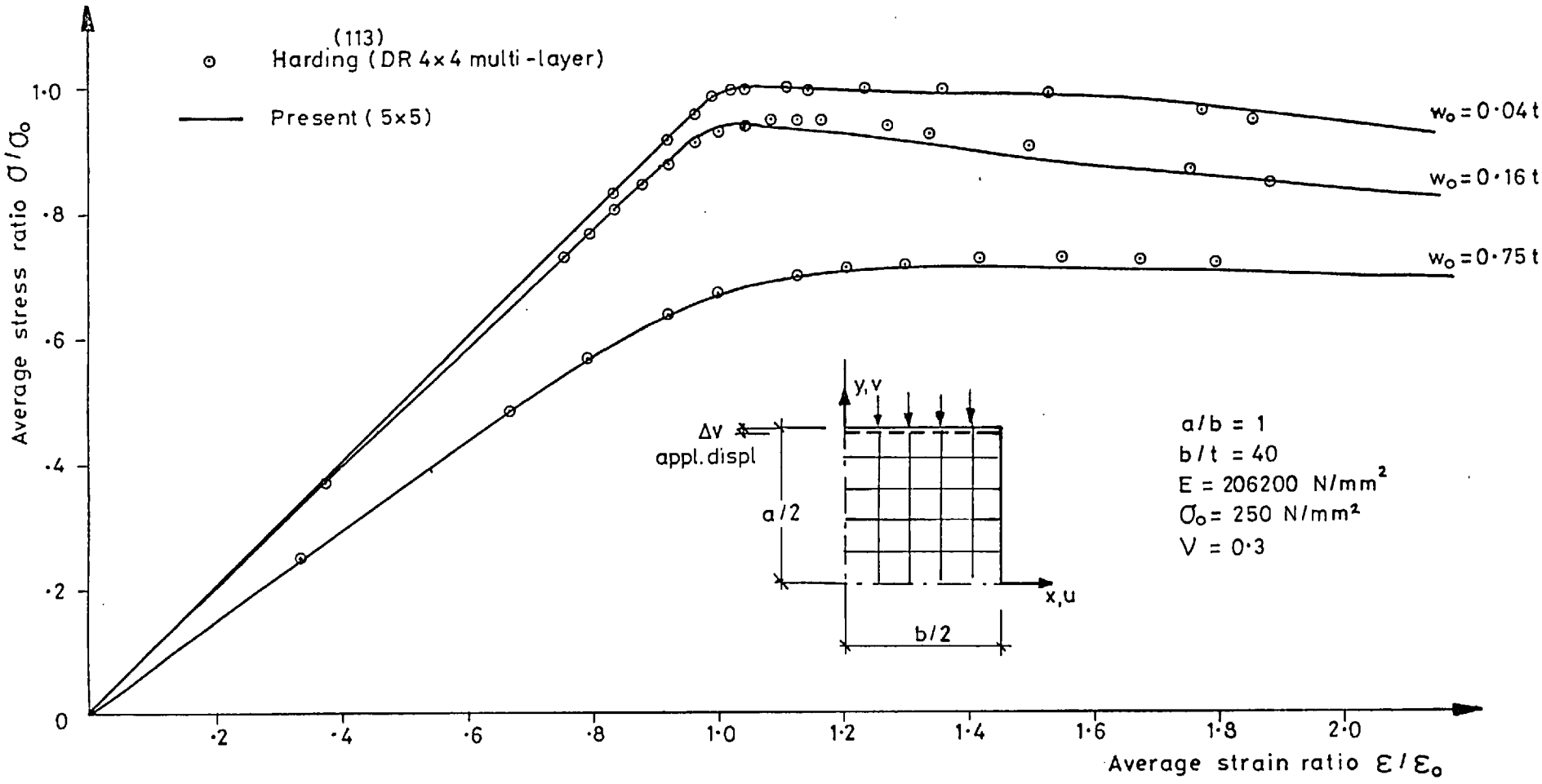

Fig. 33 Relation between average stress and average strain for simply supported plate in direct compression ($K_x = S_x = S_y = 0$)

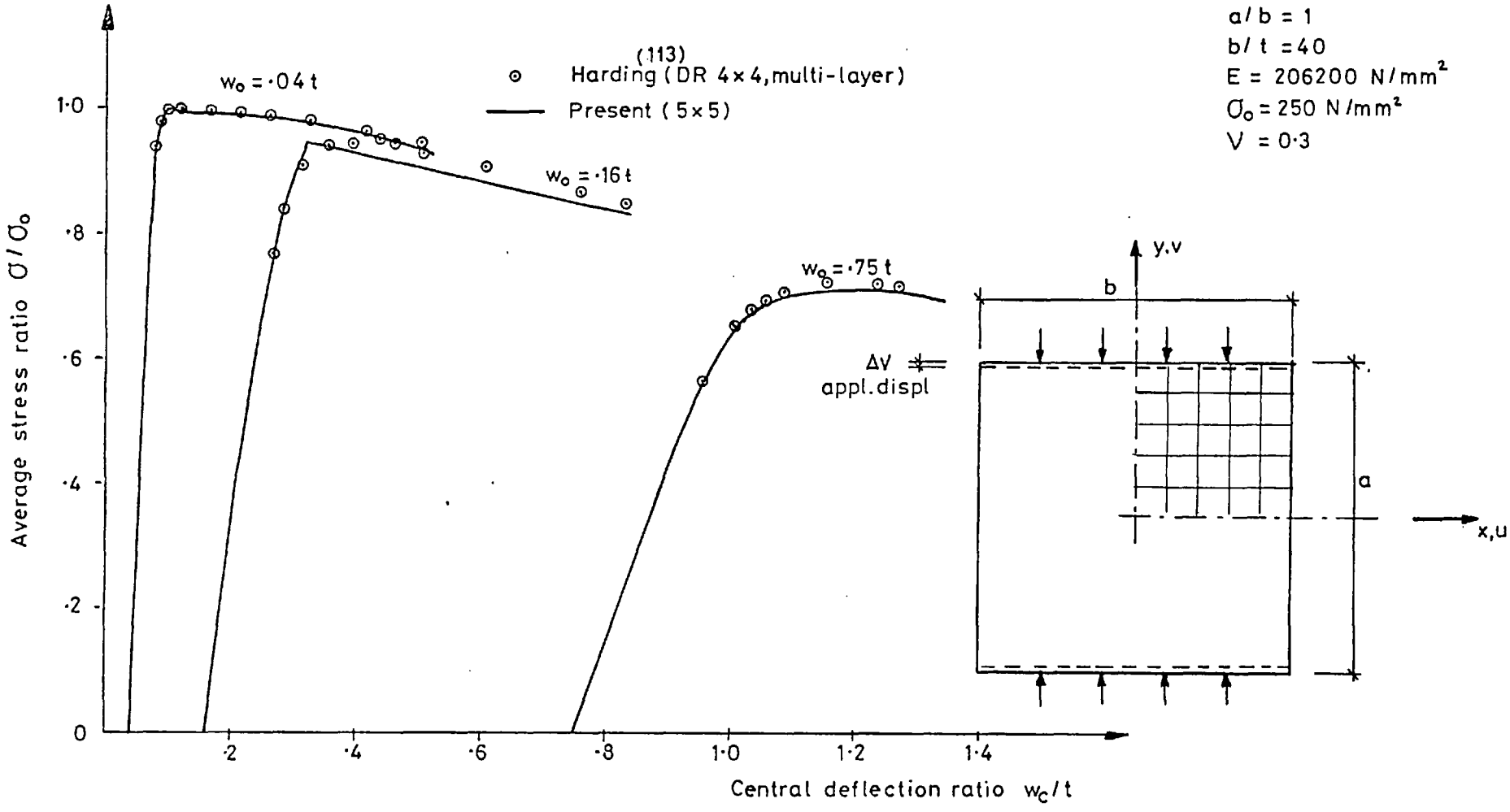

Fig. 34 Relation between average stress and central deflection for simply supported plate in direct compression (Kx = Sx = Sy = 0)

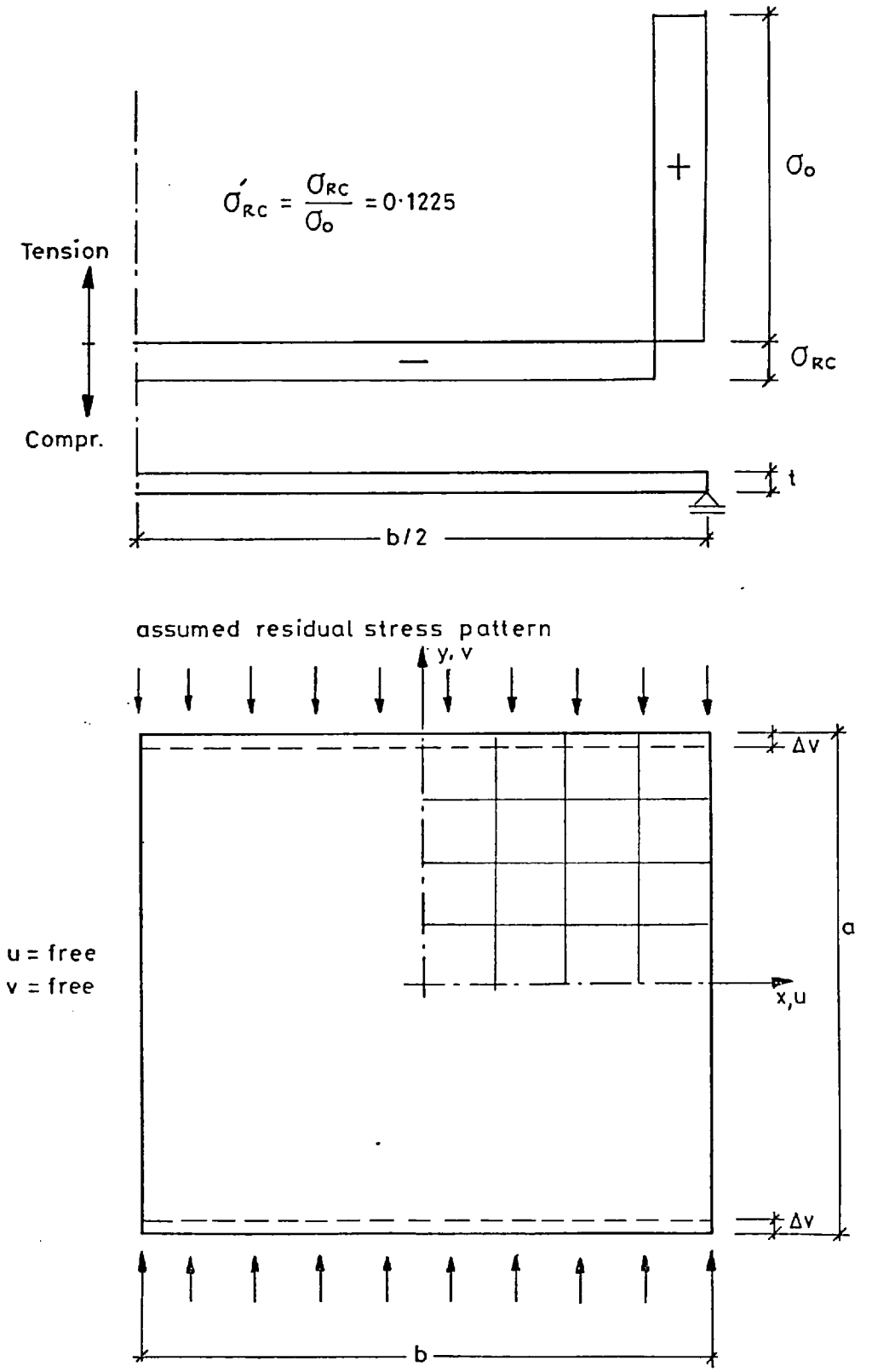

Fig. 35 Isotropic plate under uniaxial compression, assumed residual stress pattern.

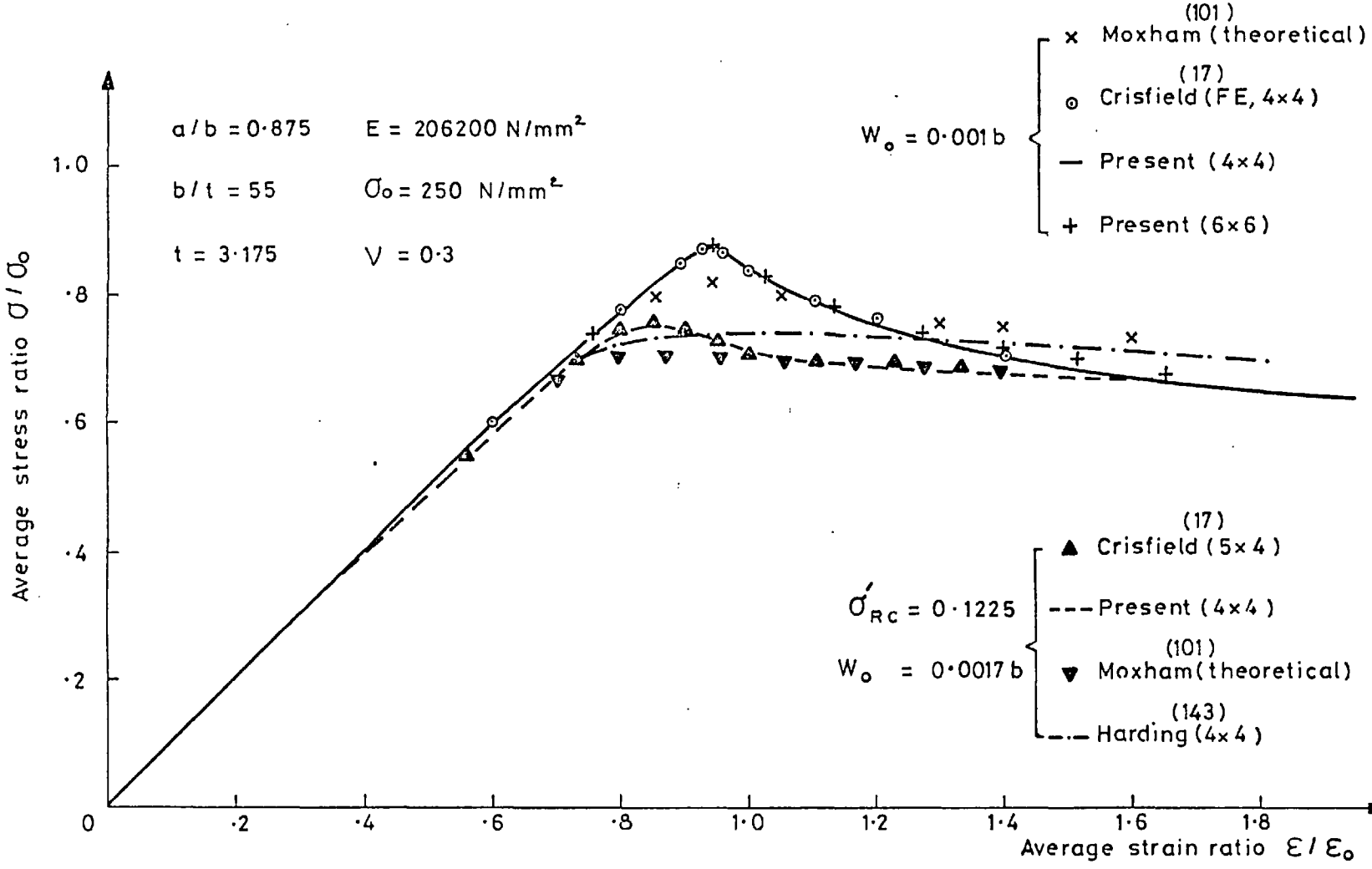

Fig. 36 Relation between average stress and average strain for simply supported plate in direct compression (Kx = Sx = Sy = 0)

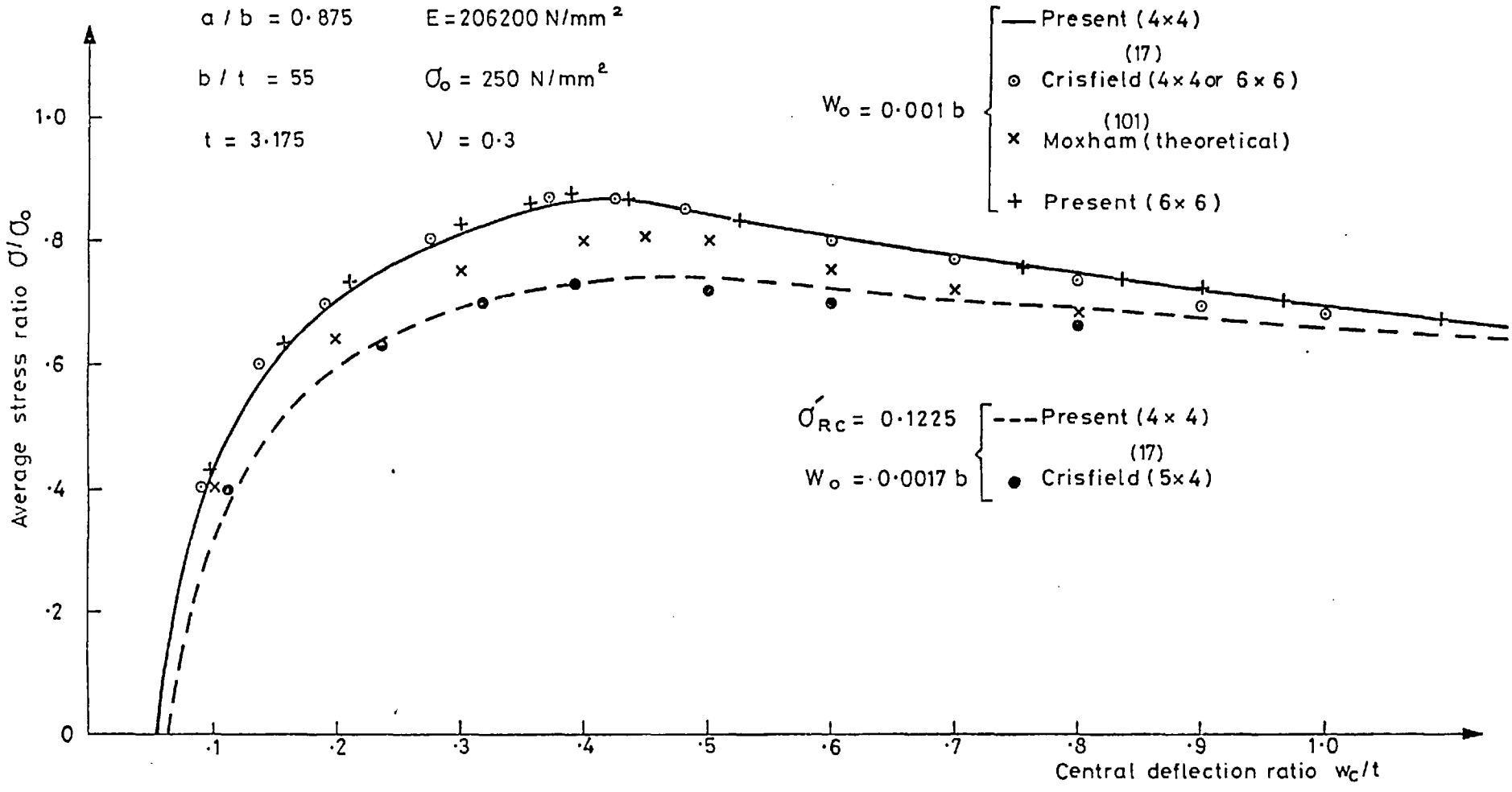

Fig.37 Relation between average stress and central deflection for simply supported plate in direct compression (Kx = Sx = Sy = 0)

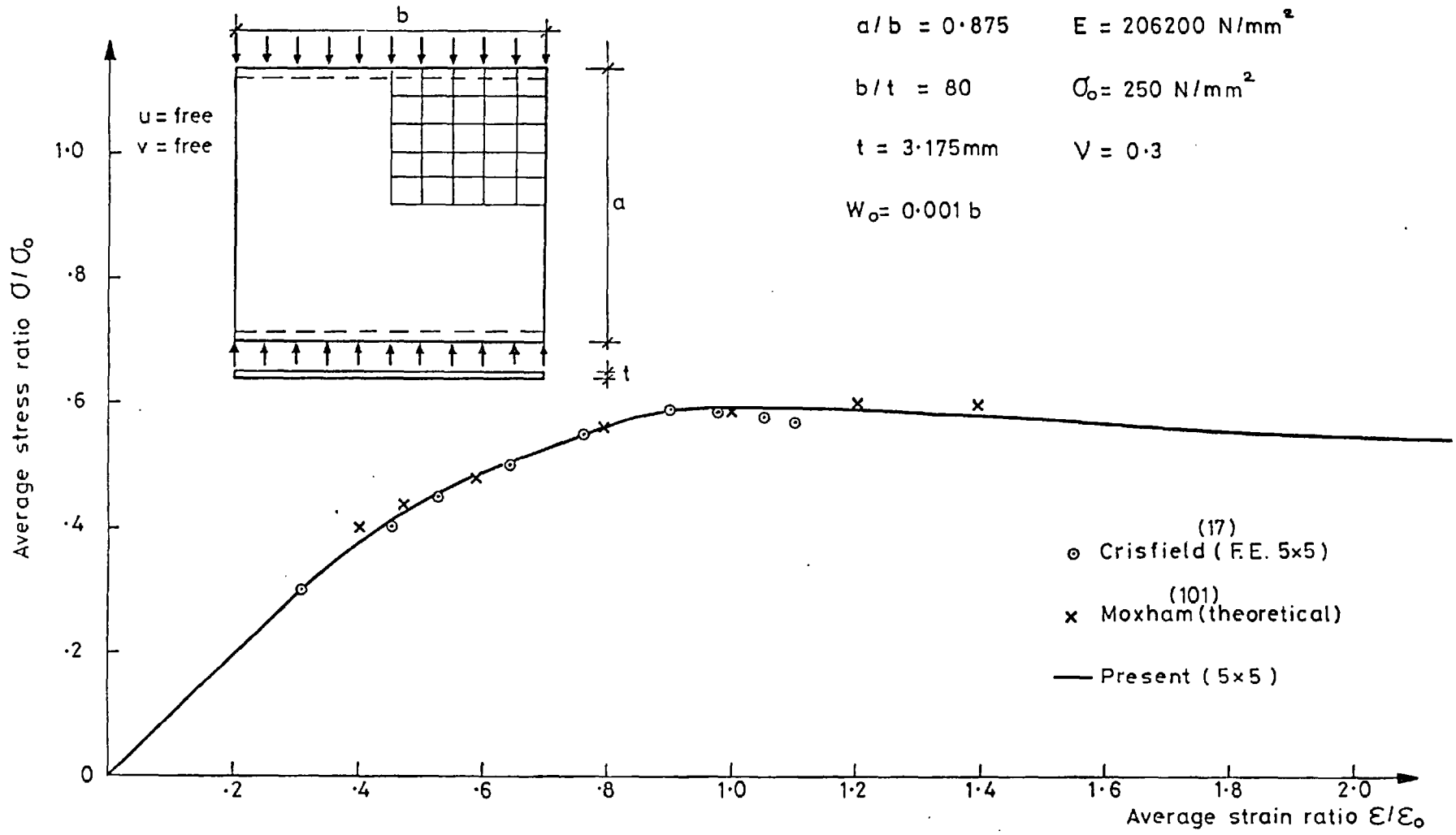

Fig.38 Relation between average stress and average strain for simply supported plate in direct compression (Kx = Sx = Sy = 0)

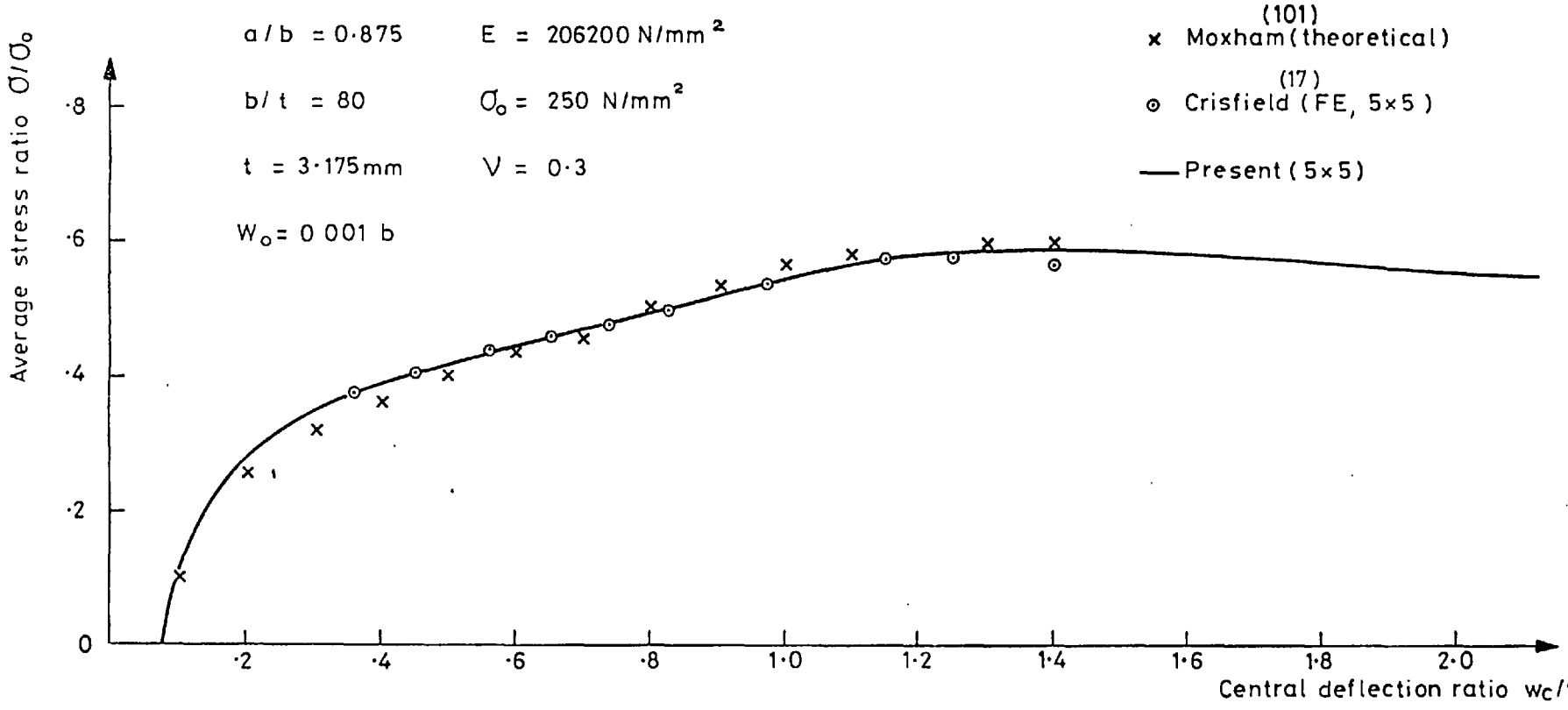

Fig. 39 Relation between average stress and central deflection for simply supported plate in direct compression (Kx = Sx = Sy = 0)

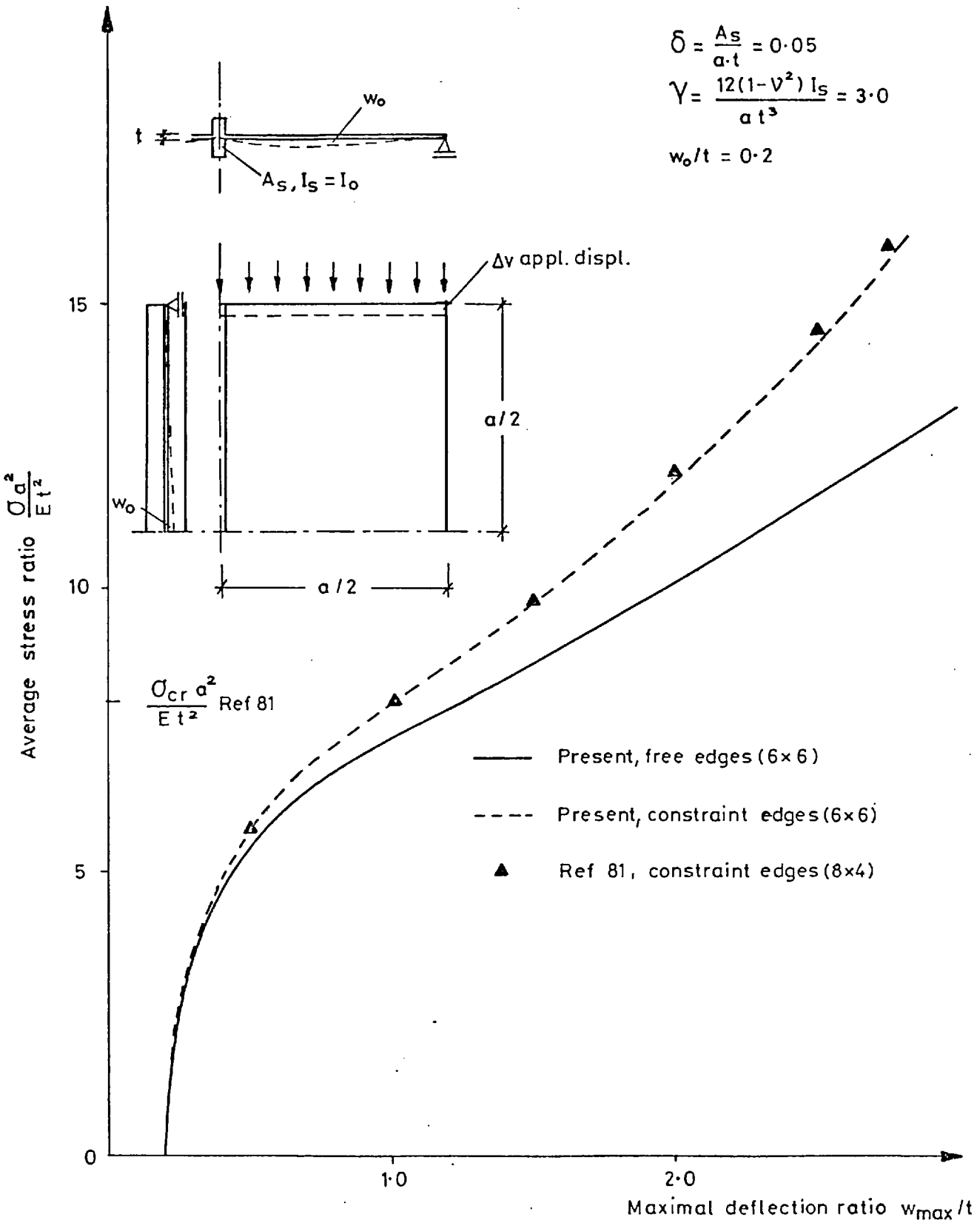

Fig. 40 Simply supported plate with one longitudinal symmetric stiffener subject to uniaxial in-plane loading

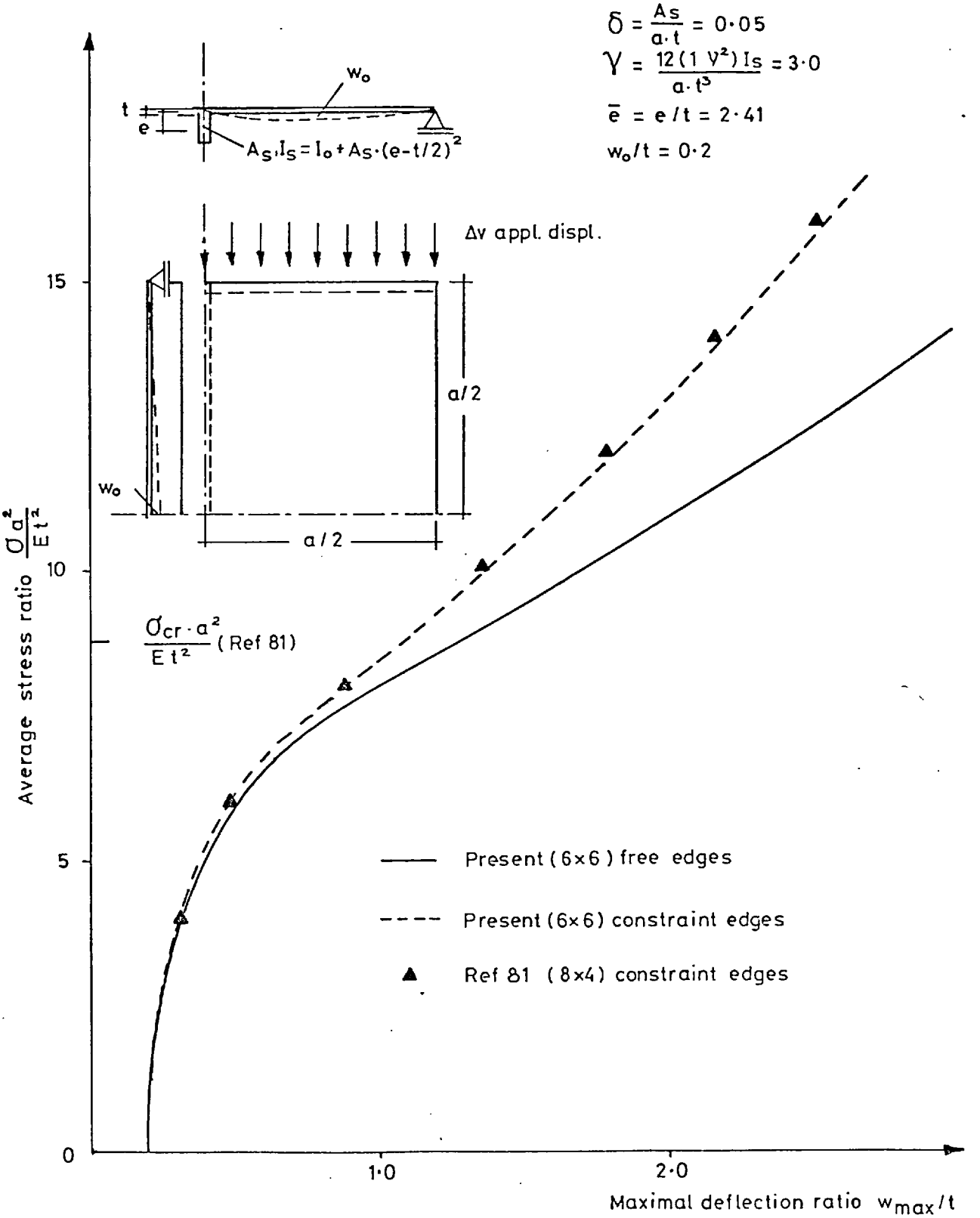

Fig. 41 Simply supported plate with one eccentric longitudinal stiffener subject to uniaxial in-plane loading

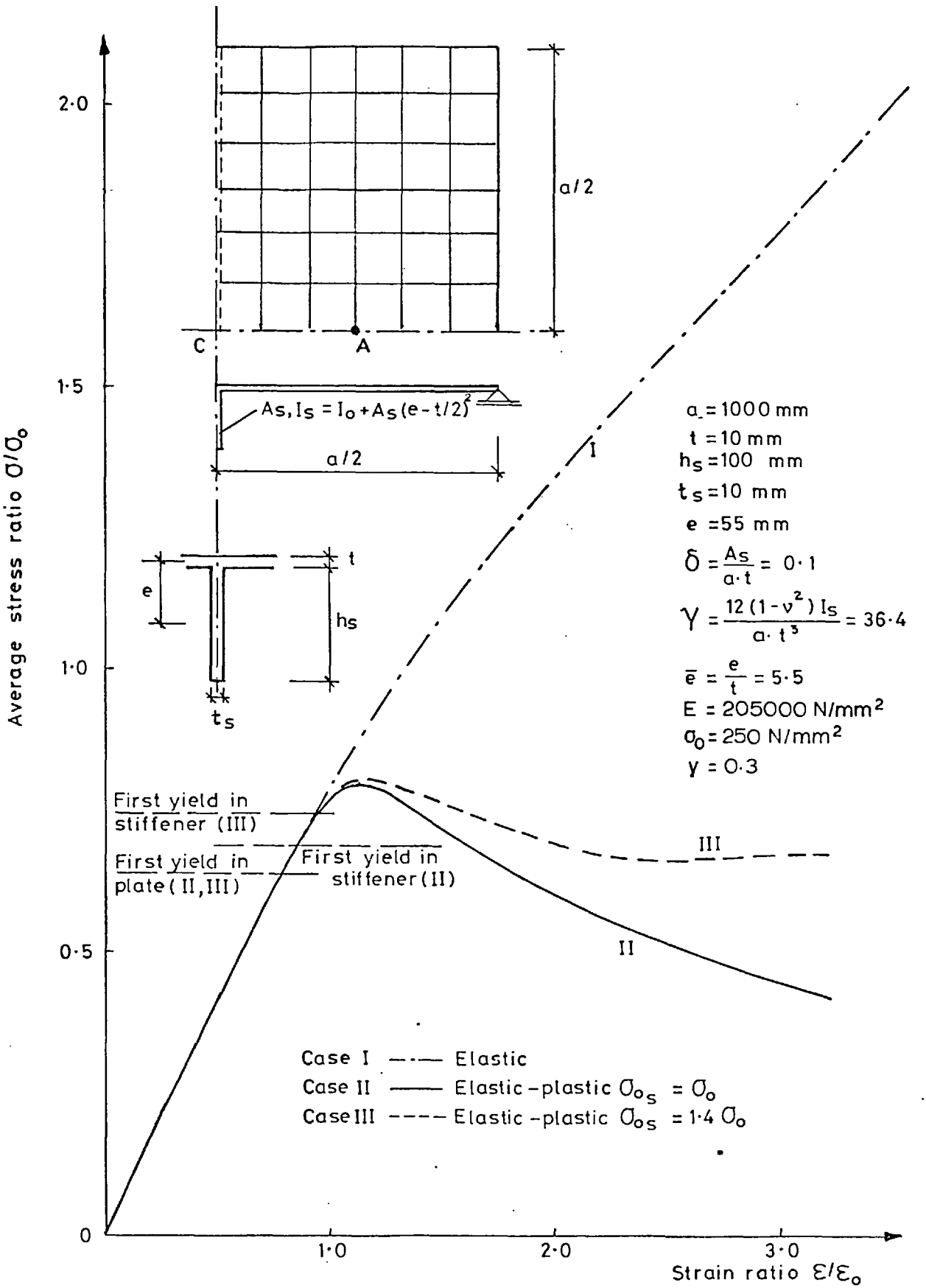

Fig. 42 Simply supported plate with one eccentric longitudinal stiffener under uniform direct compressive displacements. Relation between average stress and average strain

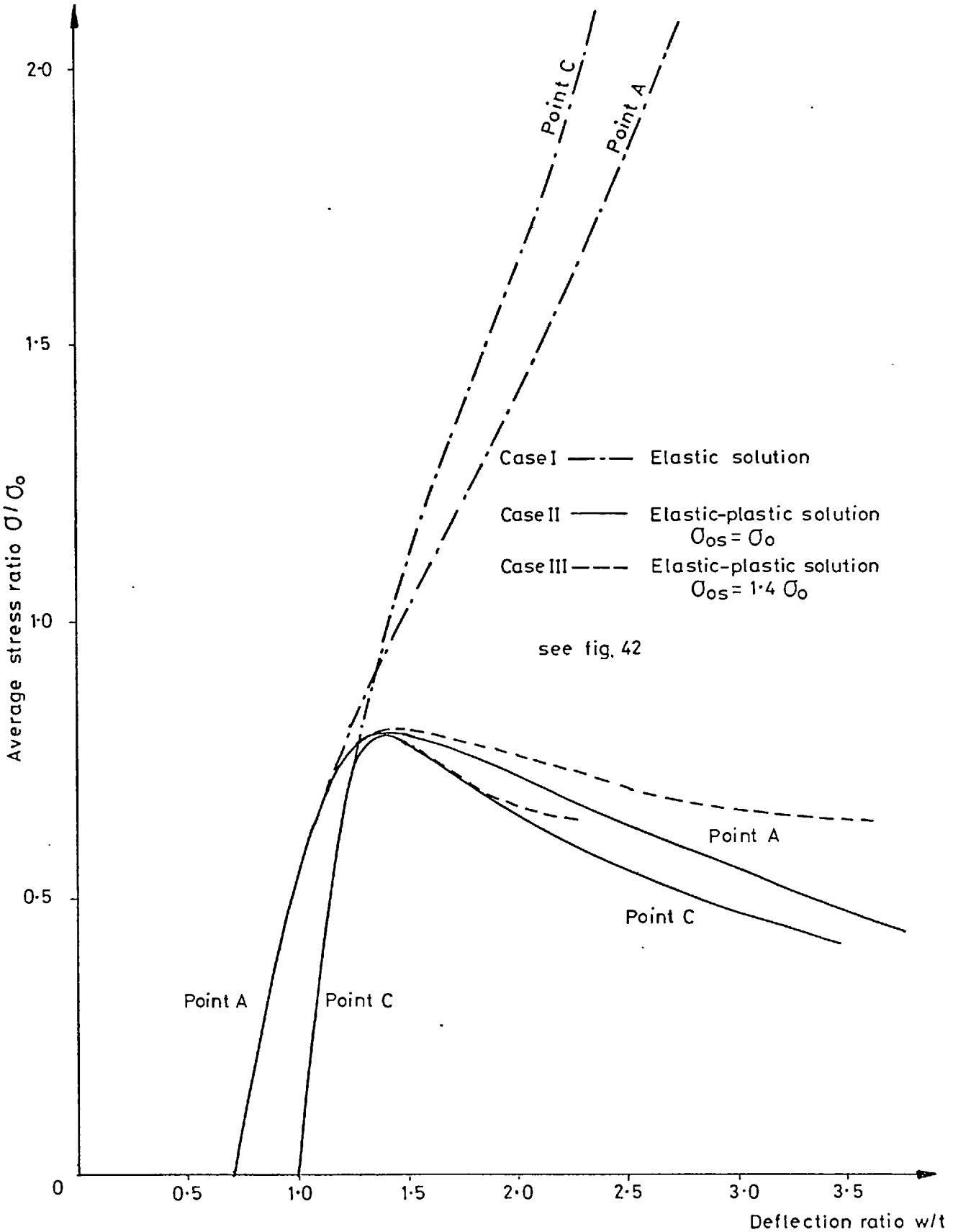

Fig. 43 Simply supported plate with one eccentric longitudinal stiffener under direct compressive displacements
Relation between average stress and deflection

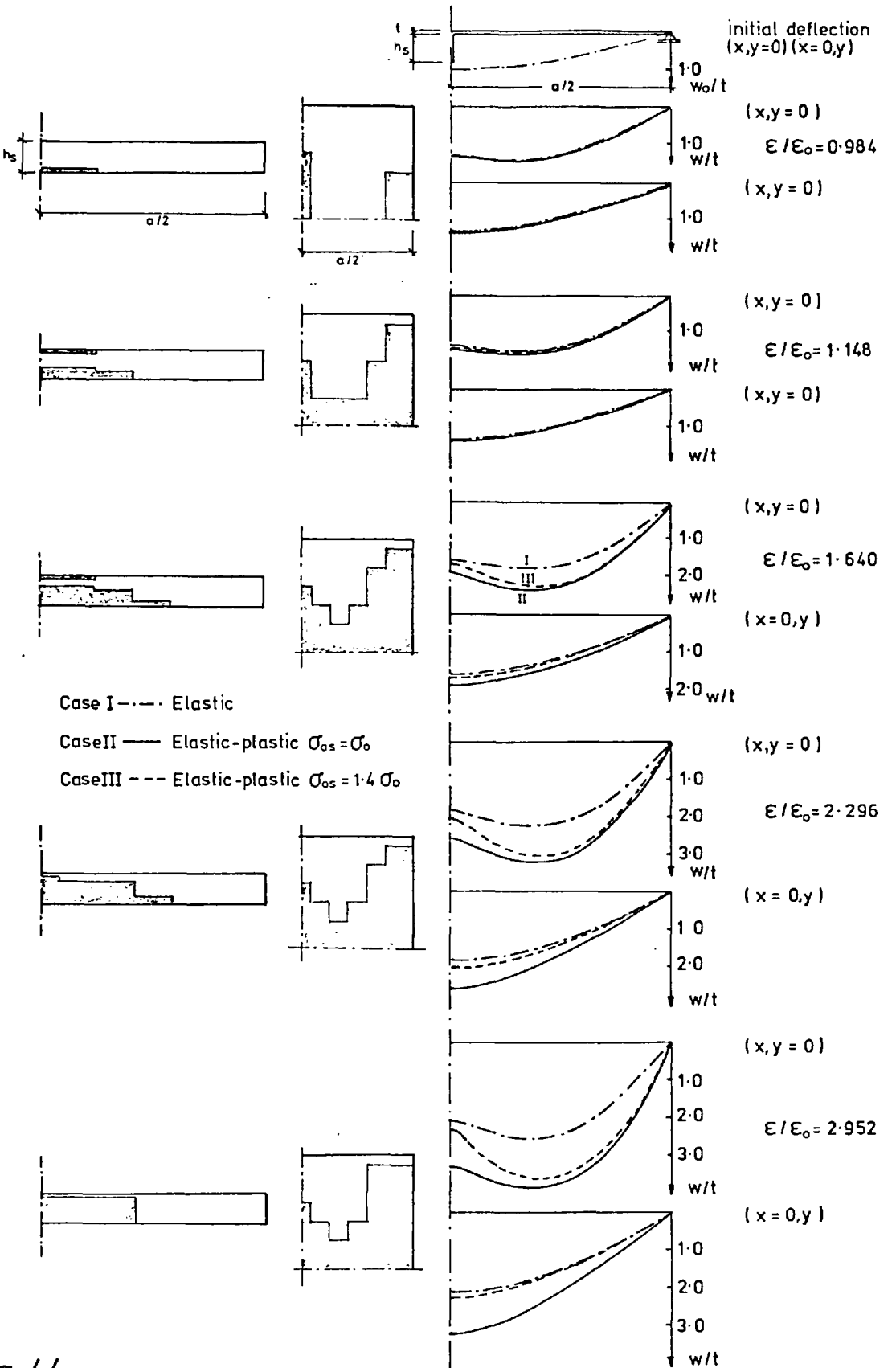

Fig. 44

Simply supported plate with one eccentric longitudinal stiffener under uniform direct compressive displacements.

Deflection profiles and growth of plasticity in plate and stiffener ($\sigma_{os} = \sigma_o$)

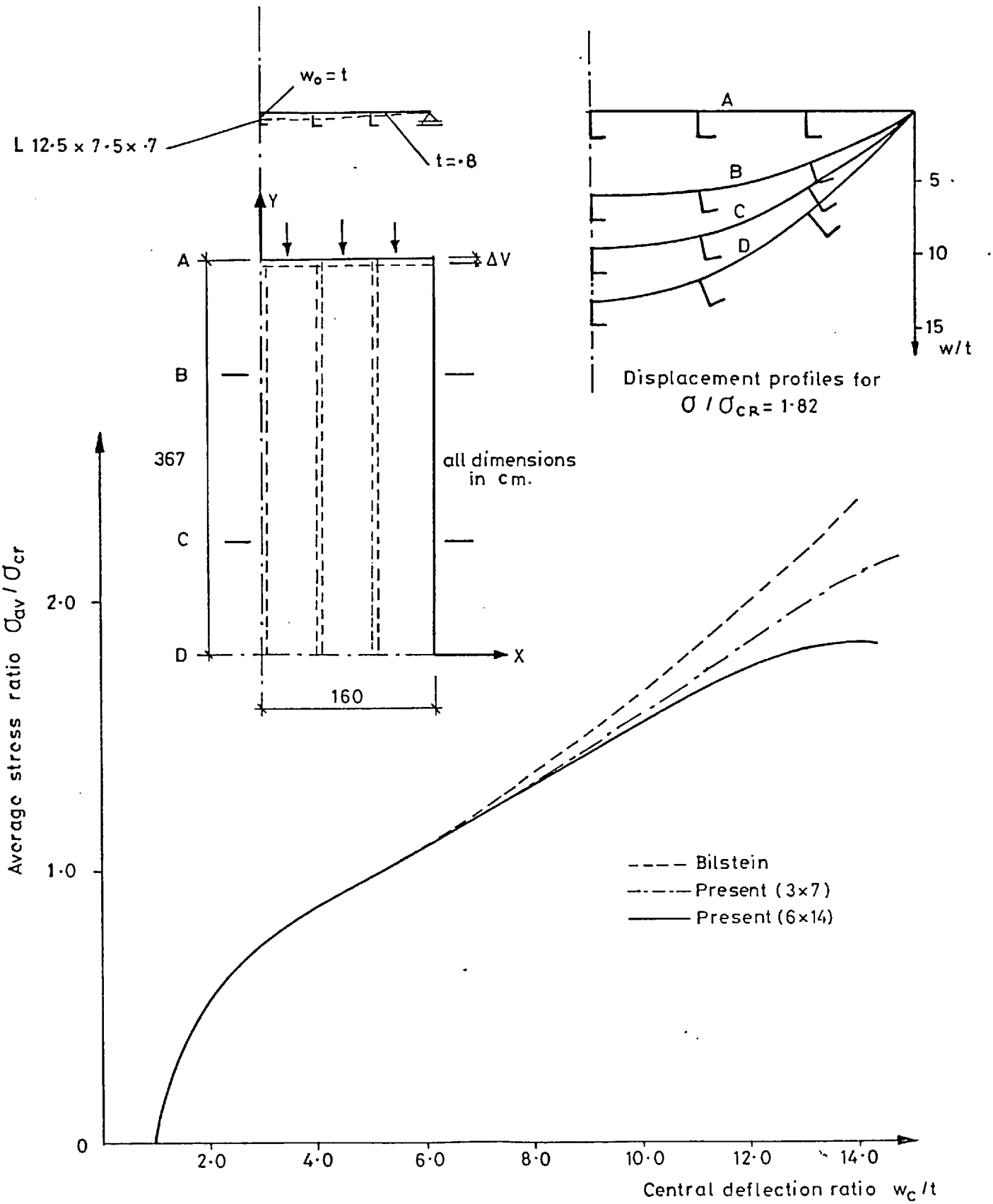

Fig. 45 · Simply supported longitudinally stiffened plate under compression.

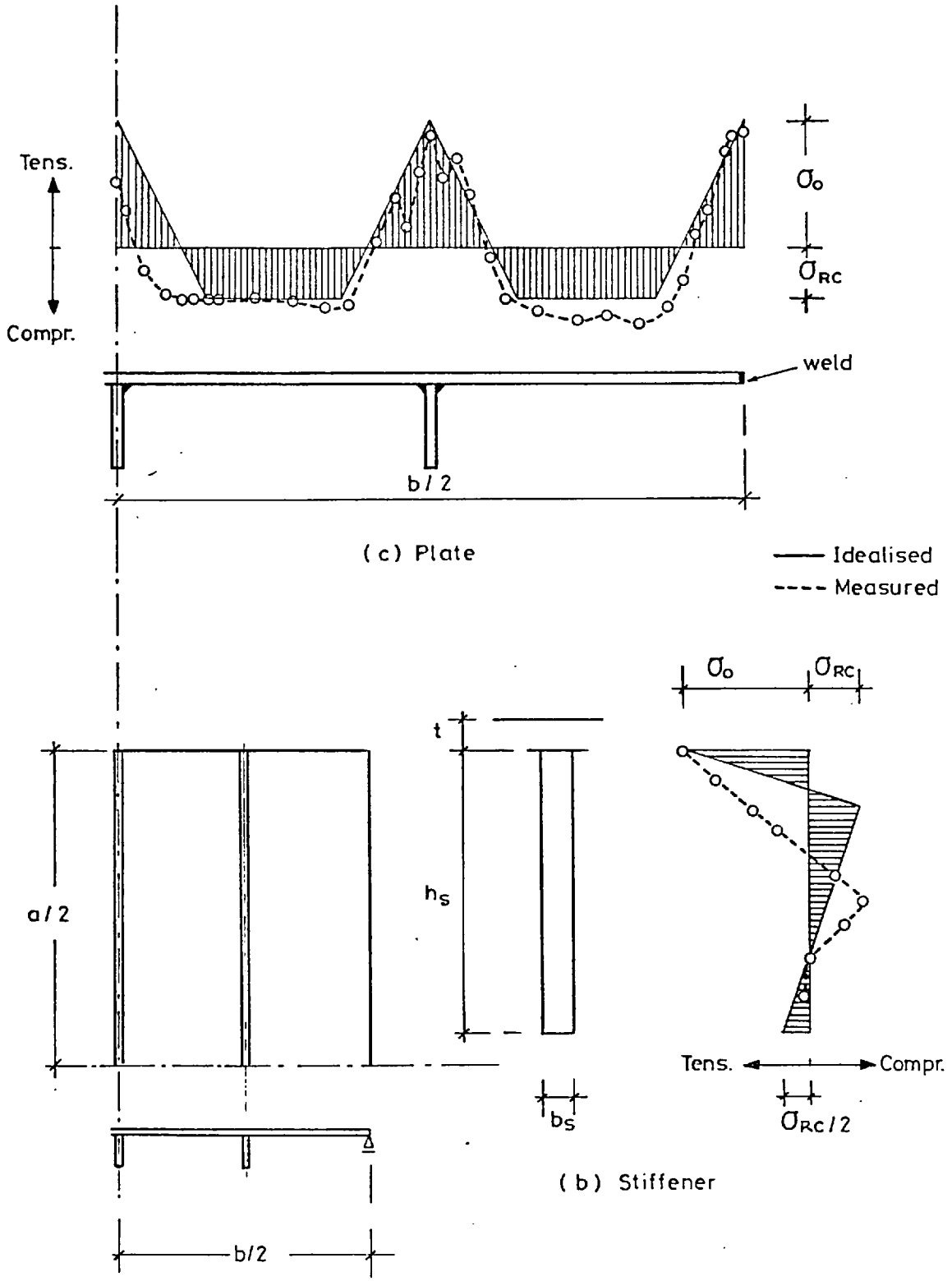

Fig. 46 Stiffened plate and assumed residual stress patterns

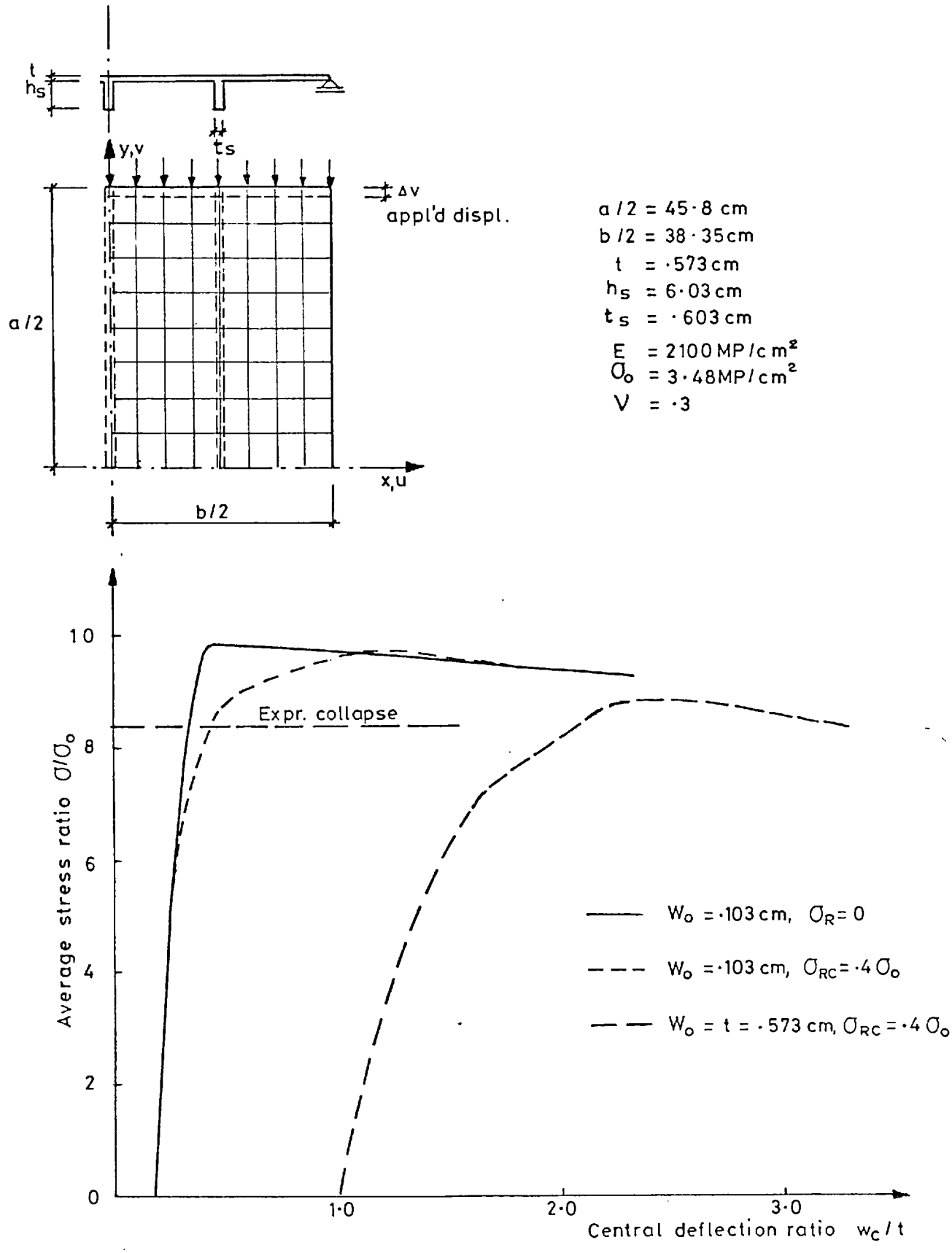

Fig. 47 Stiffened plate under uniform direct compressive displacement. Relation between average stress and central deflection

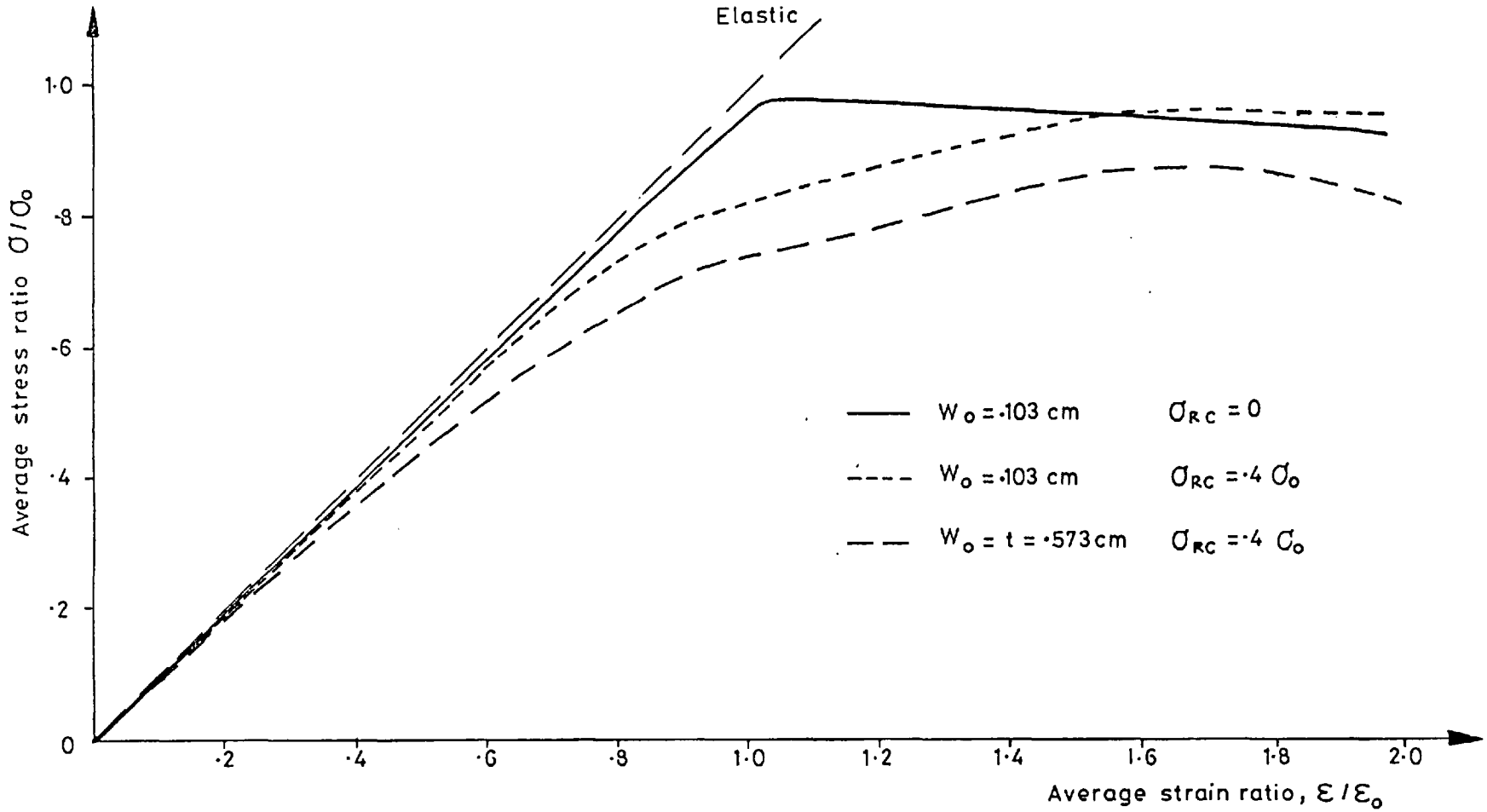

Fig. 48 Stiffened plate under uniform direct compressive displacements
Relation between average stress and average strain

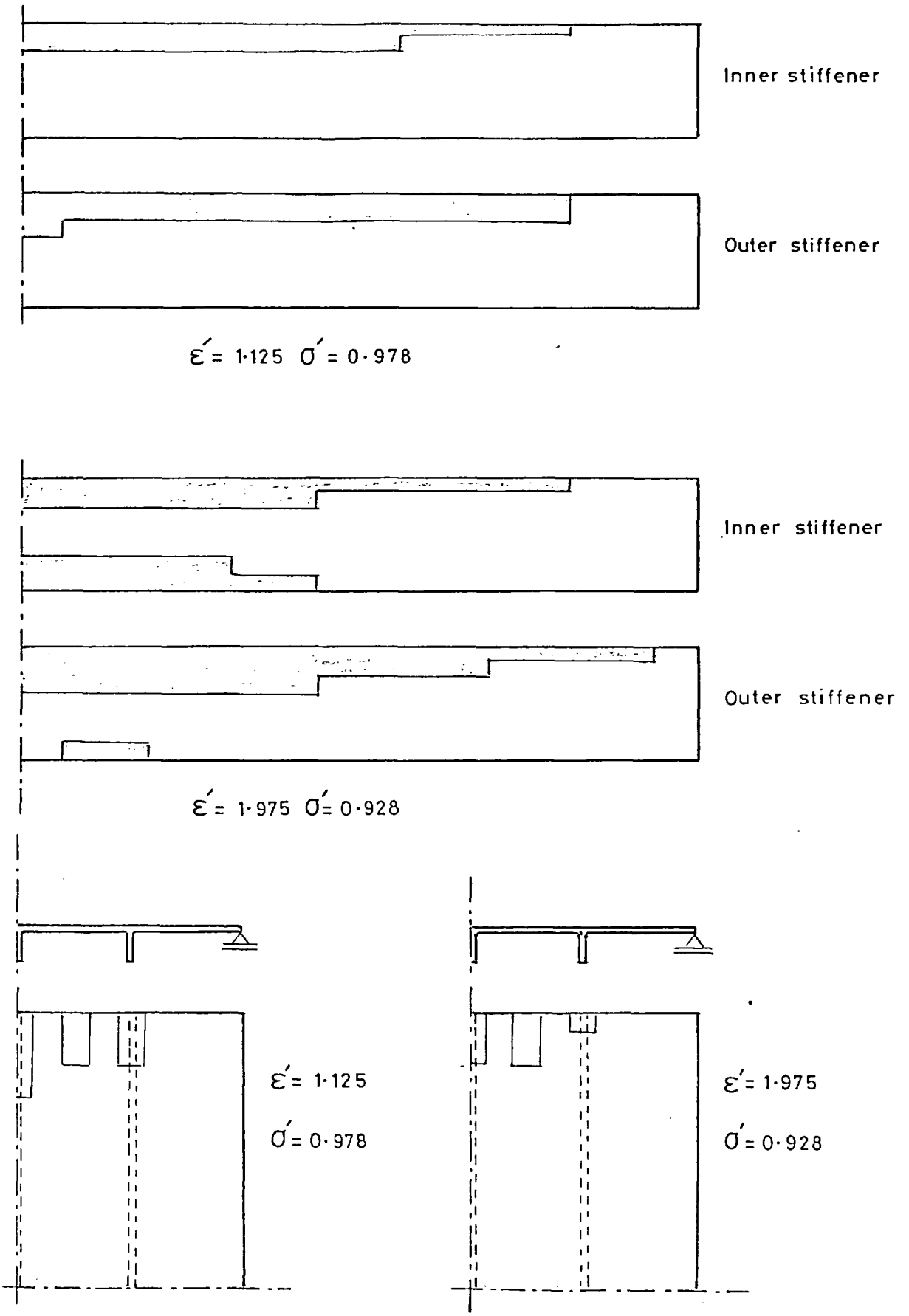

Fig. 49 Stiffened plate under uniform direct compressive displacements Growth of plasticity in plate and stiffeners.

($w_o = 0 \cdot 103$ cm, $\sigma_{RC} = 0$)

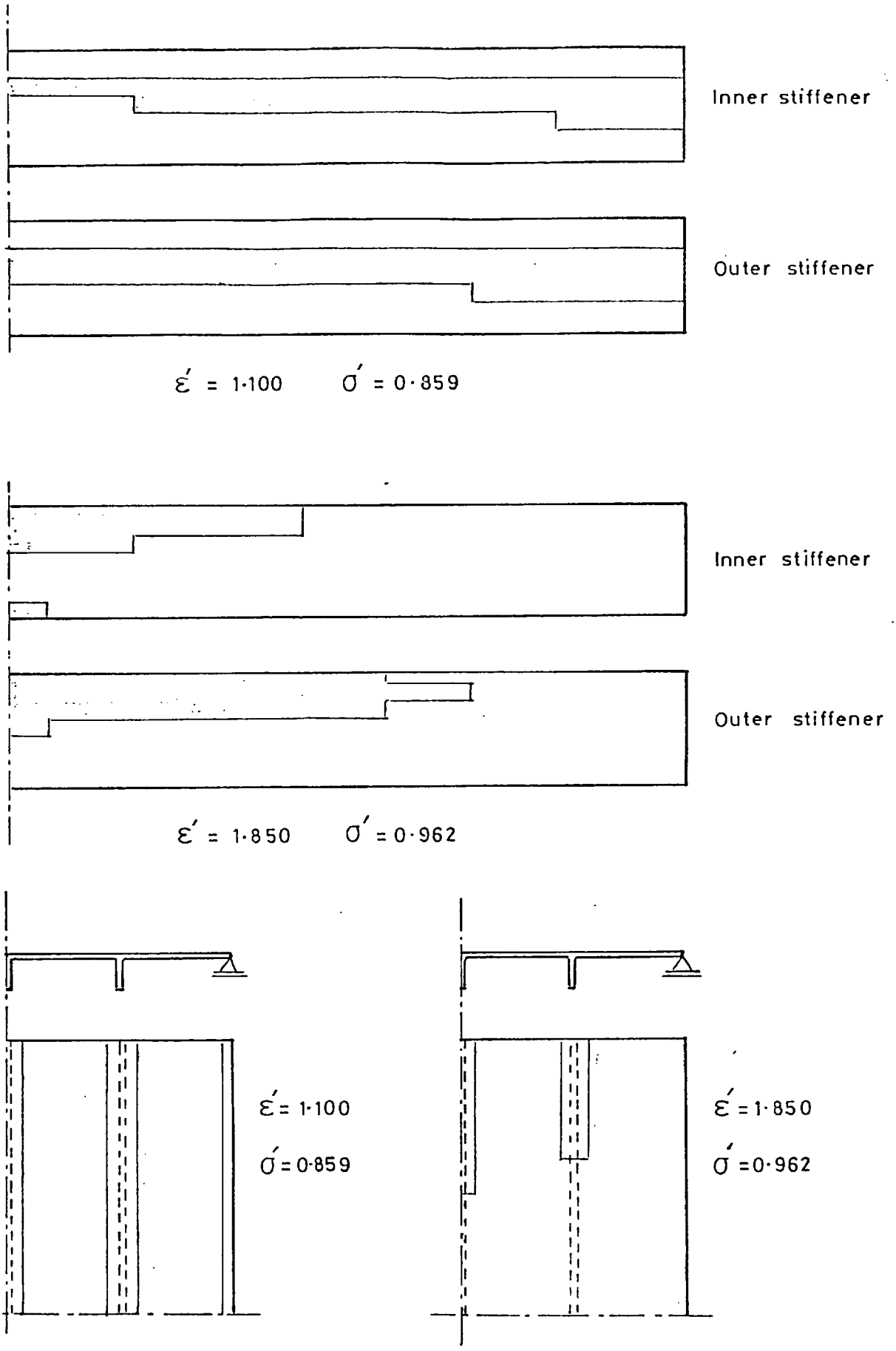

Fig.50 Stiffened plate under uniform direct compressive displacements
Growth of placity in plate and stiffeners
($w_o = 0 \cdot 103$cm, $\sigma_{RC} = 0 \cdot 4\ \sigma_o$)

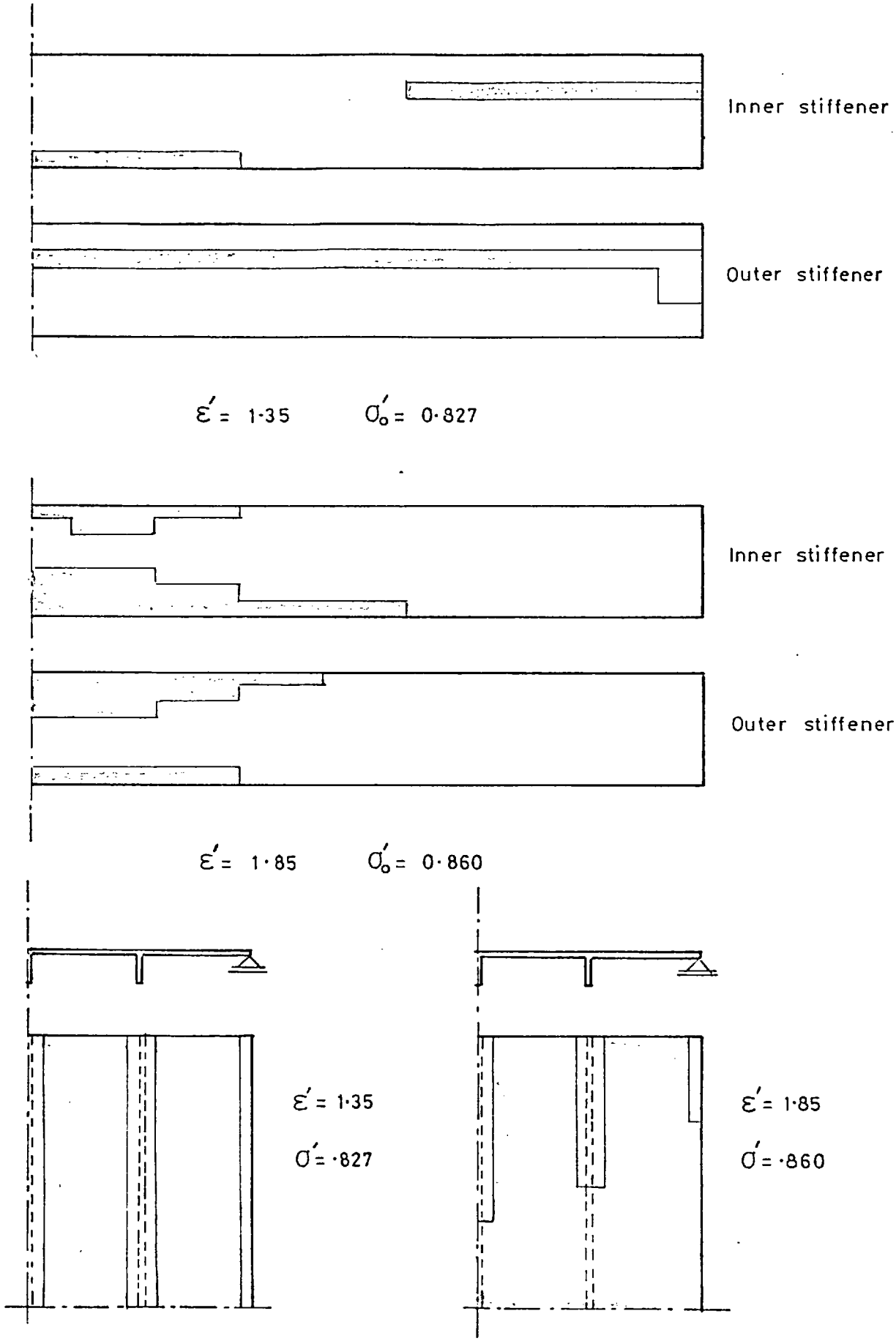

Fig. 51 Stiffened plate under uniform direct compressive displacements
Growth of plasticity in plate and stiffeners.
($w_o = t = 0{\cdot}573$ cm, $\sigma_{RC} = 0{\cdot}4\,\sigma_o$)

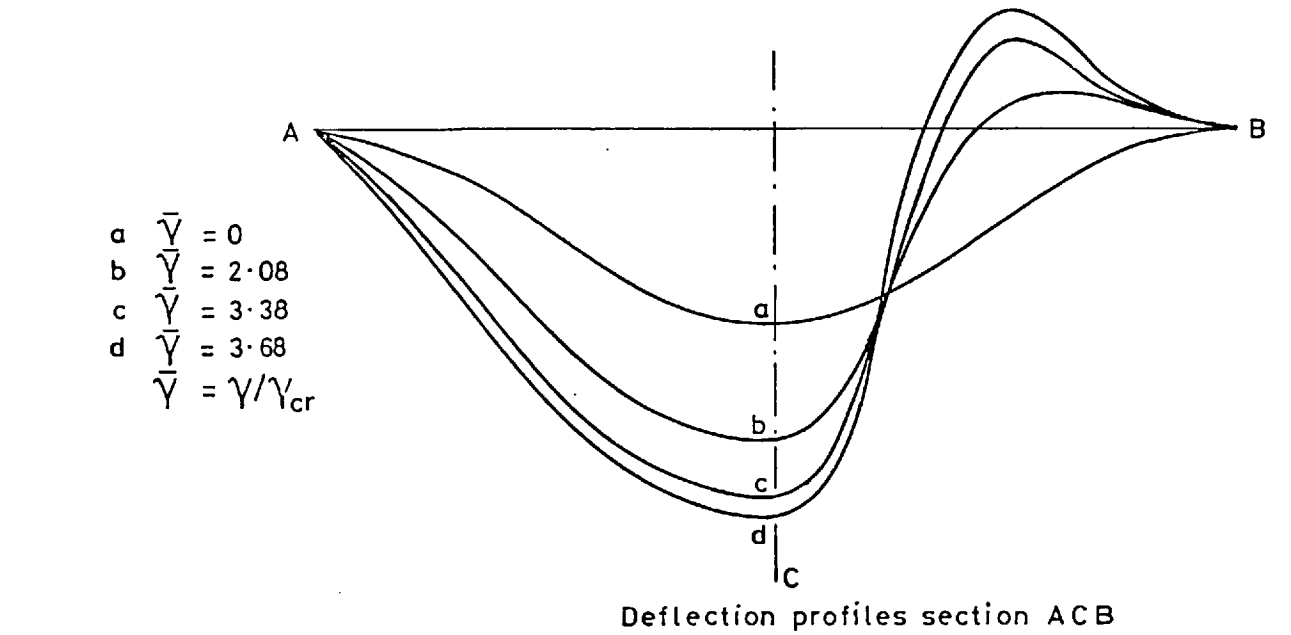

Deflection profiles section ACB

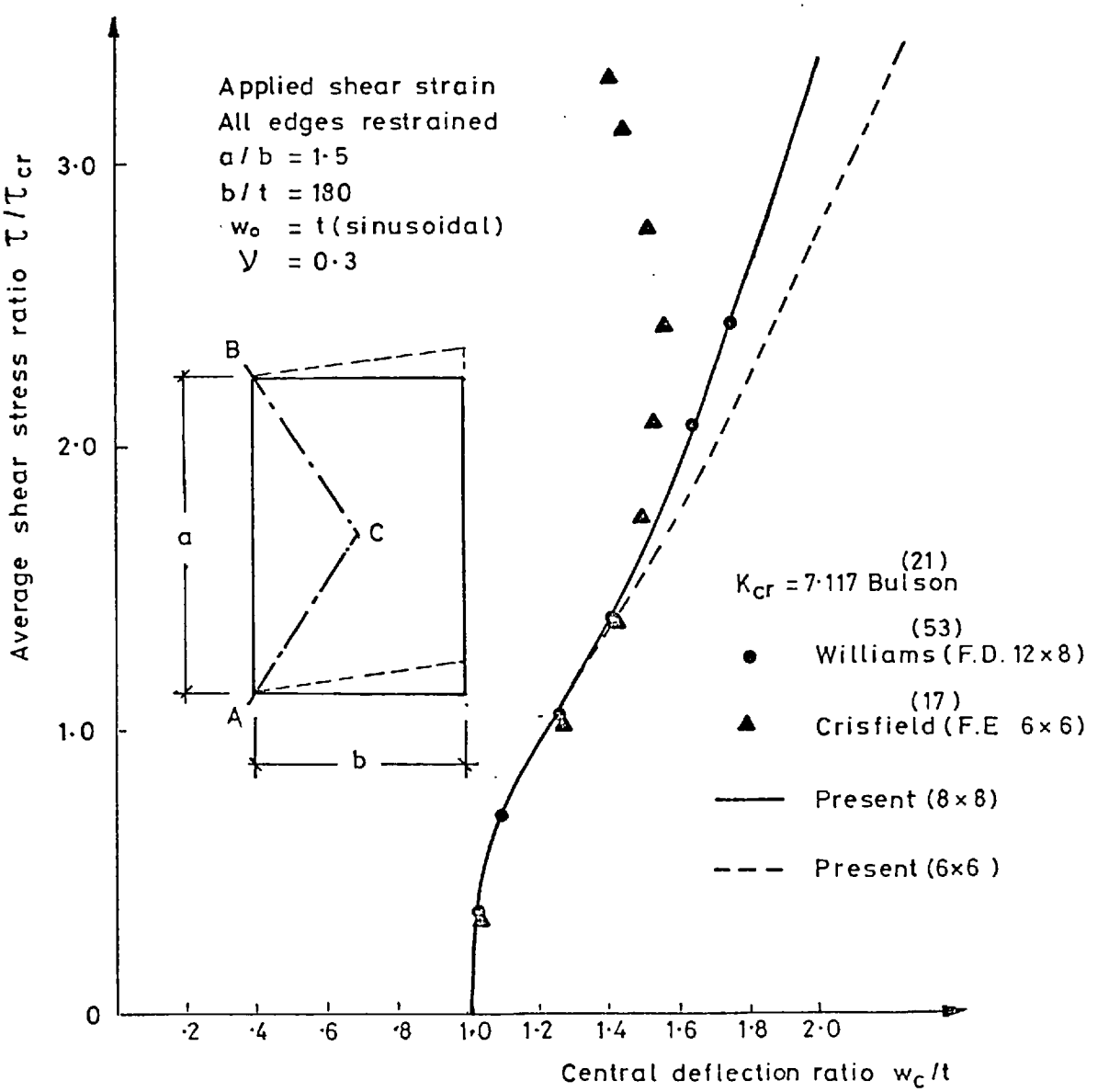

Fig. 52 Elastic simply supported isotropic plate subject to shear strain

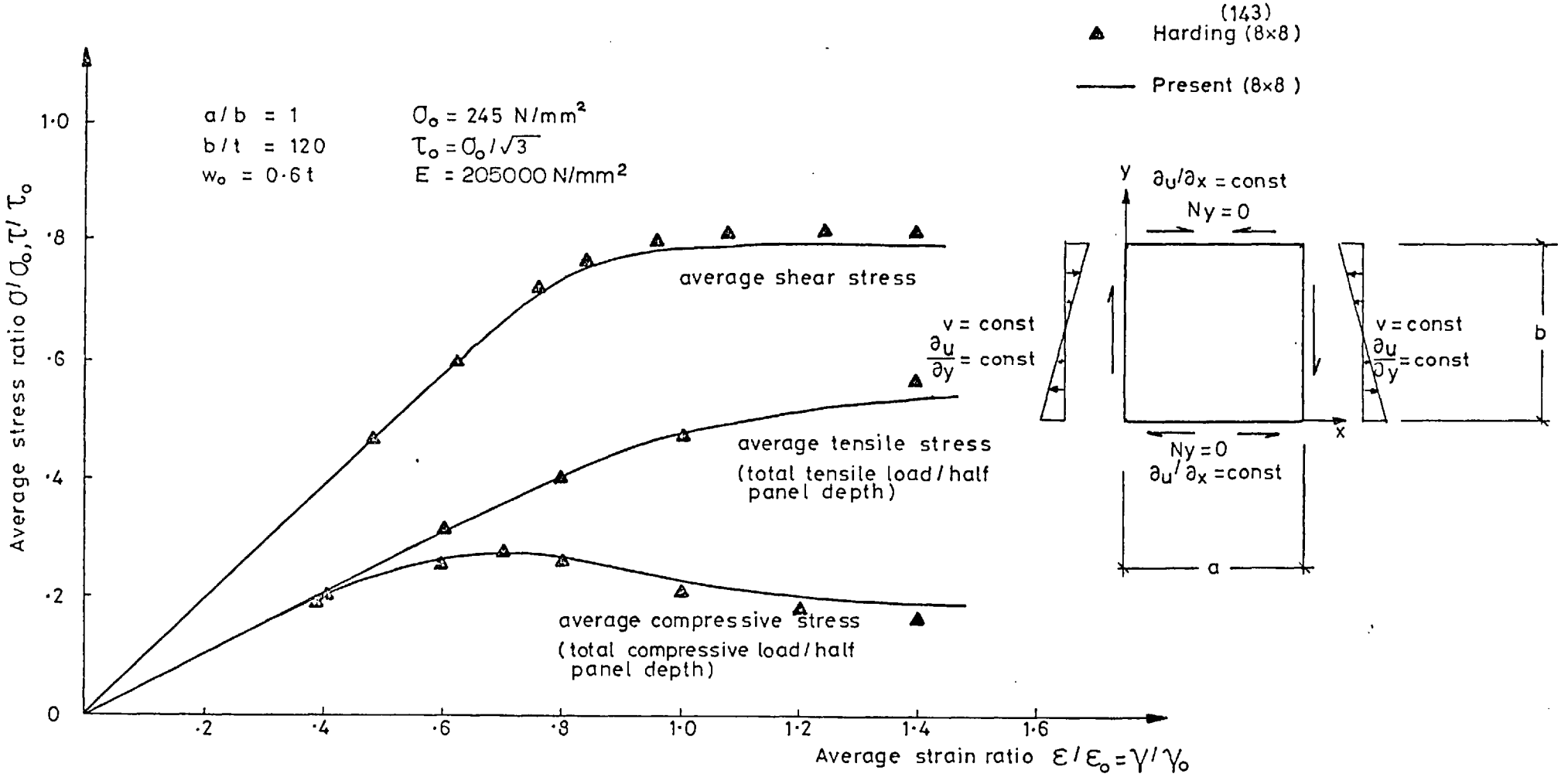

Fig. 53 Simply supported plate under shear and In-plane bending displacement. Average stress-strain curves.

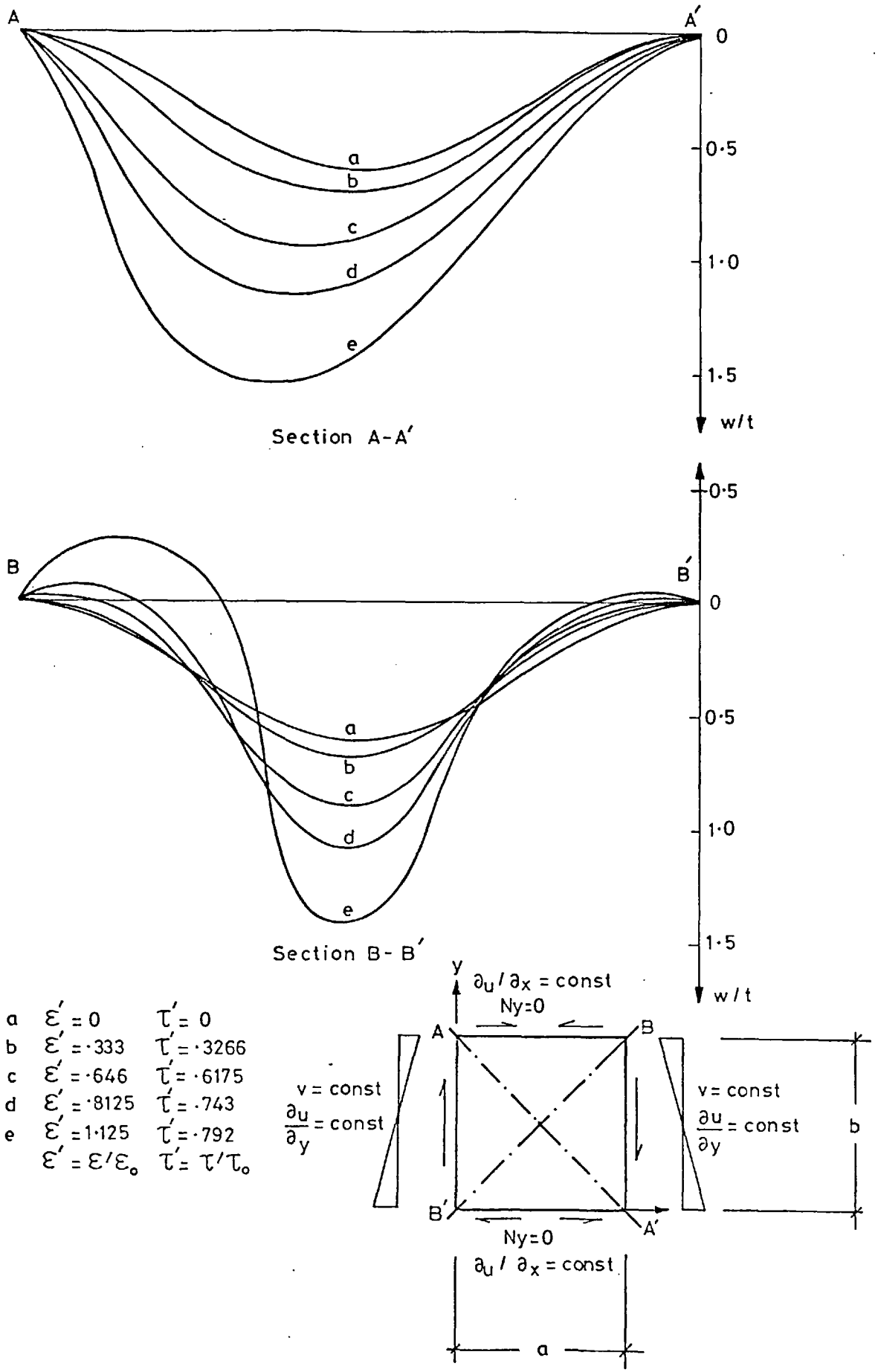

Fig. 54 Simply supported plate under shear and In-plane bending displacement. Deflection profiles.

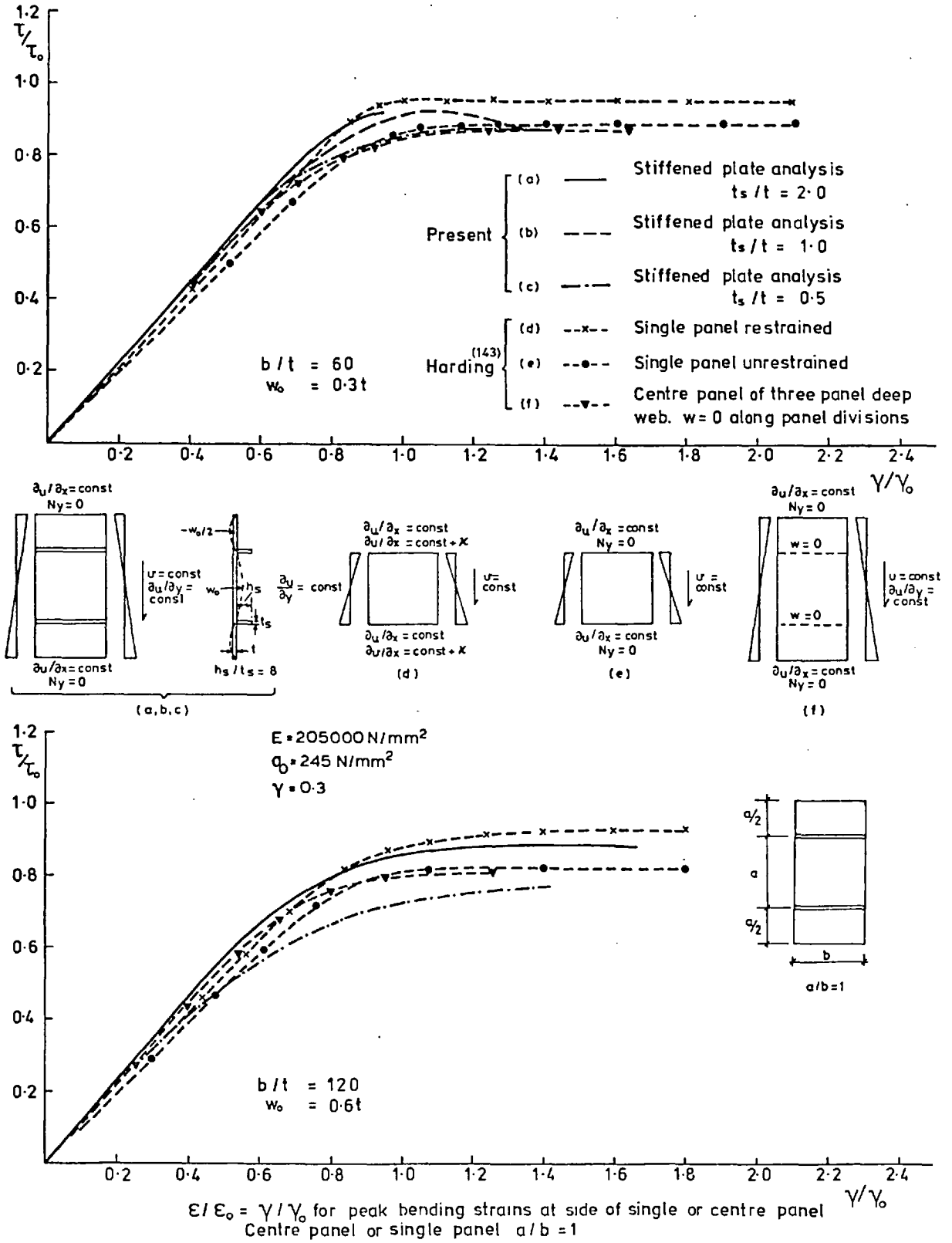

Fig. 55 Longitudinally stiffened panel under shear and In-plane bending displacement. Average shear stress-strain curves for centre panel

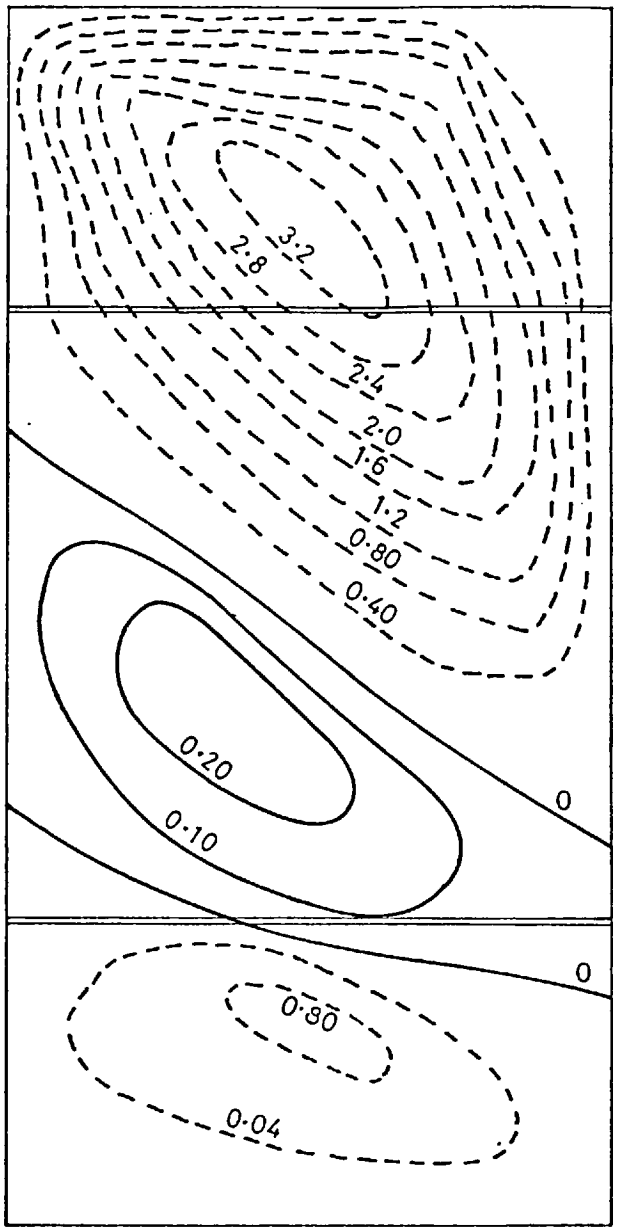

$t_s/t = 0{\cdot}5 \quad \gamma/\gamma_o = 1{\cdot}255$

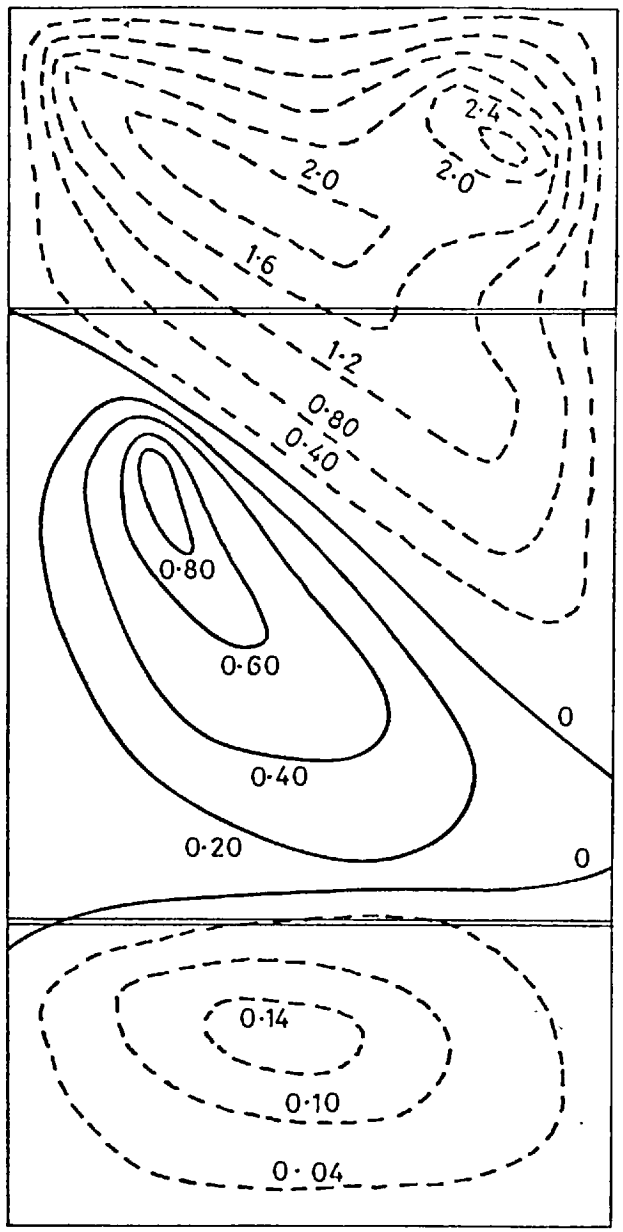

$t_s/t = 2{\cdot}0 \quad \gamma/\gamma_o = 1{\cdot}297$

b/t = 120 for centre panel

Contours are out-of-plane deformations expressed as multiples of the plate thickness

——— towards stiffener outstand

– – – – – away from stiffener outstand

$W_o = 0{\cdot}6\,t$ (see fig. 57)

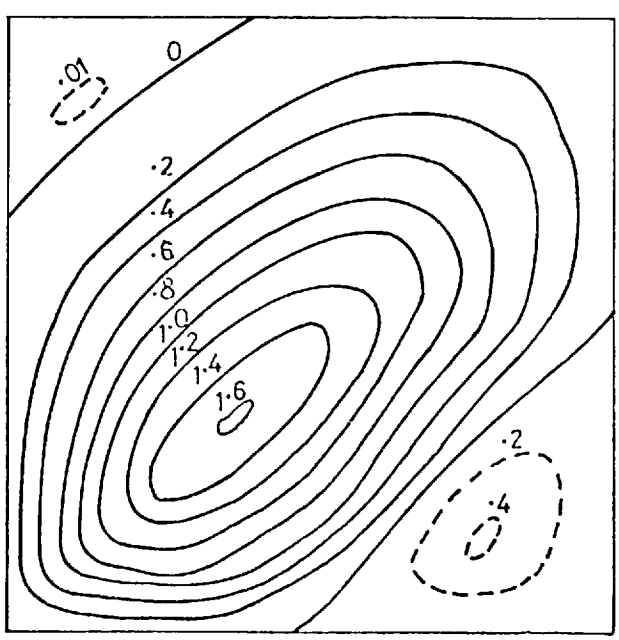

Unrestrained single panel $\gamma/\gamma_o = 1{\cdot}125$

Fig. 56 Out-of-plane deformation of stiffened panels

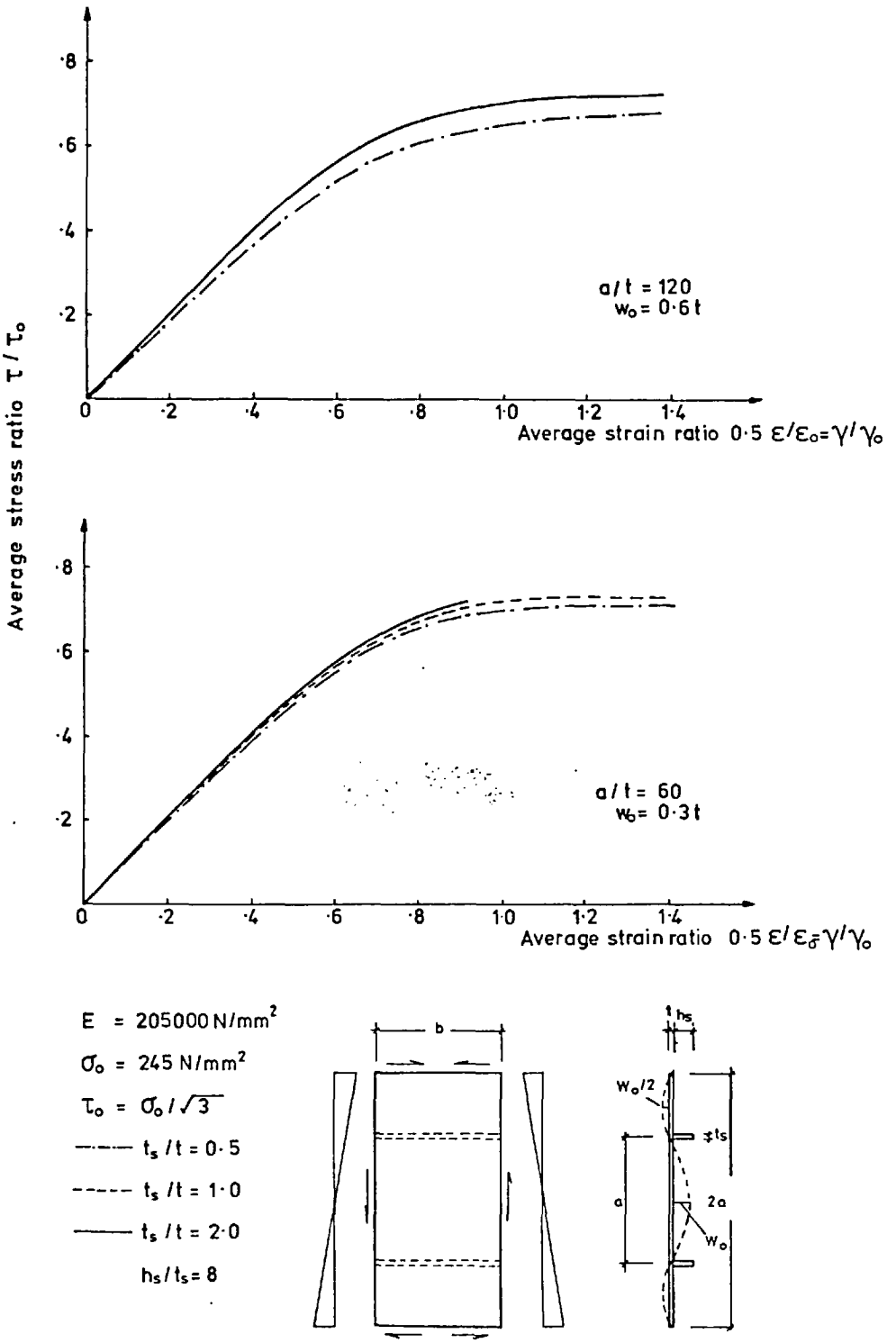

Fig.57 Longitudinally stiffened plate under combined in-plane shear and bending displacements.

Relation between average strain and average stress

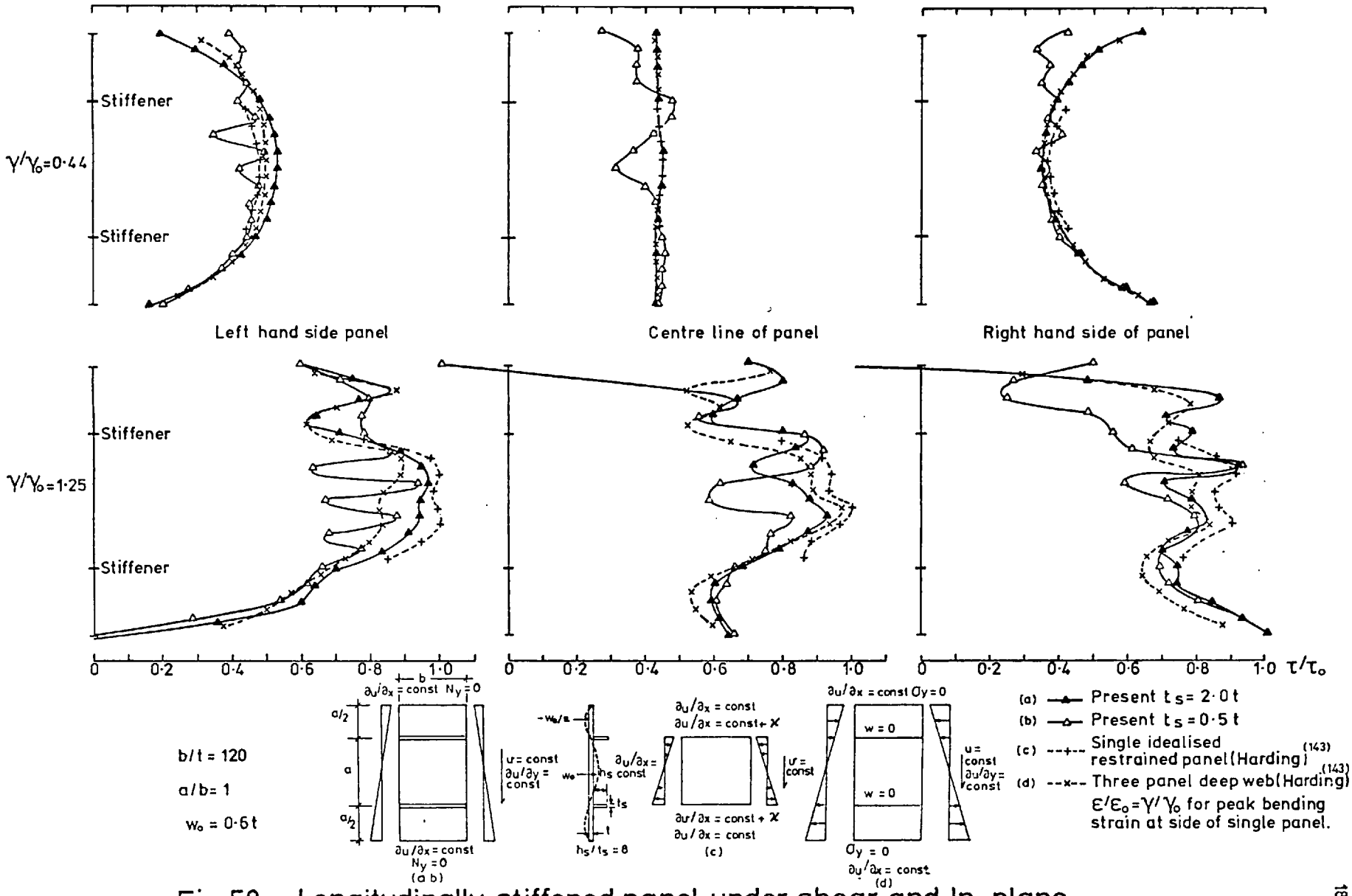

Fig. 58 Longitudinally stiffened panel under shear and In-plane bending displacement. Shear stress distribution.

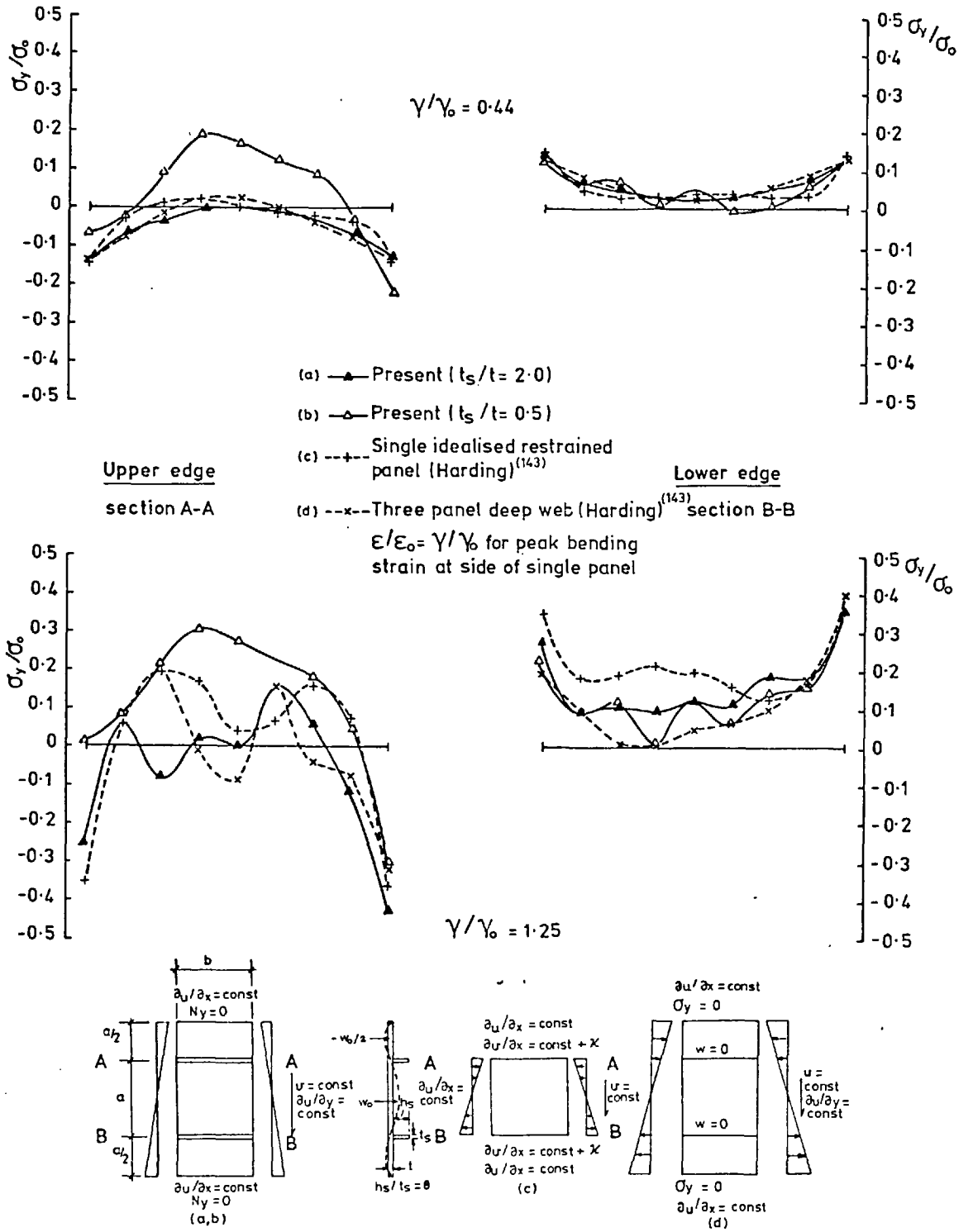

$a/b = 1 \qquad b/t = 120 \qquad w_o = 0{\cdot}6\,t$

Fig. 59 Longitudinally stiffened panel under shear and In-plane bending displacement. Transverse stress distribution along the stiffeners.

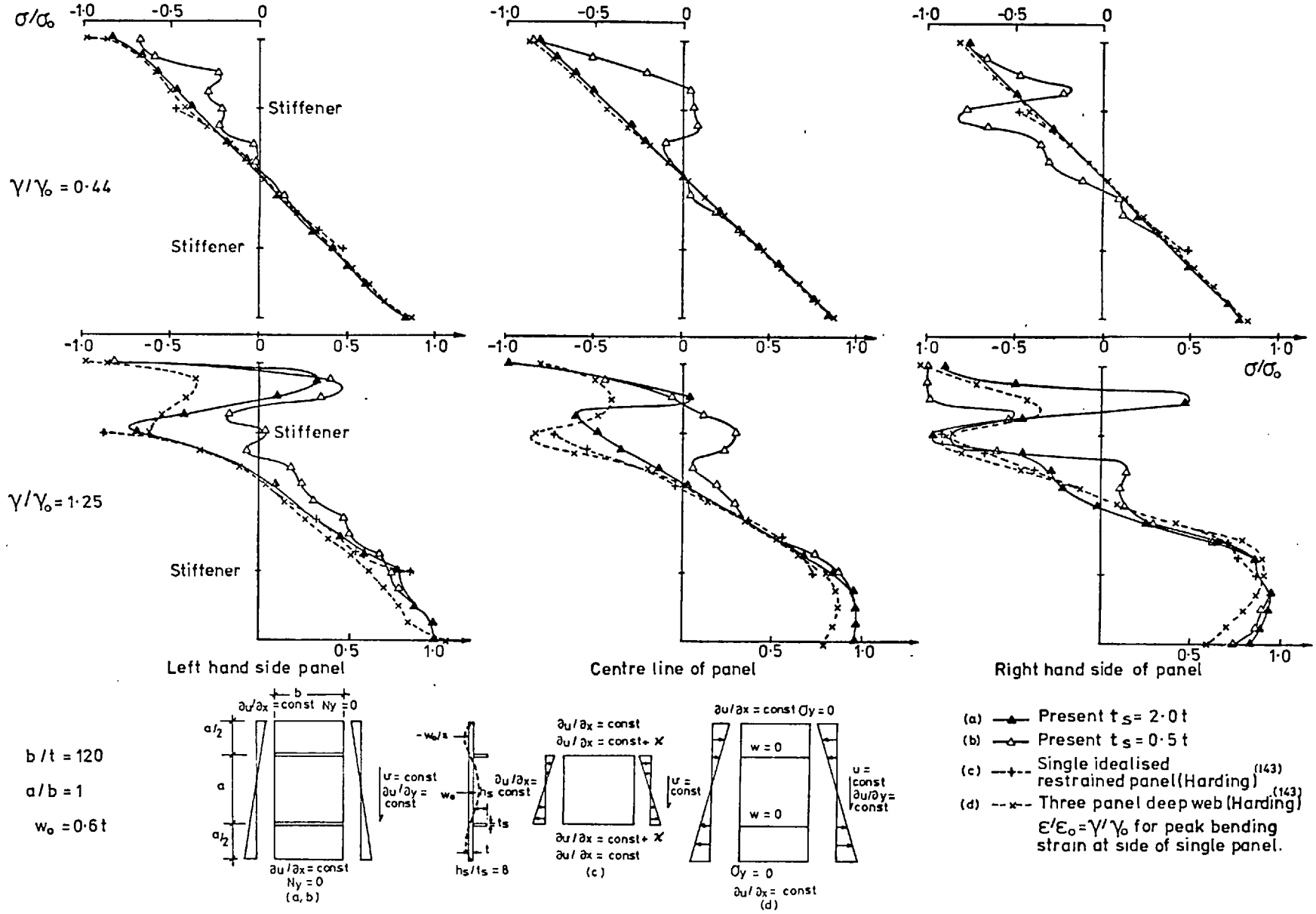

Fig. 60 Longitudinally stiffened panel under shear and In-plane bending displacement. Normal stress distribution